



Universiteit
Leiden
The Netherlands

Bitter Sweet Symphony: the impact of sugars on autoimmunity

Kissel, T.

Citation

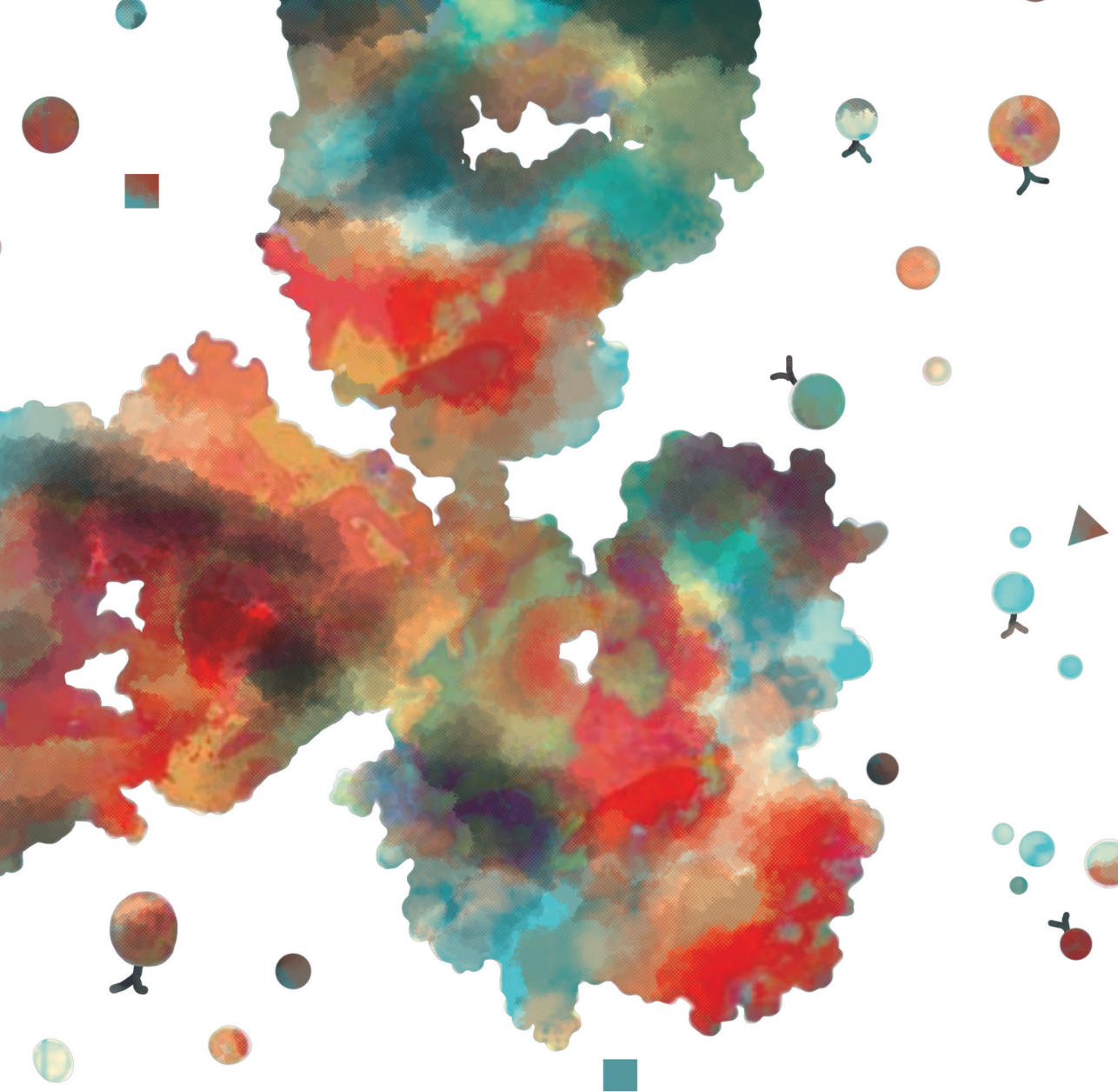
Kissel, T. (2022, December 1). *Bitter Sweet Symphony: the impact of sugars on autoimmunity*. Retrieved from <https://hdl.handle.net/1887/3492105>

Version: Publisher's Version

License: [Licence agreement concerning inclusion of doctoral thesis in the Institutional Repository of the University of Leiden](#)

Downloaded from: <https://hdl.handle.net/1887/3492105>

Note: To cite this publication please use the final published version (if applicable).



BITTER SWEET SYMPHONY **THE IMPACT OF SUGARS** **ON AUTOIMMUNITY**

Theresa Kissel

BITTER SWEET SYMPHONY

THE IMPACT OF SUGARS ON AUTOIMMUNITY

Theresa Kissel

Bitter Sweet Symphony: the impact of sugars on autoimmunity
Theresa Kissel

Copyright © 2022 T. Kissel, Leiden, The Netherlands. All rights reserved. No part of this publication may be reproduced or transmitted in any form without permission of the copyright owner.

The research described in this thesis was financially supported by the Dutch Arthritis Foundation (ReumaNederland, 17-1-402).

ISBN: 978-94-6458-453-0

Cover design and layout: © www.evelienjagtman.com
Printing: Ridderprint | www.ridderprint.nl

BITTER SWEET SYMPHONY THE IMPACT OF SUGARS ON AUTOIMMUNITY

PROEFSCHRIFT

ter verkrijging van
de graad van doctor aan de Universiteit Leiden,
op gezag van rector magnificus prof. dr. ir. H. Bijl,
volgens besluit van het college voor promoties
te verdedigen op donderdag 1 december 2022
klokke 15:00 uur

door

Theresa Kissel

geboren te Bensheim
in 1992

Promotor

Prof. dr. R.E.M. Toes

Co-promotor

Dr. H.U. Scherer

Promotiecommissie

Prof. dr. T.W.J. Huizinga

Prof. dr. M. Wuhler

Dr. T. Rispens (Sanquin, AMC)

Prof. dr. L. Nitschke (Erlangen, FAU)

Prof. dr. A. van Spriel (Radboud, UMC)

*“Challenges are what make life interesting
and overcoming them is what makes life meaningful.”*

(Joshua J. Marine)

Table of Contents

Chapter 1	General introduction	9
Chapter 2	Checkpoints controlling the induction of B cell-mediated autoimmunity in human autoimmune diseases	29
Chapter 3	Antibodies and B cells recognizing citrullinated proteins display a broad cross-reactivity towards other post-translational modifications	51
Chapter 4	On the presence of HLA-SE alleles and ACPA IgG variable domain glycosylation in the phase preceding the development of rheumatoid arthritis	83
Chapter 5	Genetic predisposition (HLA-SE) is associated with ACPA IgG variable domain glycosylation in the pre-disease phase of RA	99
Chapter 6	ACPA IgG variable domain glycosylation increases before the onset of rheumatoid arthritis and stabilizes thereafter; a cross/sectional study encompassing 1500 samples	117
Chapter 7	Surface immunoglobulin variable domain glycosylation impacts on autoantigen binding and acts as threshold for human autoreactive B-cell activation	147
Chapter 8	N-linked glycans attached to the immunoglobulin variable domain affect the recruitment of complement	209
Chapter 9	General discussion and perspectives	243
 Addendum		
	Summary	269
	Nederlandse samenvatting	273
	Deutsche Zusammenfassung	277
	Curriculum Vitae	283
	List of publications	285
	Acknowledgments	287



General introduction

Autoantibodies in Rheumatoid Arthritis

Rheumatoid Arthritis (RA) is an autoimmune disease causing chronic inflammation of the joints and other associated tissues. Characteristic is a symmetrical and persistent inflammation of the synovial tissue of small joints, particularly of the hands and feet. RA is classified based upon the American College of Rheumatology (ACR) and European League Against Rheumatism (EULAR) criteria combining clinical manifestations (joint involvement, duration of symptoms) and laboratory tests (serology, acute phase reactants)¹. RA has a slowly evolving disease course including arthralgia, a phase in which synovial inflammation is still absent, as an important pre-disease manifestation. Autoantibodies are an important hallmark of RA and about 60-70% of patients display rheumatoid factors (RF), antibodies directed against the fragment crystallizable (Fc)-tail of IgG, when these are complexed with antigen. The effective treatment with B-cell targeted therapies emphasizes that B cells and/or their secreted antibodies are central players in the disease progression^{2,3}.

The most disease-specific antibodies were first identified in 1964 as “anti-perinuclear factors”⁴. In 1998 it was found that these “anti-perinuclear factors” were directed against citrulline, a “non-encoded” amino acid generated by a post-translational modification (PTM) of arginine via protein-arginine deiminase (PAD) enzymes^{5,6}. The therefore called anti-citrullinated protein antibodies (ACPAs) are present in about 50-70% of RA patients. ACPAs can already occur several years before the onset of RA, in the phase of clinically “silent” autoimmunity, although to a rather limited extent⁷. Intriguingly, ACPA-positive patients have a more severe disease progression and a lower chance to achieve long-term drug-free remission as compared to ACPA-negative patients⁸. ACPA responses are dynamic and an increase in levels combined with a broader citrullinated epitope recognition profile associates with the transition towards RA⁹. Remarkably, ACPAs can react towards a broad spectrum of citrullinated antigens, such as α -enolase, fibrinogen, filaggrin, vimentin and type II collagen^{6,10-14}. Next to ACPAs, also other autoantibodies targeting different PTMs, such as carbamylated-(homocitrulline-presenting) and acetylated-antigens, have been identified. Anti-carbamylated protein antibodies (ACarPAs) are present in ~45% of patients with RA, while anti-acetylated protein antibodies (AAPAs) can be found in ~40% of RA patients¹⁵⁻¹⁷. The concurrent presence of different autoantibody systems in patients with RA is surprising and suggests cross-reactivity of one autoantibody to various PTMs¹⁸⁻²¹. Nevertheless, ACPAs, ACarPAs and AAPAs may possibly also represent three distinct autoantibody families^{15,17}. This assumption is reinforced by the fact that the “modified” epitopes, citrullinated-arginine residues and carbamylated-/acetylated-lysine residues, occur at different positions in the protein backbone surrounded by distinct flanking regions. In addition, the three amino acid modifications are structurally dissimilar, especially when comparing carbamylation to acetylation.

Currently it is unclear if and how the autoantibodies in RA are involved in the inflammation of the synovium, but it has been postulated that ACPAs can contribute to disease pathogenesis via the complement system. The complement system can be activated via three distinct cascades - classical, lectin, and alternative - each leading to a common terminal pathway²². It has been shown that ACPAs can activate both the classical and the alternative complement pathway in an antigen-dependent *in vitro* assay²³.

B-cell response in Rheumatoid Arthritis

The identification and isolation of citrullinated protein (CP)-directed, ACPA secreting B cells from RA patients allowed for the first time the detailed characterization of these cells²⁴. These B cells were identified using labelled citrullinated antigen-(cyclic citrullinated peptide 2) tetramers. Flow cytometry experiments revealed that they mainly circulate in the peripheral blood as class-switched CD20 and CD27 positive memory B cells at a mean frequency of 1:10,000 B cells. In addition, long-lived ACPA secreting plasmablasts and plasma cells have been detected, producing immunoglobulins (Ig) of several classes (IgM, IgG and IgA)²⁵. Interestingly, a recent study showed that CP-directed memory B cells in patients with recent-onset RA display an activated and proliferative phenotype as opposed to tetanus toxoid (TT)-directed B cells²⁶. This activated phenotype, represented by an increased expression of CD80, CD86 and Ki67, did not correlate with disease activity, indicating that autoreactive B cells in RA are continuously active and fail to reach a state of quiescence irrespective of treatment. This is also consistent with findings that ACPA-positive patients rarely seroconvert and that ACPA levels remain elevated compared with RF levels²⁷, suggesting that ACPAs are produced by long-lived plasma cells residing in niches of the bone or (chronically) inflamed tissues. Furthermore, a high positivity for HLA-DR was observed pointing towards their ability to interact with T cells in RA. Next to the increased activation status, CP-directed B cells also down-regulate the inhibitory receptor CD32 and thus escape CD32-mediated negative regulation mechanisms. Furthermore, CP-directed B cells are enriched in synovial fluid and have been detected in synovial tissue mainly as plasmablasts or plasma cells^{26,28}. CP-directed B cells isolated from the inflamed synovial compartment secreted functionally active proinflammatory cytokines, particularly IL-8, potentially able to attract neutrophils. This phenotype was less prominent in individuals with arthralgia, indicating that an activated phenotype of CP-directed B cells might be predictive for disease development²⁶. Remarkably, CP-directed B cells have introduced a high amount of somatic mutations into their B-cell receptors (BCRs), implying once again continuous T-cell help. However, despite the high amount of mutations, the ACPA response undergoes limited avidity maturation²⁹ pointing towards a different selection mechanism of the autoreactive B cells as compared to “conventional” B cells and B-cell responses against e.g. recall antigens.

Genetic factors contributing to Rheumatoid Arthritis

A consistent and reproducible genetic contribution to RA was reported for variants within the human leukocyte antigen (HLA) region on chromosome 6 (6p21.3). More specifically, it has been shown that RA associates with alleles of the class II HLA-DRB1-gene, that encode a conserved amino acid sequence in the third hypervariable region (HVR3). This region, shared by most HLA-DRB1-genes associated with RA, is referred to as the shared epitope (SE)³⁰, and hence these alleles are called HLA-SE alleles. Differences in the predominantly RA-associated alleles have been found for different ethnicities: the *0401 and *0404 alleles are associated with RA in Caucasians, *0405 in Asian populations and *0101 in Israeli Jews. The SE hypothesis suggests that these class II molecules are directly involved in the pathogenesis of RA, although the exact mechanism is still unknown. As the SE alleles are located in the antigen-binding groove of the HLA molecule, it is compelling to assume that they influence the binding and presentation of specific peptide epitopes, including arthritogenic epitopes³¹. Interestingly, the HLA-SE alleles do not predispose to RA as such, but to ACPA-positive RA, but not to RF-positive RA³². This association is mainly present for individuals with ACPA-positive disease^{32,33} and mostly lost in ACPA-positive healthy individuals³⁴. These findings are of importance and indicate that T helper cells are involved in the transition from an ACPA-positive healthy to disease state (Figure 1).

N-linked protein glycosylation

A key characteristic, found on more than 90% of the RA-specific autoantibodies, ACPA IgG, is the abundant presence of N-linked glycans in their antigen-binding domains^{35,36}. Proteins can be co- or post-translationally modified by the attachment of monosaccharides (also known as sugars, glycans or carbohydrates). The most common type of glycosylation, is the N-linked glycosylation where glycans are attached to a nitrogen atom of an asparagine residue (N). N-glycans are attached to an asparagine in the presence of N-glycosylation consensus sequences, asparagine-X-serine/threonine (N-X-S/T), where "X" can be any amino acid except for proline³⁷. To a lower degree, N-glycans are also attached to asparagine-X-cysteine (N-X-C) motives^{38,39}. More recently, N-linked glycans were also observed on reversed N-linked consensus sequences (S/T-X-N)⁴⁰ or non-consensus sequences (A-N-S-G)⁴¹. The most common N-glycan building blocks are monosaccharides, cyclic structures consisting of five carbons and one oxygen atom within the ring structure. Two monosaccharides can be enzymatically linked by condensation between the hemiacetal group of one monosaccharide and one of the hydroxyl groups of the other monosaccharide. As one monosaccharide contains several hydroxyl groups, multiple glycosidic bonds can be formed which results in branched glycan structures.

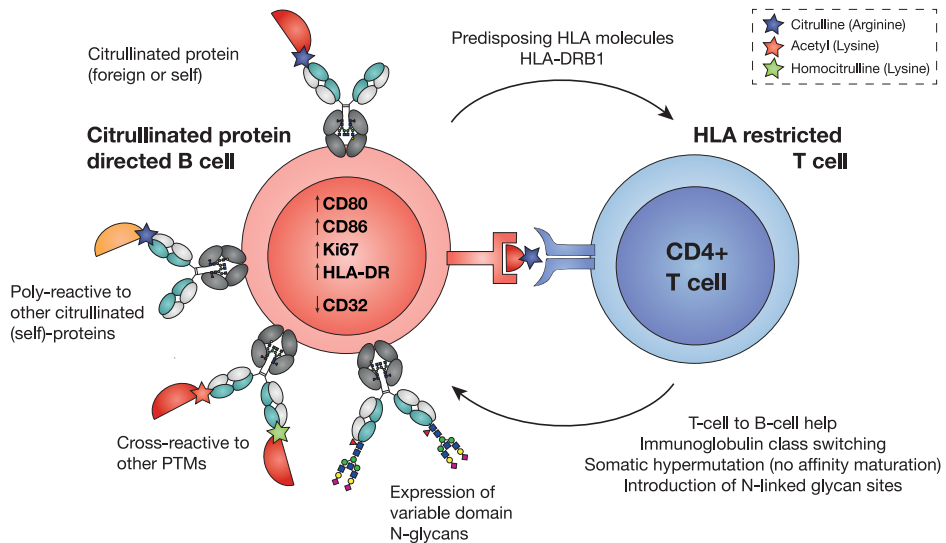


Figure 1. Schematic depiction of citrullinated protein (CP)-directed B cells. CP-directed IgG B-cell receptors (BCRs) interact with citrullinated proteins (foreign or self). CD4+ T cells recognize the citrullinated proteins presented by predisposing HLA molecules. T cells provide help to B cells followed by somatic hypermutation, which results in broadly poly- and cross-reactive BCRs and the introduction of N-linked variable domain glycans. The continuously activated CP-directed B cells depict an activated phenotype (increased expression of CD80, CD86 and Ki67, decreased expression of CD32).

Glycans are attached to proteins co- or post-translationally in the endoplasmic reticulum (ER) (Figure 2). In a first step, a precursor N-glycan consisting of two N-acetylglucosamines (GlcNAc), nine mannoses (Man) and three glucoses (Glc) is transferred from a dolichol anchor to the asparagine in the consensus sequence. The terminal Glc are then enzymatically removed. This functions as a folding-quality control mechanism and only after correct folding, the protein enters the Golgi. In the Golgi the Man residues are trimmed down to a structure containing two GlcNAcs and five Man. Later on, glycans can be extended with a GlcNAc resulting in a hybrid-type glycan. An ongoing interplay between glycosidases and glycosyltransferases shapes the formation of complex-type N-glycans and contributes to a plethora of N-glycan forms. They can be extended by GlcNAc branches (antennae), a bisecting GlcNAc (β 1,4), core and/or antennary fucoses (Fuc), antennary galactoses (Gal), N-acetylgalactosamines (GalNAc) and N-acetylneuraminic acids (Neu5Ac, α 2,6 in humans)⁴². Neu5Ac are large monosaccharides belonging to the group of sialic acids (Sia) and contain a carboxylic acid functional group⁴³. The final N-glycan composition is most likely influenced by the expression levels and localization of glycosyltransferases, glycan transporters, and glycosidases, the accessibility of the specific N-linked glycosylation sites and the immunological and metabolic state of the cell, which might influence the duration of the glycoproteins in the ER and the Golgi apparatus. Each individual glycan modification can have a substantial impact on the structure and function of the protein or its interactions with surrounding molecules⁴⁴.

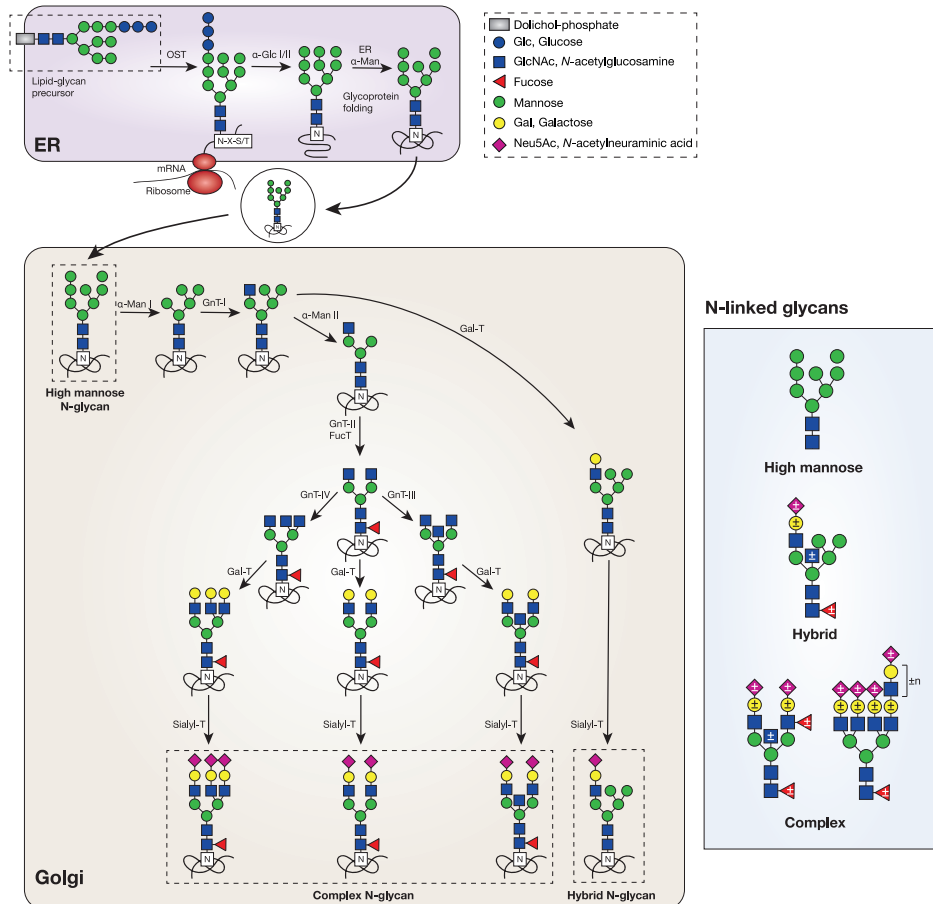


Figure 2. Biosynthesis of N-linked glycans. The biosynthesis of N-linked glycans is initiated in the endoplasmic reticulum (ER) by the transfer of a lipid/glycan precursor (dolichol phosphate bound glycan with $\text{Glc}_3\text{Man}_9\text{GlcNAc}_2$) to the nitrogen atom of an asparagine residue by the oligosaccharyltransferase (OST) enzyme. The glucose residues are trimmed down by two α -glucosidases (α -Glc I-II) and an initial mannose residue is removed by the α -mannosidase (ER α -Man). The correctly folded glycoprotein is transported via vesicles to the Golgi apparatus where the N-glycans are further trimmed by α -mannosidase I and II (α -Man I-II) and modified by glycosidases and transferases [GlcNAc-transferase I-IV (GnT-I-IV), Fucosyltransferase (FucT), β 1,4 galactosyltransferase (Gal-T), α 2,6 sialyltransferase (Sialyl-T)]. This results in the three most common types of N-glycan structures attached to human proteins: high mannose-, hybrid- and complex-type glycans (carrying optional core and antennary monosaccharide residues).

Glycosylation of immunoglobulin G

IgG is a highly abundant glycoprotein in human serum consisting of two heavy (H) and two light (L) chains both including constant (C_{H1} , C_{H2} , C_{H3} and C_L) and variable regions (V_H and V_L) (Figure 3). The fragment antigen-binding (Fab) moiety is formed by the C_L , C_{H1} , V_L and V_H and the fragment crystallizable (Fc) region consists of the C_{H2} and C_{H3} domains, which are linked by a flexible hinge region. Almost 100% of human IgG in the circulation contain a N-glycosylation consensus sequence (N297) in the C_{H2} domain of the Fc region (Figure 3)⁴⁵. Mainly complex-type and diantennary N-glycans are attached to the IgG Fc domain carrying a high amount of core fucosylation (~94%). IgG Fc N-glycans can carry a bisecting GlcNAc (~10%), present antennary galactoses (~67%) and terminal *N*-acetylneuraminic acids (~10%)^{46,47}. The conserved Fc glycans have been studied extensively and the glycosylation profile can vary with disease (e.g. Rheumatoid Arthritis), gender and age, particularly with respect to the level of galactosylation⁴⁸⁻⁵⁰. Fc glycans are essential for the structure and function of the Fc domain and already minor changes can alter the Fc conformation, change the interaction with Fc-gamma receptors (FcγRs) or the complement component C1q and thus modulate IgG effector functions⁵¹.

Additionally to the aforementioned conserved C_{H2} N-glycans, ~15-25% of IgG variable regions can carry N-glycosylation consensus sequences (Figure 3)^{47,52}. In comparison to Fc glycans, variable domain glycans (VDGs) depict higher levels of galactosylation (~94%), sialylation (~72%) and bisection (~45%), while fucosylation is reduced (~69%)^{47,53}. In addition low levels of high-mannose type structures have been described^{47,53}, depending on the consensus amino-acid motif or the location of the N-glycosylation sites⁵⁴. N-glycosylation sequences are mainly introduced into the variable domains following somatic hypermutation (SHM) during antigen-specific immune responses⁵⁵ and sequencing analyses of (auto)antibody repertoires revealed that this is likely a selective process. The naïve human B-cell antibody repertoire is almost devoid of such sites, with an exception of the IGHV1-8, IGHV4-34, IGHV5-10-1, IGLV3-12 and IGLV5-37 alleles⁵². The introduced VDG sites primarily emerge near antigen-binding regions in both H and L chains⁵⁶. IgG subclass analyses disclosed distinct VDG levels for different isotypes. Thus, lower levels were observed for IgG1 (12%), IgG2 (11%) and IgG3 (15%) as compared to IgG4 (44%)⁵⁶, which might be partially explained by their ability to Fab-arm exchange or by their slightly higher mutation rate as compared to other subclasses.

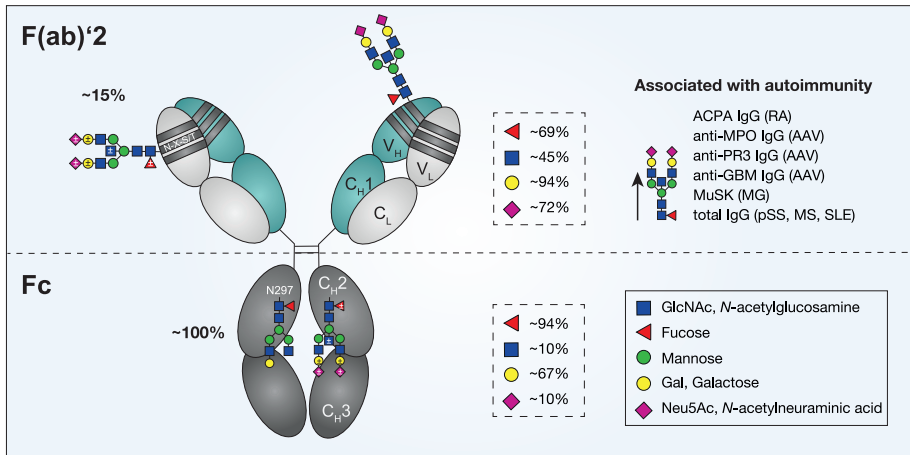


Figure 3. N-linked glycosylation of IgG. Schematic representation of an IgG molecule consisting of two heavy (H) and two light (L) chains both including constant (C_H1, C_H2, C_H3 and C_L) and variable domains (V_H and V_L). The fragment antigen-binding (Fab)² moiety is formed by the C_L, C_H1, V_L and V_H of both antibody chains linked by a flexible hinge region. The fragment crystallizable (Fc) region consists of the C_H2 and C_H3 domains. The Fc domain is ~100% N-glycosylated at N297 and the Fab domain is ~15% N-glycosylated at N-X-S/T consensus motifs in the hypervariable regions (variable domain glycans, VDGs). The percentage of fucosylation, bisection, galactosylation and sialylation of the Fc and Fab N-glycan is depicted. Variable domain glycosylation is increased on ACPA IgG from RA patients, anti-MPO/PR3 and GBM IgG from AAV patients and on total IgG from pSS, MS and SLE patients.

Variable domain glycosylation in disease

Notably, enhanced IgG variable domain glycosylation seems to be a common feature among autoimmune diseases. A hyperglycosylation of the variable domain has been shown for the RA-specific ACPA IgG, as evidenced by an increased molecular weight of the variable fragments and mass spectrometry³⁵. Sambucus nigra agglutinin (SNA)-binding studies revealed an increased binding, and thus most probably the presence of α 2,6-linked sialic acid containing VDGs, for anti-neutrophil cytoplasmic antibodies (ANCA) directed against myeloperoxidase (MPO) or proteinase 3 (PR3) and for anti-glomerular basement membrane (GBM) autoantibodies from ANCA-associated vasculitis (AAV)-patients as opposed to total IgG⁵⁷. These results have been confirmed by mass spectrometry studies of anti-MPO enriched IgG depicting disialylated and bisected glycan traits specific for the Fab domain of antibodies⁵⁸. Additionally, primary sjorgen's syndrome (pSS), multiple sclerosis (MS) and systemic lupus erythematosus (SLE) patients show a higher degree of IgG sequences with N-linked glycan sites compared to healthy donors^{59,60}. Recently, N-linked glycosylation motifs were also found to be present in the variable domains of monoclonal muscle-specific kinase (MuSK) autoantibodies suggesting a potential role for the autoimmune disease myasthenia gravis (MG)^{61,62}. Interestingly, also inflammation-associated

antibodies, such as anti-hinge antibodies (AHAs), revealed an increased variable domain glycosylation of 53% as determined by SNA-chromatography⁵⁶. Also anti-drug antibodies that emerge in patients treated with adalimumab or infliximab depict increased VDG levels suggesting that the introduction of N-glycans into the immunoglobulin variable domain is triggered by a chronic and systemic antigen exposure⁵⁶. Intriguingly, an abundant amount of N-linked glycosylation sites in the variable domain of immunoglobulins has not only been observed for several autoimmune diseases, but also for patients with follicular lymphoma, especially with diffuse large B-cell lymphoma and Burkitt's lymphoma, suggesting a key role in lymphomagenesis⁶³.

Despite all these observations, little is known about the functional role of glycans attached to the hypervariable region of (surface) immunoglobulins, most likely due to their high heterogeneity in terms of distribution, frequency and glycan composition. Also, it remains unclear why and how chronic antigen exposure facilitates the accumulation of N-glycosylation sites in BCR V-regions.

Variable domain glycosylation of ACPA IgG

ACPA IgG depict a characteristic high expression of VDGs. N-glycans were found in the variable domain on more than 90% of ACPA IgG^{35,36} and autoantibodies isolated from the site of inflammation, the synovial fluid, presented even over 100% of VDGs, implying that multiple glycans are attached to the variable region of one ACPA molecule³⁶. The underlying N-linked glycosylation sites are selectively and abundantly introduced into the ACPA IgG hypervariable regions following somatic hypermutation (SHM) and no sites were found to be present in the hypervariable regions of ACPA IgM or germline encoded sequences^{64,65}. Structural analysis revealed that ACPA IgG VDGs carry a high amount of bisection, galactosylation and terminal sialic acids³⁶. Intriguingly, recent studies show that the abundant presence of VDGs on ACPA IgG in healthy first nation Canadian individuals is a strong predictor for progression towards RA⁶⁶. As VDGs are selectively introduced, present in the vast majority of ACPA IgG molecules and predictive for disease development, it is tempting to speculate that their expression provides a selective advantage for ACPA-expressing B cells allowing them to persist for several years. The glycosylation of the hypervariable regions might provide an additional pathway for the autoreactive B cells to regulate tolerance. However, further investigations are needed to unveil the first occurrence of these glycans and to understand the biological impact of VDGs for ACPA-expressing B cells.

Influence of variable domain glycosylation on IgG structure and function

Although glycosylation is a well-known post-translational modification able to modulate the structure and function of proteins and thus to affect humoral responses, little is known about the functional impact of sugar moieties attached to the variable domains of (surface) immunoglobulins. Interestingly, more and more studies suggest that VDGs might be involved in the pathophysiology of certain autoimmune diseases and can have immunomodulatory effects. As mentioned above, N-glycosylation consensus sequences in the variable domain occur mainly near antigen-binding regions and VDGs thus potentially influence the affinity/ avidity for antigens. Indeed, previous studies have shown differential impacts of VDGs on antigen binding. Dependent on the amount and the location of the N-linked glycosylation sites⁵⁶, VDGs can increase⁶⁷⁻⁶⁹ or decrease^{69,70} binding to their cognate antigens and thus modulate the specificity of an antibody. For example, it has been hypothesized that VDGs allow BCRs to move away from auto-reactivity, while cross-reactivity to foreign-antigens can be retained⁷¹. Furthermore, VDGs, especially their composition, can have a modulatory impact on the half-life of immunoglobulins^{69,72}. In the absence of terminal sialic acid residues, asialoglycoprotein receptors presented on liver cells can interact with terminal galactoses or *N*-acetylgalactosamine residues, expressed on the variable domain of the immunoglobulins, leading to a shortened half-life⁷³. In addition high-mannose structures, that can be attached to N-glycan sites in the variable domain, are more easily cleared by mannose receptors⁷⁴. Further VDGs, without the need of terminal sialic acids, can improve antibody thermostability, possibly by shielding hydrophobic residues⁷⁵. Depending on their location and charge, VDGs could also potentially alter binding to Fc gamma receptors (FcγR), including the neonatal FcR (FcRn), thereby affecting the serum half-life of IgG. In addition to an effect on FcγRs, VDGs may also affect the propensity of immunoglobulins to form immune complexes/ aggregates⁷⁶, potentially affecting complement activation, another IgG effector mechanism. A further important functionality reported for VDGs, and glycans in general, is the interaction with glycan-binding proteins termed lectins. It has been suggested that a variable domain glycosylation of BCRs allows interactions with lectins in vicinity to the BCR (in *cis*) or on neighboring cells (in *trans*), which will provide the B cell with survival signals^{56,71,77-79}. This has for example been proposed for follicular lymphoma cells, where the interaction between mannosylated VDGs and lectins free these cells from the dependence on antigen and enhance their survival through selection based on glycan interactions^{63,80,81}.

Nonetheless, despite these possible roles assigned to VDGs on BCRs, the function or consequences of VDGs on ACPA and/or CP-directed BCRs is unknown. Given the abundant presence of these glycans on ACPA, additional insight into the role of VDGs on the biology of the ACPA response will likely yield relevant information on the emergence of this highly specific autoantibody-response hallmarking RA.

Scope of this thesis

The aim of the studies described in this thesis is to better understand the concurrent presence of the different anti-modified protein antibody responses in RA and to obtain functional insights into the role of VDGs on the biology of autoreactive B cells and the autoantibodies they produce. More specifically, the studies not only aim to illustrate the cross-reactive nature of autoreactive B cells in RA or the occurrence of VDGs across different disease stages, they also intend to gain understanding how both characteristics are potentially involved in the breach of B-cell tolerance.

In **Chapter 2** several mechanism on how human autoreactive B cells might overcome peripheral B-cell “tolerance” checkpoints are reviewed. We highlight the autoimmune disease RA and elaborate on how RA-specific autoreactive B cells, expressing ACPAs, might bypass these B-cell checkpoints. We specifically focus on the cross-reactivity of these B cells and on the abundant expression of VDGs on their (surface) immunoglobulins.

The high cross-reactive nature of RA-specific antibodies is illustrated in **Chapter 3**. This chapter describes the cross-reactivity of ACPAs on the monoclonal level and on the level of CP-directed B-cell responses. The reactivity of monoclonal ACPAs to antigens carrying distinct PTMs, such as citrullination, homcitrullination (carbamylation) or acetylation, is assessed and the joined term of anti-modified protein antibodies (AMPAs) introduced. Furthermore, the chapter illustrates the activation potential of CP-directed B cells after the exposure to different PTMs, which is highly relevant to further the understanding of the “evolution” of the autoimmune responses in RA.

The possible role of VDGs in the development of RA is reiterated in **Chapter 4**. This chapter describes the emergence of VDGs on ACPA IgG in the phase before the onset of clinical symptoms. Associations between ACPA carrying VDGs and the most prominent genetic risk factor predisposing to RA, the HLA-SE alleles, are assessed. **Chapter 5** presents additional in depth studies on the association between the HLA-SE risk alleles and ACPA IgG harboring VDGs in the phase prior to the onset of RA in three distinct cohorts. It further highlights that the HLA-SE alleles primarily associate with the highly sialylated VDGs on ACPA IgG and not with ACPA as such.

The emergence and abundance of ACPA IgG VDGs across several clinical stages of RA is illustrated in **Chapter 6**. Dynamic changes of VDGs across different disease stages are analyzed in a large data set of 1500 samples. ACPA IgG glycan profiles of 7 different cohorts including ACPA-positive healthy individuals, pre-symptomatic individuals, individuals with arthralgia, patients at the onset of RA and RA patients 4,8 and 12 months after disease-onset and treatment are assessed. Additionally, ACPA IgG VDG profiles of individuals in whom long-term drug-free remission is achieved are illustrated.

After analyzing the emergence of VDGs on ACPA IgG in the studies presented in the aforementioned chapters, **Chapter 7** focuses on the biological consequences of VDGs for autoreactive B cells and their secreted antibodies. In particular, this chapter deals with the impact of ACPA IgG VDGs on citrullinated (auto)antigen binding assessed amongst others by crystallography and antigen-binding studies. Furthermore, we studied the impact of highly sialylated VDGs on B-cell activation and BCR downmodulation to dissect the key characteristics of VDGs on human autoreactive B cells.

Chapter 8 focuses on the biological impact of VDGs on an important effector function of IgG, the activation of the complement system. Monoclonal antibodies expressing identical Fc-glycan profiles, but various amounts of N-linked glycans in their variable domains, were used to identify VDG-specific effects on complement activation.

Finally, the work described in this thesis comes together in **Chapter 9**, the general discussion, with a specific focus on the involvement of VDGs in the breach of tolerance of autoreactive B cells in RA.

References

- 1 Aletaha, D., Neogi, T., Silman, A. J., Funovits, J., Felson, D. T., Bingham, C. O., 3rd, et al., 2010 rheumatoid arthritis classification criteria: an American College of Rheumatology/European League Against Rheumatism collaborative initiative. *Ann Rheum Dis* 2010. 69: 1580-1588.
- 2 Edwards, J. C. and Cambridge, G., Prospects for B-cell-targeted therapy in autoimmune disease. *Rheumatology (Oxford)* 2005. 44: 151-156.
- 3 Edwards, J. C. W., Szczepański, L., Szechiński, J., Filipowicz-Sosnowska, A., Emery, P., Close, D. R., et al., Efficacy of B-Cell-Targeted Therapy with Rituximab in Patients with Rheumatoid Arthritis. *New England Journal of Medicine* 2004. 350: 2572-2581.
- 4 Nienhuis, R. L. and Mandema, E., A New Serum Factor in Patients with Rheumatoid Arthritis; the Antiperinuclear Factor. *Ann Rheum Dis* 1964. 23: 302-305.
- 5 Vossenaar, E. R., Zendman, A. J., van Venrooij, W. J. and Pruijn, G. J., PAD, a growing family of citrullinating enzymes: genes, features and involvement in disease. *Bioessays* 2003. 25: 1106-1118.
- 6 Schellekens, G. A., de Jong, B. A., van den Hoogen, F. H., van de Putte, L. B. and van Venrooij, W. J., Citrulline is an essential constituent of antigenic determinants recognized by rheumatoid arthritis-specific autoantibodies. *J Clin Invest* 1998. 101: 273-281.
- 7 Rantapää-Dahlqvist, S., de Jong, B. A., Berglin, E., Hallmans, G., Wadell, G., Stenlund, H., et al., Antibodies against cyclic citrullinated peptide and IgA rheumatoid factor predict the development of rheumatoid arthritis. *Arthritis Rheum* 2003. 48: 2741-2749.
- 8 van der Kooij, S. M., Goekoop-Ruiterman, Y. P., de Vries-Bouwstra, J. K., Guler-Yuksel, M., Zwinderman, A. H., Kerstens, P. J., et al., Drug-free remission, functioning and radiographic damage after 4 years of response-driven treatment in patients with recent-onset rheumatoid arthritis. *Ann Rheum Dis* 2009. 68: 914-921.
- 9 Willemze, A., Trouw, L. A., Toes, R. E. and Huizinga, T. W., The influence of ACPA status and characteristics on the course of RA. *Nat Rev Rheumatol* 2012. 8: 144-152.
- 10 Takizawa, Y., Suzuki, A., Sawada, T., Ohsaka, M., Inoue, T., Yamada, R., et al., Citrullinated fibrinogen detected as a soluble citrullinated autoantigen in rheumatoid arthritis synovial fluids. *Ann Rheum Dis* 2006. 65: 1013-1020.
- 11 Burkhardt, H., Koller, T., Engstrom, A., Nandakumar, K. S., Turnay, J., Kraetsch, H. G., et al., Epitope-specific recognition of type II collagen by rheumatoid arthritis antibodies is shared with recognition by antibodies that are arthritogenic in collagen-induced arthritis in the mouse. *Arthritis Rheum* 2002. 46: 2339-2348.
- 12 Vossenaar, E. R., Despres, N., Lapointe, E., van der Heijden, A., Lora, M., Senshu, T., et al., Rheumatoid arthritis specific anti-Sa antibodies target citrullinated vimentin. *Arthritis Res Ther* 2004. 6: R142-150.
- 13 Lundberg, K., Kinloch, A., Fisher, B. A., Wegner, N., Wait, R., Charles, P., et al., Antibodies to citrullinated alpha-enolase peptide 1 are specific for rheumatoid arthritis and cross-react with bacterial enolase. *Arthritis Rheum* 2008. 58: 3009-3019.
- 14 Ioan-Facsinay, A., el-Bannoudi, H., Scherer, H. U., van der Woude, D., Menard, H. A., Lora, M., et al., Anti-cyclic citrullinated peptide antibodies are a collection of anti-citrullinated protein antibodies and contain overlapping and non-overlapping reactivities. *Ann Rheum Dis* 2011. 70: 188-193.
- 15 Trouw, L. A., Rispens, T. and Toes, R. E. M., Beyond citrullination: other post-translational protein modifications in rheumatoid arthritis. *Nat Rev Rheumatol* 2017. 13: 331-339.
- 16 Juarez, M., Bang, H., Hammar, F., Reimer, U., Dyke, B., Sahbudin, I., et al., Identification of novel antiacetylated vimentin antibodies in patients with early inflammatory arthritis. *Ann Rheum Dis* 2016. 75: 1099-1107.
- 17 Shi, J., Knevel, R., Suwannalai, P., van der Linden, M. P., Janssen, G. M., van Veelen, P. A., et al., Autoantibodies recognizing carbamylated proteins are present in sera of patients with rheumatoid arthritis and predict joint damage. *Proc Natl Acad Sci U S A* 2011. 108: 17372-17377.

- 18 Lloyd, K. A., Wigerblad, G., Sahlstrom, P., Garimella, M. G., Chemin, K., Steen, J., et al., Differential ACPA Binding to Nuclear Antigens Reveals a PAD-Independent Pathway and a Distinct Subset of Acetylation Cross-Reactive Autoantibodies in Rheumatoid Arthritis. *Front Immunol* 2018. 9: 3033.
- 19 Reed, E., Jiang, X., Kharlamova, N., Ytterberg, A. J., Catrina, A. I., Israelsson, L., et al., Antibodies to carbamylated alpha-enolase epitopes in rheumatoid arthritis also bind citrullinated epitopes and are largely indistinct from anti-citrullinated protein antibodies. *Arthritis Res Ther* 2016. 18: 96.
- 20 Kampstra, A. S. B., Dekkers, J. S., Volkov, M., Dorjee, A. L., Hafkenscheid, L., Kempers, A. C., et al., Different classes of anti-modified protein antibodies are induced on exposure to antigens expressing only one type of modification. *Ann Rheum Dis* 2019. 78: 908-916.
- 21 Steen, J., Forsstrom, B., Sahlstrom, P., Odowd, V., Israelsson, L., Krishnamurthy, A., et al., Recognition of Amino Acid Motifs, Rather Than Specific Proteins, by Human Plasma Cell-Derived Monoclonal Antibodies to Posttranslationally Modified Proteins in Rheumatoid Arthritis. *Arthritis Rheumatol* 2019. 71: 196-209.
- 22 Sjoberg, A. P., Trouw, L. A. and Blom, A. M., Complement activation and inhibition: a delicate balance. *Trends Immunol* 2009. 30: 83-90.
- 23 Trouw, L. A., Haisma, E. M., Levarht, E. W., van der Woude, D., Ioan-Facsinay, A., Daha, M. R., et al., Anti-cyclic citrullinated peptide antibodies from rheumatoid arthritis patients activate complement via both the classical and alternative pathways. *Arthritis Rheum* 2009. 60: 1923-1931.
- 24 Kerkman, P. F., Fabre, E., van der Voort, E. I., Zaldumbide, A., Rombouts, Y., Rispen, T., et al., Identification and characterisation of citrullinated antigen-specific B cells in peripheral blood of patients with rheumatoid arthritis. *Ann Rheum Dis* 2016. 75: 1170-1176.
- 25 Kerkman, P. F., Kempers, A. C., van der Voort, E. I., van Oosterhout, M., Huizinga, T. W., Toes, R. E., et al., Synovial fluid mononuclear cells provide an environment for long-term survival of antibody-secreting cells and promote the spontaneous production of anti-citrullinated protein antibodies. *Ann Rheum Dis* 2016. 75: 2201-2207.
- 26 Kristyanto, H., Blomberg, N. J., Slot, L. M., van der Voort, E. I. H., Kerkman, P. F., Bakker, A., et al., Persistently activated, proliferative memory autoreactive B cells promote inflammation in rheumatoid arthritis. *Sci Transl Med* 2020. 12.
- 27 Bos, W. H., Bartelds, G. M., Wolbink, G. J., de Koning, M. H., van de Stadt, R. J., van Schaardenburg, D., et al., Differential response of the rheumatoid factor and anticitrullinated protein antibodies during adalimumab treatment in patients with rheumatoid arthritis. *J Rheumatol* 2008. 35: 1972-1977.
- 28 Corsiero, E., Bombardieri, M., Carlotti, E., Pratesi, F., Robinson, W., Migliorini, P., et al., Single cell cloning and recombinant monoclonal antibodies generation from RA synovial B cells reveal frequent targeting of citrullinated histones of NETs. *Ann Rheum Dis* 2016. 75: 1866-1875.
- 29 Suwannalai, P., Scherer, H. U., van der Woude, D., Ioan-Facsinay, A., Jol-van der Zijde, C. M., van Tol, M. J., et al., Anti-citrullinated protein antibodies have a low avidity compared with antibodies against recall antigens. *Ann Rheum Dis* 2011. 70: 373-379.
- 30 Gregersen, P. K., Silver, J. and Winchester, R. J., The shared epitope hypothesis. An approach to understanding the molecular genetics of susceptibility to rheumatoid arthritis. *Arthritis Rheum* 1987. 30: 1205-1213.
- 31 Koning, F., Thomas, R., Rossjohn, J. and Toes, R. E., Coeliac disease and rheumatoid arthritis: similar mechanisms, different antigens. *Nat Rev Rheumatol* 2015. 11: 450-461.
- 32 Huizinga, T. W., Amos, C. I., van der Helm-van Mil, A. H., Chen, W., van Gaalen, F. A., Jawaheer, D., et al., Refining the complex rheumatoid arthritis phenotype based on specificity of the HLA-DRB1 shared epitope for antibodies to citrullinated proteins. *Arthritis Rheum* 2005. 52: 3433-3438.
- 33 Hensvold, A. H., Magnusson, P. K., Joshua, V., Hansson, M., Israelsson, L., Ferreira, R., et al., Environmental and genetic factors in the development of anticitrullinated protein antibodies (ACPAs) and ACPA-positive rheumatoid arthritis: an epidemiological investigation in twins. *Ann Rheum Dis* 2015. 74: 375-380.

- 34 Terao, C., Ohmura, K., Ikari, K., Kawaguchi, T., Takahashi, M., Setoh, K., et al., Effects of smoking and shared epitope on the production of anti-citrullinated peptide antibody in a Japanese adult population. *Arthritis Care Res (Hoboken)* 2014. 66: 1818-1827.
- 35 Rombouts, Y., Willemze, A., van Beers, J. J., Shi, J., Kerkman, P. F., van Toorn, L., et al., Extensive glycosylation of ACPA-IgG variable domains modulates binding to citrullinated antigens in rheumatoid arthritis. *Ann Rheum Dis* 2016. 75: 578-585.
- 36 Hafkenscheid, L., Bondt, A., Scherer, H. U., Huizinga, T. W., Wuhrer, M., Toes, R. E., et al., Structural Analysis of Variable Domain Glycosylation of Anti-Citrullinated Protein Antibodies in Rheumatoid Arthritis Reveals the Presence of Highly Sialylated Glycans. *Mol Cell Proteomics* 2017. 16: 278-287.
- 37 Marshall, R. D., Glycoproteins. *Annu Rev Biochem* 1972. 41: 673-702.
- 38 Zielinska, D. F., Gnad, F., Wisniewski, J. R. and Mann, M., Precision mapping of an in vivo N-glycoproteome reveals rigid topological and sequence constraints. *Cell* 2010. 141: 897-907.
- 39 Bause, E. and Legler, G., The role of the hydroxy amino acid in the triplet sequence Asn-Xaa-Thr(Ser) for the N-glycosylation step during glycoprotein biosynthesis. *Biochem J* 1981. 195: 639-644.
- 40 Valliere-Douglass, J. F., Eakin, C. M., Wallace, A., Ketchem, R. R., Wang, W., Treuheit, M. J., et al., Glutamine-linked and non-consensus asparagine-linked oligosaccharides present in human recombinant antibodies define novel protein glycosylation motifs. *J Biol Chem* 2010. 285: 16012-16022.
- 41 Valliere-Douglass, J. F., Kodama, P., Mujacic, M., Brady, L. J., Wang, W., Wallace, A., et al., Asparagine-linked oligosaccharides present on a non-consensus amino acid sequence in the CH1 domain of human antibodies. *J Biol Chem* 2009. 284: 32493-32506.
- 42 Kornfeld, R. and Kornfeld, S., Assembly of asparagine-linked oligosaccharides. *Annu Rev Biochem* 1985. 54: 631-664.
- 43 Schauer, R. and Kamerling, J. P., Exploration of the Sialic Acid World. *Adv Carbohydr Chem Biochem* 2018. 75: 1-213.
- 44 Lis, H. and Sharon, N., Protein glycosylation. Structural and functional aspects. *Eur J Biochem* 1993. 218: 1-27.
- 45 Stavenhagen, K., Plomp, R. and Wuhrer, M., Site-Specific Protein N- and O-Glycosylation Analysis by a C18-Porous Graphitized Carbon-Liquid Chromatography-Electrospray Ionization Mass Spectrometry Approach Using Pronase Treated Glycopeptides. *Anal Chem* 2015. 87: 11691-11699.
- 46 Bakovic, M. P., Selman, M. H., Hoffmann, M., Rudan, I., Campbell, H., Deelder, A. M., et al., High-throughput IgG Fc N-glycosylation profiling by mass spectrometry of glycopeptides. *J Proteome Res* 2013. 12: 821-831.
- 47 Bondt, A., Rombouts, Y., Selman, M. H., Hensbergen, P. J., Reiding, K. R., Hazes, J. M., et al., Immunoglobulin G (IgG) Fab glycosylation analysis using a new mass spectrometric high-throughput profiling method reveals pregnancy-associated changes. *Mol Cell Proteomics* 2014. 13: 3029-3039.
- 48 Yamada, E., Tsukamoto, Y., Sasaki, R., Yagyu, K. and Takahashi, N., Structural changes of immunoglobulin G oligosaccharides with age in healthy human serum. *Glycoconj J* 1997. 14: 401-405.
- 49 Parekh, R., Roitt, I., Isenberg, D., Dwek, R. and Rademacher, T., Age-related galactosylation of the N-linked oligosaccharides of human serum IgG. *J Exp Med* 1988. 167: 1731-1736.
- 50 Parekh, R. B., Dwek, R. A., Sutton, B. J., Fernandes, D. L., Leung, A., Stanworth, D., et al., Association of rheumatoid arthritis and primary osteoarthritis with changes in the glycosylation pattern of total serum IgG. *Nature* 1985. 316: 452-457.
- 51 Dekkers, G., Treffers, L., Plomp, R., Bentlage, A. E. H., de Boer, M., Koeleman, C. A. M., et al., Decoding the Human Immunoglobulin G-Glycan Repertoire Reveals a Spectrum of Fc-Receptor- and Complement-Mediated-Effector Activities. *Front Immunol* 2017. 8: 877.
- 52 van de Bovenkamp, F. S., Hafkenscheid, L., Rispens, T. and Rombouts, Y., The Emerging Importance of IgG Fab Glycosylation in Immunity. *J Immunol* 2016. 196: 1435-1441.

- 53 Anumula, K. R., Quantitative glycan profiling of normal human plasma derived immunoglobulin and its fragments Fab and Fc. *J Immunol Methods* 2012. 382: 167-176.
- 54 Endo, T., Wright, A., Morrison, S. L. and Kobata, A., Glycosylation of the variable region of immunoglobulin G--site specific maturation of the sugar chains. *Mol Immunol* 1995. 32: 931-940.
- 55 Dunn-Walters, D., Boursier, L. and Spencer, J., Effect of somatic hypermutation on potential N-glycosylation sites in human immunoglobulin heavy chain variable regions. *Mol Immunol* 2000. 37: 107-113.
- 56 van de Bovenkamp, F. S., Derksen, N. I. L., Ooijevaar-de Heer, P., van Schie, K. A., Kruithof, S., Berkowska, M. A., et al., Adaptive antibody diversification through N-linked glycosylation of the immunoglobulin variable region. *Proc Natl Acad Sci U S A* 2018. 115: 1901-1906.
- 57 Xu, P. C., Gou, S. J., Yang, X. W., Cui, Z., Jia, X. Y., Chen, M., et al., Influence of variable domain glycosylation on anti-neutrophil cytoplasmic autoantibodies and anti-glomerular basement membrane autoantibodies. *BMC Immunol* 2012. 13: 10.
- 58 Lardinois, O. M., Deterding, L. J., Hess, J. J., Poulton, C. J., Henderson, C. D., Jennette, J. C., et al., Immunoglobulins G from patients with ANCA-associated vasculitis are atypically glycosylated in both the Fc and Fab regions and the relation to disease activity. *PLoS One* 2019. 14: e0213215.
- 59 Hamza, N., Hershberg, U., Kallenberg, C. G., Vissink, A., Spijkervet, F. K., Bootsma, H., et al., Ig gene analysis reveals altered selective pressures on Ig-producing cells in parotid glands of primary Sjogren's syndrome patients. *J Immunol* 2015. 194: 514-521.
- 60 Visser, A., Hamza, N., Kroese, F. G. M. and Bos, N. A., Acquiring new N-glycosylation sites in variable regions of immunoglobulin genes by somatic hypermutation is a common feature of autoimmune diseases. *Ann Rheum Dis* 2018. 77: e69.
- 61 Huijbers, M. G., Vergoossen, D. L., Fillie-Grijpma, Y. E., van Es, I. E., Koning, M. T., Slot, L. M., et al., MuSK myasthenia gravis monoclonal antibodies: Valency dictates pathogenicity. *Neurol Neuroimmunol Neuroinflamm* 2019. 6: e547.
- 62 Mandel-Brehm, C., Fichtner, M. L., Jiang, R., Winton, V. J., Vazquez, S. E., Pham, M. C., et al., Elevated N-Linked Glycosylation of IgG V Regions in Myasthenia Gravis Disease Subtypes. *J Immunol* 2021. 207: 2005-2014.
- 63 Zhu, D., McCarthy, H., Ottensmeier, C. H., Johnson, P., Hamblin, T. J. and Stevenson, F. K., Acquisition of potential N-glycosylation sites in the immunoglobulin variable region by somatic mutation is a distinctive feature of follicular lymphoma. *Blood* 2002. 99: 2562-2568.
- 64 Vergroesen, R. D., Slot, L. M., Hafkenscheid, L., Koning, M. T., van der Voort, E. I. H., Grooff, C. A., et al., B-cell receptor sequencing of anti-citrullinated protein antibody (ACPA) IgG-expressing B cells indicates a selective advantage for the introduction of N-glycosylation sites during somatic hypermutation. *Ann Rheum Dis* 2018. 77: 956-958.
- 65 Vergroesen, R. D., Slot, L. M., van Schaik, B. D. C., Koning, M. T., Rispens, T., van Kampen, A. H. C., et al., N-Glycosylation Site Analysis of Citrullinated Antigen-Specific B-Cell Receptors Indicates Alternative Selection Pathways During Autoreactive B-Cell Development. *Front Immunol* 2019. 10: 2092.
- 66 Hafkenscheid, L., de Moel, E., Smolik, I., Tanner, S., Meng, X., Jansen, B. C., et al., N-Linked Glycans in the Variable Domain of IgG Anti-Citrullinated Protein Antibodies Predict the Development of Rheumatoid Arthritis. *Arthritis Rheumatol* 2019. 71: 1626-1633.
- 67 Leibiger, H., Wustner, D., Stigler, R. D. and Marx, U., Variable domain-linked oligosaccharides of a human monoclonal IgG: structure and influence on antigen binding. *Biochem J* 1999. 338 (Pt 2): 529-538.
- 68 Tachibana, H., Kim, J. Y. and Shirahata, S., Building high affinity human antibodies by altering the glycosylation on the light chain variable region in N-acetylglucosamine-supplemented hybridoma cultures. *Cytotechnology* 1997. 23: 151-159.
- 69 Coloma, M. J., Trinh, R. K., Martinez, A. R. and Morrison, S. L., Position effects of variable region carbohydrate on the affinity and in vivo behavior of an anti-(1-->6) dextran antibody. *J Immunol* 1999. 162: 2162-2170.

- 70 Schneider, D., Duhren-von Minden, M., Alkhatib, A., Setz, C., van Bergen, C. A., Benkisser-Petersen, M., et al., Lectins from opportunistic bacteria interact with acquired variable-region glycans of surface immunoglobulin in follicular lymphoma. *Blood* 2015. 125: 3287-3296.
- 71 Sabouri, Z., Schofield, P., Horikawa, K., Spierings, E., Kipling, D., Randall, K. L., et al., Redemption of autoantibodies on anergic B cells by variable-region glycosylation and mutation away from self-reactivity. *Proc Natl Acad Sci U S A* 2014. 111: E2567-2575.
- 72 Steffen Goletz, A. D., Lars Stoeckl, Fab-glycosylated antibodies <https://patentimages.storage.googleapis.com/f9/58/85/7f5bcf1970d486/WO2012020065A1.pdf> 2012.
- 73 Morell, A. G., Gregoriadis, G., Scheinberg, I. H., Hickman, J. and Ashwell, G., The role of sialic acid in determining the survival of glycoproteins in the circulation. *J Biol Chem* 1971. 246: 1461-1467.
- 74 Alessandri, L., Ouellette, D., Acquah, A., Rieser, M., Leblond, D., Saltarelli, M., et al., Increased serum clearance of oligomannose species present on a human IgG1 molecule. *MAbs* 2012. 4: 509-520.
- 75 van de Bovenkamp, F. S., Derksen, N. I. L., van Breemen, M. J., de Taeye, S. W., Ooijevaar-de Heer, P., Sanders, R. W., et al., Variable Domain N-Linked Glycans Acquired During Antigen-Specific Immune Responses Can Contribute to Immunoglobulin G Antibody Stability. *Front Immunol* 2018. 9: 740.
- 76 Courtois, F., Agrawal, N. J., Lauer, T. M. and Trout, B. L., Rational design of therapeutic mAbs against aggregation through protein engineering and incorporation of glycosylation motifs applied to bevacizumab. *MAbs* 2016. 8: 99-112.
- 77 Radcliffe, C. M., Arnold, J. N., Suter, D. M., Wormald, M. R., Harvey, D. J., Royle, L., et al., Human Follicular Lymphoma Cells Contain Oligomannose Glycans in the Antigen-binding Site of the B-cell Receptor. *Journal of Biological Chemistry* 2007. 282: 7405-7415.
- 78 Zhu, D., McCarthy, H., Ottensmeier, C. H., Johnson, P., Hamblin, T. J. and Stevenson, F. K., Acquisition of potential N-glycosylation sites in the immunoglobulin variable region by somatic mutation is a distinctive feature of follicular lymphoma. *Blood* 2002. 99: 2562-2568.
- 79 Vletter, E. M., Koning, M. T., Scherer, H. U., Veelken, H. and Toes, R. E. M., A Comparison of Immunoglobulin Variable Region N-Linked Glycosylation in Healthy Donors, Autoimmune Disease and Lymphoma. *Frontiers in Immunology* 2020. 11.
- 80 Linley, A., Krysov, S., Ponzoni, M., Johnson, P. W., Packham, G. and Stevenson, F. K., Lectin binding to surface Ig variable regions provides a universal persistent activating signal for follicular lymphoma cells. *Blood* 2015. 126: 1902-1910.
- 81 Coelho, V., Krysov, S., Ghaemmaghami, A. M., Emara, M., Potter, K. N., Johnson, P., et al., Glycosylation of surface Ig creates a functional bridge between human follicular lymphoma and microenvironmental lectins. *Proc Natl Acad Sci U S A* 2010. 107: 18587-18592.



REVIEW

Checkpoints controlling the induction of B cell-mediated autoimmunity in human autoimmune diseases

Sanne Reijm[†], Theresa Kissel[†], René E.M. Toes[†]

[†] These authors contributed equally to this work as co-first authors.

Abstract

B-cell targeting therapies are effective in various autoimmune diseases, amongst others Rheumatoid Arthritis, Pemphigus Vulgaris and Systemic Lupus Erythematosus. Given these successes, it is evident that B cells are central orchestrators in the processes leading to the signs and symptoms hallmarking many human autoimmune diseases. The pathways provoking the generation of such autoreactive B cells or mechanisms preventing their induction in health are, however, poorly explored. Nevertheless, such information is crucial for the development of preventative/curative interventions aiming to permanently deplete- or prohibit the emergence of autoreactive B cells. Hence, this review will focus on how B-cell tolerance might be breached, and which checkpoints are at play preventing the arousal of autoreactive B cells in human. Especially antigen presentation by follicular dendritic cells, somatic hypermutation and cross-reactivity to the microbiome/environment could operate as actors playing pivotal roles in the induction of B cell-mediated humoral autoimmunity. Moreover, we highlight the human autoimmune disease Rheumatoid Arthritis as a prototype where autoreactive B cells combine several mechanisms to overcome peripheral B-cell checkpoints.

Introduction

Clear evidence for a key role of B cells in human autoimmune diseases, such as Rheumatoid Arthritis (RA), Pemphigus Vulgaris (PV), Systemic Lupus Erythematosus (SLE), Myasthenia Graves or Anti-Neutrophil Cytoplasmic Antibody-Associated Vasculitis (AAV), is provided by the efficacy of B-cell targeted therapies in these diseases¹⁻⁴. B cells might contribute in several ways to these disorders, including the production of pathogenic autoantibodies, the generation of inflammatory cytokines and the presentation of antigens to T cells combined with their excellent ability to activate these cells. The different B-cell functions in human autoimmune diseases have been extensively reviewed and will not be discussed in this review^{5,6}.

During B-cell development in the bone marrow (BM), B cells start to express B-cell receptors (BCRs) with diverse antigen-binding sites, created through a random combination of variable (V), joining (J) and diversity (D) gene segments⁷. This junctional diversity during V(D)J-recombination is further increased by the introduction of palindromic- and non-templated nucleotides^{8,9}. Additionally, the association between heavy- and light chain creates further diversity in the BCR variable domains. Collectively these processes generate highly diverse BCR repertoires and B-cell populations able to recognize many different structures and molecules in a highly specific manner, including self-molecules expressed by healthy human tissues. It is estimated that approximately 50-75% of immature BM B cells carry self-reactive BCRs in both mice and humans¹⁰⁻¹². A significant proportion of these B cells will undergo receptor-editing or clonal deletion both leading to the removal of self-reactivity as experimentally evidenced within Ig transgenic mouse models¹³. During receptor-editing, autoreactive B cells against multivalent antigens will change their light chain to prevent autoreactivity. If this mechanism fails or if the B cell shows a high affinity to self-antigens, it will most likely undergo clonal deletion. These negative selection processes are responsible for central B-cell tolerance and ensure that most B cells leaving the BM do not recognize self. However, as central B-cell tolerance is incomplete, self-reactive B cells will escape into the periphery. To further hinder the emergence of autoreactive B-cell responses, several complementary peripheral tolerance mechanisms and B-cell activation checkpoints are in place to prevent the induction of humoral autoimmunity. Immature self-reactive B cells coming from the BM are, for example, competing with other B cells to enter primary follicles and exclusion will result in cell death within 1-3 days. This follicular exclusion of (auto)antigen-reactive B cells, shown in different mouse systems, will depend on the diversity and abundance of competing cells and is not absolute. Nonetheless, it further minimizes the chance that autoreactive B cells enter the follicle and survive in the periphery^{14,15}. After passaging the primary follicles, B cells can enter germinal centers (GC) where they interact with antigens presented by follicular dendritic cells (FDCs) and

receive survival signals¹⁶. The activated B cells are migrating to the T-/B-cell border to present antigen and receive “help” from T helper cells. These B cells will then undergo proliferation and somatic hypermutation (SHM) in the dark zone following antigen-driven selection by FDCs in the light zone^{17,18}. Murine studies have also shown that selected B cells can re-enter or exit the GC as memory B cells or plasmablasts/cells secreting high affinity isotype-switched antibodies. Thus, retained antigen presentation by FDCs and the recruitment of “help” from T helper cells are both essential peripheral checkpoints that are in place to permit the induction of B-cell responses by transmitting necessary survival and activation signals to B cells. We will further elaborate on the important role of T cells, antigen presentation and FDCs as peripheral checkpoints in the main part of the review. Additionally, B cells can also be activated in a T-cell independent manner by bacterial molecules such as Lipopolysaccharides (LPS). LPS, like other T-cell independent antigens, contains repetitive antigenic structures leading to an extensive BCR crosslinking and also provides additional co-stimulatory signals through toll-like receptor (TLR) activation. Although the activation of B cells by T-cell independent antigens can induce abundant IgM responses as evidenced by hyper-IgM syndrome, a primary human immune deficiency disorder characterized by defective CD40 signalling, chronic BCR crosslinking with high antigen density in the absence of T-cell help or co-stimulation, typically results in B-cell anergy. This silencing of B-cell clones has been shown to represent an additional peripheral checkpoint in mice as most self-molecules do not provide co-stimulation to B cells¹⁹.

Despite all these checkpoints cooperating in controlling self-reactive B cells (Figure 1A), negative selection through central and peripheral checkpoints often fails as evidenced by the prevalence of auto-immune diseases in humans that are frequently characterized by the presence of disease-specific autoantibodies. How or when autoreactive B cells are induced in these diseases remains, however, often obscure. In this review we will highlight several mechanisms how B cells might bypass peripheral “tolerance” checkpoints including the important role of antigen presentation by FDCs, somatic hypermutation and T-/B-cell cross-reactivity between self and microbial/environmental antigens (Figure 1B). A special focus will be given to RA, highlighting different mechanisms used by the RA-specific autoreactive B cells producing anti-citrullinated protein antibodies (ACPAs) to overrun several B-cell checkpoints.

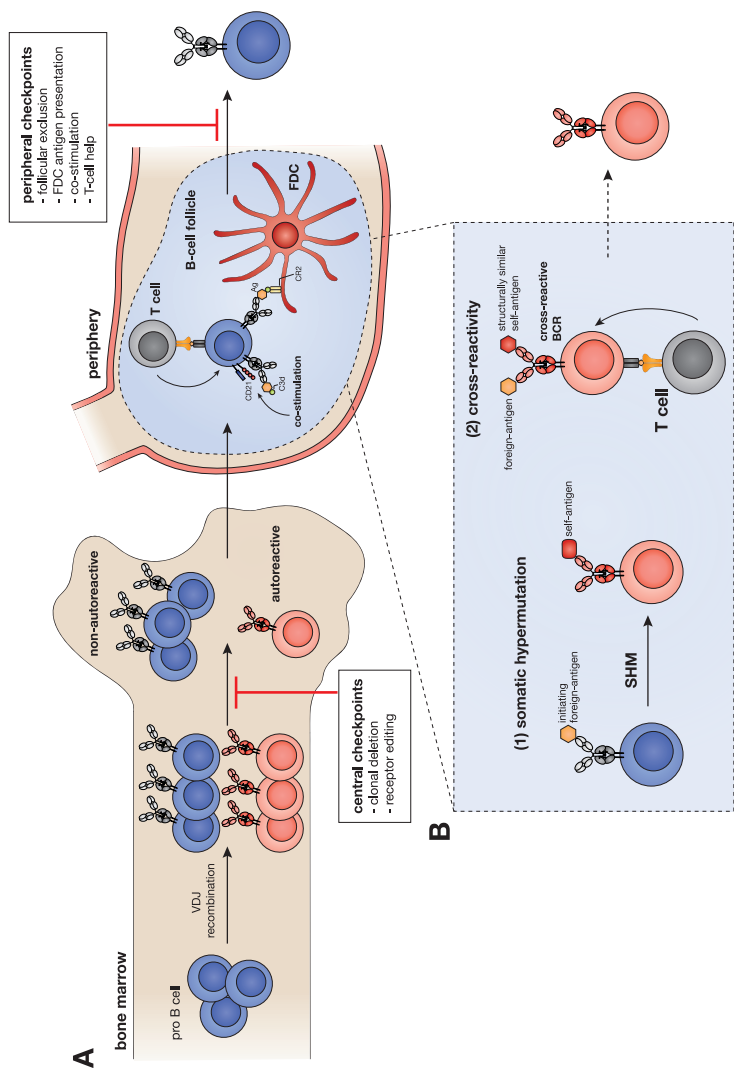


Figure 1. B-cell checkpoints and mechanisms to escape. (A) Schematic representation of the B-cell development in the BM and the periphery including the respective checkpoints. Random V(D)J-recombination of the B-cell receptor in the BM can induce autoreactive B cells. Clonal deletion and receptor editing as main central checkpoints eliminate most of these autoreactive B-cell clones. B cells that emerge into the periphery have to overcome additional checkpoints including B-cell follicular exclusion, antigen presentation by FDCs, co-stimulation by e.g. complement-C3d coated antigens and T-cell help. (B) Proposed main mechanisms of B cells to overrun peripheral checkpoints. The generation of self-reactive B cells via somatic hypermutation is one possible mechanism. B cells will alter their receptor reactivity towards self-antigens. Secondly, cross-reactive BCRs, able to recognize foreign- and structurally similar self-antigens, can overrun important gatekeepers as they receive “help” from non-autoreactive T cells.

Antigen-presentation and co-stimulation as checkpoint to control autoreactive B-cell activation

As noted above, many B-cell responses typically undergo an antigen-driven selection controlled by FDCs and follicular T helper cells in the GC. FDCs are essential for efficient GC formation and the generation of high-affinity antibodies as they are a major source of CXCL13 involved in attracting B and specific T cells to the follicles²⁰. Likewise, FDCs also produce factors promoting B-cell survival by the supply of IL-6 and the B-cell activating factor BAFF²¹. FDCs are stromal derived cells characterized by a dendritic morphology and the expression of various markers such as CD21 (CR2), CD35 (CR1), MFGE8, and Fc γ -receptors²². Furthermore, FDCs express multiple TLRs enabling them to respond to viral- or bacterial products in their vicinity. TLR2 and TLR4 stimulation of FDCs in the gut induces, for example, the production of TGF- β and BAFF involved in IgA class switching of B cells²³. Importantly, the expression of high levels of CR1 and CR2 are essential for FDC-mediated antigen retention in a complement dependent manner²⁴. FDCs retain internalized antigens, complement coated immune complexes (ICs), within cycling non-degradative endosomal compartments and periodically present them on the cell surface to B cells via CR2 during affinity maturation²². In this way, microbes and other particles or molecules that have activated the complement system become preferentially presented to B cells by FDCs. Moreover, such complement-opsonized antigens can also deliver co-stimulatory signals to responding B cells via CD21/CD35 in conjunction with BCR activation. If this complement dependent co-stimulation is lacking, B cells will not be activated properly and undergo anergy induction²⁵. Because FDCs are crucially involved in the regulation of humoral immune responses, they are also an important checkpoint controlling autoreactive B-cell responses. In general, most self-antigens will not activate the complement system and hence will not be presented efficiently by FDCs and/or recognized by B cells in a way allowing concurrent co-stimulation and BCR-engagement. Indeed, antigens conditionally expressed by FDCs in a Fc- and complement-receptor independent manner, induce B-cell tolerance in a mouse model, indicating that FDCs can play an important role in B-cell tolerance induction to sequestered self-antigens²⁶. Nonetheless, some self-constituents, such as apoptotic cells or DNA-complexes, can induce complement activation under certain pathological conditions, potentially leading to the retainment of these antigens by FDCs and induction of B-cell autoimmunity^{27,28}. The latter could be strengthened further through the ability of FDCs to attract follicular T helper cells, required for the efficient formation of T-B-cell interactions and productive GC reactions²⁹. Indeed, the important role of FDCs is also suggested by the frequent presence of ectopic lymphoid, GC-like, structures in chronically inflamed tissues of several human autoimmune diseases such as the inflamed synovium of patients with RA^{30,31}. Collectively, these findings identify FDCs as important gatekeepers governing the induction of (unwanted) B-cell responses through the control of antigen-presentation and provision of activation- and survival-signals.

De novo autoreactivity gained through somatic hypermutation

When a mature B cell recognizes its antigen, it becomes activated and can undergo SHM. During this process, random mutations might result in an enhanced antigen recognition, leading to avidity maturation of the antibody response through the selection of B cells with the highest antigen affinity. This random mutation process also bears the risk that it might lead to a shift in antigen recognition towards other (structurally similar) self-antigens. However, many such B cells will undergo apoptosis as they compete with other responding B cells for survival signals provided by FDCs and follicular T helper cells. As a consequence, many B cells will mutate away from self-reactivity as it provides a means to overcome anergy³².

Nonetheless, the development of autoimmunity in humans as a consequence of SHM has been described in several studies. For example, in Pemphigus Vulgaris, an autoimmune disease characterized by blistering and autoantibodies directed against desmoglein (DSG) proteins 1 and 3³³⁻³⁵, DSG3-specific antibodies were reverted to their respective germline sequence. As no reactivity to DSG3 could be detected anymore when these antibodies were expressed in germline configuration, the data suggest that the DSG3 reactive B cell was initially activated by another, DSG3-unrelated antigen. Interestingly, one monoclonal antibody (mAb) expressed only 4 amino acid replacements, implying that no more than a few mutations are needed to gain autoreactivity³⁶. Likewise, in pulmonary alveolar proteinosis (PAP), a rare autoimmune disease characterized by an impaired alveolar macrophage function and a shortness of breath, similar observations have been made. The disease is characterized by the presence of autoantibodies against granulocyte-macrophage colony-stimulating factor (GM-CSF), in which the reduced bioavailability of GM-CSF is causing an impaired alveolar macrophage development and function³⁷. Analyses of several patient-derived autoantibodies reverted to germline, revealed that binding to GM-CSF was strongly diminished or undetectable, indicating that somatic mutations critically determined the specificity to the autoantigen³⁸. Likewise, and in concordance with the autoimmune diseases described above, this diminished/loss of antigen recognition after germline reversion has also been described for ACPAs, the specific autoantibodies present in patients with RA³⁹⁻⁴¹. However, IgG ACPA-expressing B cells are unique as they harbor, on average, an extraordinary amount of mutations compared to other (auto)antigen-specific B cells such as anti-Tetanus Toxoid B cells, anti-DSG3 or anti-DNA antibodies^{36,42,43}. The high mutation load is, possibly, a consequence of the propensity of ACPAs to cross-react with several post-translational modifications and modified antigens^{40,44-47}, the putative chronic presence of these antigens and repetitive GC-reactions in the absence of affinity maturation. The high mutation rate complicates the determination of the correct germline sequence, increasing the chance that not the original germline sequence is investigated. In this case, investigating ACPA IgM might be more suitable as these are likely to harbor less mutations. The loss of autoreactivity after germline conversion of autoreactive IgG has also been noted in other rheumatic autoimmune diseases. For example, the analyses of a large set of mAbs, generated from BCR sequences of IgG

memory B cells from Sjögren's syndrome or SLE patients, revealed that a substantial proportion was reactive towards extractable nuclear (auto)antigens (ENA) Ro52 and La. However, when reverted to their unmutated ancestor, the ENA antibodies showed poly-reactivity with a low, non-specific, binding to Ro52 supporting the idea that SHM contributed to antibody specificity and introduction of autoreactivity^{48,49}. Similar phenomena have been described in SLE in studies where two dsDNA-directed autoantibodies did not show self-reactivity anymore when expressed in their germline configuration^{43,50}. Nevertheless, SHM is certainly not exclusively responsible for self-reactivity in these diseases, as it has also been shown that specific Ro52 reactivity is maintained after reverting somatic mutations of IgG autoantibodies to germline configuration⁵¹.

Thus, several lines of evidence indicate that autoreactivity in certain B cell-mediated diseases might be gained by SHM, although additional checkpoints at the postmutational state are likely to be present. However at this stage it is unknown, why SHM, that results in an increased avidity of most pathogen-specific responses, could also result in autoimmunity and a putative drift away from the initial T-cell help involved in the response. A possible explanation could be cross-reactivity of BCRs, as discussed in the next paragraph.

Environmental or microbial cross-reactivity as an inducer of autoimmunity

The observations described above clearly point to the possibility that autoreactive B-cell responses emerge from SHM and aberrant subsequent selection of memory B cells. Although observed in several disorders, the prevalence of this mechanism is unclear as this selection process is controlled by other mechanisms as well. For example, B cells typically require the provision of "help" from follicular T helper cells directed against the same antigenic moiety as the responding B cell. In the case of autoantigen recognition as a consequence of SHM to another (unrelated) antigen, the B cells will be severed from T-cell help due to the lack of accompanying autoreactive T cells. Therefore, such B-cell responses will not be sustained and likely disappear^{52,53}. In this respect, it is remarkable to note that many autoreactive humoral responses are directed against antigens that are tightly linked to RNA or DNA. One of these autoreactive responses is SLE, which is characterized, amongst others, by autoantibodies directed against ribonucleoproteins (RNP), such as anti-Ro (or anti SS-A), anti-La (or anti-SS-B), or anti-Sm⁵⁴. Similarly, anti-RNP and/or anti-nuclear autoantibodies are found in a variety of other autoimmune diseases such as scleroderma (anti-topoisomerase I; anti-centromere), Sjögren's syndrome (anti-SS-A/B), or dermatomyositis (anti-Jo1 recognizing histidine-tRNA ligase)⁵⁵⁻⁵⁷. Thus, all these autoantibodies recognize proteins that are intimately linked to DNA/RNA, both able to trigger Toll-like receptors (TLRs). Antigen recognition by such autoreactive B cells will lead to the concurrent provision of TLR7 or TLR9-mediated co-stimulatory signals, hence allowing effective initial activation of these B cells. Intriguingly, highly similar proteins to which these autoreactive B cells react to, are also expressed by microbes. As many DNA- and RNA-binding proteins are highly conserved across species, it is plausible that autoreactive B cells

attract “help” from T cells directed against homologous DNA-/RNA-binding proteins expressed by microbes. Noteworthy, orthologs of Ro60 with a high sequence similarity to human Ro60 can be found in multiple bacteria, including species of *Corynebacterium*, *Propionibacterium* and *Bacteroides*, which are present in the human skin, oral and gut microbiota⁵⁸. Thus, individuals chronically colonized by commensal bacteria's expressing Ro60 orthologs, might develop antibodies against both the bacterial and human Ro60 leading to B cell-mediated autoimmunity via cross-reactivity⁵⁹. In this way, the responding B cell could secure the provision of T-cell “help” by attracting microbe-specific T cells. Indeed, it has been shown that Ro60 ortholog-containing bacteria are commonly present in the human microbiome and that lupus patients with anti-Ro60 autoantibodies harbor B-cell responses to bacterial Ro60 orthologs in vitro⁵⁹. Moreover, it has been shown that the persistent presence of Ro60 orthologs repetitively stimulates short-lived Ro60-specific B cells leading to a sustained autoantibody production and a chronic disease course⁶⁰. These experimental evidences point to the notion that B-cell cross-reactivity to conserved epitopes expressed by bacterial and human DNA-/RNA-binding proteins might be central in the breach of peripheral “tolerance” checkpoints in lupus⁶¹.

Similarly, convincing evidence for a “microbe-autoreactive B-cell axis” has been presented recently in the case of the systemic autoimmune disorder antiphospholipid syndrome (APS)⁶². APS is characterized by a well-defined B-cell autoantigen, β_2 -glycoprotein I (β_2 GPI)⁶³. It has been shown in vitro and in vivo that anti- β_2 GPI B cells cross-react with mimotopes from the human gut commensal *Roseburia intestinalis*, expressed by the bacterial DNA methyltransferase (DNMT). APS patients express high levels of anti-*Roseburia intestinalis* DNMT IgG antibodies, which correlate with the anti- β_2 GPI antibody levels⁶². Additionally, immunizing mice with *Roseburia intestinalis* resulted in the generation of autoantibodies directed against human β_2 GPI, showing that bacterial proteins, conserved between man and microbe, can provide continued T-cell help and hence induce autoimmunity⁶². In these cases, the translocation of microbes to lymph nodes or systemic organs as a result of mucosal barrier breakdown⁶⁴, might be at the start of autoimmunity. Translocating bacteria are not only likely presenting antigens to the adaptive immune system but will also activate complement and other innate immune triggers, allowing efficient antigen-presentation to B cells by FDCs as well as co-stimulatory signals for the efficient initiation of B-cell responses.

Although DNA-/RNA-binding proteins are involved in the examples mentioned above, similar principles are also implicated for other autoimmune responses directed against different self-antigens. Celiac disease, although not primarily a B cell-mediated autoimmune disease, is characterized by disease-specific autoantibodies against the enzyme tissue transglutaminase (tTG)⁶⁵. It is now evident that the T cells underlying the autoreactive tTG-specific B-cell response are directed against gliadin, a foreign-antigen present in food. tTG can catalyse a specific deamidation of certain glutamine residues in gliadin, leading to the creation of modified gliadin

peptides able to bind to the Human Leukocyte Antigen (HLA)-DQ-molecules predisposing to disease and that are recognized by the disease-causing gliadin-reactive T cells. tTG can form complexes with gliadin and through the uptake of tTG-gliadin complexes, autoreactive tTG-specific B cells can recruit T-cell help through an HLA-DQ-restricted presentation of modified gliadin epitopes⁶⁶. Recently, several bacterial mimics of gliadin-epitopes have been identified that were recognized by gluten-reactive T cells from celiac disease patients. Intriguingly, the analyses of crystal structures of T-cell receptors derived from gliadin-reactive T cells in complex with HLA-DQ bound to two distinct bacterial peptides, derived from *P. fluorescens*, demonstrated that molecular mimicry drives cross-reactivity toward the gliadin epitopes⁶⁷. Thus, also in the case of celiac disease, it is indicated that T-cell reactivity towards microbial antigens displaying cross-reactivity to an antigen present in food, is at play in disease development and the formation of autoreactive B-cell responses to an ubiquitously expressed self-antigen.

However, next to microbial antigens, also other environmental triggers might provide T-cell help to support autoreactive B-cell responses. This is best exemplified for endemic Pemphigus Foliaceus in Brazil⁶⁸. Pemphigus Foliaceus is known worldwide, but an endemic variety, Fogo Selvagem, characterized by the presence of autoantibodies against DSG1, is only present in certain areas of Brazil⁶⁹. In these areas the unique combination of predisposing HLA-molecules expressed by the population⁷⁰ and a well-defined environmental trigger, the bite of a sand fly, has been shown to lead to the formation of anti-DSG1 antibodies⁶⁸. This is explained by the observation that the salivary protein LJM11 from the sand fly is recognized by Fogo Selvagem antibodies as well as anti-DSG1 mAbs derived from Fogo Selvagem patients. Although, the underlying T-cell response has not yet been defined, it is highly conceivable that also in this case the autoreactive B-cell response arises through cross-reactivity via the “help” of T cells directed against environmental antigens.

Thus, together, the picture emerges that B-cell autoimmunity often arises in the absence of autoreactive T cells. Instead, these B cells contain BCRs showing cross-reactivity between self-antigens and environmental/ microbiome triggers and thereby recruit T-cell help.

Mechanisms of ACPA-expressing B cells in RA to overrun B-cell checkpoints

As described above, the prominent human autoimmune disease RA is characterized by disease-specific autoantibodies and responsive to B-cell targeted therapies. It is manifested by synovial inflammation and progressive joint damage if left untreated. The autoantibody response in RA has been characterized in great detail in the past decade, revealing important insights that harmonize with the findings into the emergence of the autoreactive B-cell response uncovered in other autoimmune diseases. However, these studies also unveiled additional processes which are likely involved in violating checkpoints controlling B-cell activation in humans. The most disease-specific antibodies in RA are directed against citrullinated proteins, and hence,

are named anti-citrullinated protein antibodies. Remarkably, ACPAs are reactive towards a broad spectrum of citrullinated antigens, including self-proteins as well as proteins present in microbes⁷¹⁻⁷⁵. Moreover, recent studies have shown that they are not only restricted to citrulline recognition, but that they can also cross-react to other post-translational modifications (PTMs), more specifically acetylated- and carbamylated-lysine residues. This has not only been shown at the polyclonal and monoclonal autoantibody level, but also on the level of BCR signaling^{40,44-46,76-78}. Thus, in this case, autoreactive B cells expressing a BCR directed against one particular PTM antigen can not only be activated by this specific modification, but also by (other) antigens expressing different modifications⁴⁵. Hence, various antigens and PTMs could potentially drive the expansion of autoreactive B cells in RA, possibly including microbe-derived antigens. Experimental studies have reflected on a role for the oral, gut or lung microbiota in the development of RA, such as mediated by *Porphyromonas gingivalis* (*Pg*), *Aggregatibacter actinomycetemcomitans* (*Aa*) and *Proteus mirabilis* (*Pm*)^{74,79,80}. For example, a high similarity between *Pg* enolase and the human α -enolase has been shown⁷⁴. This similarity between foreign and self allows cross-reactive antibodies to bind to self-antigens, as evidenced by the correlation between ACPA levels directed against citrullinated human α -enolase and the levels of antibodies directed against citrullinated α -enolase from *P.gingivalis*⁷⁴. Additionally, it has been reported that ACPAs might evolve from immune responses to *Pg*⁸¹. For *Aggregatibacter actinomycetemcomitans* it has been suggested that a pore-forming toxin, leukotoxin A (LtxA), causes hypercitrullination and thus generates multiple citrullinated epitopes that can potentially be targeted by the cross-reactive autoantibodies⁸⁰. Nevertheless, ACPAs are not only present in individuals exposed to *Aa*⁸². Thus, also in this autoimmune disease, the prevailing humoral autoimmune response is recognizing both (modified) self- and non-self-proteins expressed by microbes. Moreover, these autoantibodies also recognize DNA-binding molecules such as histones as citrullination and acetylation represent prominent epigenomic modifications⁸³. Therefore, it is conceivable that ACPA-expressing B cells can recruit co-stimulatory signals from both (opsonized) microbes as well as (modified) protein-DNA-complexes.

Additionally, a unique feature of ACPAs is the presence of N-linked glycans in the variable (V) domain as it is found that over 90% of ACPA molecules in serum of RA patients contain V-domain glycans^{84,85}. These glycans displayed on ACPAs are primarily complex-type carbohydrates containing a high degree of sialic acids⁸⁴ and are acquired through the introduction of N-linked glycosylation sites following SHM⁸⁶. As the introduction of glycosylation sites in the BCR by SHM is a random process, and as ACPA V-domain glycans are found in the vast majority of ACPA molecules in almost all RA patients, it is likely that the expression of such glycans by anti-citrullinated protein BCRs, provides a selective advantage to ACPA-expressing B cells. Interestingly, the presence of V-domain glycans in ACPA-positive healthy subjects is associated with the transition towards disease⁸⁷. These observations, together with the recent discovery that the HLA-molecules predisposing to RA are associated with the introduction of ACPA

V-domain glycans⁸⁸, further emphasizes that the introduction of glycans into the BCR V-domain likely represents an additional mechanism involved in the “breach of B-cell tolerance” in RA and possibly other human autoimmune diseases including Anti-Nuclear Antibody (ANA)-associated vasculitis and Sjögren's syndrome^{89,90}. How V-domain glycans expressed by autoreactive anti-citrullinated protein-directed B cells contribute to the development and/or expansion of the ACPA response is presently unclear, although V-domain glycans have been shown to modulate antigen recognition and to interact with lectins in vicinity to the BCR or on neighboring cells and thereby could deliver survival signals⁹¹⁻⁹⁵.

Thus, collectively, autoreactive B-cell responses that hallmark RA are of a highly cross-reactive nature, recognizing different PTMs that are expressed on foreign- and self-proteins. Their development encompasses the introduction of V-domain glycans through the formation of N-linked glycosylation sites by SHM. Both characteristics are likely to be involved in overrunning B-cell checkpoints as cross-reactivity could trigger T-cell help as a “first hit”⁹⁶, whereas the introduction of V-domain glycans might be an additional “second hit” mechanism to gain a selective activation/survival advantage despite autoreactivity. Autoreactive B-cell responses in RA might therefore emerge from “multiple hits”, including the high cross-reactive nature of ACPAs and their abundant presence of V-domain glycans (Figure 2).

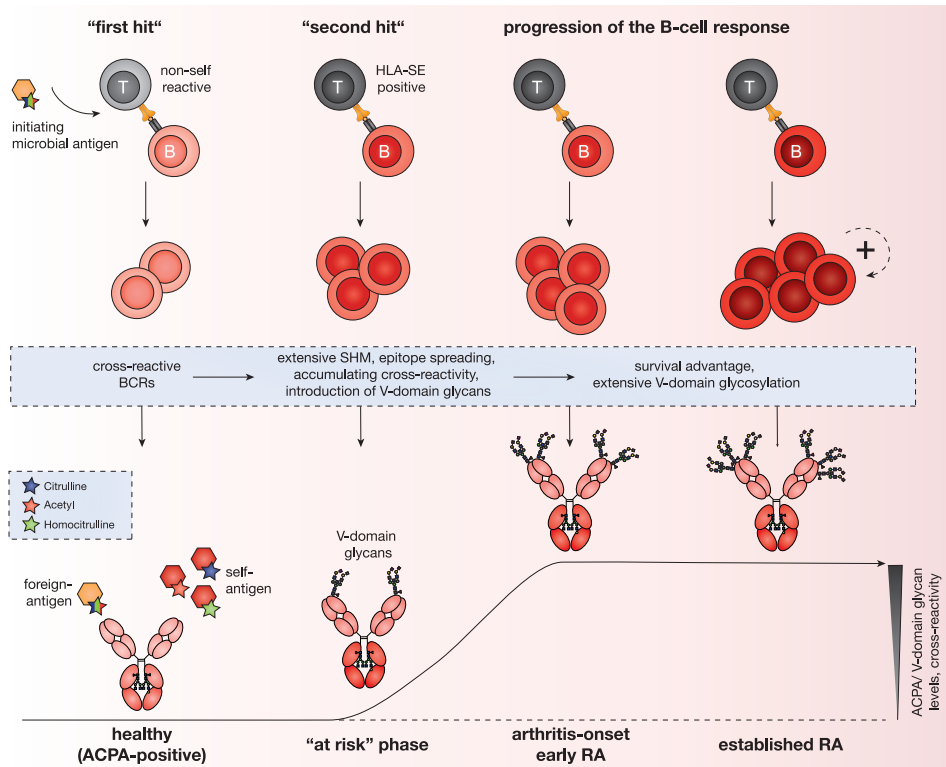


Figure 2. Escape mechanisms of ACPA-expressing B cells and RA development. "Multiple hit" theory of the ACPA-expressing B-cell response in RA and changes in ACPA characteristics towards disease-onset. The autoreactive B-cell response in RA is initiated by microbial triggers allowing T-cell help and the generation of cross-reactive, citrullinated protein-directed B cells and autoantibodies (ACPAs). These B cells are able to recognize post-translationally modified (citrullinated, acetylated, homocitrullinated) foreign- and self-antigens. This "first hit" is followed by a "second hit", including T cells restricted to HLA-molecules predisposing to RA, and results in extensive SHM leading to epitope spreading and an increase in cross-reactivity of the B-cell response. This stage is also characterized by the introduction of glycans into the variable domain of the BCRs. Current epidemiological evidence indicates that these V-domain glycans provide a selective advantage to ACPA-expressing B cells explaining the increase of V-domain glycosylated ACPAs pre-disease and the abundant presence of V-domain glycosylated ACPAs in RA. B cells presenting cross-reactive, highly V-domain glycosylated BCRs are probably able to escape important gatekeepers, which will lead to a progression of the B-cell response, a rise in autoantibody/ ACPA levels and thus in the onset of RA.

Concluding remarks

The mechanisms described in this review shed light on how autoreactive B cells might breach “tolerance” in humans. It is probable that autoreactivity arises in the periphery where B cells have to escape fewer “tolerance” checkpoints than autoreactive B cells emerging in the BM. As the induction of B-cell responses in the periphery is stringently controlled by co-stimulation from innate triggers, FDCs and T helper cells and as most autoantibodies have undergone class switch recombination and SHM, it is likely that autoreactive B-cell responses arise by misleading these gatekeepers.

Accumulating evidence suggests, although not consistent throughout diseases, that autoreactivity might be gained during SHM allowing mutated BCRs to obtain reactivity to self-antigens. SHM might also introduce cross-reactivity, which allows the BCRs to react towards both self- and foreign-antigens. Cross-reactivity to non-self as an inducer of autoimmunity is highlighted in several studies demonstrating an important role for the microbiome or environmental triggers in the induction of B cell-mediated autoimmune responses. A common denominator of these findings is the notion that autoreactive B cells cross-react between self and the “environment”/microbiome, whereas the accommodating T cells supporting these B cells do not necessarily recognize self. In this way, the need to depose both B-cell and T-cell checkpoints to induce B cell-mediated autoimmunity is overturned, conceivably explaining the relative high prevalence of B cell-mediated autoimmune responses in the human population. Additionally, glycans present in the variable domain of autoreactive BCRs might provide an additional, still poorly studied, mechanism involved in the induction of autoimmunity in humans. Further understanding of these, and other pathways controlling the induction of autoreactive B-cell responses in humans, is crucial for the development of preventative and/or curative strategies in B cell-mediated autoimmune diseases; diseases that are still incurable to date.

Funding

This work was supported by ReumaNederland 17-1-402 (to R.E.M.T.), the IMI-funded project RTCure 777357 (to T.W.J.H.), ZonMw TOP 91214031 (to R.E.M.T.), Target-to-B LSHM18055-SGF (to R.E.M.T.) and the European Research Council (ERC) Advanced grant AdG2019-884796 (to R.E.M.T.).

Conflict of interest

R.E.M.T. is named as co-inventor on a patent on ACPA IgG V-domain glycosylation. Other authors declare no competing interests.

References

- 1 Edwards, J. C. and Cambridge, G., Prospects for B-cell-targeted therapy in autoimmune disease. *Rheumatology (Oxford)* 2005. 44: 151-156.
- 2 Edwards, J. C. W., Szczepański, L., Szechiński, J., Filipowicz-Sosnowska, A., Emery, P., Close, D. R., et al., Efficacy of B-Cell-Targeted Therapy with Rituximab in Patients with Rheumatoid Arthritis. *New England Journal of Medicine* 2004. 350: 2572-2581.
- 3 Joly, P., Maho-Vaillant, M., Prost-Squarcioni, C., Hebert, V., Houivet, E., Calbo, S., et al., First-line rituximab combined with short-term prednisone versus prednisone alone for the treatment of pemphigus (Ritux 3): a prospective, multicentre, parallel-group, open-label randomised trial. *The Lancet* 2017. 389: 2031-2040.
- 4 Musette, P. and Bouaziz, J. D., B Cell Modulation Strategies in Autoimmune Diseases: New Concepts. *Frontiers in Immunology* 2018. 9.
- 5 Hampe, C. S., B Cell in Autoimmune Diseases. *Scientifica (Cairo)* 2012. 2012.
- 6 Hofmann, K., Clauder, A.-K. and Manz, R. A., Targeting B Cells and Plasma Cells in Autoimmune Diseases. *Frontiers in Immunology* 2018. 9.
- 7 Tonegawa, S., Somatic generation of antibody diversity. *Nature* 1983. 302: 575-581.
- 8 Lewis, S., Gifford, A. and Baltimore, D., DNA elements are asymmetrically joined during the site-specific recombination of kappa immunoglobulin genes. *Science* 1985. 228: 677-685.
- 9 Lewis, S., Gifford, A. and Baltimore, D., Joining of V kappa to J kappa gene segments in a retroviral vector introduced into lymphoid cells. *Nature* 1984. 308: 425-428.
- 10 Meffre, E. and Wardemann, H., B-cell tolerance checkpoints in health and autoimmunity. *Curr Opin Immunol* 2008. 20: 632-638.
- 11 Meffre, E., The establishment of early B cell tolerance in humans: lessons from primary immunodeficiency diseases. *Ann N Y Acad Sci* 2011. 1246: 1-10.
- 12 Grandien, A., Fucs, R., Nobrega, A., Andersson, J. and Coutinho, A., Negative selection of multireactive B cell clones in normal adult mice. *Eur J Immunol* 1994. 24: 1345-1352.
- 13 Hikida, M. and Ohmori, H., Rearrangement of lambda light chain genes in mature B cells in vitro and in vivo. Function of reexpressed recombination-activating gene (RAG) products. *J Exp Med* 1998. 187: 795-799.
- 14 Cyster, J. G. and Goodnow, C. C., Antigen-induced exclusion from follicles and anergy are separate and complementary processes that influence peripheral B cell fate. *Immunity* 1995. 3: 691-701.
- 15 Cyster, J. G., Hartley, S. B. and Goodnow, C. C., Competition for follicular niches excludes self-reactive cells from the recirculating B-cell repertoire. *Nature* 1994. 371: 389-395.
- 16 Allen, C. D. and Cyster, J. G., Follicular dendritic cell networks of primary follicles and germinal centers: phenotype and function. *Semin Immunol* 2008. 20: 14-25.
- 17 MacLennan, I. C., Germinal centers. *Annu Rev Immunol* 1994. 12: 117-139.
- 18 Mandel, T. E., Phipps, R. P., Abbot, A. P. and Tew, J. G., Long-term antigen retention by dendritic cells in the popliteal lymph node of immunized mice. *Immunology* 1981. 43: 353-362.
- 19 Goodnow, C. C., Brink, R. and Adams, E., Breakdown of self-tolerance in anergic B lymphocytes 1991. 352: 532-536.
- 20 Ansel, K. M., Ngo, V. N., Hyman, P. L., Luther, S. A., Forster, R., Sedgwick, J. D., et al., A chemokine-driven positive feedback loop organizes lymphoid follicles. *Nature* 2000. 406: 309-314.
- 21 Wu, Y., El Shikh, M. E., El Sayed, R. M., Best, A. M., Szakal, A. K. and Tew, J. G., IL-6 produced by immune complex-activated follicular dendritic cells promotes germinal center reactions, IgG responses and somatic hypermutation. *Int Immunol* 2009. 21: 745-756.

- 22 Heesters, B. A., Chatterjee, P., Kim, Y. A., Gonzalez, S. F., Kuligowski, M. P., Kirchhausen, T., et al., Endocytosis and recycling of immune complexes by follicular dendritic cells enhances B cell antigen binding and activation. *Immunity* 2013. 38: 1164-1175.
- 23 Suzuki, K., Maruya, M., Kawamoto, S., Sitnik, K., Kitamura, H., Agace, W. W., et al., The sensing of environmental stimuli by follicular dendritic cells promotes immunoglobulin A generation in the gut. *Immunity* 2010. 33: 71-83.
- 24 Fischer, M. B., Goerg, S., Shen, L., Prodeus, A. P., Goodnow, C. C., Kelsoe, G., et al., Dependence of germinal center B cells on expression of CD21/CD35 for survival. *Science* 1998. 280: 582-585.
- 25 Roozendaal, R. and Carroll, M. C., Complement receptors CD21 and CD35 in humoral immunity. *Immunol Rev* 2007. 219: 157-166.
- 26 Yau, I. W., Cato, M. H., Jellusova, J., Hurtado de Mendoza, T., Brink, R. and Rickert, R. C., Censoring of self-reactive B cells by follicular dendritic cell-displayed self-antigen. *J Immunol* 2013. 191: 1082-1090.
- 27 Hanayama, R., Tanaka, M., Miyasaka, K., Aozasa, K., Koike, M., Uchiyama, Y., et al., Autoimmune disease and impaired uptake of apoptotic cells in MFG-E8-deficient mice. *Science* 2004. 304: 1147-1150.
- 28 Baumann, I., Kolowos, W., Voll, R. E., Manger, B., Gaipl, U., Neuhuber, W. L., et al., Impaired uptake of apoptotic cells into tingible body macrophages in germinal centers of patients with systemic lupus erythematosus. *Arthritis Rheum* 2002. 46: 191-201.
- 29 Victoratos, P. and Kollias, G., Induction of autoantibody-mediated spontaneous arthritis critically depends on follicular dendritic cells. *Immunity* 2009. 30: 130-142.
- 30 Humby, F., Bombardieri, M., Manzo, A., Kelly, S., Blades, M. C., Kirkham, B., et al., Ectopic lymphoid structures support ongoing production of class-switched autoantibodies in rheumatoid synovium. *PLoS Med* 2009. 6: e1.
- 31 Randen, I., Mellbye, O. J., Forre, O. and Natvig, J. B., The identification of germinal centres and follicular dendritic cell networks in rheumatoid synovial tissue. *Scand J Immunol* 1995. 41: 481-486.
- 32 Reed, J. H., Jackson, J., Christ, D. and Goodnow, C. C., Clonal redemption of autoantibodies by somatic hypermutation away from self-reactivity during human immunization 2016. 213: 1255-1265.
- 33 Berkowitz, P., Chua, M., Liu, Z., Diaz, L. A. and Rubenstein, D. S., Autoantibodies in the autoimmune disease pemphigus foliaceus induce blistering via p38 mitogen-activated protein kinase-dependent signaling in the skin. *Am J Pathol* 2008. 173: 1628-1636.
- 34 Amagai, M., Hashimoto, T., Shimizu, N. and Nishikawa, T., Absorption of pathogenic autoantibodies by the extracellular domain of pemphigus vulgaris antigen (Dsg3) produced by baculovirus. *J Clin Invest* 1994. 94: 59-67.
- 35 Amagai, M., Klaus-Kovtun, V. and Stanley, J. R., Autoantibodies against a novel epithelial cadherin in pemphigus vulgaris, a disease of cell adhesion. *Cell* 1991. 67: 869-877.
- 36 Di Zenzo, G., Di Lullo, G., Corti, D., Calabresi, V., Sinistro, A., Vanzetta, F., et al., Pemphigus autoantibodies generated through somatic mutations target the desmoglein-3 cis-interface. *Journal of Clinical Investigation* 2012. 122: 3781-3790.
- 37 Kitamura, T., Tanaka, N., Watanabe, J., Uchida, Kanegasaki, S., Yamada, Y., et al., Idiopathic pulmonary alveolar proteinosis as an autoimmune disease with neutralizing antibody against granulocyte/macrophage colony-stimulating factor. *J Exp Med* 1999. 190: 875-880.
- 38 Piccoli, L., Campo, I., Fregni, C. S., Rodriguez, B. M. F., Minola, A., Sallusto, F., et al., Neutralization and clearance of GM-CSF by autoantibodies in pulmonary alveolar proteinosis. *Nature Communications* 2015. 6: 7375.
- 39 Kongpachith, S., Lingampalli, N., Ju, C. H., Blum, L. K., Lu, D. R., Elliott, S. E., et al., Affinity Maturation of the Anti-Citrullinated Protein Antibody Paratope Drives Epitope Spreading and Polyreactivity in Rheumatoid Arthritis. *Arthritis & Rheumatology* 2019. 71: 507-517.
- 40 Steen, J., Forsstrom, B., Sahlstrom, P., Odowd, V., Israelsson, L., Krishnamurthy, A., et al., Recognition of Amino Acid Motifs, Rather Than Specific Proteins, by Human Plasma Cell-Derived Monoclonal Antibodies to Posttranslationally Modified Proteins in Rheumatoid Arthritis. *Arthritis Rheumatol* 2019. 71: 196-209.

- 41 Ozawa, T., Ouhara, K., Tsuda, R., Munenaga, S., Kurihara, H., Kohno, H., et al., Physiological target, molecular evolution and pathogenic functions of a monoclonal ACPA obtained from an RA patient. *Arthritis & Rheumatology* 2020.
- 42 Vergroesen, R. D., Slot, L. M., Hafkenscheid, L., Koning, M. T., Van Der Voort, E. I. H., Grooff, C. A., et al., B-cell receptor sequencing of anti-citrullinated protein antibody (ACPA) IgG-expressing B cells indicates a selective advantage for the introduction of N-glycosylation sites during somatic hypermutation. *Annals of the Rheumatic Diseases* 2017: annrheumdis-201.
- 43 Sakakibara, S., Arimori, T., Yamashita, K., Jinzai, H., Motooka, D., Nakamura, S., et al., Clonal evolution and antigen recognition of anti-nuclear antibodies in acute systemic lupus erythematosus. *Scientific Reports* 2017. 7.
- 44 Kampstra, A. S. B., Dekkers, J. S., Volkov, M., Dorjee, A. L., Hafkenscheid, L., Kempers, A. C., et al., Different classes of anti-modified protein antibodies are induced on exposure to antigens expressing only one type of modification. *Ann Rheum Dis* 2019. 78: 908-916.
- 45 Kissel, T., Reijm, S., Slot, L. M., Cavallari, M., Wortel, C. M., Vergroesen, R. D., et al., Antibodies and B cells recognising citrullinated proteins display a broad cross-reactivity towards other post-translational modifications. *Ann Rheum Dis* 2020. 79: 472-480.
- 46 Reed, E., Jiang, X., Kharlamova, N., Ytterberg, A. J., Catrina, A. I., Israelsson, L., et al., Antibodies to carbamylated alpha-enolase epitopes in rheumatoid arthritis also bind citrullinated epitopes and are largely indistinct from anti-citrullinated protein antibodies. *Arthritis Res Ther* 2016. 18: 96.
- 47 Figueiredo, C. P., Bang, H., Cobra, J. F., Englbrecht, M., Hueber, A. J., Haschka, J., et al., Antimodified protein antibody response pattern influences the risk for disease relapse in patients with rheumatoid arthritis tapering disease modifying antirheumatic drugs. *Ann Rheum Dis* 2017. 76: 399-407.
- 48 Mietzner, B., Tsuiji, M., Scheid, J., Velinzon, K., Tiller, T., Abraham, K., et al., Autoreactive IgG memory antibodies in patients with systemic lupus erythematosus arise from nonreactive and polyreactive precursors. *Proceedings of the National Academy of Sciences* 2008. 105: 9727-9732.
- 49 Takeshita, M., Suzuki, K., Kaneda, Y., Yamane, H., Ikeura, K., Sato, H., et al., Antigen-driven selection of antibodies against SSA, SSB and the centromere 'complex', including a novel antigen, MIS12 complex, in human salivary glands. *Annals of the Rheumatic Diseases* 2020. 79: 150-158.
- 50 Wellmann, U., Letz, M., Herrmann, M., Angermuller, S., Kalden, J. R. and Winkler, T. H., The evolution of human anti-double-stranded DNA autoantibodies 2005. 102: 9258-9263.
- 51 Reed, J. H., Gorny, M. K., Li, L., Cardozo, T., Buyon, J. P. and Clancy, R. M., Ro52 autoantibodies arise from self-reactive progenitors in a mother of a child with neonatal lupus. *Journal of Autoimmunity* 2017. 79: 99-104.
- 52 Mesin, L., Ersching, J. and Victora, G. D., Germinal Center B Cell Dynamics. *Immunity* 2016. 45: 471-482.
- 53 Schwickert, T. A., Victora, G. D., Fooksman, D. R., Kamphorst, A. O., Mugnier, M. R., Gitlin, A. D., et al., A dynamic T cell-limited checkpoint regulates affinity-dependent B cell entry into the germinal center. *J Exp Med* 2011. 208: 1243-1252.
- 54 Dema, B. and Charles, N., Autoantibodies in SLE: Specificities, Isotypes and Receptors. *Antibodies (Basel)* 2016. 5.
- 55 Stochmal, A., Czuwara, J., Trojanowska, M. and Rudnicka, L., Antinuclear Antibodies in Systemic Sclerosis: an Update. *Clinical Reviews in Allergy & Immunology* 2020. 58: 40-51.
- 56 Fayyaz, A., Kurien, B. T. and Scofield, R. H., Autoantibodies in Sjögren's Syndrome. *Rheumatic Disease Clinics of North America* 2016. 42: 419-434.
- 57 Mileti, L. M., Strek, M. E., Niewold, T. B., Curran, J. J. and Sweiss, N. J., Clinical Characteristics of Patients With Anti-Jo-1 Antibodies. *JCR: Journal of Clinical Rheumatology* 2009. 15: 254-255.
- 58 Sim, S. and Wolin, S. L., Emerging roles for the Ro 60-kDa autoantigen in noncoding RNA metabolism. *Wiley Interdiscip Rev RNA* 2011. 2: 686-699.

- 59 Greiling, T. M., Dehner, C., Chen, X., Hughes, K., Iniguez, A. J., Boccitto, M., et al., Commensal orthologs of the human autoantigen Ro60 as triggers of autoimmunity in lupus. *Sci Transl Med* 2018. 10.
- 60 Lindop, R., Arentz, G., Bastian, I., Whyte, A. F., Thurgood, L. A., Chataway, T. K., et al., Long-term Ro60 humoral autoimmunity in primary Sjogren's syndrome is maintained by rapid clonal turnover. *Clin Immunol* 2013. 148: 27-34.
- 61 McClain, M. T., Heinlen, L. D., Dennis, G. J., Roebuck, J., Harley, J. B. and James, J. A., Early events in lupus humoral autoimmunity suggest initiation through molecular mimicry. *Nat Med* 2005. 11: 85-89.
- 62 Ruff, W. E., Dehner, C., Kim, W. J., Pagovich, O., Aguiar, C. L., Yu, A. T., et al., Pathogenic Autoreactive T and B Cells Cross-React with Mimotopes Expressed by a Common Human Gut Commensal to Trigger Autoimmunity. *Cell Host Microbe* 2019. 26: 100-113 e108.
- 63 Ruiz-Irastorza, G., Crowther, M., Branch, W. and Khamashta, M. A., Antiphospholipid syndrome. *Lancet* 2010. 376: 1498-1509.
- 64 Manfredo Vieira, S., Hiltensperger, M., Kumar, V., Zegarra-Ruiz, D., Dehner, C., Khan, N., et al., Translocation of a gut pathobiont drives autoimmunity in mice and humans. *Science* 2018. 359: 1156-1161.
- 65 Caja, S., Mäki, M., Kaukinen, K. and Lindfors, K., Antibodies in celiac disease: implications beyond diagnostics. *Cellular & Molecular Immunology* 2011. 8: 103-109.
- 66 Caio, G., Volta, U., Sapone, A., Leffler, D. A., De Giorgio, R., Catassi, C., et al., Celiac disease: a comprehensive current review. *BMC Medicine* 2019. 17.
- 67 Petersen, J., Ciacchi, L., Tran, M. T., Loh, K. L., Kooy-Winkelaar, Y., Croft, N. P., et al., T cell receptor cross-reactivity between gliadin and bacterial peptides in celiac disease. *Nature Structural & Molecular Biology* 2020. 27: 49-61.
- 68 Qian, Y., Jeong, J. S., Maldonado, M., Valenzuela, J. G., Gomes, R., Teixeira, C., et al., Cutting Edge: Brazilian Pemphigus Foliaceus Anti-Desmoglein 1 Autoantibodies Cross-React with Sand Fly Salivary LJM11 Antigen 2012. 189: 1535-1539.
- 69 Diaz, L. A., Sampaio, S. A. P., Rivitti, E. A., Martins, C. R., Cunha, P. R., Lombardi, C., et al., Endemic Pemphigus Foliaceus (Fogo Selvagem): II. Current and Historic Epidemiologic Studies 1989. 92: 4-12.
- 70 Moraes, J. R., Moraes, M. E., Fernandez-Vina, M., Diaz, L. A., Friedman, H., Campbell, I. T., et al., HLA antigens and risk for development of pemphigus foliaceus (fogo selvagem) in endemic areas of Brazil. *Immunogenetics* 1991. 33: 388-391.
- 71 Takizawa, Y., Suzuki, A., Sawada, T., Ohsaka, M., Inoue, T., Yamada, R., et al., Citrullinated fibrinogen detected as a soluble citrullinated autoantigen in rheumatoid arthritis synovial fluids. *Ann Rheum Dis* 2006. 65: 1013-1020.
- 72 Burkhardt, H., Koller, T., Engstrom, A., Nandakumar, K. S., Turnay, J., Kraetsch, H. G., et al., Epitope-specific recognition of type II collagen by rheumatoid arthritis antibodies is shared with recognition by antibodies that are arthritogenic in collagen-induced arthritis in the mouse. *Arthritis Rheum* 2002. 46: 2339-2348.
- 73 Vossenaar, E. R., Despres, N., Lapointe, E., van der Heijden, A., Lora, M., Senshu, T., et al., Rheumatoid arthritis specific anti-Sa antibodies target citrullinated vimentin. *Arthritis Res Ther* 2004. 6: R142-150.
- 74 Lundberg, K., Kinloch, A., Fisher, B. A., Wegner, N., Wait, R., Charles, P., et al., Antibodies to citrullinated alpha-enolase peptide I are specific for rheumatoid arthritis and cross-react with bacterial enolase. *Arthritis Rheum* 2008. 58: 3009-3019.
- 75 Ioan-Facsinay, A., el-Bannoudi, H., Scherer, H. U., van der Woude, D., Menard, H. A., Lora, M., et al., Anti-cyclic citrullinated peptide antibodies are a collection of anti-citrullinated protein antibodies and contain overlapping and non-overlapping reactivities. *Ann Rheum Dis* 2011. 70: 188-193.
- 76 Lloyd, K. A., Wigerblad, G., Sahlstrom, P., Garimella, M. G., Chemin, K., Steen, J., et al., Differential ACPA Binding to Nuclear Antigens Reveals a PAD-Independent Pathway and a Distinct Subset of Acetylation Cross-Reactive Autoantibodies in Rheumatoid Arthritis. *Front Immunol* 2018. 9: 3033.

- 77 Shi, J., Knevel, R., Suwannalai, P., van der Linden, M. P., Janssen, G. M., van Veelen, P. A., et al., Autoantibodies recognizing carbamylated proteins are present in sera of patients with rheumatoid arthritis and predict joint damage. *Proc Natl Acad Sci U S A* 2011. 108: 17372-17377.
- 78 Dekkers, J. S., Verheul, M. K., Stoop, J. N., Liu, B., Ioan-Facsinay, A., van Veelen, P. A., et al., Breach of autoreactive B cell tolerance by post-translationally modified proteins. *Ann Rheum Dis* 2017. 76: 1449-1457.
- 79 Rashid, T., Jayakumar, K. S., Binder, A., Ellis, S., Cunningham, P. and Ebringer, A., Rheumatoid arthritis patients have elevated antibodies to cross-reactive and non cross-reactive antigens from Proteus microbes. *Clin Exp Rheumatol* 2007. 25: 259-267.
- 80 Konig, M. F., Abusleme, L., Reinholdt, J., Palmer, R. J., Teles, R. P., Sampson, K., et al., Aggregatibacter actinomycetemcomitans-induced hypercitrullination links periodontal infection to autoimmunity in rheumatoid arthritis. *Sci Transl Med* 2016. 8: 369ra176.
- 81 Li, S., Yu, Y., Yue, Y., Liao, H., Xie, W., Thai, J., et al., Autoantibodies From Single Circulating Plasmablasts React With Citrullinated Antigens and Porphyromonas gingivalis in Rheumatoid Arthritis. *Arthritis Rheumatol* 2016. 68: 614-626.
- 82 Volkov, M., Dekkers, J., Loos, B. G., Bizzarro, S., Huizinga, T. W. J., Praetorius, H. A., et al., Comment on "Aggregatibacter actinomycetemcomitans-induced hypercitrullination links periodontal infection to autoimmunity in rheumatoid arthritis". *Sci Transl Med* 2018. 10.
- 83 Dieker, J. and Muller, S., Epigenetic Histone Code and Autoimmunity 2010. 39: 78-84.
- 84 Hafkenscheid, L., Bondt, A., Scherer, H. U., Huizinga, T. W., Wuhler, M., Toes, R. E., et al., Structural Analysis of Variable Domain Glycosylation of Anti-Citrullinated Protein Antibodies in Rheumatoid Arthritis Reveals the Presence of Highly Sialylated Glycans. *Mol Cell Proteomics* 2017. 16: 278-287.
- 85 Rombouts, Y., Willemze, A., van Beers, J. J., Shi, J., Kerkman, P. F., van Toorn, L., et al., Extensive glycosylation of ACPA-IgG variable domains modulates binding to citrullinated antigens in rheumatoid arthritis. *Ann Rheum Dis* 2016. 75: 578-585.
- 86 Vergroesen, R. D., Slot, L. M., Hafkenscheid, L., Koning, M. T., van der Voort, E. I. H., Grooff, C. A., et al., B-cell receptor sequencing of anti-citrullinated protein antibody (ACPA) IgG-expressing B cells indicates a selective advantage for the introduction of N-glycosylation sites during somatic hypermutation. *Ann Rheum Dis* 2018. 77: 956-958.
- 87 Hafkenscheid, L., de Moel, E., Smolik, I., Tanner, S., Meng, X., Jansen, B. C., et al., N-Linked Glycans in the Variable Domain of IgG Anti-Citrullinated Protein Antibodies Predict the Development of Rheumatoid Arthritis. *Arthritis Rheumatol* 2019. 71: 1626-1633.
- 88 Kissel, T., van Schie, K. A., Hafkenscheid, L., Lundquist, A., Kokkonen, H., Wuhler, M., et al., On the presence of HLA-SE alleles and ACPA-IgG variable domain glycosylation in the phase preceding the development of rheumatoid arthritis. *Ann Rheum Dis* 2019. 78: 1616-1620.
- 89 Holland, M., Yagi, H., Takahashi, N., Kato, K., Savage, C. O., Goodall, D. M., et al., Differential glycosylation of polyclonal IgG, IgG-Fc and IgG-Fab isolated from the sera of patients with ANCA-associated systemic vasculitis. *Biochim Biophys Acta* 2006. 1760: 669-677.
- 90 Hamza, N., Hershberg, U., Kallenberg, C. G., Vissink, A., Spijkervet, F. K., Bootsma, H., et al., Ig gene analysis reveals altered selective pressures on Ig-producing cells in parotid glands of primary Sjogren's syndrome patients. *J Immunol* 2015. 194: 514-521.
- 91 van de Bovenkamp, F. S., Derksen, N. I. L., Ooijevaar-de Heer, P., van Schie, K. A., Kruithof, S., Berkowska, M. A., et al., Adaptive antibody diversification through N-linked glycosylation of the immunoglobulin variable region. *Proc Natl Acad Sci U S A* 2018. 115: 1901-1906.
- 92 Sabouri, Z., Schofield, P., Horikawa, K., Spierings, E., Kipling, D., Randall, K. L., et al., Redemption of autoantibodies on anergic B cells by variable-region glycosylation and mutation away from self-reactivity. *Proc Natl Acad Sci U S A* 2014. 111: E2567-2575.

- 93 Radcliffe, C. M., Arnold, J. N., Suter, D. M., Wormald, M. R., Harvey, D. J., Royle, L., et al., Human Follicular Lymphoma Cells Contain Oligomannose Glycans in the Antigen-binding Site of the B-cell Receptor. *Journal of Biological Chemistry* 2007. 282: 7405-7415.
- 94 Zhu, D., McCarthy, H., Ottensmeier, C. H., Johnson, P., Hamblin, T. J. and Stevenson, F. K., Acquisition of potential N-glycosylation sites in the immunoglobulin variable region by somatic mutation is a distinctive feature of follicular lymphoma. *Blood* 2002. 99: 2562-2568.
- 95 Vletter, E. M., Koning, M. T., Scherer, H. U., Veelken, H. and Toes, R. E. M., A Comparison of Immunoglobulin Variable Region N-Linked Glycosylation in Healthy Donors, Autoimmune Disease and Lymphoma. *Frontiers in Immunology* 2020. 11.
- 96 van Heemst, J., Jansen, D. T., Polydorides, S., Moustakas, A. K., Bax, M., Feitsma, A. L., et al., Crossreactivity to vinculin and microbes provides a molecular basis for HLA-based protection against rheumatoid arthritis. *Nat Commun* 2015. 6: 6681.



Antibodies and B cells recognizing citrullinated proteins display a broad cross-reactivity towards other post-translational modifications

Theresa Kissel[†], Sanne Reijm[†], Linda M. Slot, Marco Cavallari, Corrie M. Wortel, Rochelle D. Vergroesen, Gerrie Stoeken-Rijsbergen, Joanneke C. Kwekkeboom, Arieke S.B. Kampstra, E.W. Nivine Levarht, Jan W. Drijfhout, Holger Bang, Kim M. Bongers, George M.C. Janssen, Peter A. van Veelen, Tom W.J. Huizinga, Hans U. Scherer, Michael Reth, René E.M. Toes

[†] These authors contributed equally to this work as co-first authors.

Abstract

Autoantibodies against antigens carrying distinct post-translational modifications (PTMs), such as citrulline, homocitrulline or acetyl-lysine, are hallmarks of Rheumatoid Arthritis (RA). The relation between these anti-modified protein antibody (AMPA)-classes is poorly understood as is the ability of different PTM antigens to activate B-cell receptors (BCRs) directed against citrullinated proteins. Insights into the nature of PTMs able to activate such B cells are pivotal to understand the “evolution” of the autoimmune response conceivable underlying the disease. Here, we investigated the cross-reactivity of monoclonal AMPAs and the ability of different types of PTM antigens to activate citrullinated protein (CP)-reactive BCRs.

Therefore, BCR sequences from B cells isolated using citrullinated or acetylated antigens were used to produce monoclonal antibodies (mAb) followed by a detailed analysis of their cross-reactivity towards PTM antigens. Ramos B-cell transfectants expressing CP-reactive IgG BCRs were generated and their activation upon stimulation with PTM antigens investigated.

Most mAbs were highly cross-reactive towards multiple PTMs, while no reactivity was observed to the unmodified controls. B cells carrying CP-reactive BCRs showed activation upon stimulation with various types of PTM antigens.

Our study illustrates that AMPAs exhibit a high cross-reactivity towards at least two PTMs indicating that their recognition pattern is not confined to one type of modification. Furthermore, our data show that CP-reactive B cells are not only activated by citrullinated, but also by carbamylated and/or acetylated antigens. These data are vital for the understanding of the breach of B-cell tolerance against PTM antigens and the possible contribution of these antigens to RA-pathogenesis.

Introduction

Autoreactive B cells and their secreted autoantibodies are important players in many autoimmune diseases and often implicated in disease pathogenesis. Rheumatoid arthritis (RA) is hallmarked by the presence of several autoantibodies, such as rheumatoid factor (RF) and anti-citrullinated protein antibodies (ACPAs). The presence of these autoantibody families is routinely tested to aid RA-diagnosis and included into the EULAR/ACR-criteria for RA classification¹. ACPAs are present in 50-70% of RA patients and are known to recognize multiple citrullinated antigens, such as α -enolase, fibrinogen, filaggrin, vimentin and type II collagen²⁻⁷. Their recognition profile is generally broad and the serological ACPA response expands closer to disease-onset (epitope spreading) probably reflecting an escalation in the activation of citrullinated protein (CP)-reactive B cells⁸⁻¹⁰. Recently, autoantibodies recognizing other post-translationally modified (PTM) antigens, such as anti-carbamylated protein antibodies (ACarPAs) and anti-acetylated protein antibodies (AAPAs), were identified¹¹⁻¹³. ACPAs are directed against homocitrulline-containing (carbamylated) antigens and present in approximately 45% of RA patients, while AAPAs target acetylated-lysine residues and are found in 40% of RA patients^{12,13}. So far, it is unclear how these autoantibodies are generated and if their underlying B-cell responses are interrelated. As citrullination targets arginine residues, while carbamylation/acetylation predominantly lysine residues, the “modified” epitopes are, by definition, unrelated as they occur at different positions in the protein backbone and hence are surrounded by different flanking regions. Likewise, although homocitrullination and acetylation are both lysine modifications, they are structurally dissimilar. Consequently, ACPAs, ACPAs and AAPAs are often considered as three independent autoantibody classes¹¹. Nevertheless, these autoantibodies often occur concurrently in RA and cross-reactivity has been reported, both on a polyclonal- and monoclonal-level, within an ELISA setting¹³⁻¹⁷. Hence, it is clearly relevant to understand the (in)dependence of these different autoantibody responses in greater detail and to delineate the possibility that autoreactive B cells expressing a B-cell receptor (BCR) against one particular PTM can be activated by other modifications as well. Such understanding would not only be relevant for the comprehension of the breach of B-cell tolerance in RA, but also to uncover the antigens that could drive the expansion of autoreactive B cells conceivably present in the inflamed joint. Likewise, insights into the relations between AAPAs, ACPAs and their cross-reactivity, could not only help understanding RA-initiation, it could also lead to more refined serological markers for RA-diagnosis. Therefore, we characterized the properties of monoclonal IgG generated from BCR sequences of citrullinated and acetylated antigen-reactive B cells. Additionally, we generated, for the first time, human B-cell transfectants expressing CP-reactive BCRs to investigate the hypothesis that B cells recognizing citrullinated antigens are cross-reactive and can be activated by other PTMs.

Results

Isolation and successful production of monoclonal ACPA and AAPA IgG from peripheral blood B cells of RA patients

To characterize the reactivity patterns of various AMPA IgG, we produced 14 monoclonal IgG1 antibodies from BCR sequences of single cell sorted B cells from ACPA⁺ and AAPA⁺ RA patients. 11 antibodies were obtained from cyclic citrullinated peptide 2 (CCP2)-reactive B cells, one antibody from citrullinated-fibrinogen (7E4) and two antibodies from acetylated-vimentin (HC55)-reactive B cells (Table 1)¹⁸. All monoclonal antibodies (mAbs) were successfully produced as IgG1 molecules and exhibited the expected apparent molecular weight as determined by SDS-PAGE (Figure 1A). The mAbs were subsequently tested for reactivity towards peptides carrying the same modification as used for the isolation of the B cell from which the mAbs were generated (Figure 1B). All 12 ACPA IgG showed a high reactivity to CCP2 but not to its arginine control variant (CArgP2). Likewise, the AAPA IgG molecules showed acetylated-vimentin (HC55) reactivity, but no reactivity to the unmodified lysine-vimentin peptide (HC56).

Cross-reactivity of ACPA and AAPA IgG towards various PTM antigens

Having verified the successful production of monoclonal PTM antigen-directed IgGs, we next determined their binding characteristics towards various PTM peptides and proteins. We analyzed their reactivity to four linear peptides (fibrinogen α 27-43, fibrinogen β 36-52, vimentin 59-74 and enolase 5-20) and three cyclic peptides (CCP1, CCP2 and CCP4) carrying three different modifications: citrulline (cit), homocitrulline (hcit) and acetyl-lysine (ac). Likewise, reactivity to their arginine (arg), respectively lysine (lys)-containing controls was determined (Table S2, Figure 2 and Figure S5). Noteworthy, none of the mAbs was exclusively reactive towards the PTM that was originally used for the isolation of the autoreactive B cell. In fact, all mAbs showed reactivity towards at least two different PTMs, whereas several mAbs recognized all three PTMs (1F2, D9, 2C4 and 2F5) within the same antigenic backbone (Figures 2, A and B). No binding was observed for the non-modified control peptides indicating PTM antigen-specific reactivity.

To further validate these findings, we next analyzed the cross-reactivity of the mAbs towards modified proteins, using three PTM proteins (fibrinogen, OVA and vinculin) as well as carbamylated FCS (Figures 2, C and D). The results obtained largely confirmed the results of the peptide ELISA studies. We observed no reactivity of the ACPA and AAPA mAbs to the unmodified control proteins, but extensive cross-reactivity to the PTM proteins (Figures 2, C and D). The cross-reactive nature of the antibodies was further confirmed in another experimental setting examining three mAbs in western blot analyses. These antibodies (2G9, 7E4 and 2C4) were selected on the basis of their differential binding patterns in the peptide

and protein ELISAs. The results obtained by western blot indicated that monoclonal AMPA IgG recognize different epitopes within the PTM-fibrinogen α , β and λ chains (Figure 2E). More importantly, 7E4 recognized citrullinated- and acetylated-fibrinogen, as also observed in ELISA. Likewise, in agreement with the ELISA data, 2C4 reacted to all three PTM-variants of fibrinogen, whereas 2G9 mainly reacted to citrullinated-fibrinogen (Figure 2E).

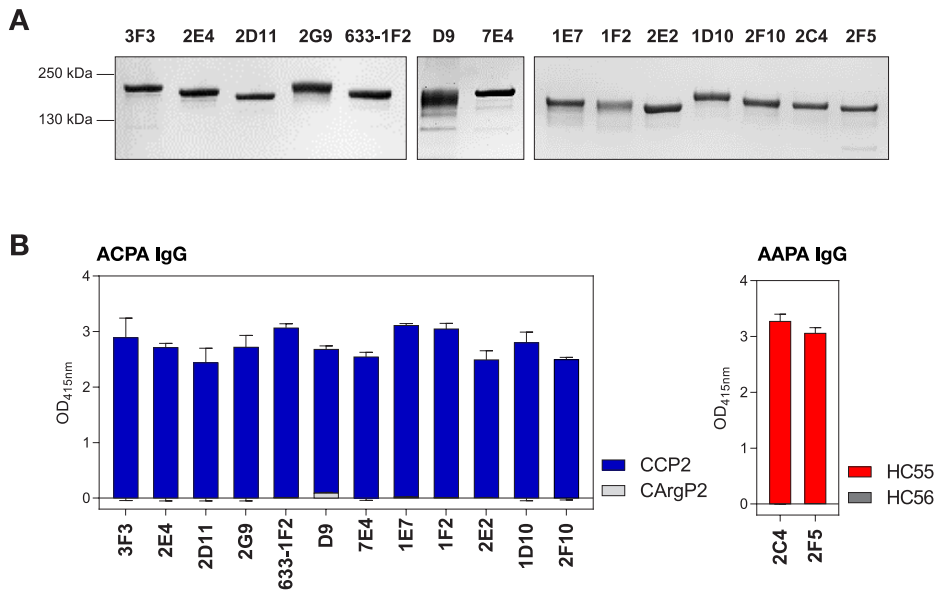


Figure 1. Production of 14 monoclonal AMPA IgG. (A) SDS-PAGE of purified monoclonal AMPA IgG using 4-15% gradient protein gels (BioRad). The size was determined using the PageRuler™ Plus Prestained Protein Ladder (Thermo Fisher Scientific). Molecular weights are higher than 150 kDa and vary between monoclonals due to the expression of different amounts of N-linked glycans within their V-domains. (B) Stacked bar graph of the CCP2/ CArgP2 (patent protected sequences) and acetylated-vimentin (HC55)/ lysine-vimentin (HC56) peptide ELISA of 12 purified monoclonal ACPA IgG and two AAPA IgG respectively. Reactivities were determined by the OD at 415 nm represented on the y-axis. The data represent the mean and standard error of 3 technical replicates.

Table 1. Monoclonal AMPA variable region sequences.

Tetramer[*]	AMPA	Patient	IGH-CDR3aa[†]	(nt) mut HC V-gene[†]	IGHV[†]	Identity [%][†]
CCP2	3F3	1	CARGTYLPVDESAAFDVW	56	IGHV1-2*02	80.56
CCP2	2E4	1	CARGSFLERPESVPFHPW	71	IGHV1-2*02	75.35
CCP2	2D11	2	CARRGGKDNVWGDW	21	IGHV5-51*01	92.71
CCP2	2G9	2	CVRWGEDRTEGLW	63	IGHV4-34*02	78.60
CCP2	633-1F2	2	CVRGGSLGIFGGSVGW	45	IGHV7-4-1*01	84.72
CCP2	D9	3	CARDLSKIFPLYGMDVW	54	IGHV3-30-3*01	81.25
Cit-fibrinogen	7E4 ¹⁸	4	CVRIRGGSSNWLDPW	63	IGHV4-39*01	77.08
CCP2	1E7	5	CARGIGLDVICEGFDVW	48	IGHV4-30-4*01	83.45
CCP2	1F2	5	CARGFGSAEELVCYGMVDW	50	IGHV4-30-4*04	82.76
CCP2	2E2	5	CARLQCSNGLCYLGDTFDIW	29	IGHV4-34*01	89.82
CCP2	1D10	5	CARGLGKTSLWGVDAFDVW	55	IGHV4-30-4*08	81.1
CCP2	2F10	5	CARALGKPLVWGVDSFDVW	38	IGHV4-30-4*01	86.94
Ac-vimentin	2C4	6	CATRHDDIWGHSSVIFDWTW	57	IGHV4-39*01	80.76
Ac-vimentin	2F5	6	CATRHYYDIRGRSSVIFETW	53	IGHV4-39*01	81.79

^{*} Tetramer used for single B cell isolation via flow cytometry.

[†] Determined by IMG/ V-QUEST.

To substantiate and further characterize the cross-reactive nature of the ACPA and AAPA IgG in a third experimental setting, we performed cross-inhibition studies using 2G9, 7E4 and 2C4 in combination with both modified peptides, C(C/Hcit/Ac)P2 and C(C/Hcit/Ac)P4 as well as proteins, citrullinated-, carbamylated- and acetylated-fibrinogen. The cross-inhibition studies showed that the reactivity of 7E4 to CCP2 and CCP4 could not only be inhibited by the citrullinated peptide itself, but also by its acetylated counterpart, while almost no inhibition could be observed after incubation with CHcitP2/CHcitP4 (Figures 3, A and S4). Similarly, reactivity towards citrullinated- and acetylated-fibrinogen could be inhibited by both the citrullinated version as well as the acetylated version of fibrinogen (Figure 3B). In agreement with titration ELISAs showing some reactivity of 7E4 towards carbamylated-fibrinogen at high concentrations (Figure S1A), binding of 7E4 to citrullinated- and acetylated-fibrinogen could be inhibited after pre-incubation with high amounts of carbamylated-fibrinogen (Figure 3B). Thus, together, these cross-inhibition results show that the mAb reactivity towards one particular PTM can be inhibited by another PTM and thereby confirm the reactivity data obtained by ELISA. Likewise, as depicted in Figures 3, A and B, similar findings were made for 2G9 and 2C4 reaffirming the outcome of the reactivity patterns observed by the peptide/protein ELISAs (Figure 2 and Figure 3, A and B).

IGHD [†]	IGHJ [†]	IGL-CDR3aa [†]	(nt) mut LC V-gene [†]	LC	IGK/LV [†]	Identity [%] [†]	IGLJ [†]
IGHD2-8*01	IGHJ3*01	CQQYYEAPYTF	39	κ	IGKV4-1*01	87.54	IGKJ2*01
IGHD3-3*01	IGHJ3*01	CLQYHAEPYTF	61	κ	IGKV4-1*01	79.46	IGKJ2*01
IGHD3-3*01	IGHJ4*02	CQQYNDWPVTF	11	κ	IGKV3-15*01	96.06	IGKJ2*01
IGHD2-21*02	IGHJ5*02	CMQRLRFPLTF	31	κ	IGKV2-40*01	89.56	IGKJ4*01
IGHD3-10*02	IGHJ4*03	CQSYRGDWVL	47	λ	IGLV6-57*02	84.19	IGLJ3*02
IGHD3-3*01	IGHJ6*02	CHHYGFSPCSF	26	κ	IGKV3-20*01	90.78	IGKJ2*04
IGHD2-15*01	IGHJ5*02	CAAWNGRLSAFVF	48	λ	IGLV1-51*01	83.86	IGLJ1*01
IGHD3-10*01	IGHJ3*01	CQSFDSGLIF	30	λ	IGLV6-57*01	90.38	IGLJ2*01
IGHD2-15*01	IGHJ6*02	CQSYDVSGLVF	15	λ	IGLV6-57*01	95.53	IGLJ2/J3*01
IGHD2-8*01	IGHJ3*02	CQQYVSYSTF	18	κ	IGKV1-5*01	93.55	IGKJ1*01
IGHD3-16*02	IGHJ3*01	CQQSNSSSSITF	43	κ	IGKV1-39*01	85.66	IGKJ4*01
IGHD2-15*01	IGHJ3*01	CQQSNSTLSLTF	36	κ	IGKV1-39*01	87.10	IGKJ4*01
IGHD3-16*01	IGHJ5*02	CQSADSEGLDILF	54	λ	IGLV3-25*03	80.65	IGLJ2/J3*01
IGHD3-16*01	IGHJ5*02	CQSSDSTGEDILF	44	λ	IGLV3-25*03	84.23	IGLJ2/J3*01

Altogether, these data indicate that all ACPA and AAPA mAbs analyzed cross-react to a varying extent to at least one other PTM and hence should be regarded as anti-modified protein antibodies (AMPAs) rather than as antibodies with a single specificity.

Human B cells expressing CP-reactive BCRs are activated upon stimulation with different PTM antigens

The data described above show a high degree of cross-reactivity of AMPAs towards several modifications and hence suggest that also CP-reactive B cells could react to multiple PTMs. To determine whether such B cells can indeed be activated by several PTMs, we next expressed three different IgGs (7E4, 3F3 and 2G9), isolated from CP-reactive B cells of RA patients, in a membrane-bound (mIgG) state on a human reporter B-cell line. To this end, we used the human lymphoma Ramos B-cell line in which the genes encoding the endogenous IgD and IgM heavy- and light-chain sequences and the gene encoding for activation-induced cytidine deaminase (AID) have been deleted, (MDL-AID). This “triple knockout (KO)” cell line is unable to show BCR signaling as it lacks an endogenous BCR. Moreover, it cannot modify a transduced BCR as it lacks AID. Upon transduction Ramos B-cell lines showed GFP and BCR expression, indicating a successful transduction and expression of CP-reactive BCRs. Indeed, binding of the CCP2 antigen, but not of the arginine containing control peptide CArgP2, was observed after incubating the transduced B cells with these antigens (Figure S2).

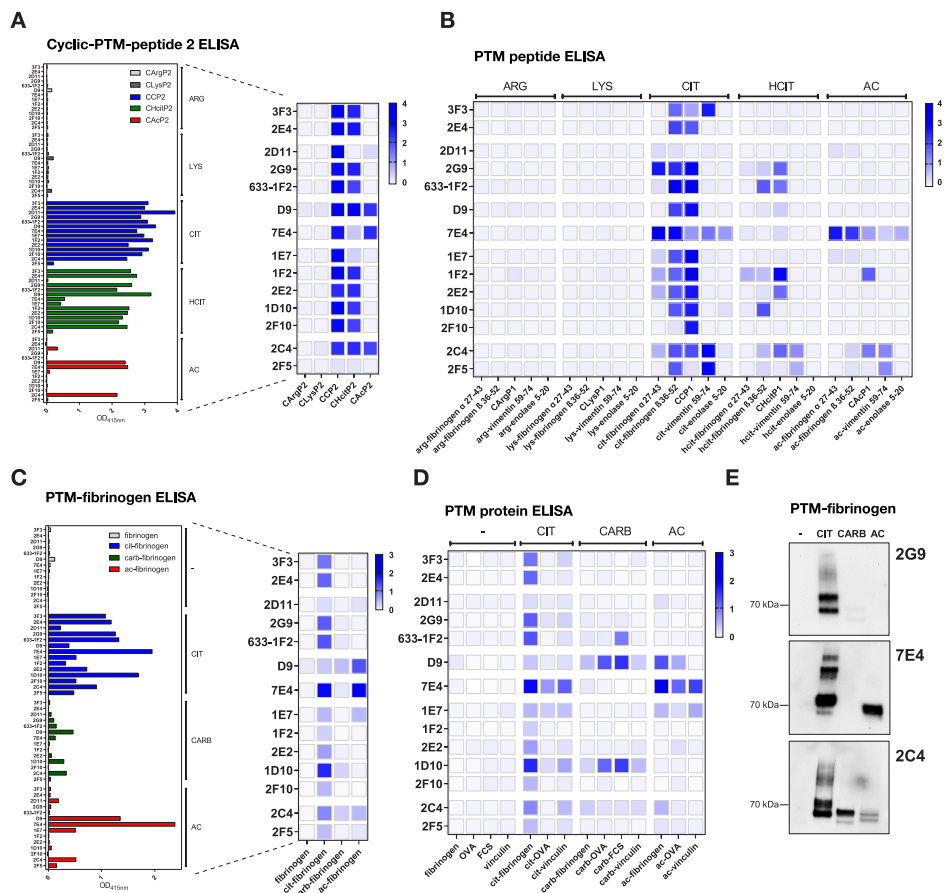


Figure 2. Cross-reactivity of monoclonal AMPA IgG determined by ELISA and western blot analysis. (A) Bar graph and heatmap of a cyclic-PTM-peptide 2 (C/C/Hcit/Ac)P2) ELISA of 14 monoclonal AMPA IgG. Monoclonal AMPA IgG reactivity towards the CCP2 (patent protected sequence) peptide in five modifications (citrulline, homocitrulline, acetyl-lysine, arginine, lysine) was tested. (B) Heatmap of PTM peptide ELISAs of 14 monoclonal AMPA IgG. Monoclonal reactivity to four linear PTM peptides (fibrinogen α 27-43, fibrinogen β 36-52, vimentin 59-74 and enolase 5-20) and the CCP1 peptide in five modifications (arg, lys, cit, hcit, ac) was analyzed. (C) Bar graph and heatmap of PTM-fibrinogen ELISA of 14 monoclonal AMPA IgG. Monoclonal AMPA IgG reactivity to the fibrinogen protein in four different versions (unmodified, cit, carb and ac) was tested. (D) Heatmap of PTM protein ELISAs of 14 monoclonal AMPA IgG. Monoclonal reactivity to fibrinogen, OVA and vinculin proteins in four different modifications (unmodified, cit, carb and ac) as well as to carb-FCS and unmodified FCS was analyzed. Reactivities were determined by the OD at 415 nm represented on the x-axis (bar graphs) or by color (blue, high OD values, light gray, low OD values) within the heatmaps. Monoclonal AMPA IgG were tested in a concentration of 10 μ g/ml. 2D11 was analyzed in a concentration of 20 μ g/ml within the cyclic-PTM-peptide 2 ELISA. All ELISA experiments were repeated independently 2 to 3 times. (E) Western blot analysis of monoclonal AMPA IgG 2G9, 7E4 and 2C4. Binding towards citrullinated-, carbamylated- and acetylated-fibrinogen and to the unmodified version (-) was analyzed under reducing conditions (separately to the α , β and λ chain). Western blot analysis was repeated 3 times within independent experiments.

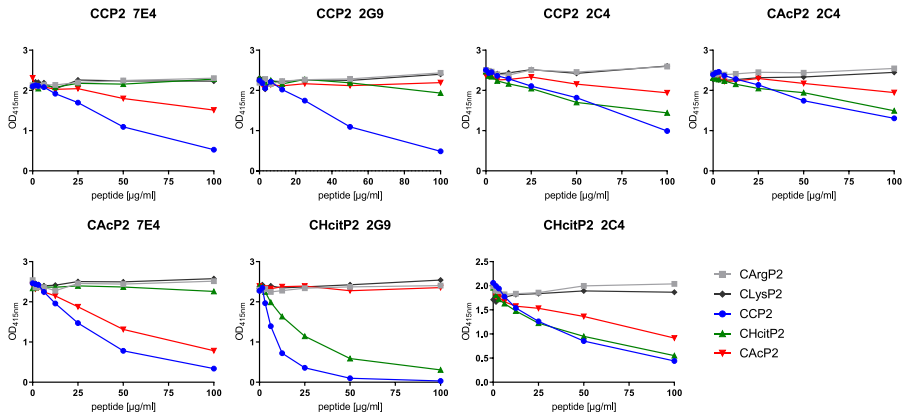
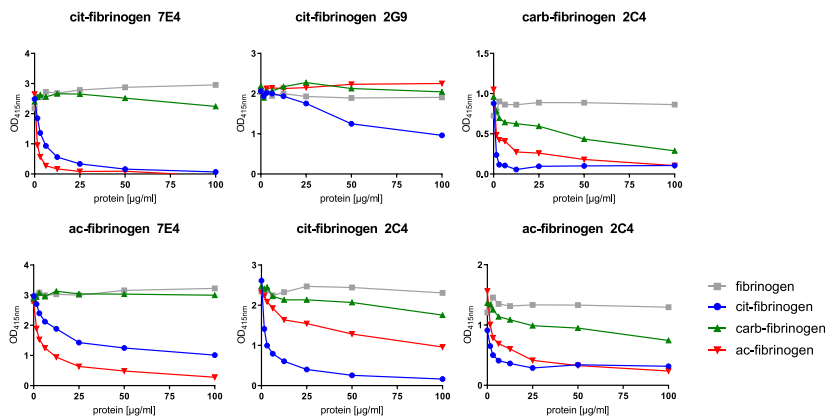
A**Cyclic-PTM-peptide 2****B****PTM-fibrinogen protein**

Figure 3. Cross-inhibition studies of monoclonal AMPA IgG determined by ELISA. (A) Cross-inhibition ELISA with cyclic-PTM-peptide 2 as an inhibitor depicted for 7E4 using CCP2- as well as CACp2-coated plates, for 2G9 using CCP2- and CHcitP2-coated plates and for 2C4 using CCP2-, CHcitP2- and CACp2-coated ELISA plates. Cross-inhibition was performed with increasing concentrations of the C-PTM-P2 peptide in all three modifications (cit, hcit and ac) and with the negative control peptides CArgP2 and CLysP2. The C-PTM-P2 peptide sequences are patent protected. **(B)** PTM-fibrinogen cross-inhibition ELISA curves of 7E4 for citrullinated- and acetylated-fibrinogen coated plates, of 2G9 for a citrullinated-fibrinogen coated plate and of 2C4 for citrullinated-, carbamylated- and acetylated-fibrinogen coated plates. Cross-inhibition was performed with increasing concentrations of all four different versions of fibrinogen (unmodified, cit, carb and ac). Monoclonals were tested in concentrations that bound within the linear range of the respective peptide or protein titration ELISA (Figure S1). Binding is represented by the OD at 415 nm on the y-axis. Cross-inhibition studies were performed 2-times within independent experiments. Light gray octagon: arginine, dark gray diamond: lysine, blue circle: citrulline, red triangle: acetyl, green square: homocitrulline/carbamyl.

Next, we used the cells to study BCR activation via phosphorylation of intracellular Syk (pSyk) 5 min after stimulation with different PTM antigens. The non-transduced MDL-AID KO cell line (BCR-GFP) was taken along as a negative/gating control. As depicted in Figures 4 and S3, Syk was phosphorylated after stimulating the 7E4, 3F3 and 2G9 Ramos B-cell transfectants with the respective PTM antigen. To quantify B-cell activation, the percentage of pSyk⁺GFP⁺ cells was determined. 7E4 mIgG carrying B cells readily reacted to stimulation with citrullinated peptides ($25.25 \pm 7.142\%$) and to stimulation with acetyl-lysine-containing peptides ($22.35 \pm 7.990\%$). In contrast, the cells did not respond to stimulation with a homocitrulline-containing peptide ($0.9450 \pm 0.8560\%$) (Table S6, Figure 4B). These data indicate that the results obtained in the “non-functional assays” described above translate to the functional activation of 7E4 CP-reactive B cells. More importantly, these results also show that such B cells respond to several PTMs. Similar results were obtained in the activation assays using 3F3- and 2G9-derived B cells, showing not only activation upon stimulation with citrullinated peptides (3F3: $28.85 \pm 2.475\%$; 2G9: $15.00 \pm 4.950\%$), but also with homocitrullinated peptides (3F3: $21.30 \pm 2.828\%$; 2G9: $14.49 \pm 6.944\%$). In line with our results obtained by ELISA these cell lines did not respond to acetyl-lysine-containing peptides (3F3: $0.8250 \pm 0.2470\%$; 2G9: $0.0000 \pm 0.0000\%$) (Table S6, Figure 4, C and D). To expand the findings described above to the recognition of protein antigens, we next analyzed the ability of the different modified forms of fibrinogen to stimulate the CP-reactive B cells. As shown in Figure 2B, 3F3 and 2G9 bind solely to citrullinated-fibrinogen in ELISA. In agreement, Ramos cells transduced with these IgG sequences displayed only reactivity to this modification (Figure S3). More importantly, and in agreement with the data presented in Figure 2B, Ramos B cells transduced with 7E4 not only responded to citrullinated-fibrinogen, but also displayed reactivity towards the acetylated counterpart (Table S7, Figure 4B), indicating that CP-reactive B-cells can respond to several PTM proteins. Together, these data show that autoreactive B cells expressing a BCR directed against one type of modification can also be activated by other PTMs.

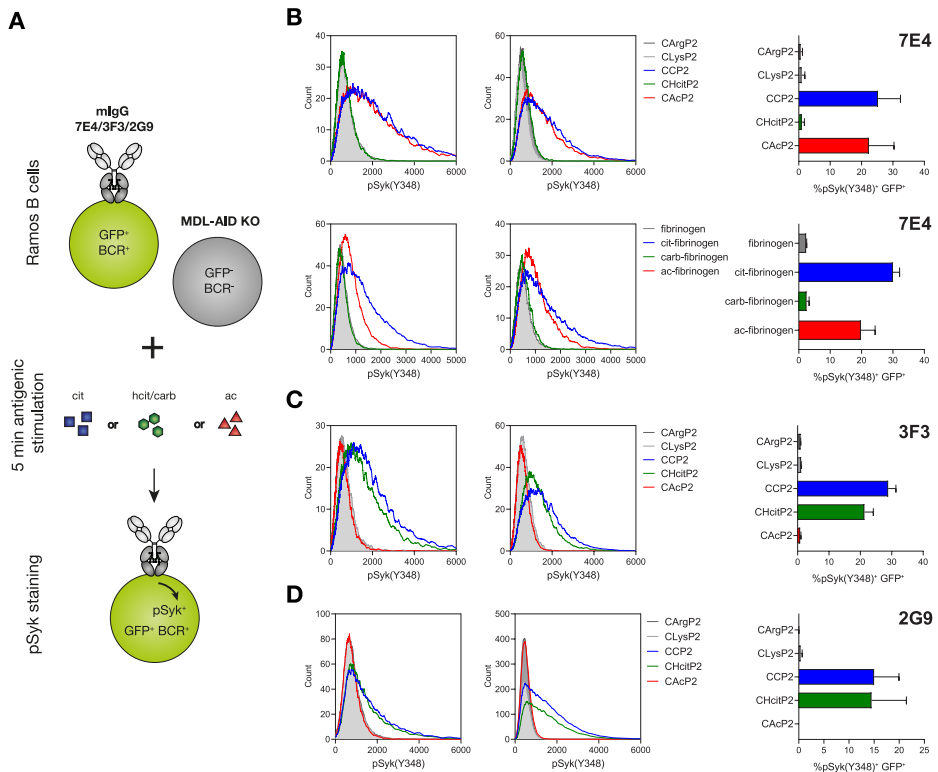


Figure 4. B-cell receptor signaling (pSyk expression) of CP-reactive BCR⁺GFP⁺ Ramos B-cell transfectants after stimulation with PTM antigens. (A) Schematic depiction of the experimental activation assay design. GFP⁺mIgG BCR⁺ Ramos B-cell transfectants and the untransfected GFP BCR⁺ control MDL-AID KO cell line were stimulated for 5 min with PTM antigens. BCR activation was determined as the proportion/percentage of GFP⁺pSyk(Y348)⁺ B cells. Stimulation with cit-antigens leads to an “ACPA” response (blue), hcit/carb-activation results in an “ACarPA” response (green) and ac-antigen activation leads to an “AAPA” response (red). (B) Histograms of two biological replicates and a bar graph (n = 2) showing the percentage of pSyk(Y348)⁺GFP⁺ 7E4 mIgG Ramos B-cells after stimulation with cyclic-PTM-peptide 2 and PTM-fibrinogen (C) Histograms of two biological replicates and a bar graph (n = 2) showing the percentage of pSyk(Y348)⁺GFP⁺ 3F3 mIgG Ramos B cells after stimulation with cyclic-PTM-peptide 2 (D) Histograms of two biological replicates and a bar graph (n=2) showing the percentage of pSyk(Y348)⁺GFP⁺ 2G9 mIgG Ramos B cells after stimulation with cyclic-PTM-peptide 2. The C-PTM-P2 peptide sequences are patent protected. All activation assays were repeated 2 to 3 times within independent experiments. CArgP2 = dark gray, CLysP2 = light gray, CCP2 = blue, CHcitP2 = green, CACp2 = red. Unmodified fibrinogen = light gray, cit-fibrinogen = blue, carb-fibrinogen = green, ac-fibrinogen = red.

Discussion

Insights into the dynamics of autoimmune responses are vital to understand the breach of tolerance to self-antigens and the “evolution” of the autoimmune response conceivably underlying the disease. Even though the ACPA response is considered as the dominating AMPA-response linked to the most prominent genetic risk factors for RA (the HLA-SE alleles), it is clear that autoantibody responses present in RA patients extend towards several modifications, such as acetylation and/or carbamylation. AMPA-responses are currently considered to consist of different autoantibody classes that are largely distinct in origin and development. Nonetheless, AMPAs also display a certain degree of cross-reactivity and often occur concurrently in individual patients. Recently, we made the crucial observation that vaccinating mice with an acetylated protein leads to the formation of autoantibodies against carbamylated proteins, indicating that different AMPA-responses can evolve from the exposure to only one type of modification. These data provide a conceptual framework for the simultaneous presence of different AMPA-responses in RA by showing that the inciting antigen responsible for the induction of e.g. ACPAs does not have to be carbamylated, but could be represented by an acetylated protein. We now show that human monoclonal ACPAs and AAPAs isolated from AMPA-positive RA patients (Figure S5) are highly cross-reactive towards various PTM antigens (Figure 2). Noteworthy, all ACPA and AAPA IgG analyzed were able to recognize at least two diverse modifications. This finding has general importance, as it indicates that ACPAs, ACPAs and AAPAs should be considered as AMPAs that are not specific for one type of PTM. Furthermore, our results indicate that not only the affinity of the mAb towards a particular modification, but also the antigenic backbone and consequently the flanking regions around a modification can contribute to the reactivity-pattern of AMPA IgG. Depending on the antigen tested (CCP2 peptide or fibrinogen protein), and thus the flanking amino acids around a modification, the AMPAs showed a higher reactivity towards one or another PTM as detected in titration and cross-inhibition ELISAs (Figures 3 and S1). We consider it unlikely that these observations can solely be explained by the number of modifications per protein, which likely differ per PTM generated and might explain the higher mAb reactivity to carb-FCS compared to carb-fibrinogen, as this pattern is not consistent across different antibodies analyzed. Nonetheless, it is clear that additional analyses are required to elucidate the potential contribution of flanking regions to the reactivity of AMPAs towards PTMs.

Most importantly, our data show that B-cell lines transfected with a BCR derived from one type of defined “ACPA” can not only be activated by citrullinated, but also by other PTM antigens. For these studies, we implemented a unique and novel tool by expressing different CP-reactive IgG as BCRs in human Ramos B cells, an accepted model cell line to study BCR responses upon stimulation¹⁹. This enabled us to study human autoreactive B-cell responses on the cellular level. Our observations support the notion that B cells expressing a BCR against citrullinated antigens

could be activated by other, non-citrulline containing PTM antigens. Conceptually, these results are highly relevant to further understand and define the antigens that could be recognized in inflamed joints or at other locations in the body (mucosal tissues) which could be involved in the induction of autoimmunity. Likewise, these findings point to the possibility that a first encounter with a particular PTM can not only initiate an AMPA-response, but also determines the direction of it, conceivably dictating a progression towards “ACPA-, ACarPA- or AAPA-dominated” B-cell responses. It is tempting to hypothesize that subsequent antigenic contacts, with different PTM antigens, could (re)direct the B-cell response towards other modifications, or reinforce the original direction of the AMPA-response. In this way, the concurrent presence of multiple AMPA-reactivities, as observed in many RA patients, can be explained, and the observation that in other patients the response can be dominated by one AMPA-response towards e.g. citrullinated, carbamylated or acetylated proteins. It would be interesting to investigate the extent of cross-reactivity in different disease stages, ranging from health to arthralgia, undifferentiated arthritis and RA within future studies. Here, we suggest that AMPA B-cell responses should be considered dynamic responses without a “fixed” categorization into different AMPA-classes. We speculate that the inciting and subsequent encounters with particular PTM antigens define the course of the autoreactive B-cell responses, resulting in the heterogeneous reactivity-pattern observed in patients with RA (Figure 5).

Thus, our data disclose a strong relationship and high cross-reactivity between various autoantibodies and their B cells in RA patients, explaining the concurrent presence of ACPA-, ACarPA- and AAPA-responses. These findings are important to further our understanding of the breach of B-cell tolerance in RA and to unmask the antigens recognized in inflamed tissues.

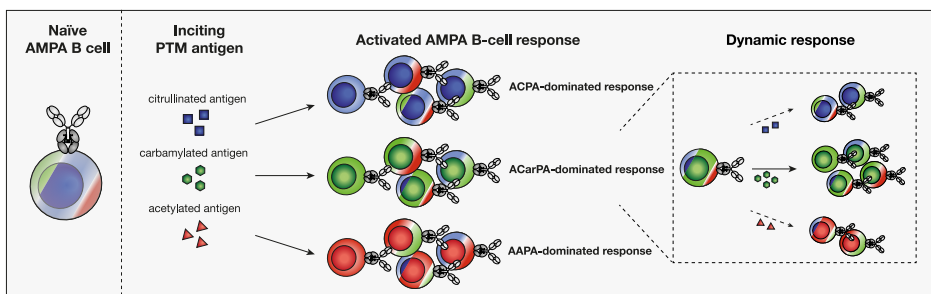


Figure 5. Schematic depiction of an hypothesis proposing the course of autoreactive AMPA B-cell responses.

Naïve B cells expressing BCRs directed against PTM antigens display reactivity towards citrullinated (blue), carbamylated (green) or acetylated (red) antigens. The inciting trigger could represent either a citrullinated, carbamylated or acetylated antigen. Dependent on this initial priming, the B cells are directed towards an “ACPA-, ACarPA- or AAPA-dominated” B-cell response. Upon subsequent encounter of other PTMs, the AMPA-response can be (re)directed towards another AMPA-class (dynamic response) or the original direction of the AMPA-response can be reinforced (outgrowth of e.g. “ACarPA-dominated” B-cell responses).

Materials and Methods

Patient and public involvement - Peripheral blood samples from ACPA⁺ or ACPA⁺/AAPA⁺ RA patients visiting the outpatient clinic of the Rheumatology Department at the Leiden University Medical Center (LUMC) were included in this study. RA patients included in this study were selected on their high anti-CCP2 positivity (ACPA⁺, >340 U/ml) based on in-house CCP2 ELISAs (see ELISA section). Patient 6, used for the monoclonal AAPA isolation, was selected based on AAPA-positivity determined by an acetylated-vimentin (HC55) ELISA (Orgentec)²⁰. All patients fulfilled the EULAR/ACR 2010-criteria for classification of RA and provided written informed consent prior to inclusion¹. None of the patients was previously treated with B-cell depletion therapies. Ethical permission was obtained from the institutional review board. Further clinical patient characteristics, including AMPA status, are given in Table S1.

Protein modification and mass spectrometry (MS) analysis - Vinculin, fibrinogen, and ovalbumin (OVA, Sigma Aldrich) protein modification (citrullination, carbamylation and acetylation) as well as FCS carbamylation was performed as previously described^{13,16}. Mass spectrometry (MS) of PTM-fibrinogen was performed as previously described¹⁶. Briefly, in-gel tryptic digestion of reduced PTM-fibrinogen (native, citrullinated, acetylated, carbamylated) was performed. Tryptic peptides were extracted from the gel, lyophilized, dissolved and analyzed by on-line C18 nano HPLC MS/MS with a system consisting of an Easy nLC 1200 gradient HPLC system (Thermo, Bremen, Germany), and an orbitrap Fusion LUMOS mass spectrometer (Thermo). In a post-analysis process, the raw data were first converted to peak lists using Proteome Discoverer version 2.2 (Thermo Electron), and then submitted to the Uniprot Homo sapiens canonical database (67911 entries), using Mascot v. 2.2.07 (www.matrixscience.com) for protein identification. Mascot searches were with 10 ppm and 0.02 Da deviation for precursor and fragment mass, respectively, and trypsin as enzyme. Up to two missed cleavages were allowed. The following modifications were set for the searches: oxidation (on M), carbamylation (on K and on peptide N-terminus), citrullination (on R), acetylation (on K and on peptide N-terminus) and deamidation (on N-terminus) were set as a variable modification; carbamidomethyl (on C) was set as a fixed modification. An FDR threshold of 0.01 was initially set. All spectra of the post-translationally modified peptides were manually evaluated for proper identification. In addition, all citrullinated peptides identified after PAD treatment were specifically cross checked in the other post-translationally modified samples as well as in the native control to exclude cross-contamination. The results are listed in Table S5. The MS proteomics data have been deposited to the ProteomeXchange Consortium via the PRIDE²¹ partner repository with the dataset identifier PXD017127.

Peptide synthesis and integrity identification - Four linear N-terminal biotinylated peptides, fibrinogen α 27-42, fibrinogen β 36-52, vimentin 59-74 and enolase 5-20, and three cyclic N-terminal biotinylated peptides, C(C/Hcit/Ac)P1, C(C/Hcit/Ac)P2 (patent EP2071335) and C(C/Hcit/Ac)P4, were synthesized in five different modifications including the altered amino acid residue(s) at the same positions within the peptide sequence (citrulline, arginine, homocitrulline, acetyl-lysine, lysine)^{10,22}. The CCP4 peptides were cyclized as previously described²³. The patent protected C(C/Hcit/Ac)P2 peptides were provided by J. W. Drijfhout (LUMC, The Netherlands). The HC55 and HC56 peptides, used for the isolation of AAPA IgG sequences, were synthesized and provided by H. Bang (Orgentec, Germany)²⁰. The known peptide sequences are listed in Table S2. The integrity of the synthesized peptides after purification was examined by ultra-performance liquid chromatography (UPLC) on a Acquity instrument (Waters) and the exact mass measured via MS on a Microflex instrument (Bruker) and crosschecked with the calculated masses (Tables S3 and S4).

Production of monoclonal AMPA IgG based on BCR sequences from RA patients - 11 ACPA IgG sequences were isolated from ACPA⁺ RA patients. CCP2- and CArgP2-streptavidin tetramers were used for the isolation of CP-reactive B cells as previously described²⁴. Single sorted cells were cultured on irradiated CD40L-cells and a cytokine mixture in complex IMDM (Gibco) medium for 10 to 12 days²⁵. RNA isolation, cDNA synthesis, ARTISAN PCR and sequencing were performed as previously described^{26,27}. The same methodology using acetylated-vimentin-(HC55) and lysine-vimentin-(HC56) streptavidin tetramers was used to isolate two AAPA IgG sequences. The ACPA IgG 7E4 sequence was provided by T. Rispen (Sanquin, The Netherlands)¹⁸. Codon optimized AMPA heavy chain (HC) and light chain (LC) V gene sequences, including 5'-BamHI and 3'-XhoI restriction sites, the Kozak sequence, and the IGHV1-18*01 leader sequence, were designed, ordered from GeneArt (Life Technologies) and ligated into a pcDNA3.1 (+) expression vector (Invitrogen) carrying the IGHG1 or the IGLC3/IGKC constant regions (UniProt) respectively flanking 3'-XhoI site. The ACPA IgG HC and LC containing vectors were transfected into FreestyleTM 293-F cells (Gibco). Cells were cultured in FreestyleTM 293 expression medium (Gibco) at 37 °C, 8% CO₂ on a shaking platform. Transfection was performed in Opti-MEM[®] (Gibco) together with the expression enhancing plasmids, encoding the large T antigen of the SV40 virus (GeneArt) and the cell cycle inhibitors p21 and p27 (Invivogen), as well as 293-FectinTM (Invitrogen) as previously described²⁸. Glycoengineering was performed by adding D-galactose substrate to the medium before transfection (Sigma Aldrich, G0750-5G). Further, to generate complex-type N-glycans on the antibody V-domains, recombinant AMPA IgG were co-expressed with 1% β -1,4-N-acetylglucosaminyltransferase III (GnTIII), 2.5% α 2,6-sialyltransferase 1 (ST6galT) and 1% β -1,4-Galactosyltransferase 1 (B4GalT1). The supernatants were harvested 5 to 6 days post-transfection.

Protein G affinity purification and size exclusion chromatography of AMPA IgG -

The IgG1 antibodies were purified using a 1ml HiTrap® Protein G HP affinity column (GE Healthcare) according to the manufacturer's instructions. Size exclusion chromatography (SEC) was performed for buffer exchange and for the exclusion of single HCs or LCs using a 53 ml HiPrep™ 26/10 Desalting column (GE Healthcare) according to the manufacturer's instructions. Monoclonal antibodies (mAbs) were concentrated with Amicon® Ultra-15 50 K filter devices (Merck) to a final concentration of 1 mg/ml and used for further experiments.

Generation of human Ramos B-cell transfectants expressing CP-reactive IgG BCRs

- 7E4, 2G9 and 3F3 ACPA IgG1 HC and LC containing single vector constructs were created with the In-Fusion HD Cloning Kit (Clontech) using the pMIG-IRES-GFP-2AP vector as a backbone including the IGHG1 transmembrane domain. The lymphoma Ramos cell line expressing the murine cationic amino-acid transporter 1 (*slc7a1*) under blasticidine resistance to be able to infect them with Moloney Murine Leukemia Virus (MoMLV)-based retrovirus particles, was provided by Dr. Engels (University Göttingen, Germany). The MDL-AID (IGHM, IGHD, IGLC and activation-induced cytidin deaminase, AID) knock-out (KO) variant of the *slc7a1* expressing Ramos cells was generated by Dr. He (University Freiburg, Germany). All inserts were verified by sequencing. Ramos cell lines were cultured in RPMI1640/GlutaMAX™/10% FCS/10 mM Hepes medium (Thermo Fisher Scientific) with 100 units/ml penicillin/streptomycin (P/S) (Lonza). Retroviral transductions in Ramos cells were performed as previously described²⁹. Briefly, Phoenix-ECO (ATCC CRL-3212™) cells were transfected with PolyJet DNA transfection reagent following the manufacturer's instructions (SigmaGen Laboratories). Retrovirus containing supernatants were collected 72 hours after transfection and used for the transduction into MDL-AID KO Ramos cells carrying *slc7a1*.

Enzyme-linked immunosorbent assays (ELISA) - Briefly, 1 µg/ml biotinylated C-PTM-P2 and 10 µg/ml biotinylated PTM peptides were coupled to pre-coated streptavidin plates (Microcoat, #65001) via incubation at RT for 1 hour. 10 µg mAbs were added in PBS/1%BSA/0.05% Tween (PBT) (Sigma Aldrich) and samples incubated for 1 hour at 37 °C. Protein ELISAs were performed as previously described¹³. Briefly, 10 µg/ml PTM protein was directly coupled to Nunc Maxisorp plates (Thermo Fisher Scientific) and incubated overnight on ice at 4 °C. Following blocking with PBS/2% BSA for 6 hours, 10 µg of the monoclonal was added in PBT and incubated overnight on ice at 4 °C. Concentrations used for titration ELISAs are mentioned within the legend to the figure. Monoclonal AMPA IgG binding was detected using an HRP-conjugated rabbit-anti-human IgG secondary antibody (DAKO, P0214). ELISA read-out was performed using ABTS and H2O2. Reactivity to PTM peptides and proteins was determined based on the unmodified protein or the arginine or lysine version of the peptide. For cross-inhibition studies, mAbs were pre-incubated

with increasing concentrations (0 to 100 $\mu\text{g/ml}$) of either unmodified, citrullinated-, carbamylated- or acetylated-fibrinogen protein, C(Arg/Lys/C/Hcit/Ac)P2 or C(Arg/Lys/C/Hcit/Ac)P4 peptides for 1 hour at RT. The antibody-antigen complexes were added to PTM-fibrinogen, cyclic-PTM-peptide 2 or cyclic-PTM-peptide 4 coated plates respectively and the ELISA read-out was performed as described above.

SDS-PAGE and western blot analysis - For SDS-PAGE, 1.5 μg of each monoclonal AMPA IgG in PBS was diluted in 4 \times Laemmli buffer (Bio Rad) and incubated for 5 min at 95 $^{\circ}\text{C}$. 10 μl sample and 3 μl PageRuler™ Plus Prestained Protein Ladder (Thermo Fisher Scientific) were loaded on 4-15% SDS-polyacrylamide gels (Bio Rad). Western blot analysis was performed as previously described¹³. In brief, PTM-fibrinogen proteins (fibrinogen, cit-, carb- and ac-fibrinogen) were subjected to 4-15% SDS-polyacrylamide gels (Bio Rad). Subsequently immunoblotting was performed on a Nitrocellulose membrane (Bio Rad). Blots were incubated in blocking buffer (3% skim milk powder/PBS/0.05% tween) for 1 hour at RT. Following washing with PBS/0.05% tween (PT), the blots were incubated with 1 to 3 $\mu\text{g/ml}$ monoclonal AMPA IgG diluted in 5 ml blocking buffer at 4 $^{\circ}\text{C}$ overnight. After washing with PT, blots were incubated for 1 hour at RT with 5 ml HRP-conjugated rabbit-anti-human IgG secondary antibody (DAKO, P0214), diluted 1:5000 in blocking buffer. Blots were washed and bound antibodies visualized using enhanced chemiluminescence (GE Healthcare, RPN2109).

Activation assays of Ramos B cells expressing CP-reactive BCRs - GFP⁺BCR⁺ (7E4, 2G9, 2C4) Ramos B-cell lines (1 $\times 10^6$ cells) were stimulated with C(Arg/Lys/C/Hcit/Ac)P2-streptavidin tetramers (10 $\mu\text{g/ml}$)²⁴ for 5 min at 37 $^{\circ}\text{C}$ in stimulation medium (RPMI/GlutaMAX™/1% FCS/10 mM Hepes/100 units/ml P/S). Additionally, stimulation was performed with unmodified, citrullinated-, carbamylated- and acetylated-fibrinogen proteins (50 $\mu\text{g/ml}$). Afterwards, cells were fixed (Biolegend Fixation Buffer, 420801) and permeabilized (True-Phos™ Perm Buffer, 425401). After washing, cells were stained with mouse anti-human pSyk(Y348)-PE mAb (moch1ct, eBioscience™) diluted 1:20 in PBS/0.5% BSA/0.02% NaN₃. The rate of pSyk expression in Ramos cells was calculated as the percentage and proportion of pSyk⁺GFP⁺ double positive cells. Gating was based on the MDL-AID KO control cell line stimulated with the citrullinated antigen and on isotype control staining's using mouse IgG1 kappa isotype control-PE mAb (P3.6.2.8.1, eBioscience™). Stained cells were analyzed on a BD LSR-II flow cytometry instrument. Data were analyzed with FlowJo_V10.

Acknowledgments

The authors would like to thank Natasja Dolezal (LUMC, Leiden, The Netherlands) for synthesizing the PTM peptides and Dr. Theo Rispens (Sanquin, Amsterdam, The Netherlands) for providing the 7E4 ACPA IgG BCR sequence.

Funding

This work was supported by ReumaNederland 17-1-402 (to R.E.M.T.), the IMI-funded project RTCure 777357 (to T.W.J.H.), ZonMw TOP 91214031 (to R.E.M.T.), Target-to-B LSHM18055-SGF (to R.E.M.T.), NWO-ZonMW clinical fellowship 90714509 (to H.U.S.), NWO-ZonMW VENI grant 91617107 (to H.U.S.), ZonMW Enabling Technology Hotels grant 435002030 (to H.U.S.), Dutch Arthritis Foundation 15-2-402 and 18-1-205 (to H.U.S.), Excellence Initiative of the German Federal and State Governments EXC 294 (to M.R.), DFG through TRR130-PO2 (to M.R.), RO1 grant A031503 (to M.R.) and by the Investment Grant NWO Medium 91116004, which is (partially) financed by ZonMw. (to P.A.v.V.)

Conflict of interest

No.

Author contributions

All authors were involved in drafting the article or revising it critically for important intellectual content, and all authors approved the final version to be published. Conceptualization: T.K., S.R., T.W.J.H., H.U.S., M.R., and R.E.M.T. Methodology: T.K., S.R., L.M.S., M.C., C.M.W., R.D.V. and G.M.C.J. Software: T.K., J.W.D., H.B., G.M.C.J. and P.A.v.V. Investigation: T.K., S.R., L.M.S., M.C., C.M.W., R.D.V., G.S.-R., J.C.K., A.S.B.K., E.W.N.L., J.W.D., H.B., K.M.B., G.M.C.J., P.A.v.V. Visualization: T.K. Supervision: M.R., T.W.J.H., H.U.S., and R.E.M.T. Writing—original draft: T.K. and R.E.M.T. Writing—review and editing: S.R., L.M.S., M.C., C.M.W., R.D.V., G.S.-R., J.C.K., A.S.B.K., E.W.N.L., J.W.D., H.B., K.M.B., G.M.C.J., P.A.v.V., T.W.J.H., H.U.S. and M.R.

References

- 1 Aletaha, D., Neogi, T., Silman, A. J., Funovits, J., Felson, D. T., Bingham, C. O., 3rd, et al., 2010 rheumatoid arthritis classification criteria: an American College of Rheumatology/European League Against Rheumatism collaborative initiative. *Ann Rheum Dis* 2010. 69: 1580-1588.
- 2 Schellekens, G. A., de Jong, B. A., van den Hoogen, F. H., van de Putte, L. B. and van Venrooij, W. J., Citrulline is an essential constituent of antigenic determinants recognized by rheumatoid arthritis-specific autoantibodies. *J Clin Invest* 1998. 101: 273-281.
- 3 Takizawa, Y., Suzuki, A., Sawada, T., Ohsaka, M., Inoue, T., Yamada, R., et al., Citrullinated fibrinogen detected as a soluble citrullinated autoantigen in rheumatoid arthritis synovial fluids. *Ann Rheum Dis* 2006. 65: 1013-1020.
- 4 Burkhardt, H., Koller, T., Engstrom, A., Nandakumar, K. S., Turnay, J., Kraetsch, H. G., et al., Epitope-specific recognition of type II collagen by rheumatoid arthritis antibodies is shared with recognition by antibodies that are arthritogenic in collagen-induced arthritis in the mouse. *Arthritis Rheum* 2002. 46: 2339-2348.
- 5 Vossenaar, E. R., Despres, N., Lapointe, E., van der Heijden, A., Lora, M., Senshu, T., et al., Rheumatoid arthritis specific anti-Sa antibodies target citrullinated vimentin. *Arthritis Res Ther* 2004. 6: R142-150.
- 6 Lundberg, K., Kinloch, A., Fisher, B. A., Wegner, N., Wait, R., Charles, P., et al., Antibodies to citrullinated alpha-enolase peptide 1 are specific for rheumatoid arthritis and cross-react with bacterial enolase. *Arthritis Rheum* 2008. 58: 3009-3019.
- 7 Ioan-Facsinay, A., el-Bannoudi, H., Scherer, H. U., van der Woude, D., Menard, H. A., Lora, M., et al., Anti-cyclic citrullinated peptide antibodies are a collection of anti-citrullinated protein antibodies and contain overlapping and non-overlapping reactivities. *Ann Rheum Dis* 2011. 70: 188-193.
- 8 Ge, C., Xu, B., Liang, B., Lonnblom, E., Lundstrom, S. L., Zubarev, R. A., et al., Structural Basis of Cross-Reactivity of Anti-Citrullinated Protein Antibodies. *Arthritis Rheumatol* 2019. 71: 210-221.
- 9 van der Woude, D., Rantapaa-Dahlqvist, S., Ioan-Facsinay, A., Onnekink, C., Schwarte, C. M., Verpoort, K. N., et al., Epitope spreading of the anti-citrullinated protein antibody response occurs before disease onset and is associated with the disease course of early arthritis. *Ann Rheum Dis* 2010. 69: 1554-1561.
- 10 Schellekens, G. A., Visser, H., de Jong, B. A., van den Hoogen, F. H., Hazes, J. M., Breedveld, F. C., et al., The diagnostic properties of rheumatoid arthritis antibodies recognizing a cyclic citrullinated peptide. *Arthritis Rheum* 2000. 43: 155-163.
- 11 Trouw, L. A., Rispen, T. and Toes, R. E. M., Beyond citrullination: other post-translational protein modifications in rheumatoid arthritis. *Nat Rev Rheumatol* 2017. 13: 331-339.
- 12 Juarez, M., Bang, H., Hammar, F., Reimer, U., Dyke, B., Sahbudin, I., et al., Identification of novel antiacetylated vimentin antibodies in patients with early inflammatory arthritis. *Ann Rheum Dis* 2016. 75: 1099-1107.
- 13 Shi, J., Knevel, R., Suwannalai, P., van der Linden, M. P., Janssen, G. M., van Veelen, P. A., et al., Autoantibodies recognizing carbamylated proteins are present in sera of patients with rheumatoid arthritis and predict joint damage. *Proc Natl Acad Sci U S A* 2011. 108: 17372-17377.
- 14 Lloyd, K. A., Wigerblad, G., Sahlstrom, P., Garimella, M. G., Chemin, K., Steen, J., et al., Differential ACPA Binding to Nuclear Antigens Reveals a PAD-Independent Pathway and a Distinct Subset of Acetylation Cross-Reactive Autoantibodies in Rheumatoid Arthritis. *Front Immunol* 2018. 9: 3033.
- 15 Reed, E., Jiang, X., Kharlamova, N., Ytterberg, A. J., Catrina, A. I., Israelsson, L., et al., Antibodies to carbamylated alpha-enolase epitopes in rheumatoid arthritis also bind citrullinated epitopes and are largely indistinct from anti-citrullinated protein antibodies. *Arthritis Res Ther* 2016. 18: 96.
- 16 Kampstra, A. S. B., Dekkers, J. S., Volkov, M., Dorjee, A. L., Hafkenscheid, L., Kempers, A. C., et al., Different classes of anti-modified protein antibodies are induced on exposure to antigens expressing only one type of modification. *Ann Rheum Dis* 2019. 78: 908-916.

- 17 Steen, J., Forsstrom, B., Sahlstrom, P., Odowd, V., Israelsson, L., Krishnamurthy, A., et al., Recognition of Amino Acid Motifs, Rather Than Specific Proteins, by Human Plasma Cell-Derived Monoclonal Antibodies to Posttranslationally Modified Proteins in Rheumatoid Arthritis. *Arthritis Rheumatol* 2019. 71: 196-209.
- 18 van de Stadt, L. A., van Schouwenburg, P. A., Bryde, S., Kruithof, S., van Schaardenburg, D., Hamann, D., et al., Monoclonal anti-citrullinated protein antibodies selected on citrullinated fibrinogen have distinct targets with different cross-reactivity patterns. *Rheumatology (Oxford)* 2013. 52: 631-635.
- 19 Villar, R. F., Patel, J., Weaver, G. C., Kanekiyo, M., Wheatley, A. K., Yassine, H. M., et al., Reconstituted B cell receptor signaling reveals carbohydrate-dependent mode of activation. *Sci Rep* 2016. 6: 36298.
- 20 Figueiredo, C. P., Bang, H., Cobra, J. F., Englbrecht, M., Hueber, A. J., Haschka, J., et al., Antimodified protein antibody response pattern influences the risk for disease relapse in patients with rheumatoid arthritis tapering disease modifying antirheumatic drugs. *Ann Rheum Dis* 2017. 76: 399-407.
- 21 Perez-Riverol, Y., Csordas, A., Bai, J., Bernal-Llinares, M., Hewapathirana, S., Kundu, D. J., et al., The PRIDE database and related tools and resources in 2019: improving support for quantification data. *Nucleic Acids Res* 2019. 47: D442-D450.
- 22 van Beers, J. J., Willemze, A., Jansen, J. J., Engbers, G. H., Salden, M., Raats, J., et al., ACPA fine-specificity profiles in early rheumatoid arthritis patients do not correlate with clinical features at baseline or with disease progression. *Arthritis Res Ther* 2013. 15: R140.
- 23 Lelieveldt, L., Kristyanto, H., Pruijn, G. J. M., Scherer, H. U., Toes, R. E. M. and Bongers, K. M., Sequential Prodrug Strategy To Target and Eliminate ACPA-Selective Autoreactive B Cells. *Mol Pharm* 2018. 15: 5565-5573.
- 24 Kerkman, P. F., Fabre, E., van der Voort, E. I., Zaldumbide, A., Rombouts, Y., Rispens, T., et al., Identification and characterisation of citrullinated antigen-specific B cells in peripheral blood of patients with rheumatoid arthritis. *Ann Rheum Dis* 2016. 75: 1170-1176.
- 25 Lighaam, L. C., Vermeulen, E., Bleker, T., Meijlink, K. J., Aalberse, R. C., Barnes, E., et al., Phenotypic differences between IgG4+ and IgG1+ B cells point to distinct regulation of the IgG4 response. *J Allergy Clin Immunol* 2014. 133: 267-270 e261-266.
- 26 Huijbers, M. G., Vergoossen, D. L., Fillie-Grijpma, Y. E., van Es, I. E., Koning, M. T., Slot, L. M., et al., MuSK myasthenia gravis monoclonal antibodies: Valency dictates pathogenicity. *Neurol Neuroimmunol Neuroinflamm* 2019. 6: e547.
- 27 Koning, M. T., Kielbasa, S. M., Boersma, V., Buermans, H. P. J., van der Zeeuw, S. A. J., van Bergen, C. A. M., et al., ARTISAN PCR: rapid identification of full-length immunoglobulin rearrangements without primer binding bias. *Br J Haematol* 2017. 178: 983-986.
- 28 Vink, T., Oudshoorn-Dickmann, M., Roza, M., Reitsma, J. J. and de Jong, R. N., A simple, robust and highly efficient transient expression system for producing antibodies. *Methods* 2014. 65: 5-10.
- 29 He, X., Klasener, K., Iype, J. M., Becker, M., Maity, P. C., Cavallari, M., et al., Continuous signaling of CD79b and CD19 is required for the fitness of Burkitt lymphoma B cells. *EMBO J* 2018. 37.

Supplemental Tables

Table S1. Clinical patient characteristics.

Patient	Age	Sex [m/f]	Ethnicity	Disease stage	Disease characteristics
1	64	f	Asian (Thai)	established (13 years)	erosive, destructive RA
2	57	f	Suriname	established (7 years)	non-erosive RA
3	57	f	Caucasian	established (6 years)	non-erosive RA
5	66	m	Caucasian	established (36 years)	erosive RA
6	53	f	Caucasian	established (6 years)	erosive RA

* based on CCP2 and CCP4 reactivity

† based on CAcP2 and CAcP4 reactivity

‡ based on CHcitP2 and CHcitP4 reactivity

Table S2. PTM peptide sequences.

Peptide	aa-sequence	Number of epitopes
HC55/HC56 vimentin ²⁰	Ttds-O-Ttds-GRVYAT-(ac)K-SSAVR/ Ttds-O-Ttds-GRVYAT-K-SSAVR	1
CCP1 (cyclic) ¹⁰	HQCHQESTXGRSRGRCGRSGSZO	1
CCP2 (cyclic)	Patent EP2071335	unknown
CCP4 (cyclic)	HQFRFXGNleSRAACZO	1
fibrinogen α 27-43 (linear) ²²	FLAEGGGVXGPRVVERHZO	1
fibrinogen β 36-52 (linear) ²²	NEEGFFSAXGHRPLDKKZO	1
vimentin 59-74 (linear) ²²	VYATXSSAVXLXSSVPZO	3
enolase 5-20 (linear) ²²	KIHAXEIFDSXGNPTVZO	2

X = arginine, lysine, citrulline, homocitrulline, acetyl-lysine.

Z = 6-aminohexanoic acid

O = lys (biotine)-amide

Ttds-linker = 1,13-diamino-4,7,10-trioxatridecane succinimic acid linker

Nle= norleucine

Table S3. Cyclic PTM peptide masses. The calculated versus the measured monoisotopic masses of C-PTM-P1 and average masses of C-PTM-P4.

Peptide	MH+, monoisotopic [m/z] calculated masses	MH+, monoisotopic [m/z] measured masses
CArgP1	2806.3	2806.6
CLysP1	2778.3	2778.5
CCP1	2807.3	2807.7
CHcitP1	2821.3	2821.6
CAcP1	2820.3	2820.5
Peptide	MH+, average [m/z] calculated masses	MH+, average [m/z] measured masses
CArgP4	2056.5	2055.9
CLysP4	2028.5	2028.5
CCP4	2057.5	2056.8
CHcitP4	2071.5	2071.7
CAcP4	2070.5	2070.2

Swollen joint count	Treatment at time of sampling	ACPA IgG status ⁺	AAPA IgG status ⁺	ACarPA IgG status ⁺	RF status
0	methotrexate, hydroxychloroquine	positive	positive	positive	positive
8	methotrexate	positive	positive	positive	positive
0	methotrexate, hydroxychloroquine	positive	positive	positive	negative
0	methotrexate	positive	positive	positive	positive
0	none	positive	positive	positive	positive

Table S4. Linear PTM peptide masses. The calculated versus the measured average masses of four linear PTM peptides.

Peptide	MH ⁺ , average [m/z] calculated masses	MH ⁺ , average [m/z] measured masses
arg-fibrinogen β 36-52	2455.8	2456.0
lys-fibrinogen β 36-52	2427.8	2429.3
cit-fibrinogen β 36-52	2456.8	2456.8
hcrit-fibrinogen β 36-52	2470.8	2470.3
ac-fibrinogen β 36-52	2469.9	2469.7
arg-fibrinogen α 27-43	2303.7	2303.2
lys-fibrinogen α 27-43	2275.7	2275.8
cit-fibrinogen α 27-43	2304.7	2304.7
hcrit-fibrinogen α 27-43	2318.7	2318.2
ac-fibrinogen α 27-43	2317.8	2317.1
arg-vimentin 59-74	2216.7	2216.7
lys-vimentin 59-74	2132.6	2131.7
cit-vimentin 59-74	2219.6	2219.1
hcrit-vimentin 59-74	2261.7	2261.4
ac-vimentin 59-74	2258.9	2258.0
arg-enlase 5-20	2307.7	2308.2
lys-enlase 5-20	2251.7	2251.0
cit-enlase 5-20	2309.7	2310.4
hcrit-enlase 5-20	2337.8	2336.6
ac-enlase 5-20	2335.9	2335.0

Table S5. Citrullinated peptides detected via MS in all four PTM-fibrinogen samples (native, citrullinated, acetylated and carbamylated).

Peptide sequences	Citrulline position within the peptide	Protein subunit
MELERPGGNEITRGGSTSYGTGSETESPR	13	alpha
GDFSSANNRDNTYNR	9	alpha
GDFSSANNRDNTYNRVSEDLR	9.15	alpha
GPRVVERHQSACKDSDWPFCSDWDWNYK	3.7	alpha
DNTYNRVSEDLR	6	alpha
VTSGSTTTTTRRSCSK	10.1	alpha
SCRGSCSRALAR	3.8	alpha
GSCSRALAR	5	alpha
TFPGFFSPMLGEFVSETESRGSESGIFTNTK	20	alpha
SSSYSKQFTSSTSYNRGDSTFESK	16	alpha
QFTSSTSYNRGDSTFESK	10	alpha
GPRVVERHQSACK	3.7	alpha
EVVTSEDCPEAMDGLTSLGIGTLDGFRHR	30	alpha
VTSGSTTTTTRRSCSKVTK	10.11	alpha
SSSYSKQFTSSTSYNRGDSTFESKSYK	16	alpha
LVTSGDKELRTGK	11	alpha
DRQHLPLIK	2	alpha
ESSSHHPGIAEFPSRGK	15	alpha
EEAPSLRPAPPPISGGGYRARPAC	19	beta
EEAPSLRPAPPPISGGGYRARPAC	7.19	beta

n.d.= no citrullination detected

Table S6. %pSyk(Y348)*GFP+ and #pSyk(Y348)*GFP+ CP-reactive mIgG expressing B cells after 5min stimulation with C-PTM-P2 (10 µg/ml).

ACPA BCR	#pSyk(Y348)*GFP+ B cells									
	CArgP2		CLysP2		CCP2		CHcitP2		CAcP2	
	Mean	SD	Mean	SD	Mean	SD	Mean	SD	Mean	SD
3F3	339	138.6	445.5	129.4	9253	1105	6953	1250	260.5	38.89
7E4	300	271.5	312.5	323.1	8491	2065	334	275.8	7469	2286
2G9	230	66.47	177.5	53.03	5273	814.6	3576	347.9	213.5	51.62

n = 2

Table S7. %pSyk(Y348)*GFP+ and #pSyk(Y348)*GFP+ CP-reactive mIgG expressing B cells after 5min stimulation with PTM-fibrinogen (50 µg/ml).

ACPA BCR	#pSyk(Y348)*GFP+ B cells							
	fibrinogen		cit-fibrinogen		carb-fibrinogen		ac-fibrinogen	
	Mean	SD	Mean	SD	Mean	SD	Mean	SD
3F3	305.5	9.192	2598	1776	391.5	65.76	443.5	183.1
7E4	691	80.61	9698	929.8	725.5	194.5	6288	1311
2G9	380.3	188.6	791.3	363.6	512.5	454.3	563.5	512.5

n = 2 to 3

Abundance of citrullinated peptides in PTM-fibrinogen samples			
native	citrullinated	acetylated	carbamylated
3.90E+06	1.00E+07	3.50E+06	1.10E+07
2.60E+07	2.20E+08	6.60E+05	6.30E+05
n.d.	8.30E+07	n.d.	n.d.
n.d.	2.50E+06	n.d.	n.d.
n.d.	3.00E+07	n.d.	n.d.
n.d.	1.20E+07	n.d.	n.d.
n.d.	1.70E+06	n.d.	n.d.
n.d.	1.10E+05	n.d.	n.d.
n.d.	3.00E+06	n.d.	n.d.
n.d.	2.40E+07	n.d.	n.d.
n.d.	5.50E+06	n.d.	n.d.
n.d.	2.70E+07	n.d.	n.d.
n.d.	1.40E+06	n.d.	n.d.
n.d.	1.60E+07	n.d.	n.d.
n.d.	1.20E+06	n.d.	n.d.
n.d.	2.70E+07	n.d.	n.d.
n.d.	1.90E+06	n.d.	n.d.
n.d.	1.30E+08	n.d.	n.d.
n.d.	2.20E+07	n.d.	n.d.
n.d.	6.20E+07	n.d.	n.d.

%pSyk(Y348)*GFP ⁺ B cells									
CArGP2		CLysP2		CCP2		CHcitP2		CAcP2	
Mean	SD	Mean	SD	Mean	SD	Mean	SD	Mean	SD
0.965	0.049	1.145	0.021	28.85	2.475	21.3	2.828	0.825	0.247
0.62	0.537	0.915	1.011	25.25	7.142	0.945	0.856	22.35	7.99
0.01	0.013	0.355	0.332	15	4.95	14.49	6.944	0	0

%pSyk(Y348)*GFP ⁺ B cells							
fibrinogen		cit-fibrinogen		carb-fibrinogen		ac-fibrinogen	
Mean	SD	Mean	SD	Mean	SD	Mean	SD
1.01	0.028	8.285	5.678	1.285	0.148	1.41	0.58
2.35	0.17	30	2.121	2.495	0.799	19.8	4.25
1.218	0.573	2.558	0.829	1.433	0.754	1.335	0.456

Supplemental Figures

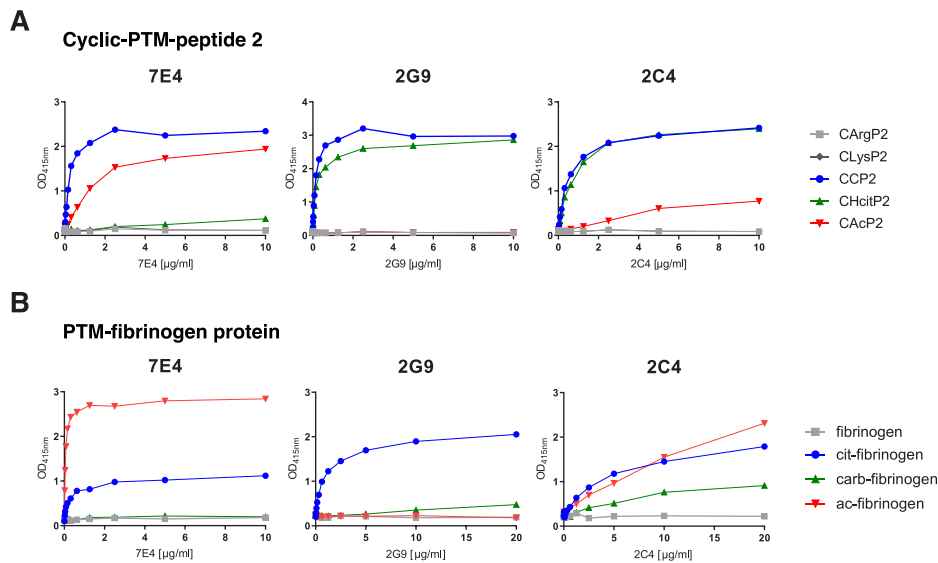


Figure S1. Titration ELISA curves of monoclonal AMPA IgG 7E4, 2G9 and 2C4. (A) Cyclic-PTM-peptide 2 (patent protected sequence) titration ELISA curves of the monoclonal AMPA IgG 7E4, 2G9 and 2C4 (0 to 10 µg/ml). **(B)** PTM-fibrinogen titration ELISA curves of the monoclonal AMPA IgG 7E4 (0 to 10 µg/ml), 2G9 and 2C4 (0 to 20 µg/ml).

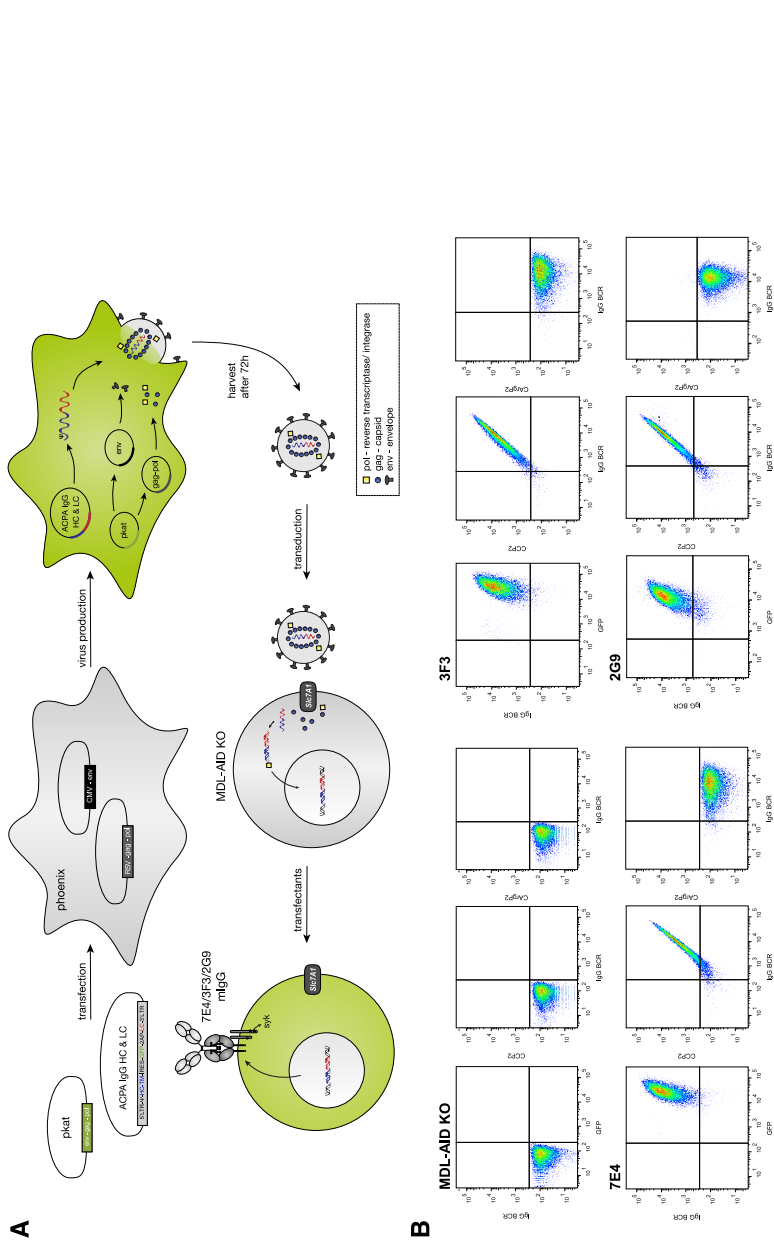


Figure S2. MDL-AID KO Ramos B-cell transfectants expressing CP-reactive BCRs. (A) Schematic depiction of the generation of human Ramos B-cell transfectants expressing CP-reactive BCRs. Phoenix-ECO cells were transfected with the help vector pkat and a single vector including the ACPA IgG HC and LC sequences as well as the selection marker GFP. Retroviruses produced by the phoenix cells were collected after 72 hours and transduced into MDL-AID KO human Ramos B-cell lines via the *slc7a1* receptor. B-cell transfectants express the CP-reactive IgG 7E4, 3F3 and 2G9 as membrane-bound BCR (mlgG) and the selection marker GFP (green). (B) Dot plot chromatograms showing GFP, mlgG-BCR expression and binding towards CCP2 and CArgP2 of the untransduced MDL-AID KO control cell line and the Ramos B-cell transfectants expressing 7E4, 3F3 and 2G9.

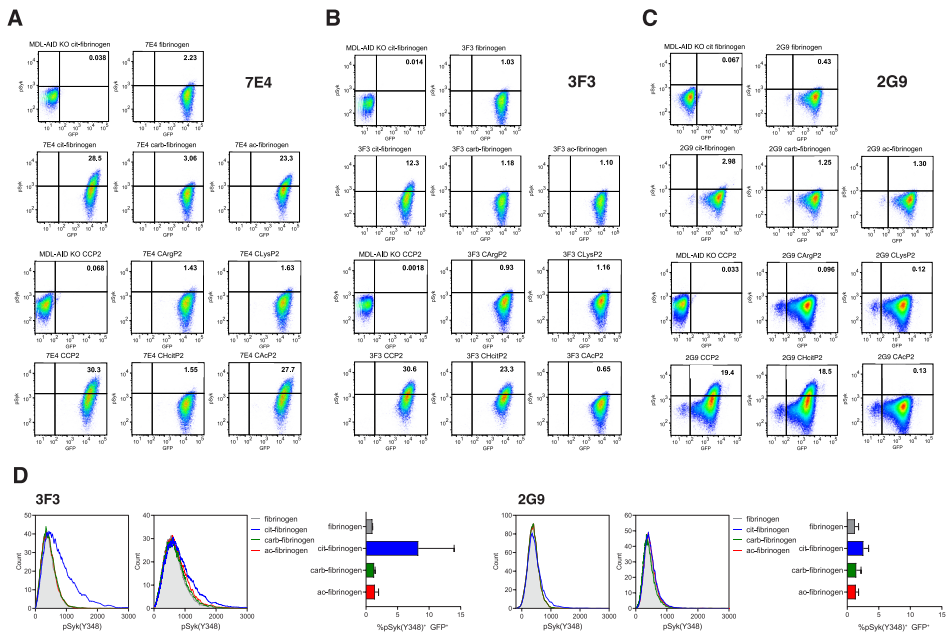
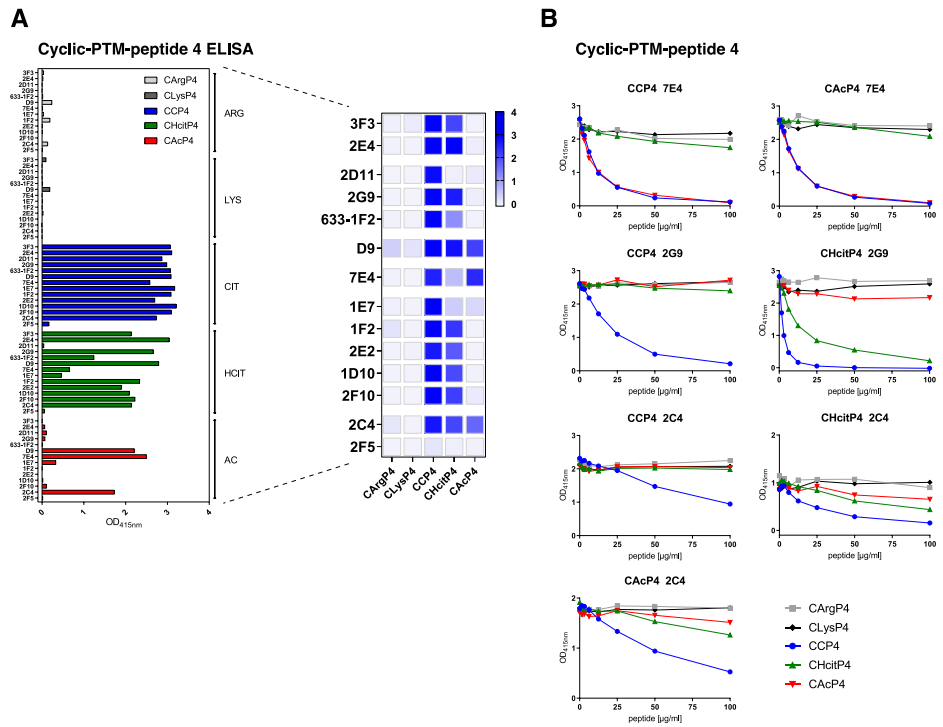


Figure S3. B-cell receptor signaling (pSyk expression) of CP-reactive BCR⁺GFP⁺ Ramos B-cell transfectants after stimulation with PTM antigens. Dot plot chromatograms showing the percentage of pSyk(Y348)⁺GFP⁺ (**A**) 7E4 mlgG Ramos cells (**B**) 3F3 mlgG Ramos cells and (**C**) 2G9 mlgG Ramos cells after stimulation with C-PTM-P2 (patent protected sequence) and PTM-fibrinogen. MDL-AID KO cell lines stimulated with CCP2 and cit-fibrinogen were used as a negative gating control in every experiment. (**D**) Histograms of two biological replicates and a bar graph (n = 2) showing the percentage of pSyk(Y348)⁺GFP⁺ 3F3 and 2G9 mlgG Ramos cells stimulated with PTM-fibrinogen (cit, carb and ac). Fibrinogen: light gray; cit-fibrinogen: blue; hcit-fibrinogen: green; ac-fibrinogen: red.



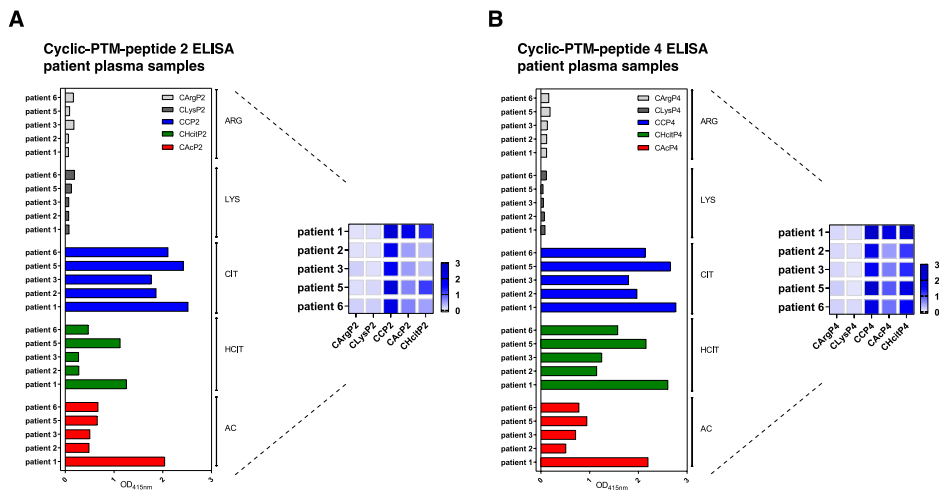


Figure S5. Cross-reactivity of selected RA patient plasma samples used for the mAb sequence isolation based on cyclic-PTM-peptide 2 and cyclic-PTM-peptide 4 ELISAs. (A) Bar graph and heatmap of a cyclic-PTM-peptide 2 (patent protected sequence) ELISA of five patients (1 to 3, 5 and 6) used for the mAb sequence isolation (Table 1). (B) Bar graph and heatmap of a cyclic-PTM-peptide 4 ELISA of five patients (1 to 3, 5 and 6) used for the mAb sequence isolation (Table 1). Shown are the RA patient plasma sample reactivities towards both peptides in five modifications (arg, lys, cit, hcit and ac) depicted as OD values at 415 nm.



On the presence of HLA-SE alleles and ACPA IgG variable domain glycosylation in the phase preceding the development of rheumatoid arthritis

Theresa Kissel, Karin A.J. van Schie, Lise Hafkenscheid, Anders Lundquist, Heidi Kokkonen, Manfred Wuhrer, Tom W.J. Huizinga, Hans U. Scherer, René E.M. Toes, Solbritt Rantapää-Dahlqvist

Abstract

Anti-citrullinated protein antibodies (ACPAs) in Rheumatoid Arthritis (RA) patients display a unique feature defined by the abundant presence of N-linked glycans within the variable domains (V-domains). Recently, we showed that N-glycosylation sites, which are required for the incorporation of V-domain glycans, are introduced following somatic hypermutation. However, it is currently unclear when V-domain glycosylation occurs. Further, it is unknown which factors might trigger the generation of V-domain glycans and whether such glycans are relevant for the transition towards RA. Here, we determined the presence of ACPA IgG V-domain glycans in paired samples of pre-symptomatic individuals and RA patients.

ACPA IgG V-domain glycosylation was analyzed using UHPLC in paired samples of pre-symptomatic individuals [median (IQR) pre-dating time: 5.8 (5.9) years; n = 201; 139 ACPA-positive and 62 ACPA-negative] and RA patients (n = 99; 94 ACPA-positive and 5 ACPA-negative).

V-domain glycans on ACPA IgG were already present up to 15 years before disease in pre-symptomatic individuals and their abundance increased closer to symptom-onset. Noteworthy, HLA-SE alleles associated with the presence of V-domain glycans on ACPA IgG.

Our observations indicate that somatic hypermutation of ACPAs, which results in the incorporation of N-linked glycosylation sites and consequently V-domain glycans, occurs already years before symptom-onset in individuals that will develop RA later in life. Moreover, our findings provide first evidence that HLA-SE alleles associate with ACPA IgG V-domain glycosylation in the pre-disease phase and thereby further refine the connection between HLA-SE and the development of ACPA-positive RA.

Introduction

Rheumatoid Arthritis (RA) is hallmarked by the presence of autoantibodies, such as rheumatoid factor (RF) and anti-citrullinated protein antibodies (ACPAs)^{1,3}. Several genetic risk factors such as the human leukocyte antigen class II shared epitope (HLA-SE) alleles are associated with ACPA-positive RA. Noteworthy, an association with HLA-SE can only be found in ACPA-positive disease and is mostly lost in ACPA-positive healthy individuals, indicating that HLA-SE-restricted T helper cell activity is likely involved in the development of ACPA-positive disease and not the initial induction of autoimmunity. Presumably, these T cells provide help to ACPA-expressing B-cells that have been activated in an earlier phase^{4,5}. ACPA IgG are glycoproteins that harbor, like all IgG, N-linked glycans in the Fc region located at Asn297⁶. Remarkably, approximately 90% of ACPA IgG molecules in sera from RA patients are also abundantly glycosylated within their variable domain (V-domain)⁷. Structural composition analysis revealed that these V-domain glycans are mostly biantennary complex-type glycans carrying sialic acids^{7,8}. To undergo N-linked glycosylation, a consensus sequence in the protein backbone is required (N-X-S/T, where X ≠ P)⁹. Previously, we have shown that N-linked glycosylation sites in ACPA IgG V-domains are introduced during somatic hypermutation¹⁰. Furthermore, in a cross-sectional study of Indigenous North American individuals, we observed that ACPA IgG V-domain glycosylation is largely absent in ACPA-positive subjects that did not transition to RA, while N-linked glycans were found on ACPA-positive healthy subjects that later developed RA¹¹.

On the basis of these and other observations, we hypothesize that V-domain glycosylation conveys a selective advantage to ACPA-expressing B cells, which potentially plays a pivotal role in disease development^{10,12}. To investigate and understand the presence and acquisition of ACPA V-domain glycans in the phase preceding arthritis in more depth, we now aimed to analyze the presence of V-domain glycans on ACPA IgG in paired samples of pre-symptomatic individuals and RA patients.

Results

ACPA IgG V-domain glycan profiles were detected in ACPA-positive pre-symptomatic individuals and RA patients

We analyzed individuals who were sampled before symptom-onset, after diagnosis of RA and randomly selected ACPA-positive and negative control samples from the same population. Chromatographic glycosylation peaks (Figure 1A) could be observed for captured ACPA IgG of 94 out of 201 pre-symptomatic individuals (89 ACPA-positive), 80 out of 99 RA patients (78 ACPA-positive) and 2 out of 43 control samples (1 ACPA-positive and 1 with an anti-CCP2 antibody level < 25 AU/ml). The results obtained strengthen the reliability of the method used,

as from the samples displaying glycan profiles only 8 (4.5%) were derived from ACPA-negative individuals (anti-CCP2 antibody level < 25 AU/ml) compared to 168 glycan profiles (> 95%) derived from samples obtained from ACPA-positive individuals (Table S2 and Figure S1). Of note, in 68 ACPA-positive samples (40.5%) no glycan profiles, including Fc glycans (positive control), could be detected, indicating a limitation of the assay sensitivity.

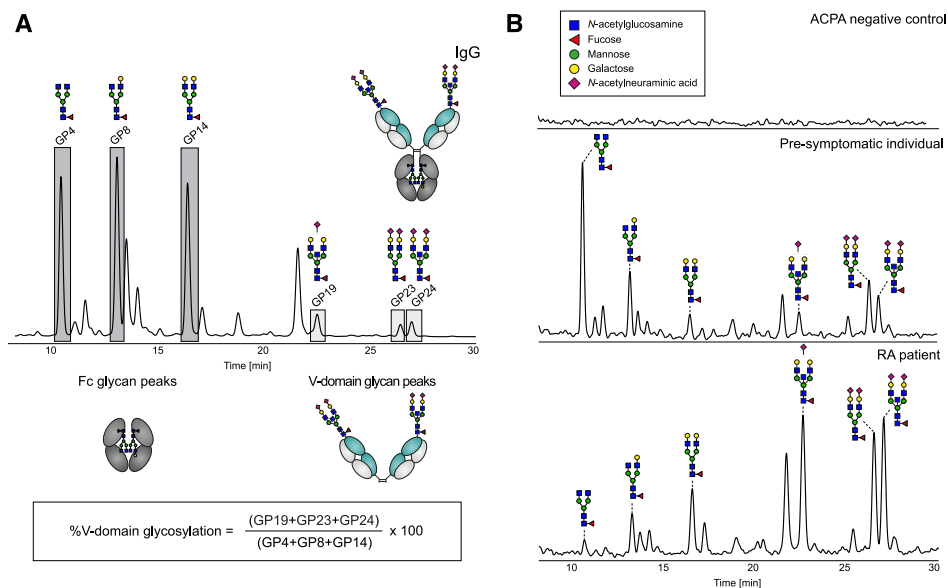


Figure 1. Representative UHPLC spectra of released N-glycans. (A) UHPLC chromatogram of healthy control IgG after IgG capturing and schematic representation of Fc- and V-domain derived glycosylation peaks. The 6 chromatographic peaks (alignment based on¹³) used for the calculation of %V-domain glycosylation are highlighted and the formula is visualized. (B) UHPLC spectra of released N-glycans after ACPA IgG capturing from an ACPA IgG negative individual (no detectable glycan peaks), an ACPA IgG positive pre-symptomatic individual (V-domain glycosylation of 55%) and an ACPA IgG positive RA patient (V-domain glycosylation of 324%). Assigned are the GP4, GP8, GP14, GP19, GP23 and GP24 chromatographic peaks of the IgG glycome based on literature^{7,8}. Blue square: N-acetylglucosamine, green circle: mannose, yellow circle: galactose, red triangle: fucose, pink diamond: α 2,6-linked N-acetylneuraminic acid.

ACPA IgG V-domain glycosylation rises towards symptom-onset and is already present years before

To address the question when V-domain glycosylation first appears, matched paired individuals were sampled before symptom-onset (between -15 and -0.5 years) as well as after diagnosis of RA (between +0.5 and +3 years) and analyzed for ACPA IgG V-domain glycosylation (Figure 1A)⁷. The data obtained revealed that V-domain glycosylation was already present in pre-symptomatic individuals (Figure 2A). Interestingly, ACPA IgG V-domain glycosylation increased

over time ($p < 0.001$) reaching a mean of 111.4% at symptom-onset, showing that, on average, more than one N-glycan is present within the V-domain of these ACPA IgG. Likewise, also analyses of the 29 matched pairs, with detectable V-domain glycan peaks, showed an increase of ACPA IgG V-domain glycosylation towards disease-onset ($p = 0.043$, paired t-test) (Figure 2B). Furthermore, we observed that rising V-domain glycosylation in pre-symptomatic individuals correlated moderately with anti-CCP2 antibody levels ($r_s = 0.504$, $p < 0.001$) (Figure 2C). This correlation could not be detected anymore after disease development (Figure 2D).

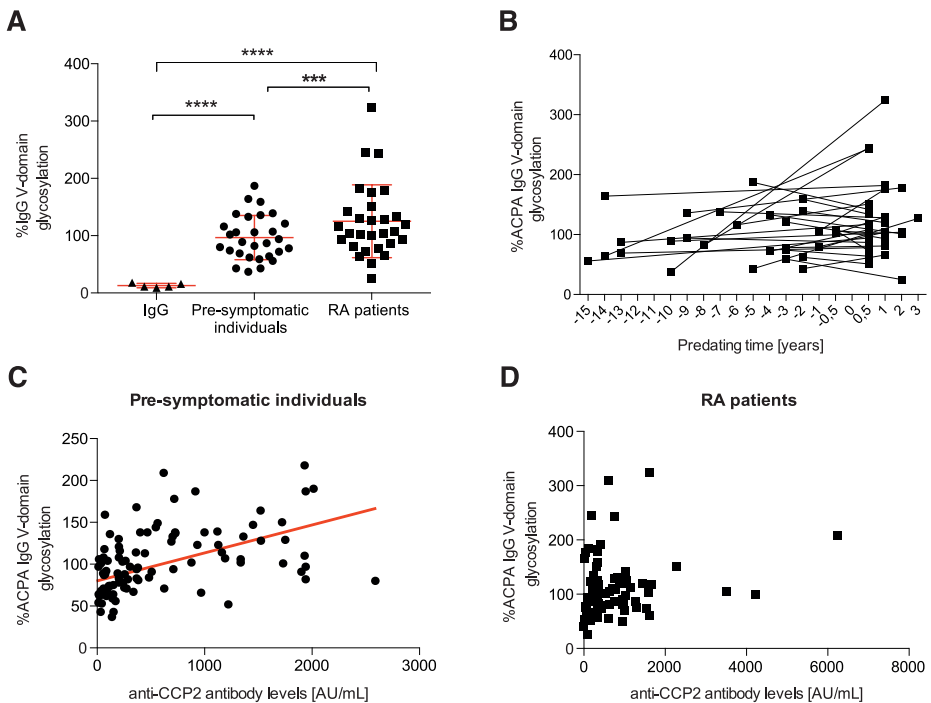


Figure 2. ACPA IgG variable domain glycosylation levels of pre-symptomatic individuals and RA patients.

(A) Percentage V-domain glycosylation of healthy control IgG samples, captured ACPA IgG from pre-symptomatic individuals and RA patients. (B) Percentage ACPA IgG V-domain glycosylation followed over pre-dating time (-15 years before until +3 years after symptom-onset) for 29 matched paired pre-symptomatic and RA patient samples that showed detectable V-domain glycan profiles. 0 indicates onset of RA. ACPA IgG V-domain glycosylation increases towards disease-onset ($p = 0.043$, paired t-test). (C) Scatter plot of percentage ACPA IgG V-domain glycosylation and anti-CCP2 antibody levels in pre-symptomatic individuals ($r_s = 0.504$, $p < 0.001$) (D) Scatter plot of percentage ACPA IgG V-domain glycosylation and anti-CCP2 antibody levels in RA patients ($r_s = 0.169$, $p = 0.133$). Significant differences are indicated by *** ($p < 0.001$) and **** ($p < 0.0001$). The cut-off used for ACPA IgG V-domain glycan peaks is defined as the average of the AUC sum intensity of all blank sample peaks plus x^* standard deviation (x^* = value defined as such that all blank and ACPA-negative healthy donor control samples fall below the cut-off).

Table 1. Logistic regression analysis of samples from pre-symptomatic individuals with detectable vs. non detectable ACPA IgG glycan profiles.

Variable	Simple		
	OR	95%CI	p-value
Anti-CCP2 ab +/-	20.29	7.63, 53.94	< 0.001
Anti-CCP2 ab levels	1.005	1.003, 1.007	< 0.001
RF +/-	7.36	3.91, 13.88	< 0.001
Sex m/f	0.78	0.44, 1.38	0.393
Ever smoking y/n	0.72	0.394, 1.317	0.286
HLA-SE +/-	1.97	1.022, 3.806	0.043
Pre-dating time, years	1.077	0.999997, 1.16	0.050008

ACPA IgG V-domain glycosylation associates with HLA-SE

To investigate possible associations of ACPA IgG V-domain glycosylation pre-disease and cohort characteristics, we performed a logistic regression analysis using detectable ACPA IgG V-domain glycan vs. non-detectable glycan profiles as an outcome. The statistical analysis showed no association between V-domain glycosylation and “sex” or “ever smoking”. Interestingly, an association between ACPA IgG V-domain glycosylation and HLA-SE was observed (OR = 1.97, p = 0.043). This association remained significant after adjusting for anti-CCP2 antibody status, and pre-dating time (OR: 2.46, p = 0.023) as well as after adjusting for RF and pre-dating time (OR: 2.54, p = 0.015) (Table 1). However, this association was non-significant after correcting for anti-CCP2 antibody levels although a clear trend remained (OR = 2.06, p = 0.086). In contrast, no association was found when a reciprocal analysis was performed addressing the question whether HLA-SE associates with anti-CCP2 antibody positivity pre-disease (OR = 1.01, 95%CI = 0.51 to 1.98).

Discussion

In this study we have captured ACPA IgG from pre-symptomatic individuals and RA patients and analyzed their glycan profiles using UHPLC. The observed glycan profiles were derived from samples of ACPA-positive individuals in more than 95% of the cases. These results indicate the high reliability of the implemented methodology (Figure S1). Glycan profile detection in 8 out of 107 ACPA-negative samples may be explained by the presence of ACPA levels slightly below the ELISA cut-off. In fact, 3 out of these 8 subjects in whom ACPA V-domain glycans were detected, while displaying ACPA-negativity based on the ELISA cut-off, had been tested positive for reactivity towards other citrullinated antigens, which could explain capturing by the CCP2-coated beads. A clear limitation of the present study is that not all ACPA-positive samples could be analyzed for the presence of V-domain glycans as not all glycan-profiles, including Fc glycans, could be detected. This is likely due to technical constraints such as low ACPA levels or limited sample amounts.

Multiple			Multiple			Multiple		
OR	95%CI	p-value	OR	95%CI	p-value	OR	95%CI	p-value
32.13	10.54, 97.91	< 0.001	-			-		
-			1.005	1.003, 1.008	< 0.001	-		
-			-			7.59	3.85, 14.96	< 0.001
-			-			-		
-			-			-		
2.46	1.13, 5.33	0.023	2.06	0.90, 4.70	0.086	2.54	1.20, 5.36	0.015
0.94	0.85, 1.04	0.206	0.98	0.89, 1.08	0.747	1.01	0.93, 1.10	0.804

At present ACPA IgG is used as one of the most relevant biomarkers in RA. However, ACPA detection in subjects at risk does not always correlate with the progression to RA¹⁴. Our data show that N-linked V-domain glycans are a specific feature of ACPA IgG, which can be present already years before the onset of RA. These results are in line with a recent study indicating that the presence of V-domain glycans could potentially be used as a biomarker to identify ACPA-positive individuals at risk to develop RA¹¹. Together our studies show that V-domain glycosylation occurs in almost all ACPA-positive individuals who will develop RA despite different ethnic and environmental backgrounds. Moreover, the current study shows that V-domain glycans appeared already up to 15 years before diagnosis (Figure 2B). Furthermore, our data reveal that V-domain glycosylation increases towards disease-onset, conceivably due to the generation of de-novo N-glycosylation sites or the expansion of N-glycosylation site-bearing clones, and that this increase associates with higher ACPA levels (Figure 2C). These results are in line with the notion that ACPA-expressing B cells gain a selective advantage through the generation of V-domain glycans.

Additionally, we did observe an association between ACPA IgG V-domain glycosylation pre-disease and HLA-SE alleles. This association remains after including anti-CCP2 status into the model. Likewise, a clear, although non-significant trend remains after correcting for anti-CCP2 antibody levels.

Unfortunately, we could not study a possible correlation between V-domain glycosylation and epitope spreading of the ACPA response as we did not have sufficient data on the citrullinated-epitope recognition profile of the samples available. Nonetheless, an association between HLA-SE status and ACPA IgG V-domain glycosylation is intriguing as it suggests that HLA-SE predispose to the formation of N-linked glycosylation sites in ACPA pre-disease and not to ACPA-positivity itself. This assumption is in line with findings indicating that the association between HLA-SE and ACPA-positivity is mostly lost in healthy individuals^{4,5}. However, although

appealing, additional replication is warranted as the present study could have introduced bias due to e.g. limited sample size or assay-sensitivity. Nonetheless, we consider it highly relevant to perform such studies as it could provide novel insights into the role of HLA-SE-restricted T cells on the development of ACPA-positive RA. HLA-SE T cells might facilitate the introduction of N-linked glycosylation sites on ACPA-expressing B cells allowing their expansion as conceivably explaining the rise in ACPA levels pre-disease.

In summary, our data disclose that V-domain glycosylation precedes the development of ACPA-positive RA and may serve as aid to improve current algorithms predicting RA development thereby allowing early treatment of high risk individuals. Noteworthy, our findings suggest that the action of HLA-SE could be explained by the contribution to facilitate the introduction of N-linked glycosylation sites into ACPA IgG pre-disease.

Materials and Methods

Patient and public involvement - Patients were involved in this study by donating blood at the Medical Biobank of Northern Sweden, when attending population surveys.

Ethical considerations - All participants have given their written informed consent when included into the surveys and the Regional Ethical Review Board Committee at Umeå University approved the study.

Study cohort - Individuals, diagnosed with RA later in life, were sampled prior to symptom-onset [median (IQR) pre-dating time: 5.8 (5.9) years; n = 201; 139 ACPA-positive and 62 ACPA-negative] and after diagnosis of RA (n = 99, 94 ACPA-positive and 5 ACPA-negative as specificity control). Further, randomly selected control samples (n = 43, 3 ACPA-positive and 40 ACPA-negative) were included. The RA patients fulfilled the 1987 ARA classification criteria¹⁵. Descriptive cohort information is presented in supplementary Table 1.

Laboratory analyses - Anti-citrullinated protein antibodies (ACPAs) were analyzed in blood samples of pre-symptomatic individuals and RA patients using anti-cyclic citrullinated peptide 2 (CCP2) enzyme linked immunoassays from Euro-Diagnostica (Malmö, Sweden) with a positivity cut-off set at 25 AU/mL according to the manufacturer's instructions.

ACPA IgG isolation - ACPA were isolated from plasma samples using NeutrAvidin Plus resin (Thermo Fisher Scientific) coupled with 0.1 µg/µl CCP2-biotin as previously described¹⁶. In brief, 50 µl of CCP2-coupled beads were transferred onto each well of a 96-well polypropylene filter plate (Orochem). Prior to sample application, bead-coated filter plates were washed with 150 µl

PBS by centrifugation (500×g for 2 min). Serum samples (25 µl) were diluted in 175 µl PBS, added to the bead-coated filter plates and incubated for 2 hours at 600 rpm on a plate shaker. Sample flowthrough was collected by centrifugation (500×g for 2 min). Washing steps with 150 µl PBS followed by 150 µl 25 mM ammonium bicarbonate (pH 7 to 7.5) and two times 150 µl PBS were performed. CCP2 specific antibodies were eluted with 100 µl 0.1 M formic acid (pH 2.5). Eluted samples were neutralized with 2 M TRIS until pH reached 7 to 7.5. ACPA isolation was followed by IgG isolation using FcXL affinity beads (Thermo Fisher Scientific) as previously described¹⁶. In brief, 100 µl bead slurry was transferred onto each well of a 96-well polypropylene filter plate (Orochem). 500 µl PBS was added and the plates centrifuged at 50×g for 2 min. The bead-coated plates were washed three times with 200 µl PBS. Captured ACPA from the serum samples was added to the bead-coated plates and incubated for 1 hour at 900 rpm on a plate shaker. The flowthrough was collected by centrifugation (50×g for 1 min). The plate was washed three times with 200 µl PBS. 100 µl 100 mM formic acid (pH 2.5) was added in two steps, incubated for 5 min at 900 rpm and the eluted ACPA IgG collected by centrifugation (1 min at 500 rpm). The ACPA IgG samples were evaporated using a speedvac for 3 hours at 45 °C.

N-linked glycan release, labeling and UHPLC analysis - N-linked glycans from captured ACPA IgG samples were released using PNGase F as previously described⁷. Released N-glycans were subsequently labeled with 2-aminobenzoic acid (2-AA, Sigma Aldrich) and 2-picoline borane (2-PB, Sigma Aldrich) and purified via hydrophilic interaction liquid chromatography-solid phase extraction (HILIC SPE) using GHP membrane filter plates (Pall Life Science) as previously described¹⁷. 2-AA labelled and HILIC SPE purified N-linked glycans were diluted in ACN to obtain a final concentration of 75% ACN and analyzed using a Dionex Ultimate 3000 (Thermo Fisher Scientific) instrument, a FLR fluorescence detector set with excitation and emission wavelengths of 330 and 420 nm and a Acquity UHPLC BEH Glycan column (1.7 µm 2.1 mm × 100 mm; Waters, Milford, MA). Separation was performed at 60 °C with a flow rate of 0.6 ml/min. 100% ACN (solvent A) and 100 mM ammonium formate pH 4.4 (solvent B) were used for gradient generation. Column equilibration was performed for 0.5 min using 85% of solvent A. Sample loading occurred in 75% of solvent A followed by a column wash with 85% solvent A for 10 min. The separation was achieved using a start gradient of 75% solvent A and 25% solvent B, which decreased linearly to 63% solvent A within 30 min. For re-equilibration the column was flushed for 4 min with 40% solvent A and 10 min 85% solvent A. The generated chromatograms were analyzed and exported as excel files using Chromeleon version 7.1.2.1713 (Thermo Fisher Scientific). All chromatograms were aligned in the same manner and separated into 24 peaks. Glycan composition in each chromatographic peak was defined as previously described¹⁸.

Data analysis and processing - Calibration was performed using HappyTools version 0.0.2¹⁸ and the elution time of five calibrant peaks (GP4, GP8, GP14, GP23, GP24). Integration and baseline correction were performed using the elution time of all chromatographic peaks and

the following settings: General settings: start t = 8 min, end t = 30 min; Peak detection settings: minimum intensity: 0.05, sigma value: 2.0; calibration settings: minimum peaks: 4, minimum S/N: 1; Quantitation settings: datapoints: 100, baseline order: 1, background window: 1.0, MT slice points: 5. The amount of N-glycans in each peak was expressed as the total integrated area under the curve (AUC). A cut-off was defined using the average of the AUC sum intensity of all blank samples plus $x \times$ standard deviation (x = value defined such that all blank and healthy donor control samples fall below the cut-off). The percentage ACPA IgG V-domain glycosylation was calculated based on the three most abundant Fc-glycan peaks (positive control for IgG capturing) and the three most abundant V-domain glycan peaks using the following formula: $[(GP19+GP23+GP24) / (GP4+GP8+GP14)] \times 100^{11,18}$.

Statistical analyses – Statistical calculations were performed using SPSS for Windows version 25.0 (IBM Corp., NY, USA). Continuous data were analyzed using non-parametric methods (Mann-Whitney's U-test and Wilcoxon signed-rank test) and parametric tests when appropriate. Correlation analyses were performed using Spearman rank-order correlation (r_s). All p-values are two-sided and $p < 0.05$ was considered as statistically significant. Simple and multiple logistic regression analyses were performed for different variables associated with ACPA IgG V-domain glycosylation.

Acknowledgments

The authors would like to thank the Department of Biobank Research at Umeå University, Västerbotten Intervention Programme, the Northern Sweden MONICA study and the County Council of Västerbotten for providing data and samples. We would like to thank Dr. Jan Wouter Drijfhout (LUMC, Leiden, The Netherlands) for providing the CCP2 peptide.

Funding

This work has been financially supported by ReumaNederland 17-1-402 (to R.E.M.T.), the IMI-funded project RTCure 777357 (to T.W.J.H.), ZonMw TOP 91214031 (to R.E.M.T.), the Swedish Research Council VR 2017-00650 (to S.R.-D.) as well as the King Gustaf V's 80-Year Fund, the King Gustaf V's and Queen Victoria's Fund and the Swedish Rheumatism Association (to S.R.-D.).

Conflict of interest

H.U.S., T.W.J.H. and R.E.M.T. are mentioned inventors on a patent on ACPA IgG V-domain glycosylation.

Author contributions

All authors were involved in drafting the article or revising it critically for important intellectual content, and all authors approved the final version to be published. Conceptualization: T.K., K.A.J.v.S., L.H., R.E.M.T. and S.R.-D. Methodology: T.K., K.A.J.v.S., L.H., A.L., H.K. Software: T.K., A.L., H.K. Investigation: T.K., K.A.J.v.S., L.H. Visualization: T.K. Supervision: H.U.S., R.E.M.T. and S.R.-D. Writing—original draft: T.K., R.E.M.T. and S.R.-D. Writing—review and editing: K.A.J.v.S., L.H., A.L., H.K., M.W., T.W.J.H. and H.U.S.

References

- 1 Schellekens, G. A., de Jong, B. A., van den Hoogen, F. H., van de Putte, L. B. and van Venrooij, W. J., Citrulline is an essential constituent of antigenic determinants recognized by rheumatoid arthritis-specific autoantibodies. *J Clin Invest* 1998. 101: 273-281.
- 2 Aletaha, D., Neogi, T., Silman, A. J., Funovits, J., Felson, D. T., Bingham, C. O., 3rd, et al., 2010 Rheumatoid arthritis classification criteria: an American College of Rheumatology/European League Against Rheumatism collaborative initiative. *Arthritis Rheum* 2010. 62: 2569-2581.
- 3 Aho, K., Heliovaara, M., Maatela, J., Tuomi, T. and Palosuo, T., Rheumatoid factors antedating clinical rheumatoid arthritis. *J Rheumatol* 1991. 18: 1282-1284.
- 4 Hensvold, A. H., Magnusson, P. K., Joshua, V., Hansson, M., Israelsson, L., Ferreira, R., et al., Environmental and genetic factors in the development of anticitrullinated protein antibodies (ACPAs) and ACPA-positive rheumatoid arthritis: an epidemiological investigation in twins. *Ann Rheum Dis* 2015. 74: 375-380.
- 5 Terao, C., Ohmura, K., Ikari, K., Kawaguchi, T., Takahashi, M., Setoh, K., et al., Effects of smoking and shared epitope on the production of anti-citrullinated peptide antibody in a Japanese adult population. *Arthritis Care Res (Hoboken)* 2014. 66: 1818-1827.
- 6 Arnold, J. N., Wormald, M. R., Sim, R. B., Rudd, P. M. and Dwek, R. A., The impact of glycosylation on the biological function and structure of human immunoglobulins. *Annu Rev Immunol* 2007. 25: 21-50.
- 7 Hafkenscheid, L., Bondt, A., Scherer, H. U., Huizinga, T. W., Wuhler, M., Toes, R. E., et al., Structural Analysis of Variable Domain Glycosylation of Anti-Citrullinated Protein Antibodies in Rheumatoid Arthritis Reveals the Presence of Highly Sialylated Glycans. *Mol Cell Proteomics* 2017. 16: 278-287.
- 8 Rombouts, Y., Willemze, A., van Beers, J. J., Shi, J., Kerkman, P. F., van Toorn, L., et al., Extensive glycosylation of ACPA-IgG variable domains modulates binding to citrullinated antigens in rheumatoid arthritis. *Ann Rheum Dis* 2016. 75: 578-585.
- 9 Shakin-Eshleman, S. H., Spitalnik, S. L. and Kasturi, L., The amino acid at the X position of an Asn-X-Ser sequon is an important determinant of N-linked core-glycosylation efficiency. *J Biol Chem* 1996. 271: 6363-6366.
- 10 Vergoesen, R. D., Slot, L. M., Hafkenscheid, L., Koning, M. T., van der Voort, E. I. H., Grooff, C. A., et al., B-cell receptor sequencing of anti-citrullinated protein antibody (ACPA) IgG-expressing B cells indicates a selective advantage for the introduction of N-glycosylation sites during somatic hypermutation. *Ann Rheum Dis* 2018. 77: 956-958.
- 11 Hafkenscheid, L., de Moel, E., Smolik, I., Tanner, S., Meng, X., Jansen, B. C., et al., N-Linked Glycans in the Variable Domain of IgG Anti-Citrullinated Protein Antibodies Predict the Development of Rheumatoid Arthritis. *Arthritis Rheumatol* 2019. 71: 1626-1633.
- 12 Scherer, H. U., Huizinga, T. W. J., Kronke, G., Schett, G. and Toes, R. E. M., The B cell response to citrullinated antigens in the development of rheumatoid arthritis. *Nat Rev Rheumatol* 2018. 14: 157-169.
- 13 Pucic, M., Knezevic, A., Vidic, J., Adamczyk, B., Novokmet, M., Polasek, O., et al., High throughput isolation and glycosylation analysis of IgG-variability and heritability of the IgG glycome in three isolated human populations. *Mol Cell Proteomics* 2011. 10: M111 010090.
- 14 van Beers, J. J., Willemze, A., Jansen, J. J., Engbers, G. H., Salden, M., Raats, J., et al., ACPA fine-specificity profiles in early rheumatoid arthritis patients do not correlate with clinical features at baseline or with disease progression. *Arthritis Res Ther* 2013. 15: R140.
- 15 Arnett, F. C., Edworthy, S. M., Bloch, D. A., McShane, D. J., Fries, J. F., Cooper, N. S., et al., The American Rheumatism Association 1987 revised criteria for the classification of rheumatoid arthritis. *Arthritis Rheum* 1988. 31: 315-324.

- 16 Habets, K. L., Trouw, L. A., Levarht, E. W., Korpelaar, S. J., Habets, P. A., de Groot, P., et al., Anti-citrullinated protein antibodies contribute to platelet activation in rheumatoid arthritis. *Arthritis Res Ther* 2015. 17: 209.
- 17 Jansen, B. C., Bondt, A., Reiding, K. R., Scherjon, S. A., Vidarsson, G. and Wuhler, M., MALDI-TOF-MS reveals differential N-linked plasma- and IgG-glycosylation profiles between mothers and their newborns. *Sci Rep* 2016. 6: 34001.
- 18 Jansen, B. C., Hafkenscheid, L., Bondt, A., Gardner, R. A., Hendel, J. L., Wuhler, M., et al., HappyTools: A software for high-throughput HPLC data processing and quantitation. *PLoS One* 2018. 13: e0200280.

Supplemental Tables

Table S1. Descriptive information of the sample cohort.

Variables	Controls N = 43	Pre-symptomatic individuals N = 201	RA patients N = 99
Females, n (%)	32 (74.4)	126 (62.7)	67 (67.7)
Age at sampling, mean±SD, years	51.3 ± 9.6	51.4 ± 9.4	59.0 ± 9.5
Anti-CCP2 abs, n (%)	3 (6.98)	139 (69.2)	94 (95.0)
RF, n (%)	3 (6.98)	107 (53.2)	82 (82.8)
Ever smoker, n (%)	14 (32.6)	140 (69.7)	72 (72.7)
HLA-SE, n (%)	-	141 (70.2)	76 (76.8)
Pre-dating time, median (IQR), years	-	5.8 (5.9)	-

Table S2. Detectable ACPA IgG V-domain glycosylation profiles within the sample cohort.

	n	anti-CCP2 antibody level > 25AU/ml	Detectable glycan profiles	Non detectable glycan profiles
Controls	43	pos	3	2
		neg	40	39
Pre-symptomatic individuals	201	pos	139	50
		neg	62	57
RA patients	99	pos	94	16
		neg	5	3

Supplemental Figure

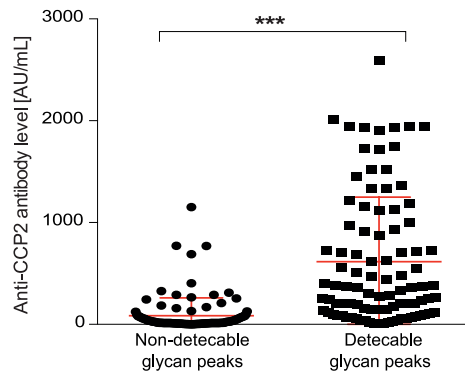


Figure S1. Detectability of ACPA IgG V-domain glycosylation correlates with anti-CCP2 antibody positivity.

Anti-CCP2 antibody levels stratified for detectable vs. non-detectable ACPA IgG V-domain glycan peaks within all samples tested.



LETTER

Genetic predisposition (HLA-SE) is associated with ACPA IgG variable domain glycosylation in the pre-disease phase of RA

Theresa Kissel[†], Tineke J. Wesemael [†], Anders Lundquist, Heidi Kokkonen, Atsushi Kawakami, Mami Tamai, Dirkjan van Schaardenburg, Manfred Wuhler, Tom W.J. Huizinga, Hans U. Scherer, Diane van der Woude, Solbritt Rantapää-Dahlqvist, René E.M. Toes

[†] These authors contributed equally to this work as co-first authors.

In addition to Fc glycans, Immunoglobulin G (IgG) can carry N-linked glycans in the variable domain. The abundant presence of disialylated variable domain glycans (VDGs) is a special feature of ACPA IgG and possibly other autoantibodies. The introduction of glycosylation sites is mediated by somatic hypermutation (SHM), a T-cell dependent process¹. The high frequency of glycosylation sites does not correlate with the number of SHM, pointing towards a selective advantage of B cells expressing variable domain glycosylated ACPAs². Previously, we observed that ACPA IgG VDGs are already present in the phase preceding the onset of RA and predictive for disease development³. In addition, we provided first evidence that the human leukocyte antigen (HLA) shared epitope (SE) alleles, the most prominent genetic risk factor for ACPA-positive RA, are associated with the presence of VDGs on ACPA IgG pre-disease⁴. Hence, variable domain glycosylation could possibly explain the contribution of HLA-SE restricted T cells in the maturation of the ACPA response. Building upon these results, we now hypothesized that HLA-SE alleles may not be associated with ACPA-positivity as such, but with the specific presence of variable domain glycosylated ACPA IgG, a favorable factor for the development of this multifactorial disease.

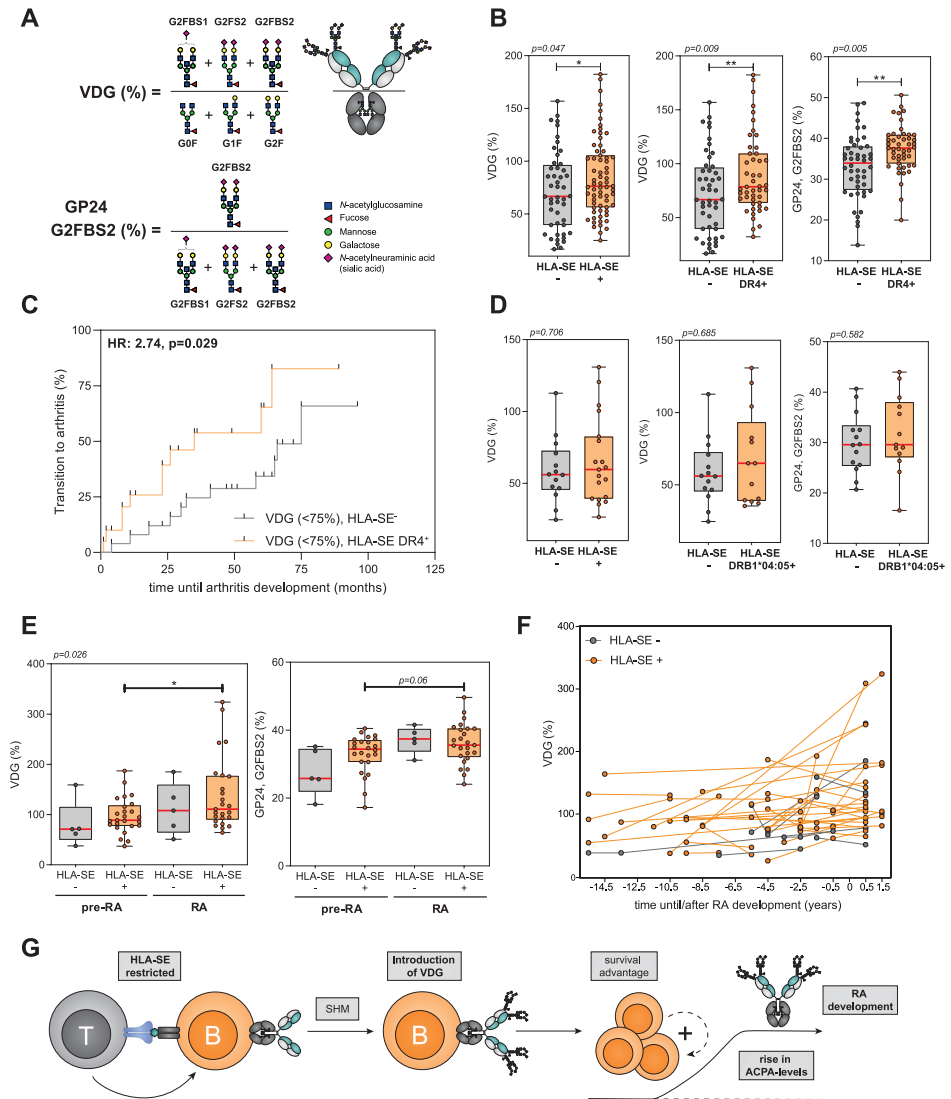
To substantiate our hypothesis, we expanded the set of pre-symptomatic individuals (n = 228) and RA patients (n = 126) from Sweden and analyzed two additional cohorts comprising ACPA-positive Dutch individuals with arthralgia (n = 239) and ACPA-positive healthy Japanese individuals (n = 58) (Table S1). We determined the presence/percentage of ACPA IgG VDGs using liquid chromatography⁵ and assessed associations with HLA-SE (supplementary materials and methods). In particular, we focused on the most prominent glycan peak (GP24) found on top of the variable domain¹, which carries a bisecting *N*-acetylglucosamine and two terminal sialic acids (G2FBS2) (Figure 1A). ACPA IgG VDGs were, with a median of 58%, already abundantly expressed in healthy individuals (Table S1), in contrast to conventional IgG molecules that yield 12% of VDGs⁶. VDG (p = 0.047) and GP24 (p = 0.003) were significantly higher in HLA-SE⁺ Dutch individuals with arthralgia compared to the HLA-SE-negative group (Figure 1B, Table S2 and S3). HLA-SE DR4⁺ (HLA-DRB1*04:01, *04:04, *04:05, *04:08 and *04:10 alleles) individuals showed the strongest increase in VDGs (p = 0.009) and GP24 (p = 0.005) compared to HLA-SE-negative individuals (Figure 1B). Even though, we observed a strong correlation between VDGs and ACPA levels (Figure S1), we could not identify an association between ACPA levels and HLA-SE (p = 0.66) (Table S4). Moreover, in line with our hypothesis, the association between HLA-SE and GP24 remained significant after correcting for ACPA levels in a multivariable analysis (HLA-SE: p = 0.03; HLA-SE DR4⁺: p = 0.07) (Table S3), indicating that HLA-SE primarily associates with abundantly variable domain glycosylated ACPA IgG.

Interestingly, individuals with an “incomplete” VDG (lower than the median of 75%) (Table S1) were more prone to transition to RA, if they were HLA-SE DR4⁺ (HR: 2.74, p = 0.029) (Figure 1C). Conceivably, HLA-SE restricted T cells increase SHM and hence the formation of glycosylation sites, impacting on a subsequent increased risk to develop disease³. Likewise, although underpowered and statistically not significant, VDGs and GP24 were numerically increased in the healthy ACPA-positive

individuals from Japan, mainly in the HLA-SE DRB1*04:05⁺ group, the predominant HLA-SE alleles in this population (Figure 1D). The association between HLA-SE and increased VDG percentages was not present in the Swedish data-set, possibly because all individuals transition to RA (Table S5). However, the findings replicated our previous data, as HLA-SE alleles associated with the presence of ACPA IgG VDGs in the pre-RA phase, after correcting for ACPA-positivity (OR: 1.998, $p = 0.040$) (Table S7). No association was found between HLA-SE and ACPA in a reciprocal analysis (i.e. after correcting for the presence of VDGs) (OR: 0.620, $p = 0.254$) (Table S8). Similar to our preceding analyses, this correlation was only found pre-disease as we could not identify a link between HLA-SE and VDGs in established disease (OR: 0.305, $p = 0.269$) (Table S9), likely because most ACPA IgG carry an abundant amount of VDGs by then (Table S1). Thus, in the phase preceding RA, HLA-SE alleles are associated with ACPAs harboring elevated amounts of VDGs. Additionally, HLA-SE⁺ individuals showed a significant increase in VDGs towards disease-onset (matched paired analysis, Figures 1, E and F).

Figure 1. Percentage of ACPA IgG variable domain glycosylation (VDG) and glycan peak 24 (GP24, G2FBS2) in HLA-SE⁻ and HLA-SE⁺ individuals.

(A) Formulas to calculate the percentage of ACPA IgG VDG and the most common complex-type disialylated glycan peak found on top of the variable domain, GP24. ACPA IgG were captured, glycans released using PNGase F, 2-AA labelled, HILIC SPE purified and analyzed using UHPLC. The formulas presented are based on the abundance of the liquid chromatography determined Fc-glycan traits G0F, G1F, G2F and VD-glycan traits G2FBS1, G2FBS2 and G2FBS2. The respective glycans and their locations on the antibody molecule are schematically illustrated. Agalactosylated (G0), monogalactosylated (G1), digalactosylated (G2), fucose attached to the core GlcNAc (F), bisecting GlcNAc (B), monosialylated (S1), disialylated (S2). Blue square: *N*-acetylglucosamine (GlcNAc), green circle: mannose, yellow circle: galactose, red triangle: fucose, pink diamond: *N*-acetylneuraminic acid. (B) ACPA IgG⁺ individuals with arthralgia from The Netherlands (Amsterdam). Increased ACPA IgG VDG of HLA-SE⁺ ($n = 67$) compared to HLA-SE⁻ ($n = 48$) individuals. Significantly higher ACPA IgG VDG and GP24 in HLA-SE DR4⁺ ($n = 47$) individuals. (C) ACPA IgG⁺ individuals with arthralgia from The Netherlands (Amsterdam) with a VDG < 75% ($n = 49$). ACPA IgG⁺ arthralgia individuals with a VDG lower than 75% are more prone to transition to disease and transition earlier, if they are HLA-SE DR4⁺ (HR: 2.74 (95% CI: 1.07 to 7.00), p -value: 0.029). (D) ACPA IgG⁺ symptom-free healthy individuals from Japan (Nagasaki). Statistically not significant trend for an increased percentage of ACPA IgG VDG and GP24 in HLA-SE⁺ ($n = 19$) particularly HLA-SE DRB1*04:05 ($n = 13$) healthy individuals compared to the HLA-SE⁻ ($n = 14$) group. (E), (F). Matched pairs of samples from pre-symptomatic individuals and RA patients from Sweden (Umeå) ($n = 59$). HLA-SE⁺ individuals show a significant increase in their percentage ACPA IgG VDG and GP24 towards disease-onset. HLA-SE⁺ pre-symptomatic individuals ($n = 24$) show already high VDG levels up to 15 years before RA-onset. (G). Graphical illustration of concluding hypothesis. HLA-SE restricted T cells give help to ACPA IgG-expressing B cells, which results in SHM and the introduction of N-linked glycan sites, and consequently VDG (associations between HLA-SE and VDG). These ACPA IgG VDG⁺ B cells expand leading to a rise in ACPA levels and ultimately towards disease development. Mann Whitney U tests or linear regression analysis were performed between non-paired and Wilcoxon signed rank test between matched paired samples. The comparison of the survival curves was performed using a Mantel-Cox test. Significant differences are denoted by * or ** and the respective p -values are represented. ►



Hence, the data presented support a concept in which HLA-SE restricted T cells stimulate the introduction of glycosylation sites in ACPA-expressing B cells, an event taking place before the development of ACPA-positive disease. HLA-SE can thus be considered as an “accelerating factor” causing the abundant expression of VDGs on ACPA IgG (Figure 1G). Our data also provide an explanation for why HLA-SE do not associate with ACPAs in healthy individuals^{7,8} as these are not yet abundantly glycosylated in their variable domains. The fact that all ACPA IgG are heavily glycosylated in established RA, explains why HLA-SE associate with ACPAs in this disease-stage and emphasizes the possibility that VDGs serve as an important “hit” involved in the unrestrained expansion of the RA-specific autoreactive B-cell response.

Acknowledgments

The authors would like to thank the Department of Biobank Research at Umeå University, Västerbotten Intervention Programme, the Northern Sweden MONICA study and the County Council of Västerbotten for providing data and samples. We would like to thank Dr. Jan Wouter Drijfhout (LUMC, Leiden, The Netherlands) for providing the CCP2 peptide.

Funding

This work has been financially supported by ReumaNederland 17-1-402 and 08-1-34 (to R.E.M.T.), the IMI-funded project RTCure 777357 (to T.W.J.H.), ZonMw TOP 91214031 (to R.E.M.T.), Target-to-B LSHM18055-SGF (to R.E.M.T.), the European Research Council (ERC) advanced grant AdG2019-884796 (to R.E.M.T.), the Swedish Research Council VR 2017-00650 (to S.R.-D.) as well as the King Gustaf V's 80-Year Fund, the King Gustaf V's and Queen Victoria's Fund and the Swedish Rheumatism Association (to S.R.-D.).

Conflict of interest

H.U.S., T.W.J.H. and R.E.M.T. are mentioned inventors on a patent on ACPA IgG V-domain glycosylation.

Author contributions

All authors were involved in drafting the article or revising it critically for important intellectual content, and all authors approved the final version to be published. Conceptualization: T.K., T.J.W., and R.E.M.T. Methodology: T.K. Software: T.K., T.J.W., A.L., H.K. Investigation: T.K., T.J.W., A.L., H.K. Visualization: T.K., T.J.W. Supervision: D.v.W., S.R.-D. and R.E.M.T. Writing—original draft: T.K., T.J.W., D.v.W., S.R.-D. and R.E.M.T. Writing—review and editing: A.L., H.K., A.K., M.T., D.v.S., M.W., T.W.J.H., H.U.S.

References

- 1 Hafkenscheid, L., Bondt, A., Scherer, H. U., Huizinga, T. W., Wuhrer, M., Toes, R. E., et al., Structural Analysis of Variable Domain Glycosylation of Anti-Citrullinated Protein Antibodies in Rheumatoid Arthritis Reveals the Presence of Highly Sialylated Glycans. *Mol Cell Proteomics* 2017. 16: 278-287.
- 2 Vergroesen, R. D., Slot, L. M., Hafkenscheid, L., Koning, M. T., van der Voort, E. I. H., Grooff, C. A., et al., B-cell receptor sequencing of anti-citrullinated protein antibody (ACPA) IgG-expressing B cells indicates a selective advantage for the introduction of N-glycosylation sites during somatic hypermutation. *Ann Rheum Dis* 2018. 77: 956-958.
- 3 Hafkenscheid, L., de Moel, E., Smolik, I., Tanner, S., Meng, X., Jansen, B. C., et al., N-Linked Glycans in the Variable Domain of IgG Anti-Citrullinated Protein Antibodies Predict the Development of Rheumatoid Arthritis. *Arthritis Rheumatol* 2019. 71: 1626-1633.
- 4 Kissel, T., van Schie, K. A., Hafkenscheid, L., Lundquist, A., Kokkonen, H., Wuhrer, M., et al., On the presence of HLA-SE alleles and ACPA-IgG variable domain glycosylation in the phase preceding the development of rheumatoid arthritis. *Ann Rheum Dis* 2019. 78: 1616-1620.
- 5 Jansen, B. C., Hafkenscheid, L., Bondt, A., Gardner, R. A., Hendel, J. L., Wuhrer, M., et al., HappyTools: A software for high-throughput HPLC data processing and quantitation. *PLoS One* 2018. 13: e0200280.
- 6 Kasermann, F., Boerema, D. J., Rueggsegger, M., Hofmann, A., Wymann, S., Zuercher, A. W., et al., Analysis and functional consequences of increased Fab-sialylation of intravenous immunoglobulin (IVIg) after lectin fractionation. *PLoS One* 2012. 7: e37243.
- 7 Hensvold, A. H., Magnusson, P. K., Joshua, V., Hansson, M., Israelsson, L., Ferreira, R., et al., Environmental and genetic factors in the development of anticitrullinated protein antibodies (ACPAs) and ACPA-positive rheumatoid arthritis: an epidemiological investigation in twins. *Ann Rheum Dis* 2015. 74: 375-380.
- 8 Terao, C., Ohmura, K., Ikari, K., Kawaguchi, T., Takahashi, M., Setoh, K., et al., Effects of smoking and shared epitope on the production of anti-citrullinated peptide antibody in a Japanese adult population. *Arthritis Care Res (Hoboken)* 2014. 66: 1818-1827.
- 9 Bos, W. H., Wolbink, G. J., Boers, M., Tijhuis, G. J., de Vries, N., van der Horst-Bruinsma, I. E., et al., Arthritis development in patients with arthralgia is strongly associated with anti-citrullinated protein antibody status: a prospective cohort study. *Ann Rheum Dis* 2010. 69: 490-494.
- 10 Kawashiri, S. Y., Tsuji, Y., Tamai, M., Nonaka, F., Nobusue, K., Yamanashi, H., et al., Effects of cigarette smoking and human T-cell leukaemia virus type 1 infection on anti-citrullinated peptide antibody production in Japanese community-dwelling adults: the Nagasaki Islands Study. *Scand J Rheumatol* 2020: 1-4.
- 11 Arnett, F. C., Edworthy, S. M., Bloch, D. A., McShane, D. J., Fries, J. F., Cooper, N. S., et al., The American Rheumatism Association 1987 revised criteria for the classification of rheumatoid arthritis. *Arthritis Rheum* 1988. 31: 315-324.
- 12 Kokkonen, H., Brink, M., Hansson, M., Lassen, E., Mathsson-Alm, L., Holmdahl, R., et al., Associations of antibodies against citrullinated peptides with human leukocyte antigen-shared epitope and smoking prior to the development of rheumatoid arthritis. *Arthritis Res Ther* 2015. 17: 125.
- 13 Jansen, B. C., Bondt, A., Reiding, K. R., Scherjon, S. A., Vidarsson, G. and Wuhrer, M., MALDI-TOF-MS reveals differential N-linked plasma- and IgG-glycosylation profiles between mothers and their newborns. *Sci Rep* 2016. 6: 34001.
- 14 Hafkenscheid, L., de Moel, E., Smolik, I., Tanner, S., Meng, X., Jansen, B. C., et al., N-linked glycans in the variable domain of ACPA-IgG predict the development of rheumatoid arthritis. *Arthritis Rheumatol* 2019.

Supplemental Tables

Table S1. Descriptive cohort data

	Cohort 1 Pre-symptomatic individuals, Sweden (Umeå) N = 228
Sex (female), n(%)	145 (64)
Age (years), mean (SD)	52.2 (9.4)
Time until symptom-onset of RA (years), median (Q3 - Q1)	4.7 (5.9)
Time until arthritis development (months), median (Q3 - Q1)	
Arthritis/RA during follow up, n (%)	228 (100)
ACPA-positive, n (%)	168 (73.7)
ACPA levels (AU/mL), median (Q3 - Q1)	126.7 (455.5)
HLA-SE positive, n(%)	165/227 (72.7)
VDG positive, n (%)	105 (46.1)
VDG%, median (Q3 - Q1)	97.4 (53.5)
GP24%, median (Q3 - Q1)	34.3 (9.5)

VDG = variable domain glycosylation
GP24 = glycan peak 24, most abundant disialylated VDG peak
ACPA titer/levels were measured as previously described^{4,9,10}

Table S2. Linear regression analysis of individuals with arthralgia from The Netherlands (Amsterdam) with VDG percentages as dependent variable.

Arthralgia	univariable (simple)			
	B	95%CI		sign.
		lower	upper	
HLA-SE	13.96	0.20	27.71	0.047
HLA-SE DR4	17.98	4.50	31.45	0.009
Sex (female)	0.80	-14.96	16.57	0.92
ACPA levels	20.66	17.68	23.64	< 0.001
Age (years)	0.32	-0.31	0.96	0.32

ACPA levels are log transformed

Table S3. Linear regression analysis of individuals with arthralgia from The Netherlands (Amsterdam) with GP24 percentages as dependent variable.

Arthralgia	univariable (simple)			
	B	95%CI		sign.
		lower	upper	
HLA-SE	3.97	1.37	6.57	0.003
HLA-SE DR4	3.73	1.14	6.32	0.005
Sex (female)	-0.003	-3.05	3.04	0.99
ACPA levels	3.19	2.46	3.92	< 0.001
Age (years)	-0.02	-0.14	0.11	0.76

ACPA levels are log transformed

Cohort 1 (Continued)	Cohort 2	Cohort 3
RA patients, Sweden (Umeå) N = 126	Individuals with arthralgia, The Netherlands (Amsterdam, Reade) N = 239	Healthy, symptom-free individuals, Japan (Nagasaki) N = 58
78 (61)	185 (77)	38 (66)
59.7 (9.3)	48.3 (11.6)	66.7 (9.9)
-	-	-
-	18.22 (30.7)	-
-	137 (57.3)	9 (15.5)
125 (98.4)	239 (100)	58 (100)
592.9 (725.3)	103 (708.5)	35.8 (79)
94/126 (74)	74/128 (73)	22/39 (56.4)
116 (92.1)	211 (87.9)	48 (83.8)
94.2 (50.8)	75.3 (48.9)	58.1 (35.6)
32.1 (9.2)	35.6 (8.98)	32.1 (9.8)

multivariable (multiple)				multivariable (multiple)			
B	95%CI		sign.	B	95%CI		sign.
	lower	upper			lower	upper	
3.47	-5.26	12.19	0.43	6.24	-2.41	14.88	0.16
20.45	17.41	23.48	< 0.001	20.22	17.19	23.25	< 0.001

multivariable (multiple)				multivariable (multiple)			
B	95%CI		sign.	B	95%CI		sign.
	lower	upper			lower	upper	
2.41	0.31	4.50	0.03	1.96	-0.15	4.06	0.07
3.04	2.31	3.77	< 0.001	3.05	2.31	3.79	< 0.001

Table S4. Linear regression analysis of ACPA-positive individuals with arthralgia (The Netherlands) with log-transformed ACPA levels as dependent variable.

Arthralgia	univariable (simple)				multivariable (multiple)			
	B	95% CI		sign.	B	95% CI		sign.
		lower	upper			lower	upper	
HLA-SE	0.18	0.61	0.97	0.66	0.09	-0.24	0.43	0.58
HLA-SE DR4	0.34	0.46	1.12	0.40				
Sex (female)	-0.11	-1.00	0.77	0.80				
Age (years)	-0.02	-0.06	0.01	0.28				
VDG%	0.030	0.026	0.034	< 0.001	0.030	0.026	0.034	< 0.001
GP24%	0.13	0.10	0.15	< 0.001				

VDG = variable domain glycosylation

GP24 = glycan peak 24, most abundant disialylated VDG peak

Table S5. Linear regression analysis of pre-symptomatic individuals from Sweden (Umeå) with VDG percentages as dependent variable.

Pre-RA	univariable (simple)			
	B	95% CI		sign.
		lower	upper	
HLA-SE	-9.536	-27.771	8.699	0.302
Sex (female)	2.747	-12.609	18.103	0.724
ACPA+/-	28.047	-7.129	63.222	0.117
ACPA levels (AU/mL)	0.019	0.010	0.029	0.000
Age (years)	-0.230	-1.026	0.566	0.568
Time until RA development (years)	0.533	-1.383	2.449	0.582

Table S6. Linear regression analysis of pre-symptomatic individuals from Sweden (Umeå) with ACPA levels as dependent variable.

Pre-RA	univariable (simple)			
	B	95% CI		sign.
		lower	upper	
HLA-SE	102.733	-67.058	272.523	0.234
VDG+/-	529.780	394.936	664.624	0.000
VDG%	6.574	3.222	9.927	0.000

VDG = variable domain glycosylation

	multivariable (multiple)				multivariable (multiple)				multivariable (multiple)			
	B	95% CI		sign.	B	95% CI		sign.	B	95% CI		sign.
		lower	upper			lower	upper			lower	upper	
	0.02	-0.42	0.45	0.93								
					0.04	-0.30	0.38	0.82	0.12	-0.31	0.55	0.57
					0.030	0.026	0.035	< 0.001				
	0.12	0.09	0.15	< 0.001					0.12	0.09	0.15	< 0.001

multivariable (multiple)				multivariable (multiple)			
B	95% CI		sign.	B	95% CI		sign.
	lower	upper			lower	upper	
-9.388	-27.498	8.721	0.306	-11.20	-28.286	5.877	0.196
27.859	-7.313	63.031	0.119	0.020	0.010	0.030	0.000

multivariable (multiple)				multivariable (multiple)			
B	95% CI		sign.	B	95% CI		sign.
	lower	upper			lower	upper	
148.491	-167.840	464.822	0.354	34.621	-117.981	187.222	0.655
				527.869	391.351	664.387	0.000
6.735	3.363	10.108	0.000				

Table S7. Logistic regression analysis of pre-symptomatic individuals from Sweden (Umeå) with detectable vs. non detectable VDG profiles.

Pre-RA	univariable (simple)			
	OR	95% CI		sign.
		lower	upper	
HLA-SE	1.675	0.920	3.049	0.091
Sex (female)	0.735	0.428	1.263	0.265
ACPA+/-	16.176	6.157	42.500	< 0.001
ACPA levels (AU/mL)	1.003	1.002	1.004	< 0.001
Age (years)	1.001	0.974	1.030	0.918
Time until RA development (years)	0.241	-0.126	0.607	0.196

VDG = variable domain glycosylation

Table S8. Logistic regression analysis of pre-symptomatic individuals from Sweden (Umeå) with detectable vs. non detectable (< 25 AU/mL) ACPA.

Pre-RA	univariable (simple)			
	OR	95% CI		sign.
		lower	upper	
HLA-SE	0.851	0.433	1.671	0.639
Sex (female)	0.735	0.428	1.263	0.265
VDG+/-	16.176	6.157	42.500	< 0.001
VDG%	1.025	0.993	1.059	0.121
Age (years)	1.006	0.974	1.038	0.730
Time until RA development (years)	1.271	1.165	1.387	< 0.001

VDG = variable domain glycosylation

Table S9. Logistic regression analysis of RA patients from Sweden (Umeå) with detectable vs. non detectable VDG profiles.

RA	univariable (simple)			
	OR	95% CI		sign.
		lower	upper	
HLA-SE	0.305	0.037	2.504	0.269
Sex (female)	1.091	0.292	4.082	0.897
ACPA+/-	0.000	0.000		0.999
ACPA levels (AU/mL)	1.003	1.000	1.005	0.027
Age (years)	0.981	0.913	1.054	0.595

OR	multivariable (multiple)			sign.	OR	multivariable (multiple)		sign.
	95% CI		lower			upper		
	lower	upper						
1.520	0.758	3.048	0.238	1.998	1.034	3.863	0.040	
				17.211	6.500	45.572	< 0.001	
1.004	1.002	1.005	< 0.001					

OR	multivariable (multiple)			sign.	OR	multivariable (multiple)		
	95% CI		sign.			95% CI		sign.
	lower	upper				lower	upper	
1.027	0.105	10.064	0.981	0.620	0.273	1.410	0.254	
				26.842	8.688	82.932	< 0.001	
1.025	0.993	1.059	0.125					
1.058	0.855	1.309	0.603	1.35	1.208	1.509	< 0.001	

	multivariable (multiple)				multivariable (multiple)			
	OR	95% CI		sign.	OR	95% CI		sign.
		lower	upper			lower	upper	
	0.331	0.039	2.811	0.311	0.297	0.036	2.446	0.259
					0.000	0.000		0.999
	1.003	1.000	1.005	0.029				

Supplemental Figure

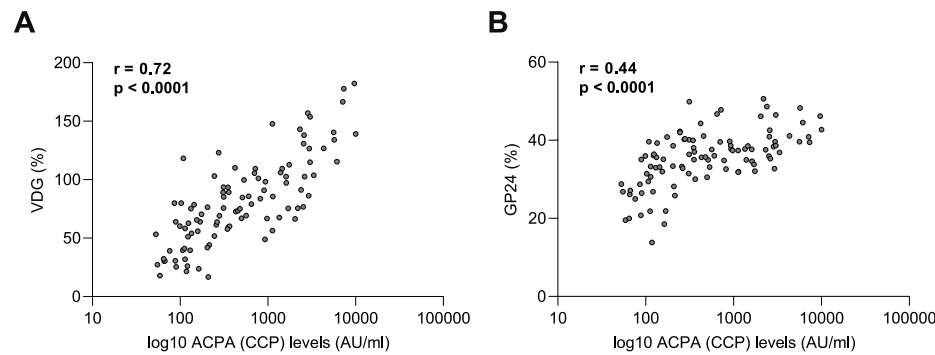


Figure S1. Correlation between ACPA levels (log transformed) and (A) ACPA IgG variable domain glycosylation (VDG) or (B) disialylated VDG (GP24, G2FBS2) in individuals with arthralgia from The Netherlands (Amsterdam). Correlation was assessed with Pearson correlation.

Supplemental Materials and Methods

Patient and public involvement - Patients were involved in this study by donating blood when attending population surveys or health checkups.

Study cohorts - The study presents data from three different cohorts. Cohort 1 includes Swedish individuals diagnosed with RA later in life and sampled at the Medical Biobank of Northern Sweden prior to symptom-onset [median (IQR) pre-dating time: 4.7 (5.9) years; $n = 228$; 168 ACPA-positive] and after diagnosis of RA ($n = 126$, 125 ACPA-positive). All RA patients fulfilled the 1987 ARA classification criteria¹¹. Cohort 2 presents data from Dutch ACPA-positive individuals with arthralgia with up to 10 years of follow-up for arthritis development sampled at the rheumatology outpatient clinic in the Amsterdam area of The Netherlands. 137 individuals (57.3%) developed arthritis during follow-up. Individuals from cohort 3 were selected as ACPA-positive healthy individuals at risk of RA, which were part of the Nagasaki Island Study performed in Japan. The prospective cohort study was based on resident health checkups. All ACPA-positive individuals were free of RA-specific symptoms (joint complaints) at the time-point of sampling and followed up to three years. 9 individuals (15.5%) developed RA during follow up. Descriptive cohort information is presented in Table S1.

Ethical considerations - All participants have given their written informed consent and the Regional Ethical Review Board Committees approved the studies.

Statistical analyses - Statistical calculations were performed using SPSS for Windows version 27.0 (IBM Corp., NY, USA) or STATA (V.16.1; STATA Corp, College Station, Texas USA). Continuous data were analyzed using non-parametric methods (Mann-Whitney's U-test and Wilcoxon signed-rank test) and parametric tests when appropriate. All p-values are two-sided and $p < 0.05$ was considered as statistically significant. Univariable (simple) and multivariable (multiple) logistic regression analyses were performed for cohort 1 (Swedish pre-symptomatic individuals) and detectable vs. non detectable VDG profiles or ACPA. Univariate and multivariate linear regression analyses were performed for cohort 1 and 2 (Dutch ACPA-positive individuals with arthralgia) and the percentages of ACPA IgG VDG and GP24 as well as for ACPA levels as dependent variables. Associations with HLA-SE were assessed. The unstandardized coefficient (B) represents the mean change in the response given a one unit change in the predictor. Correlation between ACPA levels (log transformed) and percentages of VDG was assessed with Pearson correlation.

Laboratory analyses - Anti-citrullinated protein antibodies (ACPAs) were analyzed in serum samples using anti-cyclic citrullinated peptide (CCP) enzyme linked immunosorbent assays (ELISAs) and HLA genotyping was performed as previously described^{9,10,12}. In short, ACPAs were detected in samples of pre-symptomatic individuals and RA patients from Sweden (cohort 1) using a CCP2

ELISA from Euro-Diagnostica (Malmö, Sweden) with a positivity cut-off set at 25 AU/mL. HLA-DRB1 genotyping was performed using PCR sequence-specific primers from the DR low-resolution and DRB1*04 subtyping kits (Olerup SSP AB, Saltsjöbaden, Sweden). The SE genes were defined as HLA-DRB1*01:01, 04:01, *04:04, *04:05 and *04:08¹². The CCP-status from the Dutch ACPA-positive individuals with arthralgia (cohort 2) were determined using a second-generation anti-CCP ELISA (Axis Shield, Dundee UK). The cut-off level was set at 5 AU/mL. HLA-DRB1 genotyping was performed by sequenced-based, high resolution typing (Department of Immunogenetics, Sanquin, Amsterdam). The SE alleles were defined as HLA-DRB1*01:01, *01:02, *04:01, *04:04, *04:05, *04:08, *04:10 and *10:01⁹. ACPAs from healthy individuals from Japan (cohort 3) were detected by a CLEIA (STACIA MEBLUX test CCP; MBL, Nagoya, Japan). The cut-off level was < 4.5 U/mL. HLA-DRB1 genotyping was performed with the WAKFlow HLA typing kit (Wakunaga Pharmaceutical, Osaka, Japan) based on the reverse sequence-specific oligonucleotide probes method coupled with the xMAP technology designed for the use with the Luminex system (Luminex Japan, Tokyo, Japan)¹⁰.

ACPA IgG capturing and VDG analysis - ACPA IgG capturing, total glycan release, glycan labeling, UHPLC analysis and data processing were performed as previously described^{1,4,5,13}. In brief, ACPAs were isolated from 25 µl of serum samples using NeutrAvidin Plus resin (Thermo Fisher Scientific) coupled with 0.1 µg/µl CCP2-biotin. Following, IgG isolation was performed using FcXL affinity beads (Thermo Fisher Scientific). N-linked glycans were released from captured ACPA IgG using PNGase F and subsequently labeled with 2-aminobenzoic acid (2-AA, Sigma Aldrich) and 2-picoline borane (2-PB, Sigma Aldrich). The glycans were purified via hydrophilic interaction liquid chromatography-solid phase extraction (HILIC SPE) using GHP membrane filter plates (Pall Life Science). 2-AA labelled and HILIC SPE purified N-linked glycans were analyzed using a Dionex Ultimate 3000 (Thermo Fisher Scientific) instrument, a FLR fluorescence detector set with excitation and emission wavelengths of 330 and 420 nm and a Acquity UHPLC BEH Glycan column (1.7 µm 2.1 mm × 100 mm; Waters, Milford, MA). Separation was performed as previously published⁴. The generated chromatograms were aligned and separated into 24 glycan peaks (GP) using Chromeleon version 7.1.2.1713 (Thermo Fisher Scientific). The glycan composition in each chromatographic peak was defined as previously described⁵. Calibration was performed using HappyTools version 0.0.2 and the elution time of five calibrant peaks (G0F, G1F, G2F, G2FBS1 and G2FBS2). Integration and baseline correction were performed using the following settings: *general settings*: start t = 8 min, end t = 30 min; *peak detection settings*: minimum intensity: 0.05, sigma value: 2.0; *calibration settings*: minimum peaks: 4, minimum S/N: 1; *quantitation settings*: datapoints: 100, baseline order: 1, background window: 1.0, MT slice points: 5. The amount of N-glycans in each peak was expressed as the total integrated area under the curve (AUC). The cut-off was based on the AUC of all blank and 8 ACPA-negative healthy donor samples, excluding low outliers (below $Q_1 - 1.5 \times IQR$) and high outliers (above $Q_3 + 1.5 \times IQR$). The percentage VDG was calculated based on the following formula: $[(G2FBS1 + G2FS2 + G2FBS2) / (G0F + G1F + G2F) \times 100]^{5,14}$ and the percentage of GP24 as follows: $[G2FBS2 / (G2FBS1 + G2FS2 + G2FBS2) \times 100]$.



ACPA IgG variable domain glycosylation increases before the onset of rheumatoid arthritis and stabilizes thereafter; a cross-sectional study encompassing 1500 samples

Theresa Kissel, Lise Hafkenscheid, Tineke J. Wesemael, Mami Tamai, Shin-ya Kawashiri, Atsushi Kawakami, Hani S. El-Gabalawy, Dirkjan van Schaardenburg, Solbritt Rantapää-Dahlqvist, Manfred Wuhrer, Annette H.M. van der Helm-van Mil, Cornelia F. Allaart, Diane van der Woude, Hans U. Scherer, René E.M. Toes, Tom W.J. Huizinga

Abstract

The autoimmune response in Rheumatoid Arthritis (RA) is marked by anti-citrullinated protein antibodies (ACPAs). A notable feature of ACPA IgG is the abundant expression of N-linked glycans in the variable domain. However, the presence of ACPA variable domain glycosylation (VDG) across disease stages, and its' response to therapy is poorly described. To understand its dynamics, we investigated the abundance of ACPA IgG VDG in 1498 samples from individuals in different clinical disease stages.

Using liquid chromatography, we analyzed ACPA IgG VDG profiles of 7 different cohorts from Japan, Canada, The Netherlands and Sweden. We assessed 106 healthy, 228 pre-symptomatic, 277 arthralgia, 307 patients with new-onset/ early RA and 117 RA patients 4, 8 and 12 months after disease-onset and prespecified treatment regimens. Additionally, we measured VDG of 234 samples from patients whose RA did and patients whose RA did not enter long-term drug-free remission (DFR) during up to 16 years follow-up.

Our data show that ACPA IgG VDG significantly increased ($p < 0.0001$) towards disease-onset and associates with ACPA levels and epitope spreading pre-diagnosis. A slight increase in VDG was observed in established RA and a moderate influence of treatment ($p = 0.007$). Individuals in whom DFR was later achieved, ACPA IgG VDG was already reduced at the time of RA-onset.

Thus, the abundance of ACPA IgG VDG increases towards RA-onset and correlates with maturation of the ACPA response. While, ACPA IgG VDG levels are fairly stable in established disease, a lower degree of VDG at RA-onset correlates with DFR. Although the underlying biologic mechanisms remain elusive, our data support the concept that VDG relates to an expansion of the ACPA response pre-disease and contributes to disease development.

Introduction

Rheumatoid Arthritis (RA) is a prevalent, slowly evolving autoimmune disease with arthralgia as an important pre-disease manifestation. The most specific autoimmune response for RA is characterized by the presence of anti-citrullinated protein antibodies (ACPAs), which can be found several years before the onset of clinical symptoms. ACPA-positive patients have a more severe disease course and are less likely to achieve drug-free remission (DFR) as compared to seronegative patients¹. ACPA responses are known to be dynamic during the transition towards RA, as an increase in ACPA levels combined with a broader epitope-recognition profile is associated with the development of clinical symptoms². Autoantibody levels are, however, not associated with long-term treatment response and do not predict DFR³. Glycomic analysis revealed that ACPA IgG are abundantly glycosylated in their antigen-binding fragments expressing complex-type variable domain glycans (VDGs) that are mainly disialylated and bisected⁴. A variable domain glycosylation (VDG) on more than 90% of the autoantibodies, is an outstanding characteristic of ACPA IgG and distinguishes the molecules from conventional IgG which display, next to the conserved presence of glycans in the fragment crystallizable (Fc) region, a considerably lower VDG of ~12 to 14%^{4,5}. Glycosylation sites required for the attachment of VDGs are introduced by somatic hypermutation (SHM)⁶. Although the role and dynamics of ACPA IgG Fc glycans has been studied extensively⁷⁻¹⁰, little is known about the expression levels or potential biologic implications of the VDG on ACPAs. As carbohydrates might encode important biologic information and possibly affect cellular functions, it is important to understand VDG dynamics over time in relation to the disease course of RA. Previously, we showed that ACPA IgG VDG can occur several years before RA-onset. In a Canadian population, ACPA IgG VDG was predictive for disease development^{11,12}. However, how ACPA IgG VDG changes between different clinical disease stages from healthy, symptom-free individuals to individuals with arthralgia to patients at RA-onset and with established RA has not been elucidated. Additionally, it is unclear whether VDG levels are associated with treatment outcomes, predict DFR and disease flares, or can be modified by treatment. To understand the momentum of VDGs and thereby their possible contribution to the autoreactive B-cell responses in RA, we cross-sectionally investigated the presence and abundance of ACPA IgG VDGs in 1498 samples from an ethnically diverse group of individuals in various disease stages. Importantly, by analyzing samples from a well-controlled treatment strategy trial, the Improved study, aiming to assess the most effective strategy in inducing remission in early RA, we investigated longitudinal VDG changes in established RA after treatment escalation or treatment tapering¹³. Finally, we longitudinally analyzed ACPA IgG VDG changes of individuals visiting the Leiden Early Arthritis Clinic (EAC) in whom sustained drug-free (> 1 year) remission (SDFR) was achieved and those who experienced late disease flares, with an extensive follow-up of up to 16 years¹⁴.

Results

ACPA IgG variable domain glycosylation increases toward disease-onset and remains stable in established RA

To provide a comprehensive overview of the presence and abundance of ACPA IgG VDGs (Figure 1, A and B), we analyzed 1377 ACPA-positive and 121 ACPA-negative samples from individuals in different clinical disease stages (Figure 1C and Table 1). Comparable to the results of previous studies^{11,12}, we found that high percentages of VDGs (median of 56.2%) on ACPA IgG were already present in healthy individuals (n = 106) without symptoms (Figure 1D). Cross-sectional analysis revealed a significant increase in VDG (median of 74.7%) in individuals with clinically identified arthralgia (n = 277) compared to healthy individuals (Figure 1D). A further significant increase in VDG of 18% was observed when individuals were sampled at RA-onset (n = 181) (VDG median of 92.6% in the combined dataset) (Figure 1D and Table 1).

This was, however, not apparent in all individual sample sets, as VDG changes between the arthralgia phase and RA-onset could not be observed in the statistically underpowered longitudinal dataset from cohort 5 (arthralgia, Leiden), presumably because the clinically suspect arthralgia individuals were included shortly before the onset of arthralgia (Figure S3), and an increase in VDG could have occurred earlier. Patients presenting with arthralgia, regardless of whether they did or did not subsequently develop RA, displayed a lower VDG than patients at the time of RA-onset (Figure S1E). In samples from patients with established RA after prespecified treatment (n = 346), ACPA IgG VDG remained stable, with only a moderate increase after 12 months, to a median of 105.2% (Figure 1D). As previously shown¹¹, an increase in ACPA IgG VDG toward RA-onset was also observed in a Swedish population of ACPA-positive individuals that later developed RA. The extended dataset used here also exhibited a rise in VDG when analyzed per individual in a longitudinal manner (Figure S1D)²¹, however no significance could be detected cross-sectionally (Figure S1C).

Overall, the results obtained indicate that the presence of VDG on ACPA IgG was lower in healthy individuals and increased toward RA development. However, in established disease, no further progression of ACPA IgG VDG was observed in this cross-sectional setting.

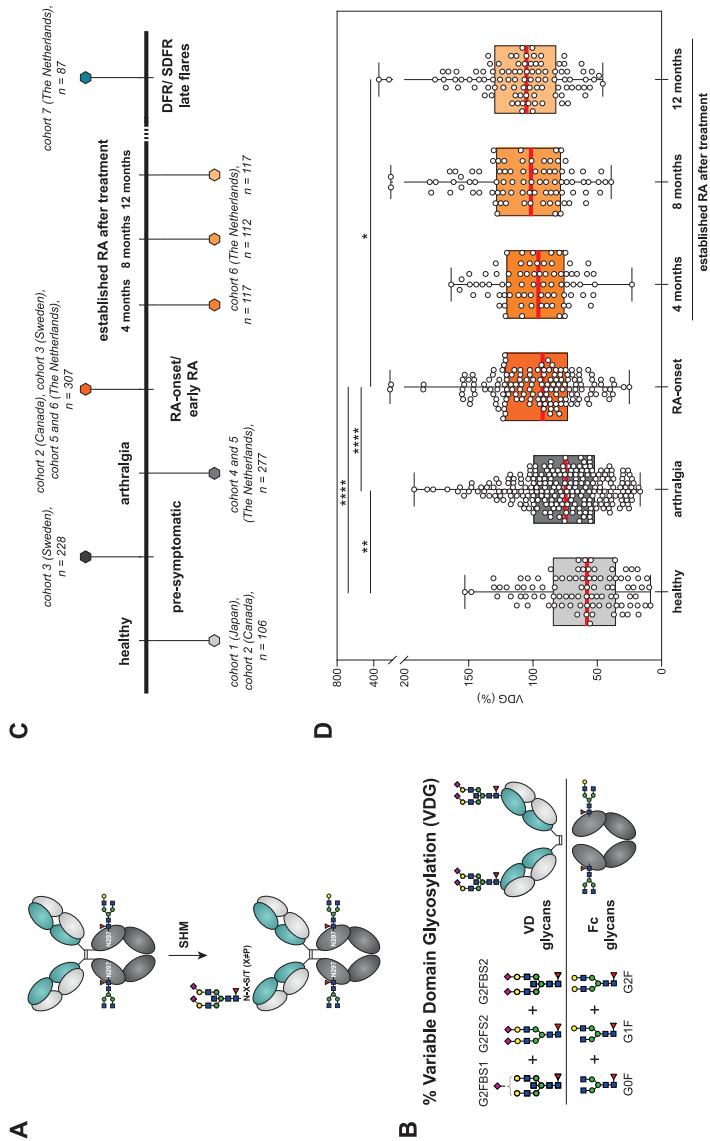


Figure 1. Percentage ACPA IgG VDG from individuals in different disease stages of RA. (A) Depiction of the process by which IgG carries N-glycans at each N297 residue in the Fc domain and can acquire additional N-linked glycosylation sites (N-X-S/T, X ≠ P) in the variable domain by somatic hypermutation (SHM). (B) Depiction of the calculation of ACPA IgG VDG, i.e., [(sum of the most abundant VDG)/(sum of the most abundant Fc glycans) × 100] or [(G2FBS1+G2FBS2+G2FBS3)/(G2FBS1+G2FBS2+G2FBS3) × 100]. The selected glycan traits are exclusively present on either the variable domain or the Fc domain of ACPA IgG. A: mono-/di-galactosylated (G0/G1/G2), core fucosylated (F), bisecting GlcNAc (B), mono-/di-sialylated (S1/S2). Blue square: N-acetylglucosamine (GlcNAc), green circle: galactose, red triangle: fucose, pink diamond: N-acetylneuraminic acid. (C) “Time-line” of clinical disease stages, the corresponding analyzed cohorts and absolute numbers of analyzed samples. (D) Percentage ACPA IgG VDG, measured by liquid chromatography, of healthy (light gray), arthralgia (dark gray), RA-onset (orange) and established RA (light orange), individuals after preprescribed treatment. Data are presented as box and whiskers including all data points. Kruskal-Wallis tests were performed for the cross-sectional datasets of cohorts 1, 2, 4 and 12 months including the Dunn’s test. Generalized estimating equation (GEE) analysis was performed for the longitudinal samples of cohort 6. Significant differences are denoted by * (p = 0.037), ** (p = 0.0032), or **** (p < 0.0001).

Table 1. Descriptive cohort data. Cohorts including samples from individuals in different disease stages from healthy symptom-free to established RA. Cohort 7 includes individuals that achieve DMARD-free remission (DFR), sustained DFR (SDFR) and individuals with late disease flares.

cohort	cohort 1, Japan (Nagasaki)	cohort 2, Canada (Manitoba)	cohort 3, Sweden (Umeå)	cohort 4, The Netherlands (Amsterdam, Reade)	cohort 5, The Netherlands (Leiden, CSA)	
disease stage	healthy, symptom-free	healthy RA-onset	pre-symptomatic 0.5 - 1.5 years after RA-onset	arthralgia	arthralgia RA-onset	
	N = 58	N = 48 N = 25	N = 228 N = 126	N = 239	N = 38 N = 26	
sex (female), n(%)	38 (66)	32 (66.7) 19 (79)	145 (64) 78 (61)	185 (77)	29 (76.3) 22 (84.6)	
age (years), mean (SD)	66.7 (9.9)	37.6 (13.5) 42 (14.7)	52.2 (9.4) 59.7 (9.3)	48.3 (11.6)	48.3 (12.5) 48.1 (12.5)	
arthritis/RA at follow up, n (%)	9 (15.5)	31 (64.6) -	228 (100) -	137 (57.3)	26 (68.4) -	
VDG-positive, n (%)	48 (83.8)	42 (33.3) 21 (84)	105 (46.1) 116 (92.1)	211 (87.9)	27 (71.1) 18 (69.2)	
VDG%, median (IQR)	58.1 (35.6)	44.9 (69.3) 99.9 (46.1)	97.4 (53.5) 94.2 (50.8)	75.3 (48.9)	70.4 (28.8) 59.1 (49.1)	
ACPA-positive, n (%)	58 (100)	37 (77.1) 22 (88)	168 (73.7) 125 (98.4)	239 (100)	33 (86.8) 21 (80.8)	
ACPA levels (aU/ml)*, median (IQR)	35.8 (79)	54 (135.5) 200 (103.3)	126.7 (455.5) 592.9 (725.3)	358 (1351)	123 (324) 25.5 (266.8)	
ACPA assay	CLEIA (STACIA MEBLux test CCP; MBL, Nagoya, Japan) ²⁰	CCP-2 kit (INOVA Diagnostics, (San Diego, CA, USA) ¹⁹	Immunoscan RA anti-CCP-2 EIA from Euro-Diagnostica (Arnhem, The Netherlands) ¹⁸	anti-CCP ELISA (Axis Shield, Dundee, UK) ¹⁷	anti-CCP-2 ELISA (Eurodiagnostica, The Netherlands) ¹⁶	

* ACPA levels (arbitrary units/ml) were determined with various assays/standards and are thus not directly comparable with each other.

	cohort 6, The Netherlands (Leiden, Improved)				cohort 7, The Netherlands (Leiden, EAC)					
	RA-onset	4 months after RA-onset	8 months after RA-onset	12 months after RA-onset	RA-onset, do not achieve DFR	RA-onset, achieve DFR	pre-remission	DRF	SDFR	DFR with late flares
	N = 130	N = 117	N = 112	N = 117	N = 59	N = 36	N = 52	N = 41	N = 35	N = 11
	88 (67.7)	79 (67.5)	78 (69.6)	78 (66.7)	42 (71.2)	24 (66.7)	37 (71.2)	27 (65.9)	27 (77.1)	7 (63.6)
	51.1 (12.5)	50.6 (12.8)	50.7 (12.4)	51.0 (12.4)	49.7 (14.5)	50.8 (13.1)	54.2 (14.8)	58.5 (13.6)	54.6 (15.1)	69.4 (14.8)
	-	-	-	-	-	-	-	-	-	-
	117 (90)	78 (66.7)	86 (76.8)	98 (83.8)	59 (100)	32 (89)	37 (71)	30 (73.2)	22 (62.9)	9 (81.8)
	96 (48.2)	95.9 (45.1)	101.7 (50.3)	105.2 (48.1)	83.8 (46)	61.4(35)	74.05 (30)	67.7 (41.5)	73.5 (42)	78.3 (26.9)
	130 (100)	117 (100)	112 (100)	117 (100)	59 (100)	29 (80.6)	38 (73)	33 (80)	29 (82.9)	10 (91)
	903.3 (1101.2)	449.9 (806.9)	602 (1061.8)	651.7 (962.5)	7340 (5984)	1933 (7296)	3583 (5302)	3010 (8975)	2616 (6765)	4210 (10709)
	anti-CCP-2 in house ELISA (The Netherlands) ^{3,15}				anti-CCP-2 in house ELISA (The Netherlands) ^{3,15}					

Interconnection between the increase in variable domain glycosylation and maturation of the ACPA immune response

To obtain further insights into ACPA IgG VDG, we investigated the possible association between VDG percentages and the “maturation” of the ACPA response by analyzing ACPA IgG levels and the broadness of the citrullinated epitope-recognition profile. Pearson's correlation analysis revealed a strong, highly significant correlation between VDG percentages and ACPA IgG levels among healthy individuals ($r = 0.728$ and $r = 0.672$) and among individuals with arthralgia ($r = 0.640$) (Figure 2A and S2). At RA-onset ($r = 0.214$) and in established RA after prespecified treatment ($r = 0.341$, $r = 0.362$ and $r = 0.215$), however, we observed only moderate correlations as depicted by the correlation coefficient r (Figure 2A and S2). Likewise, our data revealed that ACPA IgG with increased VDG showed a significantly broader recognition profile toward multiple citrullinated epitopes (Figure 2, B and C). Ordinal regression analyses confirmed these findings for individuals with arthralgia ($p < 0.001$) (Table S1) as well as in patients at RA-onset ($p = 0.004$) and over time after treatment ($p < 0.001$) (Table S2). Thus, ACPA IgG VDG associated with ACPA IgG levels and the breadth of the epitope-recognition profile, suggesting that these two features of the ACPA responses are interconnected.

Impact of immunosuppression on ACPA IgG variable domain glycosylation

By taking advantage of the design of the Improved study (Figure 3A), we investigated whether ACPA IgG VDG predicts early remission in RA or is associated with the intensity of immunosuppression.

First, we used the longitudinal dataset to identify ACPA IgG VDG changes over time by analyzing matched-paired individuals at RA-onset ($n = 130$) versus 4 ($n = 117$), 8 ($n = 112$) and 12 months ($n = 117$) after disease development. VDG appeared to be steadily and abundantly expressed on ACPA IgG in disease, although minor changes in expression levels were observed over time. A slight, but non-significant decrease was observed 4 months after disease-onset and initiation of methotrexate (MTX) and prednisone treatment (Figure 3, B and C, and Table S3). Previous studies have shown a similar decline of ACPA IgG levels after initiation of treatment, providing further evidence of a correlation between VDG and ACPA IgG levels³. After 4 months, prednisone was tapered such that patients were then treated with MTX only, if early remission ($\text{DAS} < 1.6$) had been achieved. If early remission was not achieved, patients were randomized to one of two treatment escalation arms (arm 1: MTX, prednisone, hydroxychloroquine, and sulfasalazine combination, arm 2: MTX and adalimumab combination) (Figure 3A)¹³. At 8 months, individuals in the early remission group either continued MTX treatment combined with prednisone (no drug-free group) or, if disease remission persisted, their medication was tapered (drug-free group). Individuals in the treatment escalation group (arm 1 and arm 2) continued MTX treatment, in combination with adalimumab. Overall, irrespective of the treatment arm, VDG increased moderately but significantly 12 months after RA-onset ($p = 0.037$) (Table S3).

When comparing the different treatment groups, marginal but statistically significant effects of immunosuppression on ACPA IgG VDG were observed, with a reduction in VDG 12 months after RA-onset (Figure 3, D and E, and S4A), though not at 4 and 8 months. This moderate but significant negative effect of immunosuppression on VDG was confirmed by a generalized estimating equation (GEE) analysis over time (8 vs. 12 months) [in the early remission, drug-free group: regression coefficient (B) 12.27 (95% confidence interval -7.32 to 31.87) vs. in the early remission, no drug-free and treatment escalation group: 6.42 (95% confidence interval -0.35 to 13.10); $p = 0.007$] (Table S4) and was similar to previously reported findings with regard to ACPA IgG levels³. Last, we investigated whether VDG percentage at RA-onset predicts remission after 4 months and early drug-free remission within the first year. Similar to ACPA IgG levels³, VDG percentages did not predict early (drug-free) remission (Table S5). Collectively, these results show that ACPA IgG VDG are expressed at a persistently high level in established RA and show a slight but statistically significant decrease upon immunosuppression.

Decreased VDG during active disease in patients in whom sustained DFR is later achieved

As a next step, we performed cross-sectional and longitudinal ACPA IgG VDG analyses in individuals in whom long-term DFR was achieved or who experienced DFR with late flares. We therefore made use of the unique EAC database including patients who were followed up for a period of up to 16 years after disease-onset. Using this database, we were able to identify and approach 41 individuals in whom DFR had been achieved and 35 patients in whom SDFR (> 1 year) had been achieved. The longitudinal analysis was performed for matched-paired samples from patients at RA-onset ($n = 36$), during active disease (pre-remission) ($n = 52$), during DFR ($n = 41$), during SDFR (> 1 year) ($n = 35$), and when experiencing late disease flares ($n = 11$). Again, the data showed that VDG are stably expressed in established RA. Intriguingly, however, patients whose RA achieved DFR during follow-up ($n = 36$, VDG = 61.4%) showed significantly reduced ACPA IgG VDG at the onset of disease compared to age and gender-matched patients with persistently high disease activity (DAS > 3) ($n = 59$, VDG = 83.8%) (Figure 4A and Table 1). In contrast, no statistically significant changes were observed when the ACPA IgG VDG percentages were determined over time in the DFR group or any of the other groups analyzed (Figure 4, B to D).

Thus, these longitudinal data, confirm that ACPA IgG express a constant amount of VDG after RA-onset. The cross-sectional data also indicate that among individuals in whom long-term DFR is achieved, fewer glycans are present in the variable domains of ACPA IgG at the time of RA-onset.

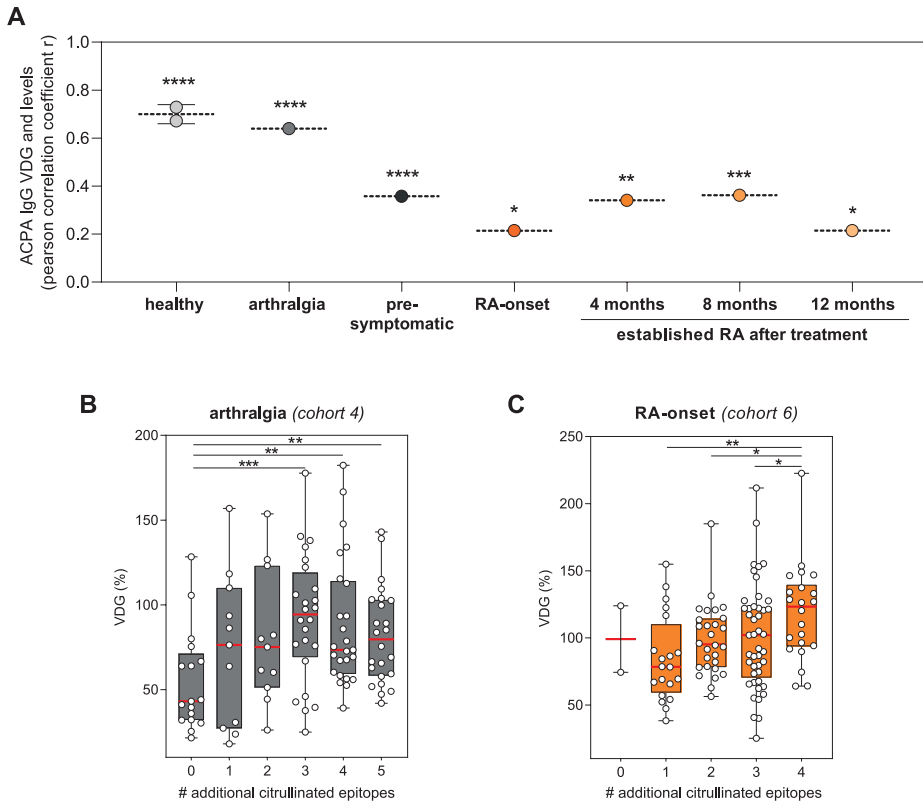


Figure 2. Correlation of ACPA IgG VDG with ACPA IgG levels and epitope spreading (maturation of the ACPA response). (A) Pearson's correlation coefficients r for the correlation between ACPA IgG VDG and ACPA IgG levels across different disease stages. P-values are two-tailed and significant differences are denoted by * (RA-onset) $p = 0.0203$, *(12 months) $p = 0.0338$, ** $p = 0.0023$, *** $p = 0.0006$ or **** $p < 0.0001$. (B) ACPA IgG VDG percentages shown for ACPA IgG isolated using CCP2 from arthralgia individuals (cohort 4, The Netherlands) and tested for binding to 0 to 5 additional citrullinated antigens (citrullinated vimentin 60-75, citrullinated fibrinogen β 36-52, α 60-74 and α 36-50 and citrullinated enolase 5-21). Kruskal-Wallis tests were performed: ** (0 vs. 4) $p = 0.0036$, ** (0 vs. 5) $p = 0.0096$, *** $p = 0.0006$. (C) ACPA IgG VDG percentages shown for ACPA IgG isolated using CCP2 from individuals at RA-onset (cohort 6, The Netherlands) and tested for recognition of 0 to 4 additional citrullinated antigens (citrullinated vimentin 59-74, citrullinated fibrinogen β 36-52 and α 27-43 and citrullinated enolase 5-20). Kruskal-Wallis tests were performed: ** (2 vs. 4) $p = 0.0411$, ** (3 vs. 4) $p = 0.0417$, *** $p = 0.0011$.

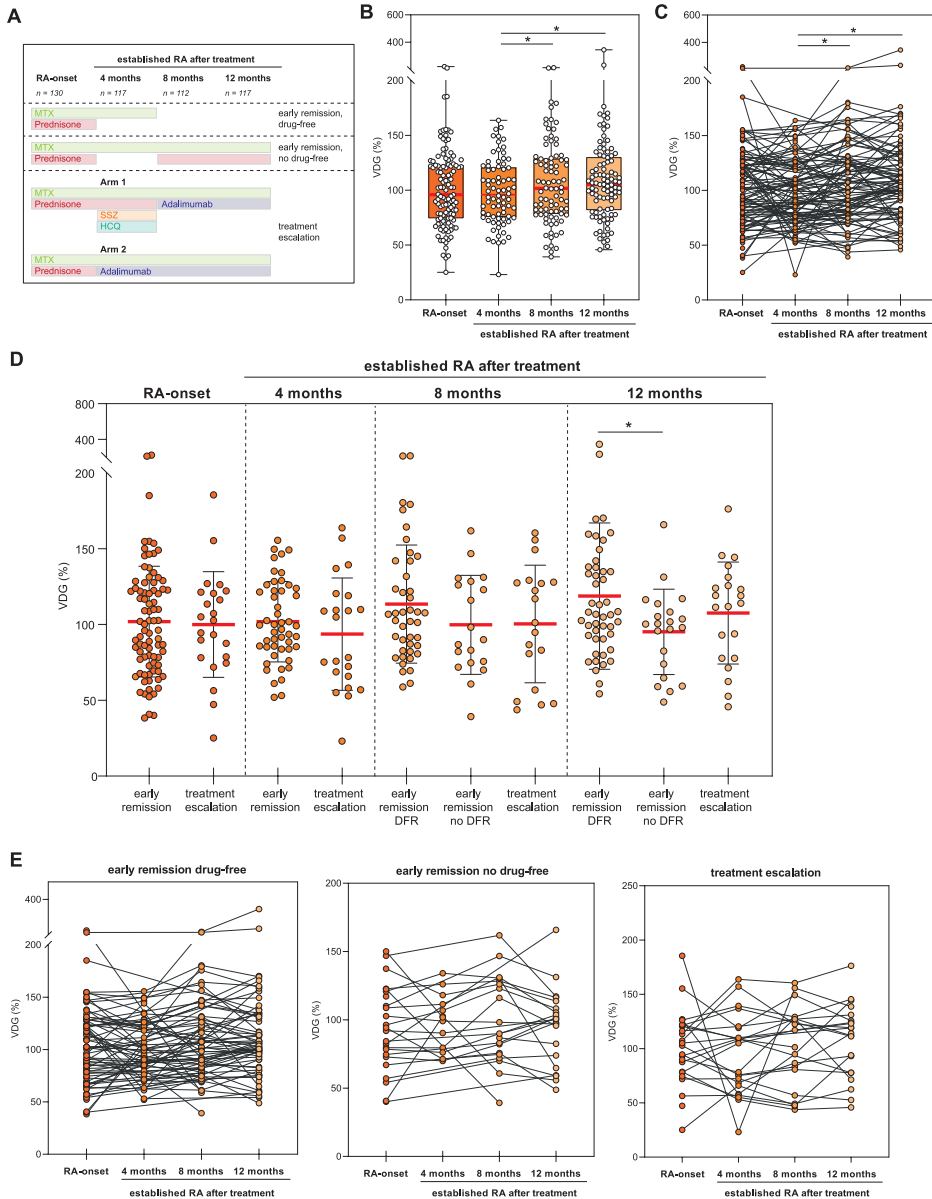


Figure 3. Longitudinal analysis of ACPA IgG VDG at RA-onset and in established RA after treatment (cohort 6, The Netherlands). (A) Treatment protocol. HCQ = hydroxychloroquine, MTX = methotrexate, SSZ = sulfasalazine (B) ACPA IgG VDG longitudinal data of patients at RA-onset and with established RA after prespecified treatment (cohort 6, The Netherlands). Data are presented as box and whiskers including all data points. Mixed-effects analysis, using Restricted Maximum Likelihood (REML), was performed including the Tukey test: $*(4 \text{ vs. } 8 \text{ months}) p = 0.0407$, $*(4 \text{ vs. } 12 \text{ months}) p = 0.0310$. (C) Longitudinal data from A are represented as matched pairs. (D) ACPA IgG VDG percentages shown by treatment group [early remission (drug-free), early remission (no drug-free) and treatment escalation]. Ordinary one-way ANOVA was performed including the Fisher's LSD test: $*p = 0.015$. (E) Longitudinal data within each treatment group, represented as matched pairs.

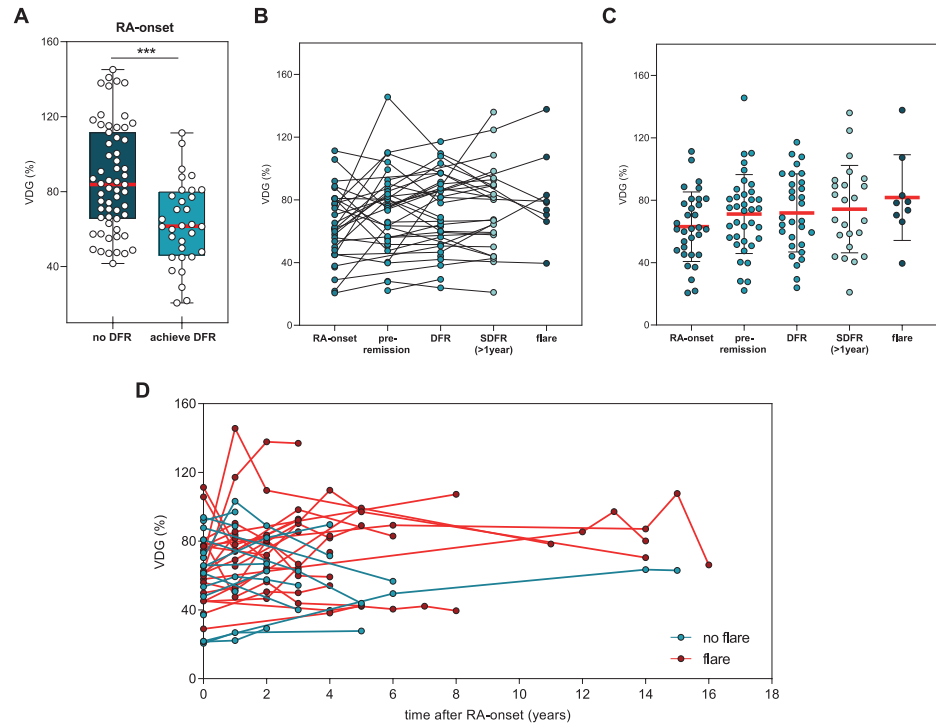


Figure 4. Cross-sectional and longitudinal analysis of ACPA IgG VDG at RA-onset and during drug-free remission (DFR) (cohort 7, The Netherlands). (A) ACPA IgG VDG percentages at RA-onset in individuals in whom DFR was not achieved and those in whom DFR was achieved. DFR was defined as the absence of clinical synovitis after discontinuation of DMARD-treatment. Mann-Whitney's U test was performed: **** $p < 0.0001$. (B) Data on ACPA IgG VDG in matched-paired samples from patients at RA-onset, pre-remission, during DFR, during SDFR (≥ 1 -year), and during late disease flares. Flare was defined as the recurrence of clinical synovitis on joint examination. (C) Same individuals as in B are depicted as scatter dot plots. Horizontal and vertical bars show the mean \pm SD. (D) ACPA IgG VDG data by assessment time point in longitudinally assessed samples from patients who did (red) and those who did not experience late flares (turquoise).

Discussion

An important key characteristic of IgG autoantibodies from patients with RA is the abundant presence of bisected and disialylated glycans in the variable domain. To gain insight into the introduction and occurrence of this unusual antibody feature across different disease stages, we have captured ACPA IgG of 1500 samples from 852 individuals in different clinical disease stages. Moreover, we analyzed the effect of therapy on the degree of variable domain glycosylation (VDG) on ACPA. The large sample size increases the power of our study, and we demonstrated that ACPA IgG VDG correlates strongly with the maturation of the ACPA immune

response prior to disease-onset, while no correlation with age was observed. We found that the abundance of ACPA IgG VDG increased significantly from the time these ACPA-positive individuals were healthy and symptom-free (58.1%) toward the pre-RA phase (arthralgia) (74.7%), with a further increase toward disease-onset (92.6%). Thus, our data strongly indicate that an increase in ACPA IgG VDG already occurs in the asymptomatic phase before symptom-onset, with a further increase during progression to arthralgia and ultimately RA-diagnosis, although the latter notion requires further detailed research with longitudinal sampling.

In established RA, we noted a constant high expression of glycans on the variable domain of ACPA IgG with a slight, but significant, increase after 12 months (105.2%). These latter findings are in agreement with our previous observations, estimating > 90% VDG on ACPA IgG in RA⁴, as well as the finding that > 80% of ACPA B-cell receptors in RA express N-linked glycosylation sites in the variable region²². Our longitudinal data from cohort 6 depict increased VDG levels in individuals in whom treatment was tapered, while patients who received more intense treatment showed reduced ACPA IgG VDG profiles over time ($p = 0.007$). This significant impact of immunosuppression was also observed for ACPA IgG levels¹⁵, confirming the correlation between ACPA IgG levels and VDG, which was strongest in the pre-disease phase. These findings are also in accordance with the notion that VDG could have a regulatory impact on the ACPA immune response. In this respect, it is intriguing to note that the HLA-shared epitope alleles predispose to ACPA harboring VDG rather than to ACPA in general¹⁰, thus linking ACPA VDG with the major genetic risk factor for RA. Indeed, a more in depth longitudinal analysis of the correlation between the presence of pre-disposing HLA-DR4 genes and the presence of VDG revealed a shorter “transit time” to RA in HLA-DR4-positive pre-disease individuals who still displayed relatively low levels of ACPA VDG, as compared to HLA-DR4-negative individuals²¹.

Of note, we observed, in the extensive “post” RA analysis, that individuals in whom long-term DFR is achieved exhibit lower VDG profiles in active disease (61.4%) compared to patients in whom long-term DFR is not achieved (83.8%). The relevance of these findings is unknown, although it is remarkable that long-term DFR, a relatively rare event in ACPA-positive RA, was associated with lower VDG on ACPA. Importantly, reduced ACPA IgG levels are not the cause of a lower variable domain glycosylation, which was controlled by titrating ACPA IgG into healthy serum samples resulting in a maintained high degree of VDG (Figure S5B). Thus it is tempting to speculate that VDG serve as an additional “hit” determining the fate of the autoreactive B-cell response and thereby exert an impact on ACPA levels.

Together with previous data, showing that N-linked glycan sites are selectively introduced into the ACPA B-cell receptor sequences upon SHM²² and that VDG are significantly elevated in ACPA-positive individuals who subsequently develop RA²³, our results provide evidence that a glycan attached to the variable domain fosters a breach of tolerance of autoreactive B cells.

As carbohydrates are known to affect cellular functions, ACPA-expressing B cells may gain a selection advantage when abundantly expressing glycans in their variable domains. The disialylated, and thus negatively charged glycans attached to the variable domain, which have also a large steric requirement, might modulate binding to autoantigens or affect B-cell receptor signaling of the citrullinated antigen-directed B cells. Further, it cannot be ruled out that VDG impact on effector mechanism and thereby autoantibody-mediated inflammation, similar to findings for Fc glycans. Next to these areas for further research, it would be interesting to investigate changes in specific VDG traits in more depth, as altered glycan composition could be associated with defined biologic implications, as also observed for Fc glycans. Recent studies have shown, for example, that not only Fc glycans on total IgG, but also ACPA IgG VDG show a decrease in the bisecting GlcNAc after COVID-19 infection^{24,25}. Interestingly, VDG are not only a feature of ACPA IgG in RA, but have also been described in other human autoimmune responses, such as in ANCA-associated vasculitis and Sjögren's syndrome, and have been observed on anti-hinge and anti-drug antibodies²⁶⁻²⁸.

A limitation of our study is that VDG profiles could be detected in only 70% of the samples analyzed, mainly explained by limited sample amounts or low ACPA IgG levels, as observed in the group of healthy individuals. Especially for rare disease stages, such as for the “DFR with late flares” group, only a limited number of samples were available to us. In addition, ACPA were captured using the highly sensitive and specific antigen CCP2. However, it cannot be excluded that certain ACPA molecules that recognize different citrullinated epitopes and do not interact with CCP2 were omitted from the analysis. Importantly though, we did not observe an effect of VDG on the binding affinity to CCP2 (data not shown), making a selection bias towards higher or lower glycosylated ACPA unlikely. Another limitation of our study is that conclusions are mainly based on cross-sectional data derived from samples collected at different sites. Although collection of such data from one site would be highly challenging, the analyses of samples from different sites could be hampered by site-specific effects. Importantly however, we also observed an increase in ACPA IgG VDG toward RA-onset in the longitudinal dataset of cohort 3, including paired samples obtained from pre-symptomatic individuals and RA patients over a time period of 15 years, as also previously described²¹. Furthermore, we observed concordant ACPA IgG VDG across different cross-sectional cohorts of healthy individuals (58.1% and 44.9%) or individuals with arthralgia (75.3% and 70.4%).

In summary, we have provided a comprehensive overview of the expression of VDG on ACPA IgG over various clinical disease stages in RA. Although the biologic implications of VDG attached to antibodies in general and ACPA specifically are still largely unexplored, our data show that VDG are a key characteristic of ACPA across disease stages in individuals of different ethnicities who develop RA. Our results show an increase in VDG towards disease progression and suggest,

taken together with previous data indicating a selective introduction of these N-linked glycan sites, that VDG may serve as a trigger for the maturation of the ACPA immune response. It will therefore be relevant to understand the biologic impact of VDG on the ACPA immune response and its detailed clinical implications.

Materials and Methods

Patient and public involvement - Individuals were involved in this study by donating blood when attending population surveys^{18,19}, medical health check-ups^{14,20}, were recruited to take part in the arthralgia study in the Amsterdam area of The Netherlands (*cohort 4*)¹⁷ or the treatment strategy study “Improved” in early RA (*cohort 6*)¹³.

Ethical considerations - All participants have given their written informed consent and the Regional Ethical Review Board Committees approved the studies.

Study cohorts - ACPA IgG VDG were analyzed in 1498 serum samples from individuals in different clinical disease stages including 121 ACPA-negative RA control samples. The descriptive cohort data are presented in Table 1. Additionally, 247 healthy donor and 150 ACPA-positive RA control samples, sampled at the Leiden rheumatology outpatient clinic, were assessed to verify the methodology used.

Cohort 1, healthy symptom-free (Japan, Nagasaki) - Healthy symptom-free individuals (n = 58) were included that were tested positive for the presence of ACPA and are part of the Nagasaki Island Study (NaiS) performed in Japan (a community-based prospective cohort study based on resident health check-ups)²⁰. The individuals included into the study showed no joint complains at the time of the resident health check-up and were thus defined as healthy. ACPA-positive individuals were further examined and followed up for a period of up to 3 years. 9 individuals (15.5%) developed RA during follow-up.

Cohort 2, healthy and RA-onset (Canada, Manitoba) - Individuals were part of the longitudinal research project “Early Identification of Rheumatoid Arthritis in First Nations” based at the Arthritis Centre at the University of Manitoba¹⁹. 48 samples of healthy individuals (first degree relatives of RA patients) were included. 25 individuals were sampled prior to RA-onset, in the absence of joint-complaints, and at the time of diagnosis of clinically-apparent RA (paired samples).

Cohort 3, pre-symptomatic and after RA-onset/ early RA (Sweden, Umeå) - Individuals were recruited into the Northern Sweden Health and Disease Study (NSHDS) or the Västerbotten Intervention Project. Blood samples of the individuals were collected and stored in a

biorepository (the Northern Sweden Medical Research Biobank). RA patients were registered based on the fulfillment of the 1987 ARA classification criteria. Individuals were retrospectively identified from the cohort as having donated blood before the onset of signs of symptoms of joint disease, defined as pre-symptomatic ($n = 228$, median (IQR) pre-dating time: 4.7 (5.9) years) and after diagnosis of RA, defined as early RA ($n = 126$; 0.5 to 1.5 years)¹⁸.

Cohort 4, arthralgia (The Netherlands, Amsterdam, Reade) – ACPA-positive individuals with arthralgia ($n = 239$) prospectively sampled at rheumatology outpatient clinics in the Amsterdam area of The Netherlands¹⁷ were selected. Individuals were followed up for a period of up to 10 years and 137 (57.3%) developed arthritis during follow-up.

Cohort 5, arthralgia and RA-onset (The Netherlands, Leiden, CSA) – Individuals, at risk of RA development, were recruited for the prospective Clinically Suspect Arthralgia (CSA) cohort in the Leiden rheumatology outpatient clinic and followed longitudinally²⁹. 38 individuals with arthralgia were included into this study. 26 of these individuals were sampled with arthralgia and at the time of diagnosis of clinically-apparent RA (paired samples).

Cohort 6, RA-onset and established RA after treatment (The Netherlands, Leiden, Improved) – Longitudinal samples of 130 RA patients at disease-onset as well as 4 months ($n = 117$), 8 months ($n = 112$) and 12 months ($n = 117$) after diagnosis and defined treatment were included. Individuals, recruited in 12 hospitals in the western area of The Netherlands, were included in the Improved (Induction therapy with Methotrexate and Prednisone in Rheumatoid Or Very Early arthritic Disease) study. This multicenter, randomized control trial was aimed to achieve DFR including treatment alteration every 4 months. Initial treatment was methotrexate (MTX) and prednisone. Patients in whom early remission was achieved (defined as DAS < 1.6) tapered prednisone. If disease was still in remission at 8 months, MTX was also tapered. If DAS was ≥ 1.6 after stopping prednisone, it was restarted. Patients in whom early remission was not achieved were randomized to one of two treatment arms: MTX, prednisone, hydroxychloroquine, and sulfasalazine combination (arm 1) or MTX and adalimumab combination (arm 2)¹³.

Cohort 7, RA-onset, DFR, SDFR and late disease flares (The Netherlands, Leiden, EAC) – Individuals at RA-onset in whom DMARD-free remission (DFR) was not achieved at later time-points ($n = 59$) and longitudinal samples ($n = 175$) of individuals in whom DFR or sustained DFR (SDFR) was achieved, were selected and recruited from the Leiden Early Arthritis Clinic (EAC) in the Leiden University Medical Center (The Netherlands)¹⁴. Samples at diagnosis of clinically apparent RA (RA-onset) ($n = 36$), during the pre-remission phase ($n = 52$), during DFR ($n = 41$), during SDFR ($n = 35$), and at the time of late disease flares ($n = 11$) were included with a follow-up of up to 16 years. DFR was defined as the absence of clinical synovitis (swollen-joints at physical examination) after discontinuation of DMARD-treatment (including systemic/ intra-

articular corticosteroids). In the 41 patients DMARDs were stopped after a median of 2.9 years (IQR 1.0 to 4.9 years). SDFR was defined as the absence of clinical synovitis after cessation of DMARD-treatment, that persisted for the entire follow-up of ≥ 1 -year. SDFR was achieved in the 35 patients after a median of 2.8 years (IQR 2.0 to 5.2 years). SDFR was maintained for 7.1 years (IQR 4.5 to 11.2 years) after DMARD-stop, showing the sustainability of DMARD-free remission. Flare was defined as the reoccurrence of clinical synovitis on joint examination. Medical files were studied on occurrence of SDFR until September 2021.

Laboratory analyses - ACPA IgG levels in aU/ml were analyzed in serum samples using standard and commercial available anti-cyclic citrullinated peptide (CCP) assays or anti-CCP-2 in house enzyme-linked immunosorbent assays (ELISA) as previously described^{3,15-20}. ACPA fine specificity for samples from cohort 6 (RA-onset and established RA, The Netherlands) was determined using anti-citrullinated vimentin 59-74, anti-citrullinated fibrinogen β 36-52 and α 27-43 and anti-citrullinated enolase 5-20 IgG in house ELISA as previously described³. ACPA fine specificity for samples from cohort 4 (arthralgia, The Netherlands) was determined using anti-citrullinated vimentin 60-75, anti-citrullinated fibrinogen β 36-52, α 60-74 and α 36-50 and anti-citrullinated enolase 5-21 IgG in house ELISA.

ACPA IgG capturing and VDG analysis using liquid chromatography - Capturing of ACPA IgG, total glycan release, glycan labeling and purification was performed as previously described¹¹. In brief, ACPA were affinity isolated from 25 μ l serum samples using NeutrAvidin Plus resin (Thermo Fisher Scientific) coupled with 0.1 μ g/ μ l CCP2-biotin followed by IgG capturing using FcXL affinity beads (Thermo Fisher Scientific). N-linked glycans were released using 0.5 U PNGase F (Roche), subsequently labelled with 2-AA and 2-PB and HILIC SPE purified using GHP membrane filter plates (Pall Life Science). Ultra-high performance liquid chromatography (UHPLC) was performed on a Dionex Ultimate 3000 (Thermo Fisher Scientific) instrument, a FLR fluorescence detector set and an Acquity BEH Glycan column (Waters, Milford, MA). Separation and glycan peak alignment were performed as previously published¹¹. HappyTools version 0.0.2 was used for calibration and peak integration³⁰. The N-linked glycan abundance in each peak was expressed as the total integrated area under the curve (AUC). The cut-off was defined based on PBS control (blank) and ACPA-negative healthy control samples of individuals donating blood in the Leiden area, excluding outliers (below or above $Q_1 - 1.5 \times \text{IQR}$ and $Q_3 + 1.5 \times \text{IQR}$). The percentage of ACPA IgG VDG was calculated based on the following formula: $[(\text{sum of the most abundant VDG})/(\text{sum of the most abundant Fc glycans}) \times 100]$ or $[(G2FBS1+G2FS2+G2FBS2)/(G0F+G1F+G2F) \times 100]$ ²³. The glycan traits were selected based on previous observations showing their exclusive presence on either the variable domain or the Fc domain of ACPA IgG molecules^{4,31}. The sum of the Fc glycans, the amount of N-linked glycans attached to the conserved Asn297 in the Fc domain of IgG antibodies, remains constant.

Statistical analyses – Continuous data were analyzed using non-parametric methods (Kruskal-Wallis test for non-paired samples and Mann-Whitney’s U-test for non-paired samples) and parametric tests (Mixed-effect analysis for matched-paired samples including missing values) when appropriate. The mixed-effect analysis model using Restricted Maximum Likelihood (REML) is comparable to repeated measures ANOVA with regard to p values and multiple comparisons tests, but can handle missing values. Correlations between ACPA IgG levels (log transformed) and percentages of VDG were assessed with Pearson correlation. All p-values are two-sided and $p < 0.05$ was considered as statistically significant. Logistic and ordinal regression analyses were performed for cohort 4 (arthralgia, The Netherlands) and cohort 6 (RA-onset, The Netherlands) to investigate the association of ACPA IgG VDG/ACPA IgG levels with epitope spreading, remission and early DFR. The unstandardized coefficient (B) represents the mean change in the response given a one unit change in the predictor. The longitudinal and repeated measures data from cohort 6 (RA-onset and established RA after treatment, Leiden) were analyzed using generalized estimating equations (GEE), as specified before³. GEE was used to assess VDG changes over time and associations with treatment/treatment decisions. The specific covariates and dependent variables are listed in the table legends, respectively. Statistical calculations were performed using STATA (V.16.1; STATA Corp, College Station, Texas USA).

Acknowledgments

The authors would like to thank the Department of Biobank Research at Umeå University, Västerbotten Intervention Programme, the Northern Sweden MONICA study and the County Council of Västerbotten for providing data and samples. We would like to thank Dr. Jan Wouter Drijfhout (LUMC, Leiden, The Netherlands) for providing the CCP2 peptide, Carolien Koeleman (LUMC, Leiden, The Netherlands) for expert assistance with liquid chromatography and Ellis Niemantsverdriet (LUMC, Leiden, The Netherlands) and Marloes Verstappen (LUMC, Leiden, The Netherlands) for assistance with sample and data collection.

Funding

This work has been financially supported by ReumaNederland 17-1-402 and 08-1-34 (to R.E.M.T.), the IMI-funded project RTCure 777357 (to T.W.J.H.), ZonMw TOP 91214031 (to R.E.M.T.), Target-to-B LSHM18055-SGF (to R.E.M.T.), the European Research Council (ERC) advanced grant AdG2019-884796 (to R.E.M.T.), NWO-ZonMW clinical fellowship 90714509 (to H.U.S.), NWO-ZonMW VENI grant 91617107 (to H.U.S.), ZonMW Enabling Technology Hotels grant 435002030 (to H.U.S.), Dutch Arthritis Foundation 15-2-402 and 18-1-205 (to H.U.S.), the Swedish Research

Council VR 2017-00650 (to S.R-D.), the King Gustaf V's 80-Year Fund, the King Gustaf V's and Queen Victoria's Fund, the Swedish Rheumatism Association (to S.R-D.) and the Canadian Institutes of Health Research (CIHR) grant MOP 77700 (to H.S.E-G.).

Conflict of interest

H.U.S., T.W.J.H. and R.E.M.T. are mentioned inventors on a patent on ACPA IgG V-domain glycosylation.

Author contributions

All authors were involved in drafting the article or revising it critically for important intellectual content, and all authors approved the final version to be published. Conceptualization: T.K., R.E.M.T., T.W.J.H. Methodology: T.K., L.H., T.J.W. Software: T.K., L.H., T.J.W. Investigation: T.K., L.H., T.J.W. Visualization: T.K., T.J.W. Supervision: D.v.d.W., H.U.S., R.E.M.T. and T.W.J.H. Writing—original draft: T.K., R.E.M.T. and T.W.J.H. Writing—review and editing: L.H., T.J.W., M.T., S.Y.K., A.K., H.S.E.-G., D.v.S., S.R.-D., M.W., A.H.M.v.d.H.-v.M., C.F.A., D.v.d.W. and H.U.S.

References

- 1 van der Kooij, S. M., Goekoop-Ruiterman, Y. P., de Vries-Bouwstra, J. K., Guler-Yuksel, M., Zwinderman, A. H., Kerstens, P. J., et al., Drug-free remission, functioning and radiographic damage after 4 years of response-driven treatment in patients with recent-onset rheumatoid arthritis. *Ann Rheum Dis* 2009. 68: 914-921.
- 2 Willemze, A., Trouw, L. A., Toes, R. E. and Huizinga, T. W., The influence of ACPA status and characteristics on the course of RA. *Nat Rev Rheumatol* 2012. 8: 144-152.
- 3 de Moel, E. C., Derksen, V., Trouw, L. A., Bang, H., Collee, G., Lard, L. R., et al., In rheumatoid arthritis, changes in autoantibody levels reflect intensity of immunosuppression, not subsequent treatment response. *Arthritis Res Ther* 2019. 21: 28.
- 4 Hafkenscheid, L., Bondt, A., Scherer, H. U., Huizinga, T. W., Wuhrer, M., Toes, R. E., et al., Structural Analysis of Variable Domain Glycosylation of Anti-Citrullinated Protein Antibodies in Rheumatoid Arthritis Reveals the Presence of Highly Sialylated Glycans. *Mol Cell Proteomics* 2017. 16: 278-287.
- 5 Kasermann, F., Boerema, D. J., Rueggesser, M., Hofmann, A., Wymann, S., Zuercher, A. W., et al., Analysis and functional consequences of increased Fab-sialylation of intravenous immunoglobulin (IVIg) after lectin fractionation. *PLoS One* 2012. 7: e37243.
- 6 Vergoesen, R. D., Slot, L. M., Hafkenscheid, L., Koning, M. T., van der Voort, E. I. H., Grooff, C. A., et al., B-cell receptor sequencing of anti-citrullinated protein antibody (ACPA) IgG-expressing B cells indicates a selective advantage for the introduction of N-glycosylation sites during somatic hypermutation. *Ann Rheum Dis* 2018. 77: 956-958.
- 7 Rombouts, Y., Ewing, E., van de Stadt, L. A., Selman, M. H., Trouw, L. A., Deelder, A. M., et al., Anti-citrullinated protein antibodies acquire a pro-inflammatory Fc glycosylation phenotype prior to the onset of rheumatoid arthritis. *Ann Rheum Dis* 2015. 74: 234-241.
- 8 Scherer, H. U., van der Woude, D., Ioan-Facsinay, A., el Bannoudi, H., Trouw, L. A., Wang, J., et al., Glycan profiling of anti-citrullinated protein antibodies isolated from human serum and synovial fluid. *Arthritis Rheum* 2010. 62: 1620-1629.
- 9 Bondt, A., Hafkenscheid, L., Falck, D., Kuijper, T. M., Rombouts, Y., Hazes, J. M. W., et al., ACPA IgG galactosylation associates with disease activity in pregnant patients with rheumatoid arthritis. *Ann Rheum Dis* 2018. 77: 1130-1136.
- 10 Ercan, A., Cui, J., Chatterton, D. E., Deane, K. D., Hazen, M. M., Brintnell, W., et al., Aberrant IgG galactosylation precedes disease onset, correlates with disease activity, and is prevalent in autoantibodies in rheumatoid arthritis. *Arthritis Rheum* 2010. 62: 2239-2248.
- 11 Kissel, T., van Schie, K. A., Hafkenscheid, L., Lundquist, A., Kokkonen, H., Wuhrer, M., et al., On the presence of HLA-SE alleles and ACPA-IgG variable domain glycosylation in the phase preceding the development of rheumatoid arthritis. *Ann Rheum Dis* 2019. 78: 1616-1620.
- 12 Hafkenscheid, L., de Moel, E., Smolik, I., Tanner, S., Meng, X., Jansen, B. C., et al., N-Linked Glycans in the Variable Domain of IgG Anti-Citrullinated Protein Antibodies Predict the Development of Rheumatoid Arthritis. *Arthritis Rheumatol* 2019. 71: 1626-1633.
- 13 Heimans, L., Wevers-de Boer, K. V., Visser, K., Goekoop, R. J., van Oosterhout, M., Harbers, J. B., et al., A two-step treatment strategy trial in patients with early arthritis aimed at achieving remission: the IMPROVED study. *Ann Rheum Dis* 2014. 73: 1356-1361.
- 14 van Aken, J., van Bilsen, J. H., Allaart, C. F., Huizinga, T. W. and Breedveld, F. C., The Leiden Early Arthritis Clinic. *Clin Exp Rheumatol* 2003. 21: S100-105.

- 15 de Moel, E. C., Derksen, V., Stoeken, G., Trouw, L. A., Bang, H., Goekoop, R. J., et al., Baseline autoantibody profile in rheumatoid arthritis is associated with early treatment response but not long-term outcomes. *Arthritis Res Ther* 2018. 20: 33.
- 16 van Steenberghe, H. W., Mangnus, L., Reijnders, M., Huizinga, T. W. and van der Helm-van Mil, A. H., Clinical factors, anticitrullinated peptide antibodies and MRI-detected subclinical inflammation in relation to progression from clinically suspect arthralgia to arthritis. *Ann Rheum Dis* 2016. 75: 1824-1830.
- 17 Bos, W. H., Wolbink, G. J., Boers, M., Tjhuis, G. J., de Vries, N., van der Horst-Bruinsma, I. E., et al., Arthritis development in patients with arthralgia is strongly associated with anti-citrullinated protein antibody status: a prospective cohort study. *Ann Rheum Dis* 2010. 69: 490-494.
- 18 Rantapää-Dahlqvist, S., de Jong, B. A., Berglin, E., Hallmans, G., Wadell, G., Stenlund, H., et al., Antibodies against cyclic citrullinated peptide and IgA rheumatoid factor predict the development of rheumatoid arthritis. *Arthritis Rheum* 2003. 48: 2741-2749.
- 19 Smolik, I., Robinson, D. B., Bernstein, C. N. and El-Gabalawy, H. S., First-degree relatives of patients with rheumatoid arthritis exhibit high prevalence of joint symptoms. *J Rheumatol* 2013. 40: 818-824.
- 20 Kawashiri, S. Y., Tsuji, Y., Tamai, M., Nonaka, F., Nobusue, K., Yamanashi, H., et al., Effects of cigarette smoking and human T-cell leukaemia virus type 1 infection on anti-citrullinated peptide antibody production in Japanese community-dwelling adults: the Nagasaki Islands Study. *Scand J Rheumatol* 2020: 1-4.
- 21 Kissel, T., van Wesemael, T. J., Lundquist, A., Kokkonen, H., Kawakami, A., Tamai, M., et al., Genetic predisposition (HLA-SE) is associated with ACPA-IgG variable domain glycosylation in the predisease phase of RA. *Ann Rheum Dis* 2021.
- 22 Vergroesen, R. D., Slot, L. M., van Schaik, B. D. C., Koning, M. T., Rispens, T., van Kampen, A. H. C., et al., N-Glycosylation Site Analysis of Citrullinated Antigen-Specific B-Cell Receptors Indicates Alternative Selection Pathways During Autoreactive B-Cell Development. *Front Immunol* 2019. 10: 2092.
- 23 Hafkenscheid, L., de Moel, E., Smolik, I., Tanner, S., Meng, X., Jansen, B. C., et al., N-linked glycans in the variable domain of ACPA-IgG predict the development of rheumatoid arthritis. *Arthritis Rheumatol* 2019.
- 24 Derksen, V., Kissel, T., Lamers-Karnebeek, F. B. G., van der Bijl, A. E., Venhuizen, A. C., Huizinga, T. W. J., et al., Onset of rheumatoid arthritis after COVID-19: coincidence or connected? *Ann Rheum Dis* 2021.
- 25 Chakraborty, S., Gonzalez, J., Edwards, K., Mallajosyula, V., Buzzanco, A. S., Sherwood, R., et al., Proinflammatory IgG Fc structures in patients with severe COVID-19. *Nat Immunol* 2021. 22: 67-73.
- 26 Vletter, E. M., Koning, M. T., Scherer, H. U., Veelken, H. and Toes, R. E. M., A Comparison of Immunoglobulin Variable Region N-Linked Glycosylation in Healthy Donors, Autoimmune Disease and Lymphoma. *Front Immunol* 2020. 11: 241.
- 27 Biermann, M. H., Griffante, G., Podolska, M. J., Boeltz, S., Sturmer, J., Munoz, L. E., et al., Sweet but dangerous - the role of immunoglobulin G glycosylation in autoimmunity and inflammation. *Lupus* 2016. 25: 934-942.
- 28 van de Bovenkamp, F. S., Derksen, N. I. L., Ooijevaar-de Heer, P., van Schie, K. A., Kruithof, S., Berkowska, M. A., et al., Adaptive antibody diversification through N-linked glycosylation of the immunoglobulin variable region. *Proc Natl Acad Sci U S A* 2018. 115: 1901-1906.
- 29 Newsum, E. C., van der Helm-van Mil, A. H. and Kaptein, A. A., Views on clinically suspect arthralgia: a focus group study. *Clin Rheumatol* 2016. 35: 1347-1352.
- 30 Jansen, B. C., Hafkenscheid, L., Bondt, A., Gardner, R. A., Hendel, J. L., Wuhler, M., et al., HappyTools: A software for high-throughput HPLC data processing and quantitation. *PLoS One* 2018. 13: e0200280.
- 31 Rombouts, Y., Willemze, A., van Beers, J. J., Shi, J., Kerkman, P. F., van Toorn, L., et al., Extensive glycosylation of ACPA-IgG variable domains modulates binding to citrullinated antigens in rheumatoid arthritis. *Ann Rheum Dis* 2016. 75: 578-585.

Supplemental Tables

Table S1. Association between the recognition of multiple citrullinated epitopes (dependent variable) and VDG or ACPA IgG levels (independent variable) in individuals with arthralgia (cohort 4, The Netherlands).

	B (95% CI) univariable (simple)	p value
VDG	0.03 (0.02 - 0.04)	< 0.001
log ACPA levels	0.84 (0.67 - 1.02)	< 0.001

Table S2. Association between the recognition of multiple citrullinated epitopes (dependent variable) and VDG or ACPA IgG levels (independent variable) of individuals at RA-onset and in established RA after prespecified treatment (cohort 6, The Netherlands).

	B (95% CI) univariable (simple)	p value
baseline (ordinal regression analysis)		
VDG	0.142 (0.0045 - 0.0239)	0.004
ACPA levels	0.0032 (0.0025 - 0.0038)	< 0.0001
over time (GEE)		
VDG	0.0089 (0.0052 - 0.0125)	< 0.0001
ACPA levels	0.0020 (0.0017 - 0.0022)	< 0.0001

Table S3. Changes in ACPA IgG VDG after RA-onset and treatment (cohort 6, The Netherlands).

	VDG (%)	p value	VDG (%), adjusted¹	p value, adjusted
continues				
per 4 months	2.85 (0.51 - 5.19)	0.017	1.29 (-1.30 - 3.89)	0.32
per month	0.71 (0.13 - 1.30)	0.017	0.32 (-0.33 - 0.97)	0.048
per visit				
RA-onset	1 (ref)	-	1 (ref)	-
4 months	-3.83 (-10.79 - 3.12)	0.28	-0.06 (-8.76 - 8.87)	0.99
8 months	4.15 (-2.86 - 11.16)	0.25	1.51 (-7.50 - 10.51)	0.74
12 months	7.49 (0.47 - 14.52)	0.037	3.76 (-4.19 - 11.71)	0.35

¹ covariates: age, gender, CRP and ACPA levels

Table S4. Generalized estimating equation (GEE) analysis of VDG from individuals sampled 4 vs. 8 months and 8 vs. 12 months after RA-onset and prespecified treatment (cohort 6, The Netherlands). Association between VDG and prespecified treatment after 4 or 8 months respectively. The regression coefficient (B, with 95% CI) indicates changes in VDG between 4 vs. 8 months and 8 vs. 12 months for the different treatment groups.

	B (95% CI)	p value ¹ univariable (simple)
VDG (%) 4 vs. 8 months		
early remission²	7.52 (-6.79 - 21.83)	-
treatment escalation³	3.27 (-6.35 - 12.90)	0.98
VDG (%) 8 vs. 12 months		
early remission, drug-free⁴	12.27 (-7.32 - 31.87)	-
early remission no drug-free and treatment escalation⁵	6.42 (-0.35 - 13.19)	0.007

¹interaction term *treatment decision*time*

²methotrexate (MTX) monotherapy

³MTX, prednisone, hydroxychloroquine, and sulphasalazine combination (arm 1) or MTX and adalimumab combination (arm 2)

⁴MTX tapering for individuals achieving DFR

⁵continuous MTX and prednisone or adalimumab treatment

Table S5. Logistic regression analysis of individuals at RA-onset (cohort 6, The Netherlands). Association between VDG (dependent variable) at RA-onset and treatment response - remission at 4 months and early drug-free remission within 1 year (independent variable).

	OR (95% CI)	p value
remission at 4 months	1.003 (0.991 - 1.014)	0.65
drug free remission in the first year	1.00 (0.99 - 1.01)	0.50

Supplemental Figures

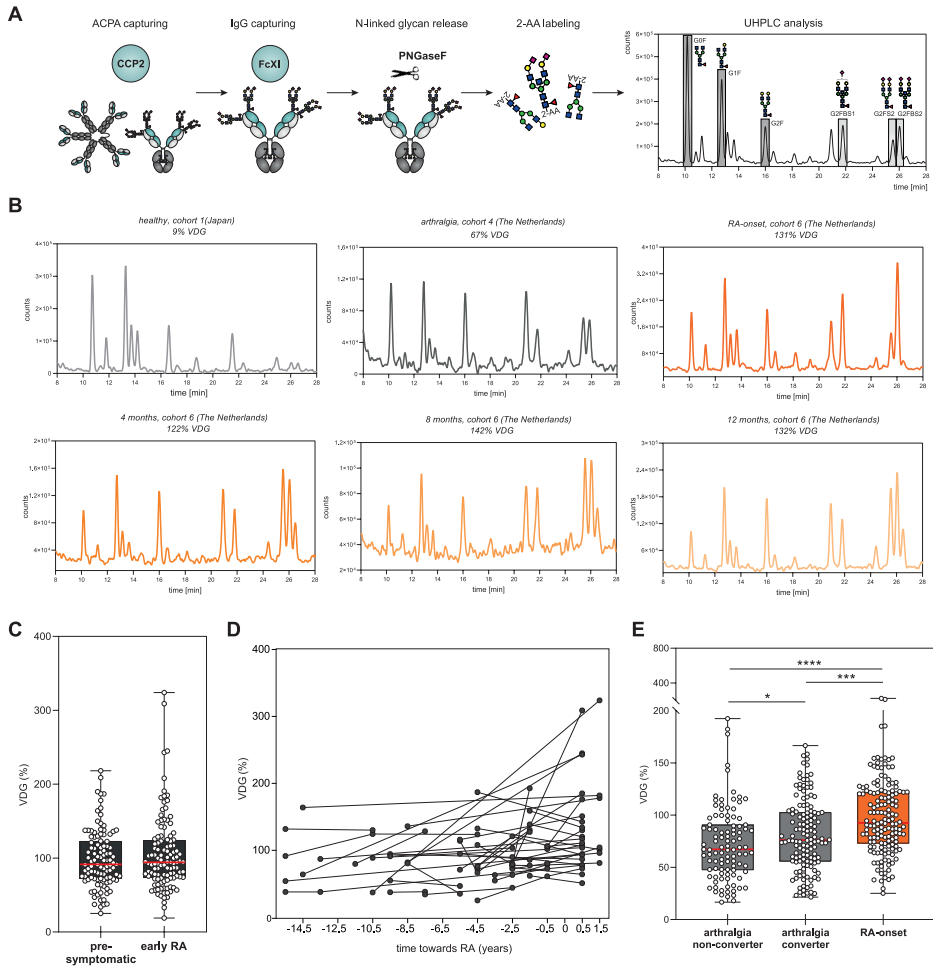


Figure S1. ACPA IgG capturing and liquid chromatography VDG analysis. (A) Experimental procedure: ACPA were captured using CCP2-streptavidin beads, followed by IgG capturing (FcXI beads). N-linked glycans were released using PNGase F and 2-AA labeled for liquid chromatography. GOF, G1F, G2F, G2FBS1, G2FBS2 and G2FBS3 glycan peaks are highlighted. A- mono-/di-galactosylated (GO/G1/G2), fucose attached to the core GlcNAc (F), bisecting GlcNAc (B), mono-/di-sialylated (S1/S2). Blue square: N-acetylglucosamine (GlcNAc), green circle: mannose, yellow circle: galactose, red triangle: fucose, pink diamond: N-acetylneuraminic acid. (B) UHPLC chromatograms of ACPA IgG VDG from a healthy individual (cohort 1), an individual with arthralgia (cohort 4) and an individual at RA-onset and 4, 8 and 12 months after disease development (cohort 6). (C) ACPA IgG VDG of individuals diagnosed with RA later in life and sampled prior to symptom-onset and after RA diagnosis (cohort 3). Data are presented as box and whiskers including all data points. (D) Matched paired samples of pre-symptomatic individuals and early RA patients (cohort 3). (E) Percentage ACPA IgG VDG of individuals with arthralgia that later convert or do not convert to RA and of patients at RA-onset. Data are presented as box and whiskers including all data points. Kruskal-Wallis tests were performed. Significant differences are denoted by * ($p = 0.0406$), *** ($p = 0.0001$), or **** ($p < 0.0001$).

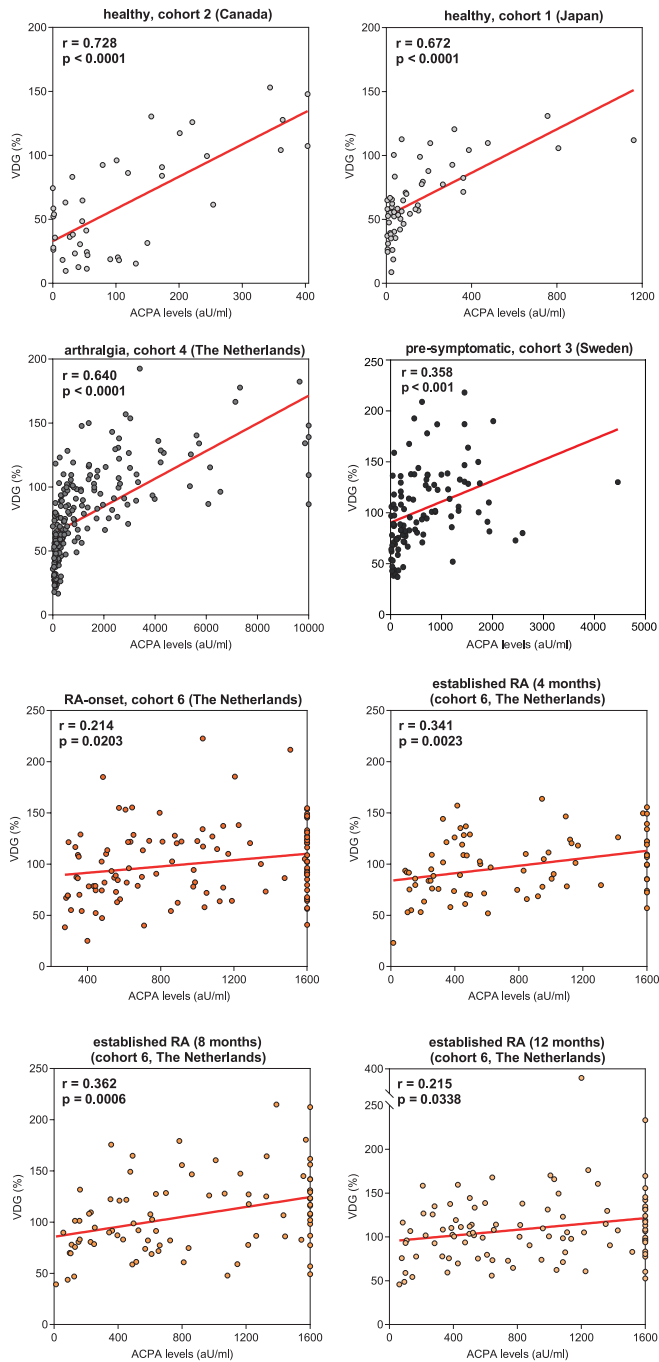


Figure S2. ACPA IgG VDG percentages correlate with ACPA IgG levels. Pearson's correlation between ACPA IgG VDG percentages and ACPA IgG levels (aU/ml). The respective p-values (two-tailed) and correlation coefficients are presented.

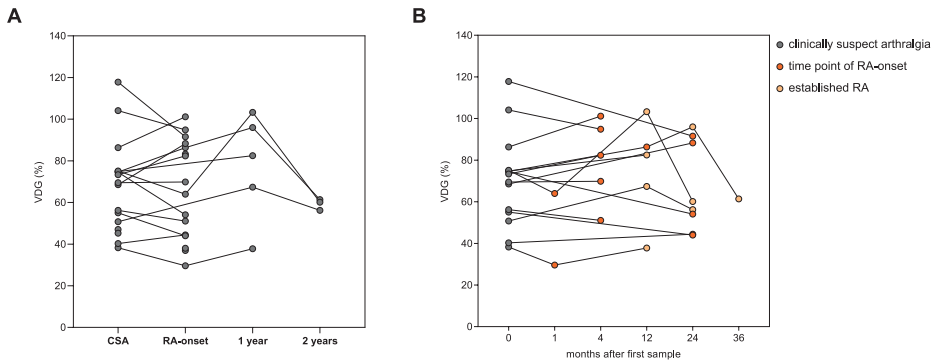


Figure S3. ACPA IgG VDG in individuals with arthralgia from cohort 5 (The Netherlands). (A) Longitudinal analysis of ACPA IgG VDG percentages from individuals with clinically suspect arthralgia (CSA), at RA-onset and 1 or 2 years after disease development. (B) "Time line" of VDG percentages up to 36 months after 1st visit. Time point of RA-onset is depicted in orange.

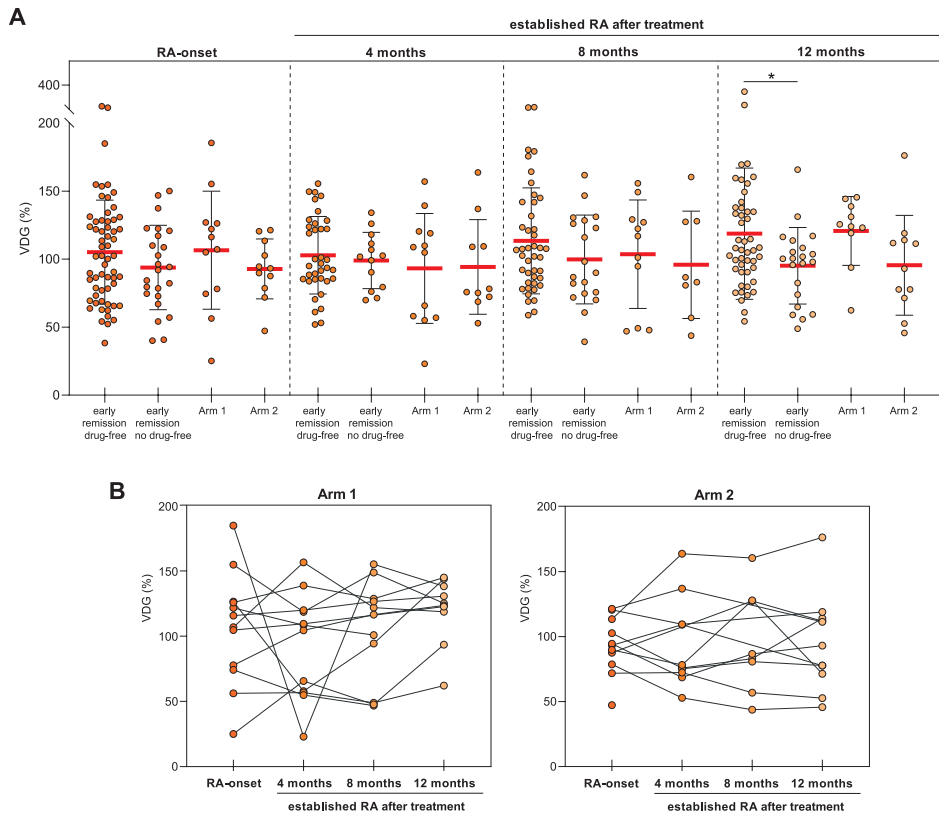


Figure S4. Longitudinal analysis of ACPA IgG VDG at RA-onset and in established RA for cohort 6 (*The Netherlands*) separated for the different treatment arms. (A) ACPA IgG VDG comparison of the four treatment groups: early remission, drug-free; early remission, no drug-free; arm 1 and arm 2. Treatment specifications are illustrated in figure 3A. Ordinary one-way ANOVA was performed including the Fisher's LSD test: * $p = 0.015$. **(B)** Longitudinal matched paired samples are shown for treatment arm 1 and 2.

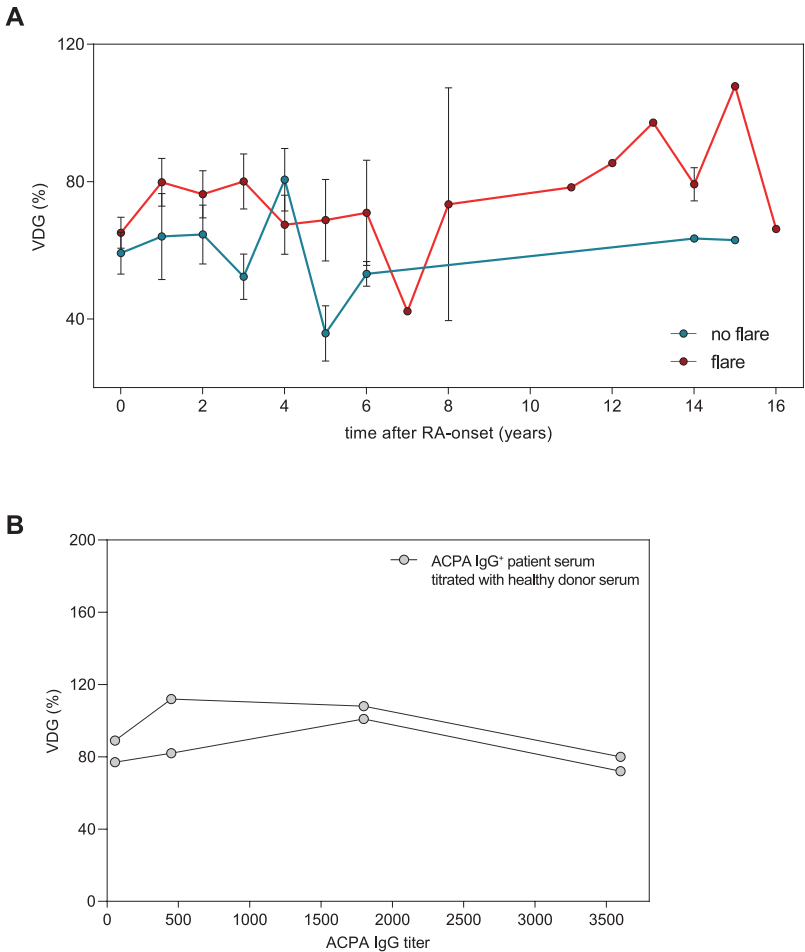
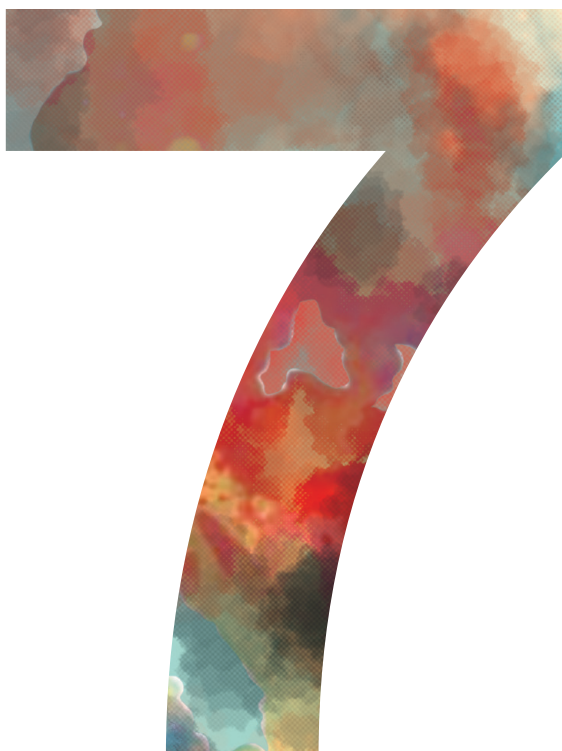


Figure S5. ACPA IgG VDG over various time-points and for different ACPA IgG titer. (A) “Time-line” of ACPA IgG VDG after RA-onset and towards drug-free remission (DFR) (*cohort 7, The Netherlands*). ACPA IgG VDG mean and SEM of the samples presented in figure 4D is depicted including patients who did and those who did not experience late flares. **(B)** Stable VDG of ACPA IgG positive patient serum measured with different titers. ACPA IgG titers were lowered by mixing the sera with ACPA-negative healthy donor sera. Two individual experiments are presented



Surface immunoglobulin variable domain glycosylation affects autoantigen binding and acts as threshold for human autoreactive B-cell activation

Theresa Kissel[†], Changrong Ge[†], Lise Hafkenscheid, Joanneke C. Kwekkeboom, Linda M. Slot, Marco Cavallari, Yibo He, Karin A.J. van Schie, Rochelle D. Vergroesen, Arieke S.B. Kampstra, Sanne Reijm, Gerrie Stoeken-Rijsbergen, Carolien Koeleman, Lennard M. Voortman, Laura H. Heitman, Bingze Xu, Ger J.M. Pruijn, Manfred Wuhrer, Theo Rispens, Tom W.J. Huizinga, Hans U. Scherer, Michael Reth, Rikard Holmdahl[‡], René E.M. Toes[‡]

[†] These authors contributed equally to this work as co-first authors.

[‡] These authors contributed equally to this work as co-senior authors.

Abstract

The hallmarking autoantibodies in Rheumatoid Arthritis (RA) are characterized by variable domain glycans (VDGs). Their abundant occurrence results from the selective introduction of N-linked glycosylation sites during somatic hypermutation, and their presence is predictive for disease development. However, the functional consequences of VDGs on autoreactive B cells remain elusive. Combining crystallography, glycobiology, and functional B-cell assays allowed us to dissect key characteristics of VDGs on human B-cell biology. Crystal structures showed that VDGs are positioned in the vicinity of the antigen-binding pocket, and dynamic modeling combined with binding assays elucidated their impact on binding. We found that VDG-expressing B-cell receptors stay longer on the B-cell surface and that VDGs enhance B-cell activation. These results provide a rationale on how the acquisition of VDGs might contribute to the breach of tolerance of autoreactive B cells in a major human autoimmune disease.

Teaser

The molecular underpinnings and the functional impact of variable domain glycans on human autoreactive B cells.

Introduction

A pathogenic role of B cells in autoimmunity is evidenced by the effective treatment of multiple autoimmune diseases, such as rheumatoid arthritis (RA), multiple sclerosis, antineutrophil cytoplasmic antibody (ANCA)-associated vasculitis, and systemic lupus erythematosus (SLE) with B-cell targeted therapies¹. Together with the observation that disease-specific autoantibody responses often characterize autoimmune diseases, these findings point to the notion that autoreactive B cells are involved in disease pathogenesis. Autoreactive B cells could contribute to disease via diverse mechanisms, such as antigen presentation to T cells, secretion of cytokines, or the production of pathogenic antibodies². To mediate these functions, an autoreactive B-cell response needs to be induced, which involves the breach of tolerance mechanisms that generally prevent the activation of pathogenic B cells. However, the mechanisms leading to the induction and survival of autoreactive B cells that contribute to autoimmune diseases remain unclear. In mouse models, it has been shown that B cells harboring autoreactive B-cell receptors (BCRs) are regulated in the bone marrow and peripheral tissues by clonal deletion, anergy induction (short-lived inactivated cells), or receptor editing³⁻⁷. This multistep process eliminates high-affinity and potentially autoreactive clones⁸. During immune responses against non-self or modified proteins carried by unwanted intruders, some initially autoreactive B cells might somatically mutate to be more efficient defense cells, thereby potentially losing affinity to self-antigens^{9,10}. This might include a role for variable domain glycans (VDGs) that could regulate self/non-self discrimination of B cells as has been described in a B-cell receptor-transgenic mouse model¹¹. Notably, the survival of autoreactive B cells involves costimulatory receptors and negative regulators, such as the sialic acid-binding lectin CD22, which will, together with the BCR, determine the outcome of the activation, the timing of T-cell help and the accessibility of antigens^{12,13}. At present, although we have some glimpses through the study of autoreactive B-cell biology in mice, the processes controlling human autoreactive B cells are largely unexplored.

The hallmarking disease-specific autoantibodies in RA, a common human autoimmune disease affecting synovial joints and cartilage, are anti-citrullinated protein antibodies (ACPAs)¹⁴. ACPAs specifically recognize a citrulline side chain and show limited interactions with the side-chains of surrounding amino acids on the protein surface, explaining their promiscuity in their protein or peptide specificity¹⁵. Recently, we have found that more than 90% of ACPA are glycosylated in their variable domains^{16,17}. The VDGs displayed on ACPAs are acquired through the introduction of N-linked glycosylation sites following somatic hypermutation¹⁸. VDGs are mainly complex-type carbohydrates containing a high percentage of sialic acids¹⁶. Intriguingly, the presence of VDGs in ACPA-positive healthy subjects is associated with the transition toward RA¹⁹. This observation, together with the selective introduction of N-linked glycosylation sites and the finding that this introduction has taken place in more than 90% of ACPA in patients with

RA^{16,18}, underlines the importance of this glycan tag and suggests that VDGs play a regulatory role for ACPA-expressing B cells. Intriguingly, variable domain glycosylation of antibodies is a characteristic not only of RA but also for some other human responses, such as ANCA-associated vasculitis, Sjögren's syndrome, anti-Hinge, and antidrug antibodies²⁰⁻²².

By combining crystallography, glycobiology, and antigen-binding studies, we show that ACPA VDGs can mask binding toward potential self-antigens. Functionally, we demonstrate that BCR VDGs enhances B-cell activation and decreases BCR downmodulation. This occurs independently of the negative regulator CD22. Together, the data demonstrate an important role of VDGs in changing the threshold of B cells to respond to self-antigens and to be activated. The generation of B cells with receptors modified by VDGs could lead to a loss of control of the self-reactive response and may play a role in the pathogenesis of RA.

Results

Generation of patient-derived monoclonal antibodies with and without VDGs

To investigate the putative effects of autoantibody VDGs on antigen binding, we generated six monoclonal antibodies (mAbs) based on full-length immunoglobulin G (IgG) BCR sequences isolated from ACPA-positive patients with RA (Figure 1A and Table 1)^{23,24}.

Figure 1. Generation of patient-derived IgG1 monoclonal anti-citrullinated protein (auto)antibodies (ACPAs) with (WT) and without (NG) variable domain glycans (VDGs). (A) Schematic representation of the generated ACPA IgG (7E4, 2E4, 1F2, 2G9, 3F3, and 2D11) carrying various amounts of N-linked glycans in the variable regions of their HC (turquoise) and LC (light gray). (B) Size shift between WT and NG ACPA under non-reduced (IgG) and reduced (HC and LC) conditions on a 4 to 15% gradient SDS protein gel (Bio Rad). The size was determined using the PageRuler™ Plus Prestained Protein Ladder (Thermo Fisher Scientific). (C) Size shift between WT and NG ACPA IgG identified via analytical size exclusion chromatography (SEC). ACPA IgG⁺ fractions were determined via the absorbance at 280 nm. (D) Schematic depiction of the four ACPA variants (WT, NG, WT+neu and NG+neu) analyzed: variable domain glycosylated (VDG⁺), Fc glycosylated (FcG⁺), sialylated (SA⁺) and non sialylated (SA⁻) after neuraminidase (neu) treatment. (E) MALDI-TOF MS analysis of N-linked variable domain and Fc glycans from WT, WT+neu, NG, and NG+neu ACPA IgG 7E4 and 3F3. Glycan structures of the most abundant N-linked glycan peaks are depicted. Blue square, *N*-acetylglucosamine (N); green circle, mannose/ hexose (H); yellow circle, galactose/ hexose (H); red triangle, fucose (F); purple diamond, α 2,6-linked *N*-acetylneuraminic (sialic acid (S). a.u., arbitrary units. ►

assisted laser desorption/ ionization-time-of-flight (MALDI-TOF)] (Figure 1E and Figure S1). The exemplarily illustrated results of 7E4 and 3F3 (Figure 1E) showed a highly sialylated glycan profile for the WT variant with a dominant complex type, bisected, and α -2,6-linked sialic acid comprising biantennary glycan peak H5N5F1S2 ($m/z=2651$) (Figure 1E), similar to the most prominent VDGs found on ACPA IgG directly isolated from patients with RA¹⁶. As we wished to determine the effect of negatively charged sialic acids (specifically *N*-acetylneuraminic acids) on antigen-binding functionalities, we treated the WT and NG mAb variants with neuraminidase (+neu). As depicted in figure 1E, this resulted in an effective cleavage of sialic acids. Likewise, the NG variant showed no sialylated glycan peaks but only the three most abundant Fc glycan forms comprising different amounts of galactose (H3N4F1, H4N4F1 and H5N4F1) (Figure 1E). Together, these results demonstrate the successful generation of patient-derived IgG mAb with engineered VDGs presenting the expected size and glycan composition as well as their NG counterparts.

Spatial orientation of VDG and antigen-binding pockets

Crystal structures of two ACPA IgG Fab fragments (3F3_{Fab} and 1F2_{Fab}) were generated to identify the structural composition of the antigen-binding pockets and the spatial orientation of the VDGs. The ACPA Fab fragments were complexed with distinct citrullinated peptides [3F3_{Fab}:cit-vim 59-74 [Protein Data Bank (PDB): 6YXK] and 1F2_{Fab}:cit-CII-C-39 (PDB: 6YXM)] selected on the basis of high reactivities within in vitro binding multiplex assays (as described in¹⁵) (Figure 2A). Additionally, 1F2_{Fab} was crystallized in an unbound state (PDB: 6YXN) (Figure 2A). The crystallographic data collection and refinement parameters are summarized in supplementary table 3. The results showed that 3F3_{Fab} and 1F2_{Fab} adopted characteristic Ig folds with well-defined binding grooves indicated by electron densities (Figure 2B). The core binding regions of the citrullinated peptides are well-defined, except for the terminal parts, which extend beyond the binding pocket (Figure 2B). Furthermore, the complexed citrullinated (CIT) peptides are visible in the antigen-binding sites and residues SSAV(CIR)L(CIT)SS of cit-vim 59-74 and LPGQ(CIT)GERG of cit-CII-C-39 could be modelled, while the other peptide residues were invisible (Figure 2C). The buried molecular surface areas of the Fab fragment and its respective peptide upon binding are 503 Å² for 1F2_{Fab} [178 Å² heavy chain (HC) and 325 Å² LC] and 622 Å² for cit-CII-C-39 as well as 659 Å² for 3F3_{Fab} (323 Å² HC and 336 Å² LC) and 789 Å² for cit-vim 59-74, respectively. The results indicate that the LC, especially for 1F2_{Fab}:cit-CII-C-39, contributed considerably to antigen binding. Superposition of the Apo-form of 1F2 (non-ligated) and its peptide-bound complex gave a backbone atom root mean square deviation (RMSD) of 0.4 Å, indicating no major changes in Ig folding upon antigen binding. When analyzing the structures of the unbound state, we found two deep pockets located within the antigen-binding region (Figure 2B), similar to pockets found in a third ACPA, 7E4_{Fab}, that has been described previously (PDB:5OCY)¹⁵. Noteworthy, these pockets, composed of polar and hydrophobic residues from HC and LC, are sufficient to accommodate a citrulline side-chain (Figure 2C). The flanking residues around the citrulline

were, in both cases, partially embedded in the binding groove, while the terminal residues of the peptides were directed towards the solvent (Figure 2C). The two peptides adopt a β -sheet like conformation atop the complementary determining regions (CDRs). To determine the structural basis required to accommodate citrullinated peptides, we performed a structural comparison between the determined ACPA 3F3_{Fab} and 1F2_{Fab} crystal structures and 7E4_{Fab}. The superposition of the three Fab structures revealed distinct structural features of paratopes formed by the CDRs including different conformations, suggesting heterogeneous antigen-binding regions among different ACPAs complexed with various peptides (Figure 2D). Moreover, there was a major difference in the electrostatic potentials that might determine the recognition of flanking residues of citrulline (Figure 2E). Noteworthy, the binding pocket of 3F3_{Fab} is positively charged, different from the negative or neutral antigen-binding pocket characteristics of the other ACPA Fab fragments described (Figure 2E).

Hence, all ACPA Fab fragments exhibit an open-ended polar/hydrophobic binding groove, fitting the binding of the citrulline side chain, which enables them to promiscuously accommodate different peptide variants, while excluding others due to steric repulsion with other amino acid side chains. This and the fact that interactions are solely formed between the terminal nitrogen and oxygen atom of the citrulline side chain could explain the low affinity toward many of their antigens and the broad cross-reactivity toward various antigens and post-translational modifications harbouring these atoms (acetylated and carbamylated antigens)²³.

Next, we characterized the spatial localization of the VDGs as this could provide insights into the potential impact of ACPA VDGs on antigen binding at the molecular level. Although N-linked glycans are highly flexible structures, the starting monosaccharides (core domain) were co-crystallized with the respective antigen-binding region of the generated monoclonal ACPA 7E4_{Fab}:cit-CII-C-48 (PDB: 6ZJG), 3F3_{Fab}:cit-vim 59-74 and 1F2_{Fab}:cit-CII-C-39 (Figure 3A). The data illustrate that the glycans are positioned outside, but in close vicinity to the peptide-binding domain. To examine whether VDGs could potentially reach the antigen-binding pocket and thereby interfere with antigenic interactions, we used the crystals as a basic framework and modeled the complete disialylated glycan compositions on top of these structures. Fab crystal structures with modeled VDGs were subsequently used for molecular dynamics (MD) simulations (Figure 3B and Figure S2A). The number of hydrogen bonds formed during simulation time was analyzed for every Fab domain and the respective HC and LC N-glycans. The results showed that up to six hydrogen-bonds were formed between the LC N-glycan and the mAb structure. The HC glycan formed fewer interactions over time, probably because it is more embedded into the protein structure and therefore more rigid (Figure 3C).

Table 1. ACPA IgG BCR variable region sequence details. ACPA IgG BCR sequences isolated from single B cells of 3 RA patients^{23,24}. Immunoglobulin (IG) heavy (H) and kappa (K) or lambda (L) light chain CDR3 amino-acid sequences are depicted and the amount of nucleotide mutations compared to germline. The N-linked glycan motifs presented in the variable heavy (V_H) or light (V_L) chain are visualized together with their respective location. The germline motifs are depicted based on the IMGT database.

ACPA IgG	IGH-CDR3 AA	IGH nt-mutations	IGK/L-CDR3 AA	IGK/L nt-mutations
7E4 ²⁴	CVRIRGGSSNW	28	CAAWNGRLSAFVF	28
2E4 ²³	CARGSFLERPESVPFHPW	71	CLQYHAEPYTF	61
1F2 ²³	CVRGGSLGIFGGSVGYW	44	CQSYRGDWVL	46
2G9 ²³	CVRWGEDRTEGLW	61	CMQRLRFPLTF	31
3F3 ²³	CARGTYLPVDESAAFDVW	56	CQQYYEAPYTF	37
2D11 ²³	CARRGGKDNVWGDW	21	CQQYNDWPVTF	11

* Amino-acid sequence and location.

† Determined by IMGT/ V-QUEST.

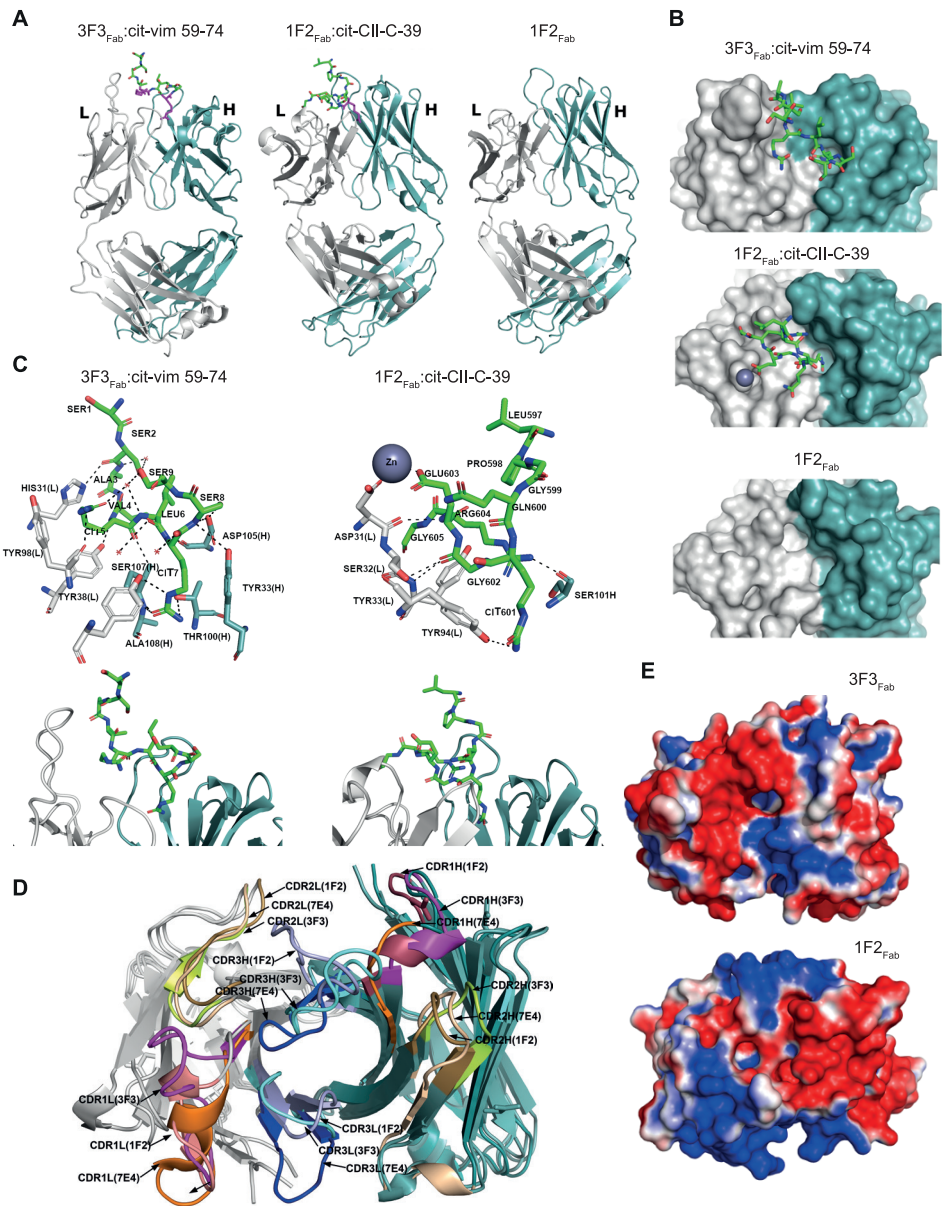
These results suggest a possibly higher impact of the LC glycan on antigen binding. We next visualized the amino acids and N-glycan monosaccharides involved in the hydrogen bond interactions as donors or acceptors within the respective three-dimensional (3D) variable domain structures based on IMGT (the international ImMunoGeneTics information system; Figure 3D and Figure S2 based on Table S4 to S6). The results show that hydrogen bonds between the core fucose or *N*-acetylglucosamine and the antibody structure were mainly formed between amino acids within or close to the N-linked glycan sites. Notably, N-glycan galactoses or terminal sialic acids also interacted with aa in the CDR1/CDR2 or even in the CDR3 (Figure 3D and Figure S2C). The negatively charged sialic acids of the 3F3 HC N-glycan interacted, for instance, with Y100, an amino acid located in the positively charged binding pocket. As amino acids located around Y100 in the HC are mainly involved in citrulline binding, an interaction with the N-linked glycan will likely affect antigen recognition (Figure 2D). Together with the structural composition of the antigen-binding pockets, these results show that carbohydrates are positioned in close vicinity to the antigen-binding pocket and are likely capable of disrupting antibody-antigen interactions by forming hydrogen bond interactions with the CDR structures directly involved in binding.

Disialylated complex-type VDG modulates binding to citrullinated antigens

As the data described above indicate that VDGs can modulate antigen binding, we next sought to validate the impact of carbohydrates attached to the variable domain on binding using the different monoclonal ACPA IgG variants. As shown by crystallography, the minor amino acid substitutions (germline back mutation) used to generate non variable domain glycosylated variants did not change CDR conformations, and hence, a potential impact on antigen-binding ability can be

N-linked glycan motifs V _H ⁺	N-linked glycan motifs V _L ⁺	Germline motifs V _H ⁺	Germline motifs V _L ⁺
NES (CDR1)	NVT (FR1)	SES (CDR1)	KVT (FR1)
NIT (FR3) and NST (FR3)	x	TMT (FR3) and STA (FR3)	x
NFS (CDR1) and NLT (CDR2-FR3)	NLT (FR1)	TFT (CDR1) and NPT (CDR2-FR3)	NFM (FR1)
NGS (CDR1), NTS (FR3) and NMT (FR3)	NIS (FR3)	GGs (CDR1), NPS (FR3) and KLS (FR3)	KIS (FR3)
NMT (FR3) and NTS (FR3)	NLT (FR3)	TMT (FR3) and STA (FR3)	TLT (FR3)
NFT (CDR1)	x	SFT (CDR1)	x

ruled out (Figure S2B). We identified the effects of various glycan compositions (WT, WT+neu, NG, and NG+neu) (Figure 1D) within six different mAbs (Table 1) on multiple antigenic interactions. Because of their heterogenous binding behaviour, different antigens were tested among different ACPA mAbs. First, binding toward several citrullinated peptides [cyclic citrullinated peptide 2 (CCP2), cit-fibrinogen α 27-43, cit-fibrinogen β 36-52, CCP1, cit-vimentin 59-74 and cit-enolase 5-20] was investigated, and our results showed an overall reduced binding capacity of the VDG-expressing WT variants (Figure 4 and Figures S3 and S4). Cleaving off negatively charged sialic acids increased binding to most antigens. The total absence of VDGs, as in the NG variants, resulted in considerably higher binding capacities (up to 90%) (Figure 4). In particular, VDGs affected the binding of ACPAs toward antigens recognized with low equilibrium K_D values, such as citrullinated enolase for the mAbs 7E4 and 1F2 or CCP1 for the mAb 3F3 (Figure 4A, Figure S4 and Table S2). Interactions with citrullinated antigens that show high maximal binding rates already at low concentrations, as observed for the CCP2 or citrullinated fibrinogen, were less affected by the presence of the carbohydrates (Figure 4A and Figure S4). Although no direct affinities could be calculated from the biphasic binding curves (Table S1), surface plasmon resonance (SPR) measurements showed a similar interference of the 7E4 VDG with citrullinated antigens. The lack of sialic acids resulted in higher response units, which raised even further, when the entire glycan structure was absent (Figure S5). Similar observations as made using citrullinated peptides as the antigenic target for ACPAs were obtained when analyzing binding toward citrullinated proteins (native autoantigens) such as citrullinated fibrinogen, vinculin, ovalbumin (OVA) and myelin basic protein (MBP). Alike the peptide binding results, the absence of VDGs raised the binding to most protein targets (Figures 4, C and D, and Figure S4), although 1F2 binding remained similar, an observation also made for some peptide antigens (Figure 4B).



◀ **Figure 2. Crystal structures of ACPA Fab fragments and their peptide-binding modes.** (A) Crystal structures of ACPA IgG Fab domains complexed with their respective peptides (3F3_{Fab}:cit-vim 59-74 and 1F2_{Fab}:cit-CII-C-39) and the unbound (APO) form of 1F2_{Fab} in a cartoon representation. The peptides bound to the Fab are shown as sticks with carbon (green), oxygen (red), and nitrogen (blue) atoms. Citrulline residues are colored in magenta. (B) Top view of the ACPA paratope and the bound peptides for 3F3_{Fab}:cit-vim 59-74 and 1F2_{Fab}:cit-CII-C-39 and for 1F2_{Fab} in an unbound state. The peptides are shown as sticks with carbon (green), oxygen (red), and nitrogen (blue) atoms. (C) Detailed paratope/epitope interactions between Fab fragments and their bound ligands shown for 3F3_{Fab}:cit-vim 59-74 and 1F2_{Fab}:cit-CII-C-39. Fab HC and LC are depicted as cartoon or sticks. All residues involved in the polar/hydrophobic interactions to the ligands are marked. Water molecules are depicted as red spheres, hydrogen bonds are depicted as black dashed lines, and the zinc ion is depicted as a dark sphere. Citrullinated residues are indicated as CIT. (D) Superposition of the CDR loops (CDR1, CDR2, and CDR3) of 3F3_{Fab}, 1F2_{Fab} and 7E4_{Fab}. (E) Electrostatic surface potentials of 3F3_{Fab} and 1F2_{Fab} are depicted. Positively charged regions are colored in red and negatively charged regions in blue. LC is depicted in light gray and HC in steel blue.

Thus, the enzyme-linked immunosorbent assay (ELISA) based binding assays of six different patient-derived monoclonal autoantibodies showed an overall negative impact of VDGs and sialic acids on binding to several potential (auto)antigens (Figure 4D and Figures S3 and S4). Thus, these data are in line with our prediction from the crystal structure analyses and indicate that VDGs can interact with and mask antigen-binding pockets of ACPAs.

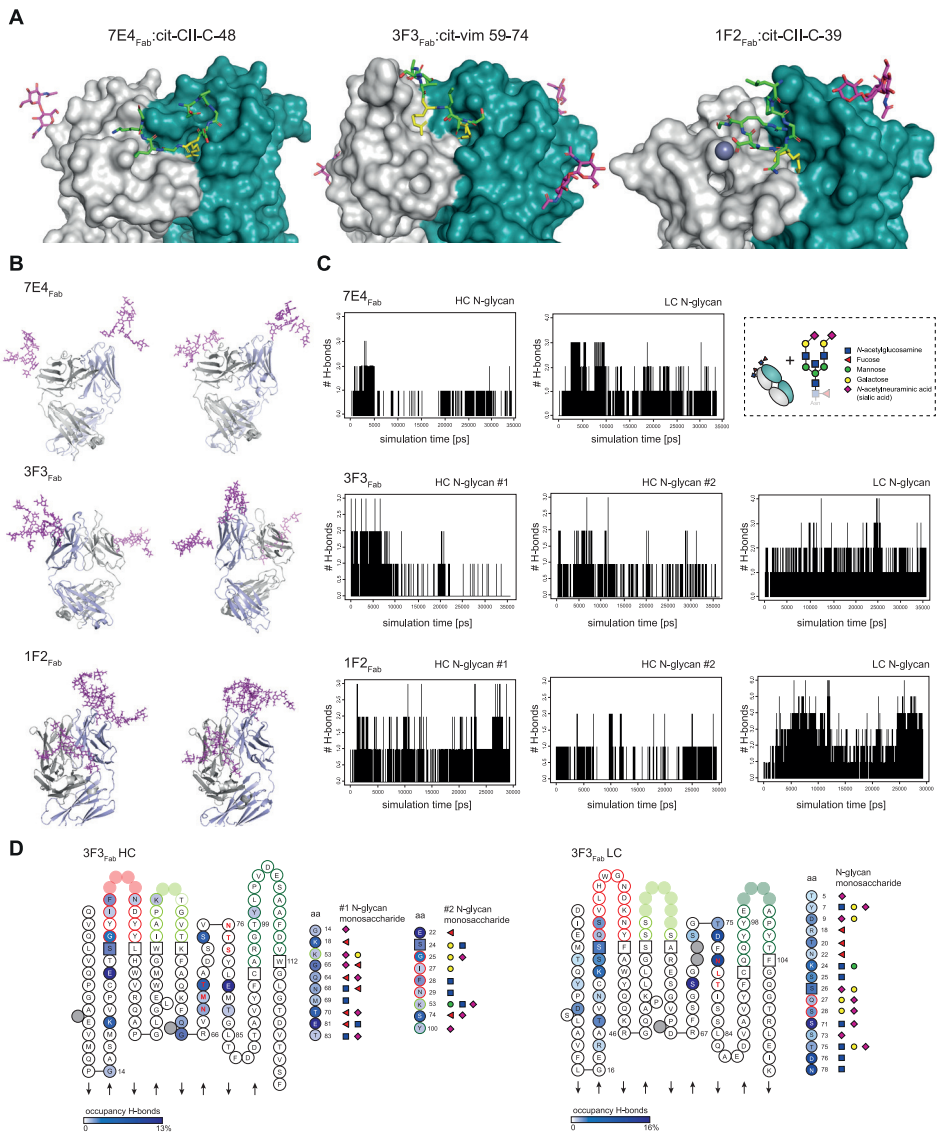
VDGs expressed by autoreactive BCRs masks antigen binding on the B-cell surface

The data described above provide novel insights into the potential influence of autoantibody VDGs on antigen binding. To address the question of whether VDG also affects autoantigen binding on the B-cell surface, we investigated the involvement of VDG on antigen binding at the cellular level. To this end, the human B-cell line Ramos, in which the endogenous IGHM, IGHD and IGLC and activation-induced cytidine deaminase were knocked out (MDL-AID KO)²³, was used to express citrullinated protein (CP)-directed BCRs. Two Ramos B-cell transfectants carrying variable domain glycosylated 3F3 and 7E4 membrane IgG (mIgG) BCRs²³ and their NG counterparts were generated (Figure 5A). NG variants were produced as mentioned above by mutating the N-linked glycan sites back to the respective germline amino acid sequences. Transduced B cells were sorted on the basis of green fluorescence protein (GFP) and mIgG expression to ensure an identical amount of WT and NG BCRs on the surface of both cell lines (Figures 5, B and C). The human Ramos B cells transduced with patient-derived autoreactive BCRs were highly GFP and mIgG BCR positive, while the non-transduced control MDL-AID KO cell line showed no BCR and GFP expression (Figure 5B). The occupancy of the N-linked glycan sites and thus the expression of VDGs on the WT mIgGs were verified by gel electrophoresis after B cell lysis and BCR capturing (Figure 5D). A size shift was present between the WT and NG BCRs for both cell lines. This mass shift was higher when comparing the 3F3 to the 7E4 BCR variants due to six N-linked glycans attached to the 3F3 BCR HC and LC chain compared to four glycans attached to the 7E4 mIgG (Figure 5D). Furthermore, we analyzed the specific IgG BCR VDG composition after an in-gel total glycan release (PNGaseF treatment) followed by

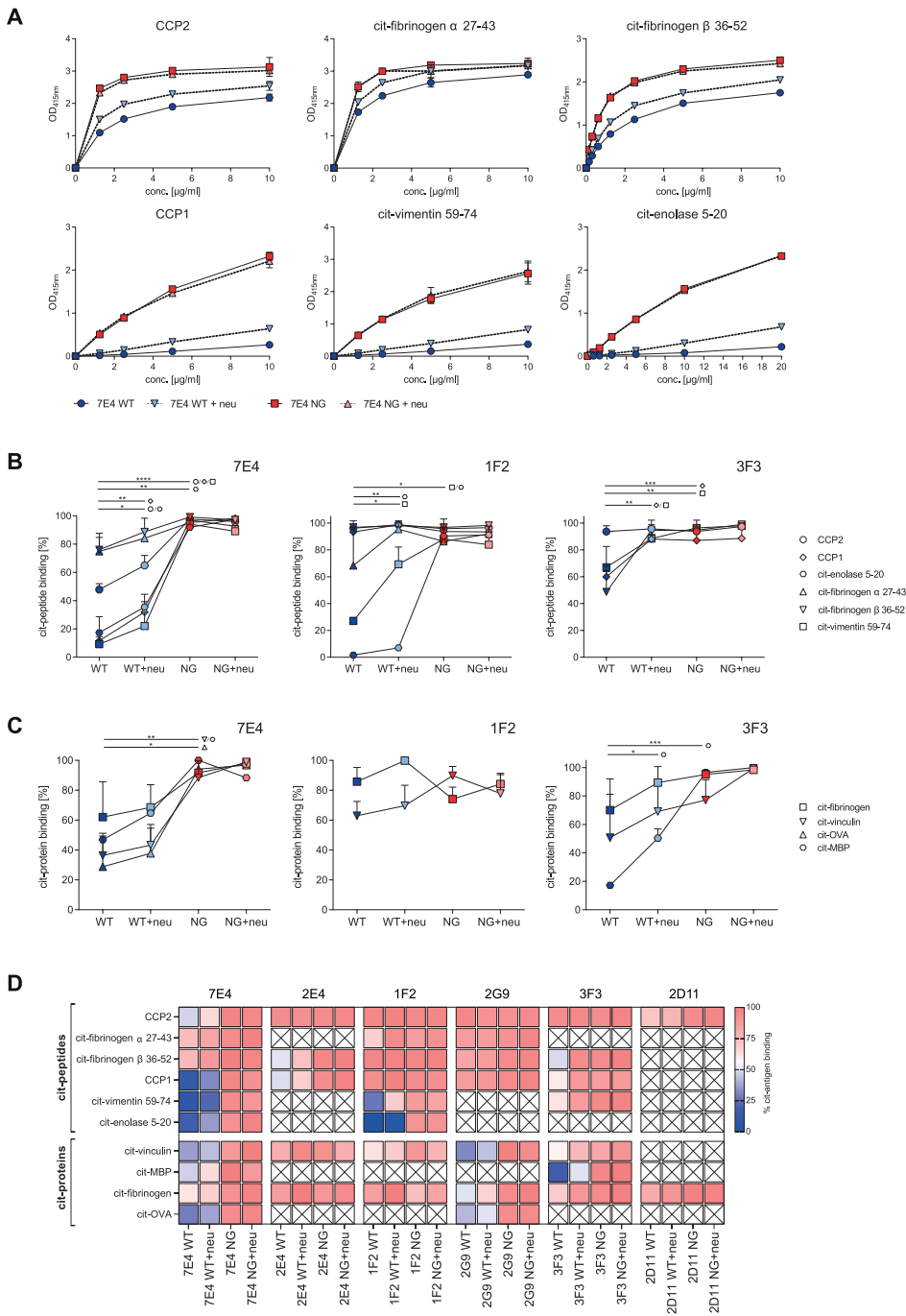
liquid chromatography-MS (LC-MS). Although this method does not allow a site-specific glycan analysis, the results obtained show that WT BCRs isolated from human Ramos B cells harbor fully processed complex type H5N5F1S2 glycans as opposed to their NG counterparts (Figures 5, F and G and Figure S6, A and B). Likewise, we observed more bisecting *N*-acetylglucosamine and sialic acid moieties on the VDG (WT) BCR compared to the non-VDG (NG) BCR, which only contained Fc glycans, while galactosylation and fucosylation were comparable between the variants (Figure 5E). We confirmed the expression of complex-type glycans on surface IgG BCRs by cell surface biotinylation and western blot analysis of the captured biotinylated BCRs. To analyze the nature of surface IgG specific glycans, we treated the biotinylated BCR with Endo H, an enzyme that is unable to cleave complex-type N-glycans and only able to remove mannosylated glycans, or PNGase F, which cleaves all N-glycan structures as also elegantly described in previous publications²⁶. The results showed a size shift toward the NG BCR after PNGase F treatment and almost no susceptibility of the BCR VDGs to Endo H treatment (Figure S6C). Thus, these data indicate that surface IgG BCRs on Ramos B cells predominantly express fully processed complex-type H5N5F1S2 glycans in their variable domains, such as the VDGs found on isolated ACPA IgG from patients, and no high-mannose structures.

Next, we used the autoreactive 7E4 and 3F3 BCR-expressing cell lines to identify the impact of mIgG H5N5F1S2 VDGs on autoantigen binding by flow cytometry analyses using labeled citrullinated peptide tetramers²⁷. The results obtained are consistent with the ELISA observations and indicate a reduction in antigen binding for B cells that express VDG BCRs (Figure 6). Similarly to the mAb data, binding of low-affinity antigens by a given ACPA, such as CCP1 for 7E4 or cit-vimentin 59-74 for 3F3, was more affected compared to binding of antigens that display higher equilibrium K_D values, such as cit-fibrinogen α 27-43 for 7E4 and CCP2 for 3F3 (Table S2 and Figure 6).

Figure 3. Fab structures crystallized with the starting (core) monosaccharides of the VDG and MD simulations to predict VDG-antibody interactions. (A) Fab structures of 7E4_{Fab}:cit-CII-C-48, 3F3_{Fab}:cit-vim 59-74, and 1F2_{Fab}:cit-CII-C-39 crystallized with the first two *N*-acetylglucosamines (GlcNAcs) of the VDG. LC is depicted in light gray and HC in steel blue. The peptides bound to the respective Fab are depicted as sticks with citrulline residues (yellow), carbon (green), oxygen (red), and nitrogen (blue) atoms. The GlcNAcs are presented as sticks in magenta. (B) MD simulation, two time points, of 7E4_{Fab}, 3F3_{Fab} and 1F2_{Fab} crystal structures modeled with full length disialylated VDGs represented as sticks in magenta. (C) Hydrogen bond (H-bond) interactions between the VDG (HC or LC) and the antibody structure are visualized over simulation time. (D) ACPA 3F3_{Fab} HC and LC variable gene amino acid sequence is depicted on the basis of IMGT (2D). Acceptors/-donors of H-bond interactions between the antibody structure and the HC (#1 and #2)/LC N-glycans are visualized. High occupancy is depicted in dark blue (HC: 13%, LC: 16%), and low occupancy is depicted in light blue (0.01 to 0.2%). Amino acids and their respective interaction partners (N-glycan monosaccharides) are shown. Blue square, GlcNAc; green circle, mannose; yellow circle, galactose; red triangle, fucose; purple diamond, α 2,6-linked *N*-acetylneuraminic acid (sialic acid). ►



Overall, our results demonstrate the first human B-cell model that can be used to study the impact of BCR glycans on autoantigen recognition, B-cell functions, or B-cell fate. Our findings show that VDGs are not only able to modulate antigen interactions on secreted autoantibodies but also capable of affecting the interplay between BCRs and their autoantigens.

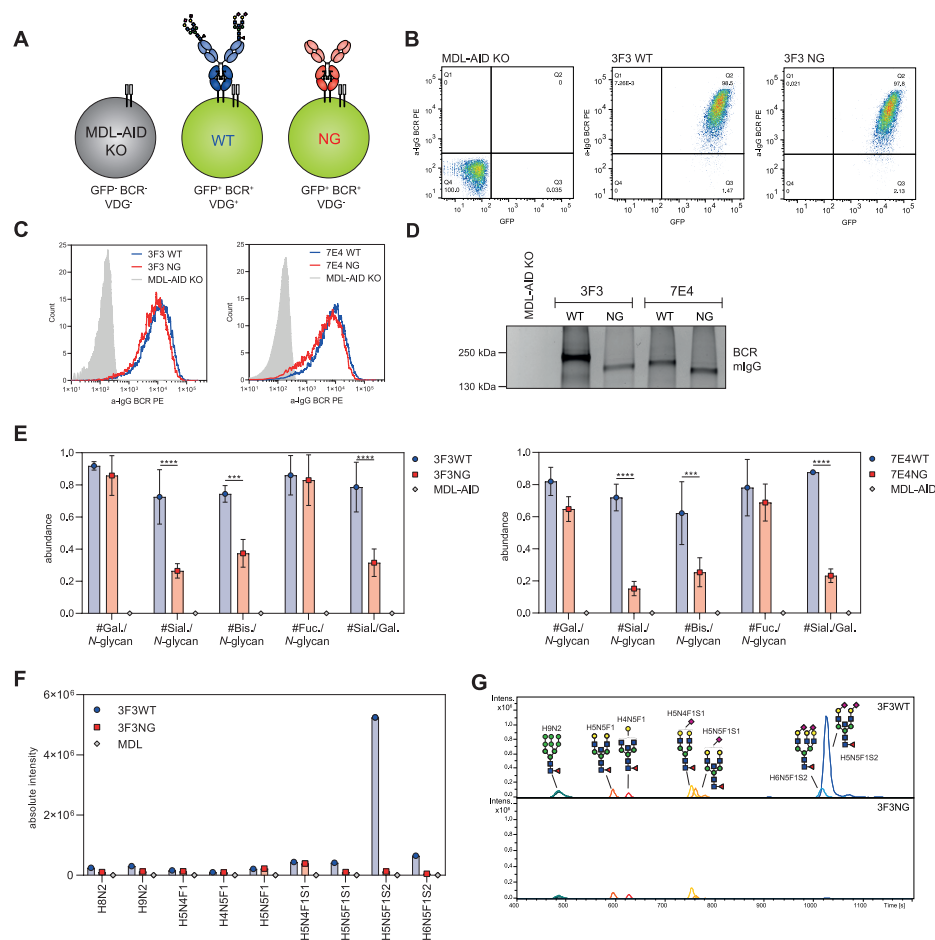


◀ **Figure 4. Impact of disialylated ACPA VDGs on citrullinated (auto)antigen binding.** (A) ELISA titration binding curves of the ACPA 7E4 (0 to 10 $\mu\text{g/ml}$) variants (WT, WT+neu, NG, and NG+neu) toward citrullinated peptides (CCP2, CCP1, cit-fibrinogen α 27-43, cit-fibrinogen β 36-52, cit-vimentin 59-74 and cit-enolase 5-20). Binding to the arginine control peptide was subtracted. Reactivity was determined via the optical density (OD) at 415 nm. Each data point represents the mean of two technical replicates, and each binding experiment was repeated two to three times. (B) Relative binding of the ACPA mAb 7E4, 1F2, and 3F3 (2 to 40 $\mu\text{g/ml}$) variants (WT, WT+neu, NG and NG+neu) to citrullinated peptides. $N = 2$ to 6. Unpaired two-tailed t- tests assuming the same SD. 7E4 WT-NG: ****p (CCP2, CCP1, cit-vimentin 59-74) < 0.0001 and **p (cit-enolase 5-20) = 0.0005; 7E4 WT-WT+neu: **p (CCP1) = 0.029, *p (CCP2) = 0.0227 and *p (cit-enolase 5-20) = 0.0419; 1F2 WT-NG: *p (cit-vimentin 59-74) = 0.0104 and *p (cit-enolase 5-20) = 0.0101; 1F2 WT-WT+neu: **p (cit-enolase 5-20) = 0.0096 and *p (cit-vimentin 59-74) = 0.0449; 3F3 WT-NG: ***p (CCP1) = 0.0009 and **p (cit-vimentin 59-74) = 0.0010; 3F3 WT-WT+neu: **p (CCP1) = 0.0017 and **p (cit-vimentin 59-74) = 0.0082. (C) Relative binding of the ACPA mAb 7E4, 1F2, and 3F3 (5 to 20 $\mu\text{g/ml}$) variants (WT, WT+neu, NG and NG+neu) to citrullinated proteins. $N = 2$. Unpaired two-tailed t-tests assuming the same SD. 7E4 WT-NG: **p (cit-vinculin) = 0.0022, **p (cit-MBP) = 0.0014 and *p (cit-OVA) = 0.0032; 3F3 WT-NG: ***p (cit-MBP) = 0.0003; 3F3 WT-WT+neu: *p (cit-MBP) = 0.0213. (D) Heat- map of relative binding (0%, blue, 100%, red) of all monoclonal ACPA (7E4, 2E4, 1F2, 2G9, 3F3, and 2D11) to citrullinated peptides and proteins. Non determined reactivities are illustrated with a cross. $N = 2$ to 3. (F) Relative binding of ACPA 7E4, 1F2, and 3F3 (5 to 20 $\mu\text{g/ml}$) variants (WT, WT+neu, NG, NG+neu) to citrullinated proteins. $N = 2$ to 6.

Functional impact of sialylated BCR VDG on B-cell activation

Next, we wished to delineate whether disialylated VDGs expressed on mIgG BCRs influence B-cell activation independently of the “masking” effect on antigen binding. For this, we performed calcium flux experiments and investigated the phosphorylation of the spleen tyrosine kinase (Syk), a central kinase in BCR signal initiation and amplification^{23,28}. Ramos WT and NG B cell lines, displaying an identical BCR surface expression (Figure 5C), were either stimulated with anti-IgG F(ab)'2 or with a citrullinated antigen (Figure 7A). For these experiments, the high-affinity antigen CCP2-streptavidin (strep.) tetramer was used, which exhibits similar binding strengths to both WT and NG BCRs (Figure 6B). Both stimuli triggered calcium flux within a few seconds, as measured by the ratio of Indo-1 in a calcium-bound and unbound state (Figures 7, B and C). No calcium flux was detected after stimulating the cells with the non-citrullinated, arginine-containing control tetramers (CArgP2-strep.) (Figure S7B). Likewise, activation with antigens that are recognized with lower affinity, such as cit-fibrinogen β 36-52, did not result in sufficient B-cell activation in this assay (Figure S7B). Intriguingly, when stimulated with either anti-IgG F(ab)'2 or the citrullinated antigen (CCP2), both WT cell lines (3F3 and 7E4) exhibited higher calcium flux peaks compared to the cells expressing NG BCRs (Figures 7, C and D). B cells expressing VDG BCRs displayed not only a higher maximal calcium flux but also a faster calcium release as indicated by the slope of the curve (Figure 7C and Figure S7A). In addition, we analyzed the phosphorylation of the BCR signal-transducing kinase Syk in these cell lines by phospho-flow and western blotting. Notably, and in line with the calcium release, both WT cell lines showed a higher pSyk level than the NG BCR carrying cells when stimulated with either anti-IgG F(ab)'2 or CCP2-strep. (Figures 7, D, F and G, and Figure S7C).

In addition, depending on the stimulus given, our data indicated not only a higher activation signal but also a prolonged Syk phosphorylation after stimulation for different time periods (2 to 20 min) (Figure 7E). Thus, these data indicate that human B-cell lines expressing a variable domain glycosylated autoreactive BCR depict a higher activation after stimulation, potentially explaining why autoreactive B cells with VDG modified BCRs have a selection advantage in RA.



◀ **Figure 5. Generation of human Ramos B-cell lines carrying disialylated VDG BCRs.** (A) Schematic depiction of generated human Ramos B-cell transfectants with mIgG VDG⁺ BCRs (WT) and VDG⁻ BCRs (NG). The untransduced MDL-AID KO cell line shows no GFP and endogenous BCR expression (GFP⁻, BCR⁻, VDG⁻). (B) GFP and BCR surface expression of the MDL-AID KO control cell line and Ramos cells expressing 3F3 mIgG with (WT) and without (NG) VDGs. (C) Histograms depicting an identical WT and NG mIgG BCR expression of the 3F3 and 7E4 Ramos B-cell lines and no BCR expression of the MDL-AID KO cell line. (D) Size shift between VDG⁺ and VDG⁻ 3F3 and 7E4 BCRs visualized on a 4 to 15% SDS polyacrylamide gel (Bio Rad). No mIgG BCR protein band was detected for the MDL-AID KO cell line. The size was determined using the PageRuler™ Plus Prestained Protein Ladder (Thermo Fisher Scientific). (E) Bar graphs of the relative abundance of galactosylation, sialylation, bisecting GlcNAc, and fucosylation per N-glycan and sialylation per galactosylation on the Ramos 3F3/7E4 WT, NG, and MDL IgG BCRs after passing quality control (QC) settings. N = 3 (biological replicates). Multiple non paired t-tests (Bonferroni-Dunn method): ****p < 0.0001, *** (3F3) p = 0.0008 and *** (7E4) p = 0.0004. (F) Absolute intensity of glycan traits expressed on the MDL and 3F3 WT and NG BCR after passing QC settings. (G) LC chromatogram of glycan traits expressed on the 3F3 WT and NG BCR after passing QC settings.

Effect of VDG on BCR downmodulation and antigen internalization

To determine whether variable domain glycosylation also regulates BCR downmodulation after antigen exposure, we stimulated the Ramos B cell lines for several minutes with the CCP2-strep. or the CArgP2-strep. control tetramer at 4 °C. We then let the cells incubate at 37 °C to allow internalization and measured mIgG BCR downmodulation using a Fab anti-human IgG detection antibody (Figure 8A). The transduced and GFP-positive Ramos cells showed no changes in cell surface BCR expression after phosphate-buffered saline (PBS) treatment or when incubated on ice. In contrast, downmodulation could be readily detected after 15 min of incubation at 37 °C (Figure 8B), indicating rapid antigen-induced BCR internalization. We identified a time-dependent decrease in BCR surface expression for both the WT and the NG B-cell line (Figure 8C). Notably, the signal of surface-bound BCRs after antigenic stimulation was significantly decreased for the B-cell lines carrying NG BCRs compared to their variable domain glycosylated counterparts (Figures 8, D to F), despite the equivalent binding intensity of CCP2 at baseline. Loss of cell surface BCR expression was faster for the 3F3 expressing cell lines as most of the mIgG was lost within 30 min, whereas no downmodulation could be detected after stimulating the cells with the control peptide (Figures 8, E and F).

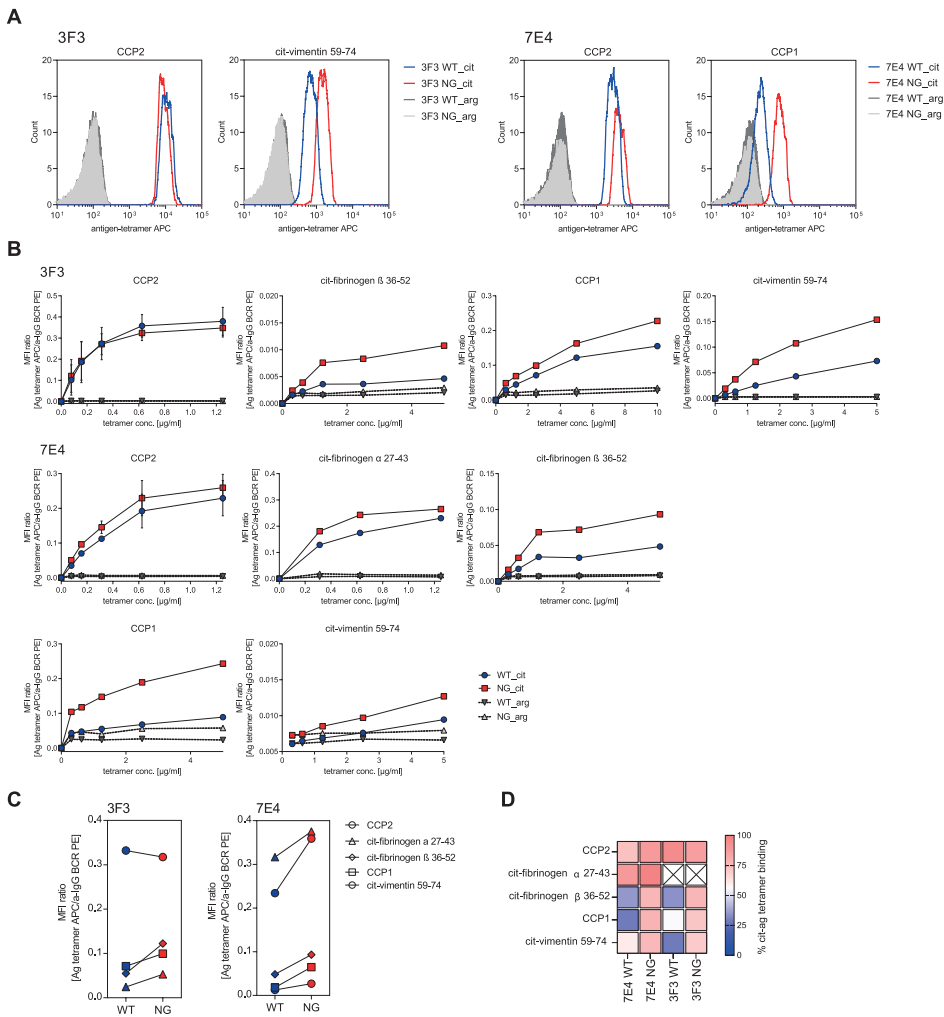
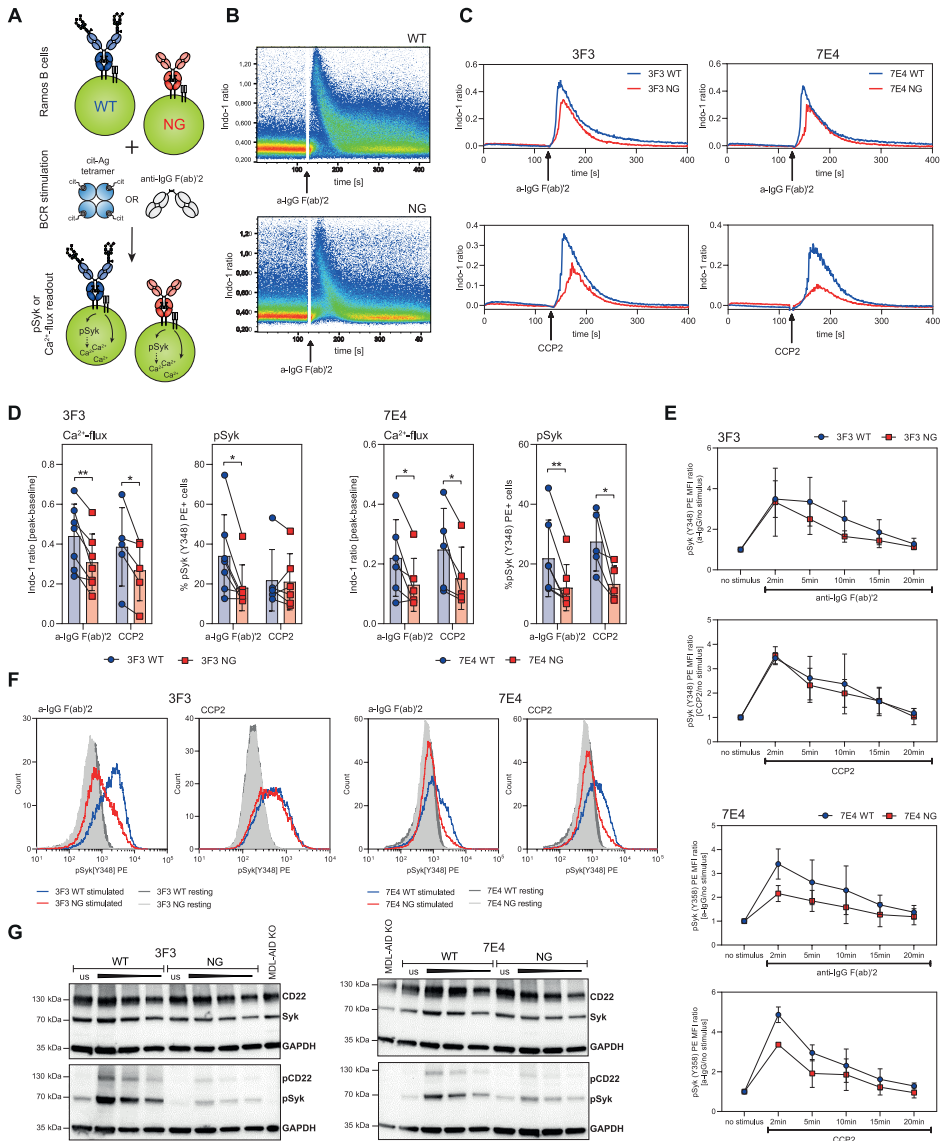


Figure 6. Binding of Ramos B cell lines carrying a VDG⁺ or VDG⁻ BCRs to citrullinated antigens. (A) Histograms of Ramos 3F3 and 7E4 B cells carrying VDG⁺ or VDG⁻ BCRs and their binding to CCP2/cit-vimentin 59-74 or CCP2/CCP1-strep. APC labeled tetramers, respectively. Binding to the arginine control peptides is shown in dark (WT) and light (NG) gray. **(B)** Binding titration curves of 7E4/ 3F3 WT and NG BCRs to citrullinated peptide-strep. tetramers (CCP2, CCP1, cit-fibrinogen α 27-43, cit-fibrinogen β 36-52, and cit-vimentin 59-74) and their respective control peptides. N = 2. The y-axis depicts the MFI ratio between antigen binding and mIgG BCR expression. **(C)** Binding of 3F3/ 7E4 WT and NG Ramos B cells to citrullinated peptide-strep. tetramers (1 to 5 μg/ml). The y axis depicts the MFI ratio between antigen binding and mIgG BCR expression. **(D)** Relative binding of 7E4/ 3F3 WT and NG BCRs towards five citrullinated peptides (0%, blue; 100%, red).

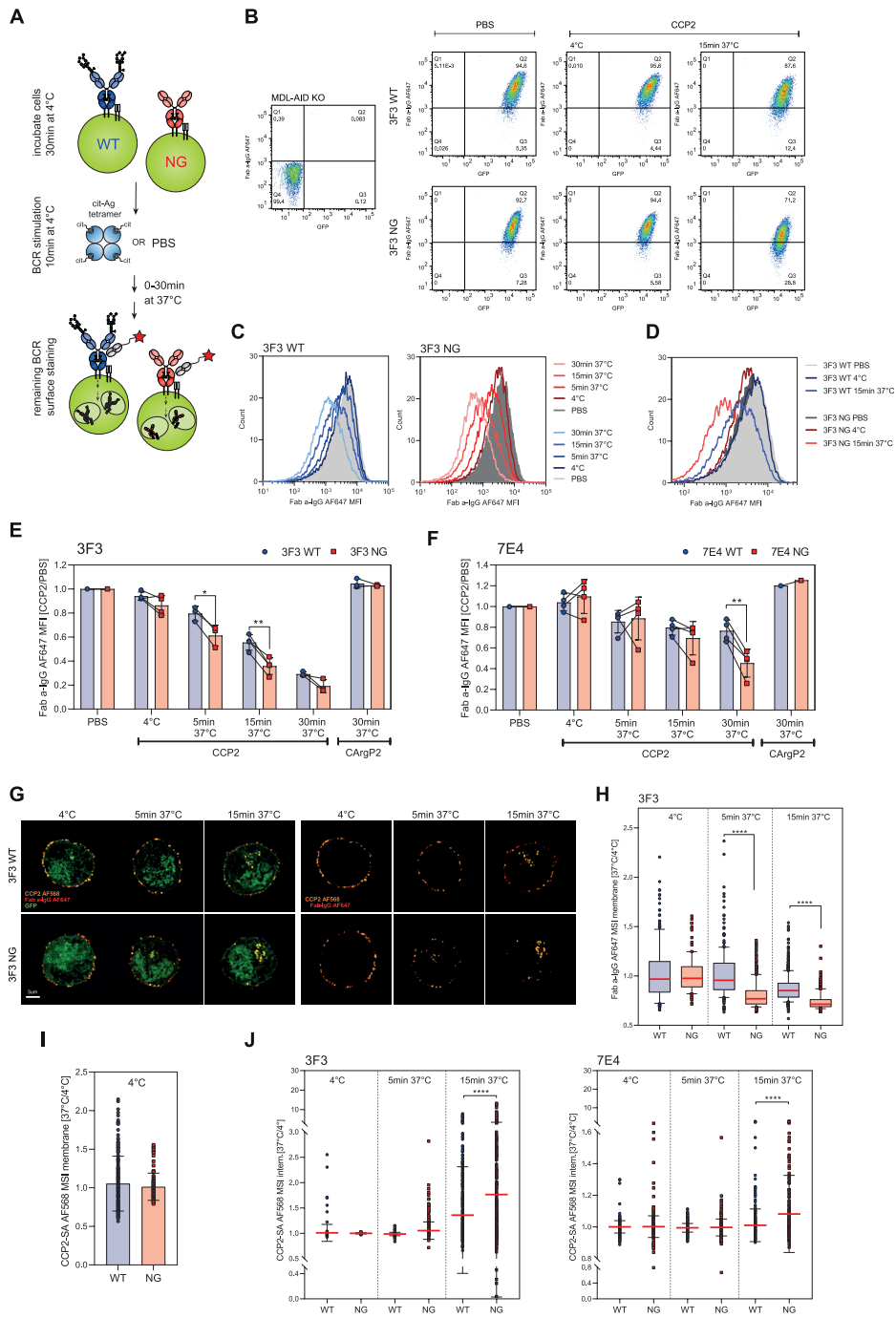
Furthermore, confocal microscopy confirmed the flow cytometry-based BCR downmodulation data. We assessed antigen internalization by stimulating the cells with AF568-labeled CCP2-strep. tetramers. BCR modulation was evaluated by staining the remaining BCRs on the fixed cell surface after antigenic stimulation. mIgG BCRs were detected using a Fab anti-human IgG antibody coupled to AF647. All antigen-bound mIgG BCRs were still located on the B-cell surface after incubation on ice. Incubating the stimulated B cells at 37 °C for several minutes induced BCR clustering followed by antigen internalization and a reduced amount of surface mIgGs (Figure 8G). The quantified results showed that especially NG BCRs were markedly downmodulated after antigenic stimulation and incubation for 5 min at 37 °C, while WT BCRs were still stably expressed on the B cell surface (Figure 8H). Despite a similar binding toward the CCP2-strep. tetramer (Figure 8I), more antigen-bound BCRs were internalized, when no VDGs were present on the 3F3 and 7E4 mIgGs (Figure 8J and Figure S7D). These results, together with the flow cytometry based BCR expression data, indicate that human BCRs harboring VDGs stay longer on the B-cell surface in an antigen-bound manner.

The role of the sialic acid-binding lectin CD22 on BCR VDG-mediated effects

To identify whether interactions with the α 2-6-linked sialic acid-binding lectin (Siglec) CD22 can explain the effect of VDGs on BCR signaling and cell surface expression, we performed CRISPR Cas9 KO in the 3F3 WT and NG BCR-expressing Ramos B cell lines. The KO was validated by flow cytometry, showing that the surface expression of CD22 was clearly absent in both the 3F3 WT and NG CD22KO cell lines compared to their non-KO counterparts (Figures 9, A to C). Furthermore, we verified the KO of the CD22 target gene by bulk sequencing. Both KO cell lines showed a gene KO efficiency of more than 90% as evidenced by TIDE (tracking of indels by decomposition) analysis (Figure S8A). Mostly nucleotide deletions (> 70%) were observed and, to a lower extent, +1 nucleotide insertions (< 20%) with the highest frequency of guanine insertions (> 85%) (Figures S8, A and B). Both CD22KO cell lines, expressing a VDG (WT) or NG BCR, as well as their CD22⁺ counterparts, were assessed in functional assays. Flow cytometry based phospho-flow depicted, in line with our previous experiments, an increased pSyk expression of stimulated 3F3 cells carrying a WT compared to a NG BCR (Figure 9D). Furthermore, we identified an increased expression of pSyk in stimulated CD22KO cell lines compared to their CD22-expressing counterparts (Figure 9D). The increased signaling capacity after the CD22KO was similar for the WT and NG variants, indicating that VDG-mediated differences in BCR signaling are independent of CD22. These results were confirmed by calcium flux (Figure 9E) and western blot analyses, which showed that the absence of CD22 did not affect an increased pSyk expression in the presence of the VDGs (Figure 9F). In addition, we could not observe an impact of the Siglec CD22 on BCR downmodulation as evidenced by the BCR surface expression data of the CD22KO cell lines after activation with a citrullinated antigen (Figure 9G). However, similar to our previously presented results, the NG BCR was downmodulated quicker compared to its VDG counterpart (Figure 9G). Together, these data point out that the highly sialylated VDGs alters BCR downmodulation and signaling via a mechanism that does not involve the sialic acid-binding lectin CD22.



◀ **Figure 7. Impact of mIgG BCR VDGs on human Ramos B-cell activation.** (A) Ramos B cells (WT and NG) were stimulated with antigen (CCP2-strep.) or anti-IgG F(ab)'2. B-cell activation was analyzed via Ca^{2+} release or the phosphorylation of Syk. (B) Ca^{2+} flux (Ca^{2+} -bound Indo-1/ unbound Indo-1) of 3F3 WT and NG Ramos B cells after stimulation with a-IgG F(ab)'2. (C) Ca^{2+} flux overlays of 7E4/ 3F3 WT and NG Ramos B cells after stimulation [a-IgG F(ab)'2 or CCP2-strep.]. (D) Paired analysis of Ca^{2+} flux and pSyk(Y348) expression after 5 min of stimulation [a-IgG F(ab)'2 or CCP2-strep.] for 3F3/ 7E4 WT and NG Ramos B cells. Paired two-tailed t-test. N = 5 to 7. 3F3 Ca^{2+} flux: **p = 0.005 and *p = 0.0316; 3F3 pSyk: *p = 0.0109; 7E4 Ca^{2+} flux: *p = 0.0309 and *p = 0.0441; 7E4 pSyk: **p = 0.0089 and *p = 0.0276. (E) pSyk (Y348) time-point analysis of 3F3/ 7E4 WT and NG Ramos B cells after adding no stimulus or 2, 5, 10, 15, and 20 min of stimulation [a-IgG F(ab)'2 or CCP2-strep.]. pSyk(Y348) MFI ratio (stimulated/ unstimulated cells) is depicted. (F) pSyk (Y348) histograms of unstimulated, CCP2-strep. or a-IgG F(ab)'2 stimulated 3F3/ 7E4 WT and NG Ramos B cells. (G) Western blot analyses of unstimulated (us) or 5 min a-IgG F(ab)'2 stimulated 3F3/ 7E4 WT and NG Ramos B cells. CD22, Syk, pCD22 (Y822) and pSyk(Y352) expression are shown. Cell lysates of 1 million (unstimulated and stimulated first slot), 0.5 million (stimulated second slot) and 0.25 million (stimulated third slot) cells were blotted. Glyceraldehyde-3-phosphate dehydrogenase (GAPDH) was used as a loading control, and 1 million MDL-AID KO cells were added as an additional control.



◀ **Figure 8. Effect of BCR VDG on antigen internalization and BCR downmodulation.** (A) Ramos B cells were incubated at 4 °C, stimulated with antigen or PBS and incubated at 4 °C or 37 °C to allow BCR downmodulation. The remaining surface BCRs were stained (Fab anti-human IgG-AF647). (B) GFP and mlgG expression of MDL-AID KO, 3F3 WT and NG cells after PBS or CCP2-strep. treatment (4 °C or 15 min at 37 °C). (C) Histograms (mlgG) of CCP2-strep. stimulated 3F3 WT or NG Ramos B cells (4 °C or 5, 15, 30 min at 37 °C). (D) Histogram (mlgG) overlay of 3F3 WT and NG Ramos B cells after PBS or CCP2-strep. treatment (4 °C or 15 min at 37 °C). (E) BCR downmodulation of 3F3 WT and NG (F) 7E4 WT and NG after PBS, CCP2-strep. or CArgP2-strep. stimulation (4 °C or 5, 15, 30 min at 37 °C). Paired two tailed t- test. N = 3 to 4. 3F3:*(5 min) $p = 0.0146$ and $**p = 0.0054$; 7E4 $**p = 0.0054$. (G) Spinning disk confocal microscopy of GFP+ 3F3 WT and NG cells after CCP2-strep.-AF568 stimulation (incubation at 4 °C or 5, 15 min at 37 °C), 2% PFA fixation and a-IgG-AF647 surface staining. (H) 3F3 WT and NG BCR expression after CCP2-strep. stimulation (4 °C or 5, 15 min at 37 °C). N = 114, 213, 474, 224, 495 and 595 cell slices respectively. Ordinary one-way ANOVA, $****p < 0.0001$. (I) CCP2-strep. binding of 3F3 WT and NG at 4 °C. (J) CCP2-strep. internalization of 3F3/7E4 WT and NG BCRs at 4 °C or after 5, 15 min incubation at 37 °C. N(3F3) = 114, 213, 474, 224, 495 and 595 cell slices respectively. N(7E4) = 619, 459, 645, 433, 738 and 302 cell slices respectively. Ordinary one-way ANOVA, $****p < 0.0001$.

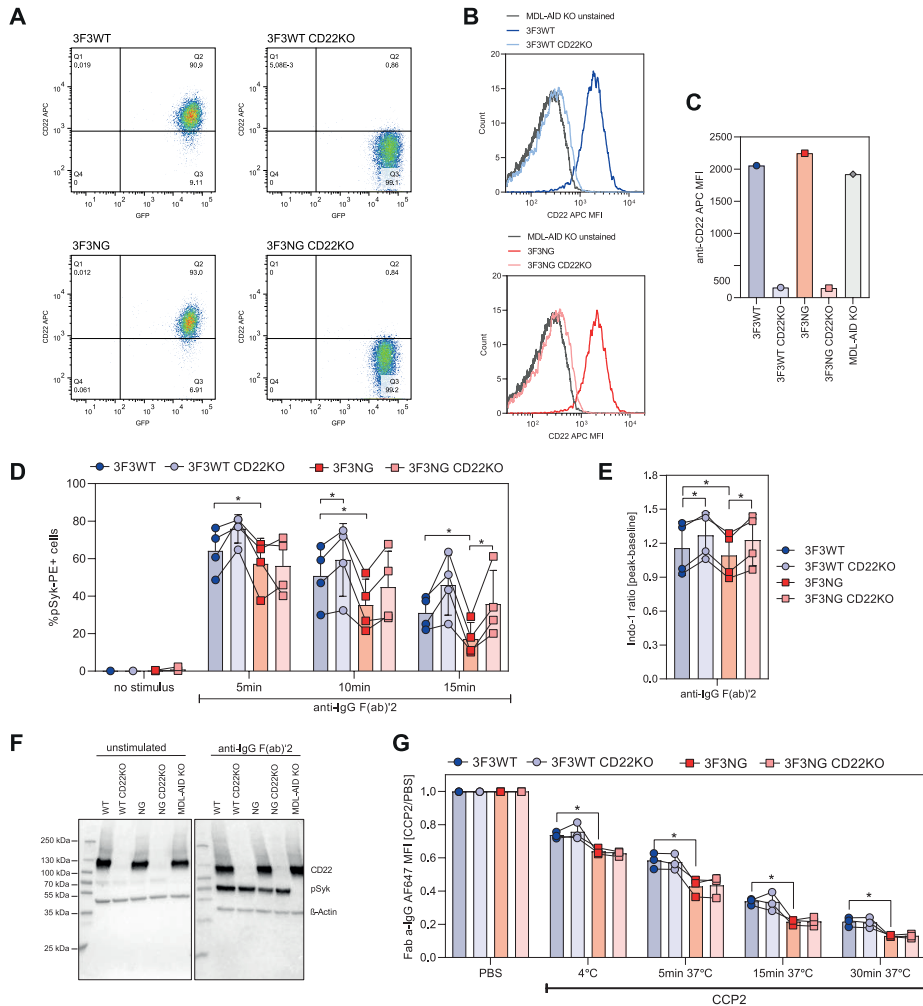


Figure 9. Impact of CD22 CRISPR Cas9 KO on BCR VDG-mediated effects. (A) GFP and CD22 (anti-CD22 APC) expression of 3F3WT, WT CD22KO, NG and NG CD22KO Ramos B cells. **(B)** Histogram overlay (CD22) of unstained cells, 3F3WT, and WT CD22KO or 3F3NG and NG CD22KO Ramos B cells. **(C)** CD22 expression of 3F3WT, WT CD22KO, NG, NG CD22KO and MDL-AID KO Ramos B cells. **(D)** Percentage of pSyk(Y348) positive cells of 3F3 WT, WT CD22KO, NG, and NG CD22KO Ramos B cells after 5, 10, and 15 min of a-IgG F(ab)2 stimulation. Paired two-tailed t-test. N = 4. 5 min: *(3F3 WT vs. NG) $p = 0.0318$; 10 min: *(3F3 WT vs. NG) $p = 0.0106$, *(3F3WT vs. WT CD22KO) $p = 0.0298$; 15 min: *(3F3WT vs. NG) $p = 0.0166$, *(3F3NG vs. NG CD22KO) $p = 0.0315$. **(E)** Ca^{2+} flux of 3F3 WT, WT CD22KO, NG, and NG CD22KO Ramos B cells after a-IgG F(ab)2 stimulation. Paired two-tailed t-test. N = 4. *(3F3 WT vs. WT CD22KO) $p = 0.0177$, *(3F3 WT vs. NG) $p = 0.0342$, *(3F3 NG vs. NG CD22KO) $p = 0.0171$. **(F)** Western blot analyses of 3F3 WT, WT CD22KO, NG and NG CD22KO Ramos B cell lysates after 5 min of a-IgG F(ab)2 stimulation. CD22 and pSyk(Y352) expression are shown. β -Actin was used as loading control and MDL-AID KO cell lysates as additional control. **(G)** BCR downmodulation of 3F3 WT, WT CD22KO, NG, and NG CD22KO Ramos B cells after PBS or CCP2-strep. stimulation and incubation at 4°C or for 5, 15 or 30 min at 37°C. Paired two-tailed t-test. N = 3. *(4°C) $p = 0.0474$, *(5 min 37°C) $p = 0.0132$, *(15 min 37°C) $p = 0.0229$, *(30 min 37°C) $p = 0.0463$.

Discussion

We here investigated the impact of VDGs on human B cell biology using citrullinated protein-directed BCR sequences isolated from ACPA-positive patients with RA. These molecules display naturally occurring N-linked glycan sites within the variable regions that are introduced during somatic hypermutation (SHM)¹⁸ and allow the incorporation of VDGs. More than 90% of ACPA IgG harbor VDGs, which makes them a hallmarking feature of the RA-specific ACPA immune response¹⁶. Although readily found on ACPA from patients with RA, VDGs are not abundantly present in healthy individuals¹⁹. Furthermore, it has become evident that the transition to ACPA-positive disease is associated with a rise in VDG levels before disease¹⁹, which is intimately connected to an increase in autoantibody levels and a “maturation” of the ACPA response as defined by an increased citrullinated antigen recognition profile and isotype usage. Notably, this maturation is not coupled to an increase in avidity as the ACPA response displays only limited avidity maturation across different (pre)disease stages²⁹. Together, these observations are intriguing as they imply that affinity maturation does not drive the selection of autoreactive ACPA-expressing memory B cells, but rather their propensity to introduce glycosylation sites into their variable domains that potentially support their expansion and/or survival³⁰. BCR analyses of ACPA-expressing B cells from patients with RA indicate that the introduction of glycosylation sites is a consequence of a selective process not explained by the number of SHM. In line with this concept, the most prominent genetic risk factor for RA, the human leukocyte antigen (HLA) class II region, does not associate with the presence of ACPA as such but mainly with ACPA-expressing VDGs^{31,32}. Hence, the acquisition of VDG represents an important event connected to the expansion of the B-cell response occurring before RA-onset that is also predictive for disease development in healthy first-degree family members of patients with RA¹⁹. Furthermore, accumulating evidence suggests that N-linked VDGs are also at play in several other human autoimmune diseases including ANCA-associated vasculitis and Sjögren's syndrome^{20,21}.

The data presented in this manuscript support a concept in which VDGs act as a “threshold” for human autoreactive B-cell activation, by showing that CP-directed B cells increase BCR signaling upon the presence of VDG. The introduction of VDGs during SHM is thus likely involved in the selection and activation process of autoreactive B cells in RA and possibly other autoimmune diseases. Next to their ability to increase B-cell activation, VDGs are able to delay BCR downmodulation after antigenic stimulation and “mask” binding to especially “low-affinity” antigens. Whether or how these functional events are interconnected and contribute in setting the “threshold” for autoreactive B-cell activation and survival is unclear. However, it is conceivable that VDGs reduce the breadth of self-antigen recognition in the GC and thereby promote B-cell survival. In case of a ubiquitous expression of self-antigens in the GC environment, self-reactive B cells might be eliminated as demonstrated in mouse

studies³³. A differential impact of VDGs on antigen binding, although not self-antigens, has been reported for high-affinity anti-adalimumab and anti-infliximab clones²² as well as for follicular lymphoma-derived VDGs artificially introduced into anti-NIP or anti-HEL BCRs and expressed in a murine B cell-derived reporter cell line³⁴. Our crystallographic data indicate that naturally occurring VDGs can interact with the antibody paratope and thereby compete with antigens for binding. This might provide a mechanism for autoreactive B cells to escape elimination through recognition of (abundantly) expressed autoantigens, while allowing activation via cross-reactivity to (higher-affinity) foreign-epitopes. Structural data together with modeling studies demonstrate that VDGs undergo hydrogen bond formations with CDR domains and can interfere with antigen binding. Our results also show that ACPAs display an open-ended binding groove and interact specifically with the modified (citrullinated) residue and, to a minor extent, with backbone structures surrounding the modification. This might explain the overall low affinity of ACPA and indicates that already marginal disturbances, by, e.g., carbohydrates, can interrupt binding.

One limitation of our study is that NG mAb variants, used for the binding assays, were generated by mutating N-linked glycan sites back into the predicted germline sequence. This prediction is based on the highest identity with the respective germline sequence but might cause altered antibody functions. However, the crystal structures of, e.g., 7E4_{Fab} showed no structural differences in CDR conformations when expressed with or without VDGs indicating no potential impact of the germline backmutation on antigen-binding ability. In line with the crystallographic results, our ELISA data illustrate that VDG of autoantibodies in RA can diminish binding to several citrullinated peptides and proteins. The interactions between VDGs and the binding pockets can be more easily disrupted by high-affinity antigens, whereas low-affinity antigens are more strongly affected by the masking carbohydrates. We assessed the impact of VDG on antigen binding not only with germline reverted variants, but also confirmed them with neuraminidase treated mAbs harboring glycan traits without the terminal sialic acids. Furthermore, the results obtained for the mAbs 7E4 and 3F3 were in line with the binding data of the variable domain glycosylated versus non variable domain glycosylated mIgG BCRs 7E4 and 3F3 expressed on human Ramos B cells.

Although BCR surface expression levels and glycan compositions might differ from the in vivo situation, we show that the Ramos model B cell lines are able to express disialylated and bisected VDG structures, similar to glycan traits observed on secreted autoantibodies from patients with RA. Despite the limitation of testing only two recombinant BCRs, our data provide the first and consistent experimental evidence that VDGs are able to boost BCR signaling, as evidenced by an increase in Syk phosphorylation and calcium release, which presumably provides an advantage to these autoreactive B cells. Enhanced variable domain glycosylation is also thought to provide a survival advantage in follicular lymphoma B cells,

although this has, so far, not been investigated experimentally^{35,36}. A limitation of our study is that we could not confirm our BCR signaling results with citrullinated protein-reactive B cells directly obtained from patients as these cells represent a rare population in peripheral blood of patients with RA (approximately 0.05% of CD19+ B cells). Moreover, at present, it is not feasible to separate these citrullinated protein-reactive B cells in subsets of cells that do or do not express VDGs.

Currently, it is unclear how VDGs affect BCR triggering and thereby set the threshold for activation. It has been suggested that sialylated VDGs interact with sialic acid-binding lectins, such as CD22³⁷, potentially leading to an altered co localization of the IgG BCR and the Siglec in a resting or activated state. Our CD22 KO data show however, no impact of CD22 on the VDG-mediated effects on BCR downmodulation and signaling. Furthermore, interactions with other Siglecs or (soluble secreted) lectins, such as galectin 9, may be involved in altered signaling, similar to the role of galectin 9 described in IgM BCR signaling³⁸. Moreover, VDG might alter the molecular organization of B-cell surface structures by forming distinct clusters that are absent on B cells expressing BCRs without VDGs. A diverse BCR organization on B cells expressing variable domain glycosylated versus non variable domain glycosylated BCRs could explain the significant differences in B-cell activation after BCR cross-linking as could differences in BCR internalization, degradation, and modulation³⁹. The presence of VDGs modulates the dynamics of the BCR surface expression after antigenic stimulation. We found a decreased BCR downmodulation and uptake after antigen exposure for variable domain glycosylated BCRs compared to NG BCRs. Thus, BCRs containing N-linked glycans show a decreased ability to be downmodulated from the cell surface and are consequently retained longer on the B-cell surface after triggering with antigen. The prolonged surface expression might modulate BCR signaling strength and duration as observed by our B-cell activation studies similar to previous studies describing increased BCR signaling after inhibition of BCR uptake pathways⁴⁰. Further studies are needed to identify whether signal attenuation and BCR internalization are directly linked and, if so, how VDG affects BCR uptake. In this respect, it will be important to delineate the temporal dynamics and spatial organization of variable domain glycosylated mIgG BCRs at the nanoscale level also in relation to its association with lipid rafts, the actin cytoskeleton, and clathrin-coated pits.

Together, we show that the presence of N-linked glycans on the variable domain affects fundamental mechanisms involved in the functionality of B cells (antigen binding, BCR signaling, and downmodulation) and thus might critically determine the outcome of the B-cell responses. In this respect, the abundance of VDG on the hallmarking autoantibody response in a prominent human autoimmune disease is noteworthy. Thus, we provide experimental evidence for the selective and abundant presence of VDG on autoreactive B cells in RA that likely conveys a signaling advantage, potentially explaining the outgrowth of these B cells and the increase of autoantibody levels towards disease-onset. Our findings are highly relevant for a better

understanding of B-cell driven autoimmune diseases as they provide a rationale on how the acquisition of VDGs might contribute to the escape of critical immune checkpoints in humans and thus the breach of B-cell tolerance.

Materials and Methods

Blood samples from patients diagnosed with RA - Peripheral blood samples from anti-citrullinated protein (auto)antibody-positive patients with RA visiting the outpatient clinic of the Rheumatology Department at the Leiden University Medical Center (LUMC) were included in this study. All patients fulfilled the EULAR/ACR 2010 criteria for the classification of RA⁴¹. None of the patients were previously treated with B cell-depletion therapies. Blood samples were taken upon obtaining written informed consent before inclusion and with approval from the local ethics committee of the LUMC, The Netherlands.

Recombinant monoclonal (auto)antibody production - Monoclonal (auto)antibodies were generated on the basis of full-length BCR sequences from APCA⁺ patients with RA^{23,24}. CCP2-strep. and CArgP2-strep. tetramers were used to isolate autoreactive B cells as described previously²⁷. Single sorted B cells were cultured on irradiated CD40L cells and a cytokine mixture in IMDM (Gibco) medium for 10 to 12 days. RNA isolation, complementary DNA (cDNA) synthesis, ARTISAN polymerase chain reaction (PCR), and BCR sequencing were performed as described earlier⁴². The 7E4 sequence was provided by T.R., Sanquin, The Netherlands²⁴. For the generation of NG variants, the N-linked glycosylation sites (N-X-S/T, X ≠ P) were specifically back-mutated into the germline sequence (based on IMGT) at the respective position (Table 1). WT sequences, including the N-glycan sites, and NG sequences were codon-optimized and the HC/LC variable genes together with 5'-BamHI and 3'-XhoI restriction sites, the Kozak sequence, and the IGHV1-18*01 leader sequence ordered from GeneArt (Life Technologies). The constructs were ligated into a pcDNA3.1 (+) expression vector (Invitrogen) carrying the IGHG1 or the IGLC3/IGKC constant regions (UniProt), respectively, flanking the 3'-XhoI site. The recombinant mAbs were produced in Freestyle™ 293-F cells (Gibco) as previously stated²³. Glycoengineering was performed by adding D-galactose substrate to the medium before transfection (Sigma Aldrich, G0750-5G). Furthermore, to generate complex-type N-glycans on the antibody variable domains, the recombinant IgGs were co-expressed with 1% β -1,4-N-acetylglucosaminyltransferase III (GnTIII), 2.5% α 2,6-sialyltransferase 1 (ST6galT) and 1% β -1,4-galactosyltransferase 1 (B4GalT1). The supernatants were harvested 5 to 6 days after transfection.

IgG purification - IgG1 antibodies were purified using a 1 ml HiTrap Protein G HP affinity column (GE Healthcare) followed by a direct buffer exchange using a 53 ml HiPrep™ 26/10 Desalting column (GE Healthcare) according to the manufacturer's instructions. The recombinant mAbs were concentrated with Amicon Ultra-15 50K filter devices (Merck) to a final concentration of 1 mg/ml and used for further experiments.

Monoclonal antibody variable domain glycosylation analysis - Human monoclonal (auto) antibodies were analyzed for levels of variable domain glycosylation via SEC, gel electrophoresis, and MALDI-TOF MS analysis. SEC was performed using a Superose6Increase 10/300 GL column (GE Healthcare) according to the manufacturer's instructions. The recombinant proteins were monitored by ultraviolet (UV) absorption at 280 nm. For SDS-PAGE, 1.5 µg of the mAbs was diluted in 4× Laemmli buffer (Bio Rad) with (reduced) or without (non-reduced) 2% β-mercaptoethanol (Sigma Aldrich) and incubated for 5 min at 95 °C. Sample (10 µl) and 3 µl of PageRuler™ Plus Prestained Protein Ladder (Thermo Fisher Scientific) were loaded on 4 to 15% SDS-polyacrylamide gels (Bio Rad). For protein detection, gels were stained with Coomassie Brilliant Blue G-250 Dye (Thermo Fisher Scientific). MS analysis of released N-glycans was performed as previously described⁴³. In brief, the IgG samples (10 µg in 5 µl) were reduced in 10 µl of 2% SDS and incubated with 0.5 U of PNGase F (Roche Diagnostics, Germany), in 10 µl 1:1 5x PBS/4% NP-40, overnight at 37 °C. The total released glycan mixture was subjected to sialic acid stabilization by adding 100 µl ethylation reagent [0.5 M 1-ethyl-3-(3-dimethylaminopropyl) carbodiimide hydrochloride and 0.5 M 1-hydroxybenzotriazole hydrate] and incubating for 1 hour at 37 °C. For glycan purification, the samples were brought to 85% acetonitrile (ACN) (Biosolve, Valkenswaard, The Netherlands) and purified with 15 µl cotton hydrophilic interaction liquid chromatography (HILIC) tips using 85% ACN and 85% ACN+1% trifluoroacetic acid for washing. Released and purified N-glycans were eluted from the HILIC tips using 10 µl MQ. Three microliters of the purified and ethyl-esterified glycans were spotted on a MALDI target (MTP AnchorChip 800/384 TF, Bruker Daltonics) together with 1 µl of super-DHB (5 mg/ml) in 50% ACN and 1 mM NaOH. Spots were dried at room temperature (RT) and analyzed on an UltrafleXtreme (Bruker Daltonics) operated under flexControl 3.3 (Build 108, Bruker Daltonics). A mass spectrum from m/z 1000 to 3000 was recorded, combining 10000 shots in a random walk pattern at 1000 Hz. The instrument was calibrated with a peptide calibration standard (Bruker Daltonics). MS data were analyzed using flexControl 3.3 and glycan peaks above S/N of nine were included into the analysis.

Fab fragment generation, crystallization and structure determination - For Fab fragment preparation, chimeric 3F3 and 1F2 antibodies were produced on the basis of human variable regions and mouse constant (Fc) domains, expressed in Expi393F™ cells (Life Technologies), purified as previously described¹⁵ and dialyzed against PBS. The 3F3 and 1F2 Fab fragments were prepared using the ImmunoPure Fab Preparation Kit (Pierce) following the manufacturer's

instructions. Cleavage was evaluated by SDS-PAGE. Fab fragments were further purified by SEC on a HiLoad 16/600 Superdex 200 column. The peptides cit-vimentin 59-74, cit-CII-C-39, and cit-CII-48 used for co-crystallization are described in previous studies^{5,23}. The crystals used for data collection were grown as follows: For $3F3_{Fab}$:cit-vimentin 59-74, the sitting drop consisted of 1 μ l of $3F3_{Fab}$ (10 mg/ml) mixed with cit-vimentin 59-74 in twofold molar excess in 20 mM tris (pH 7.5), 20 mM NaCl and 0.5 μ l of reservoir solution [0.2 M ammonium chloride (pH 6.3) and 20% (w/v) PEG 3350]. For $1F2_{Fab}$:cit-CII-C-39, the sitting drop consisted of 1 μ l of $1F2_{Fab}$ solution (10 mg/ml) in 20 mM tris (pH 7.4), 20 mM NaCl mixed with cit-CII-C-39 in twofold molar excess and 0.5 μ l of reservoir solution [20% (w/v) PEG 6000, 0.1 M Hepes 7.0 (pH 7.0) and 0.01 M zinc chloride]. For $1F2_{Fab}$, the sitting drop was set up from 1 μ l of $1F2_{Fab}$ (10 mg/ml) in 20 mM tris (pH 7.4), 20 mM NaCl, and 1 μ l of reservoir solution [0.2 M sodium acetate and 20% (w/v) PEG 3350]. For $7E4_{Fab}$:cit-CII-48, the sitting drop consisted of 1 μ l of $7E4_{Fab}$ solution (10 mg/ml) in 20 mM tris (pH 7.4), 20 mM NaCl mixed with cit-CII-C-48 in twofold molar excess and 1 μ l of reservoir solution [20% (w/v) PEG 3350, 0.1 M bis-tris propane (pH 6.5), and 0.2 M potassium thiocyanate]. The complexes were incubated overnight before crystallization. All crystals were cryoprotected by briefly soaking in the corresponding reservoir solution containing 30% (v/v) ethylene glycol or glycerol before flash-freezing in liquid nitrogen. Diffraction data were collected at the beamlines and with the statistics given in table S3. The images were processed using XIA2⁴⁴, and scaled by AIMLESS⁴⁵ from the CCP4 program suite⁴⁶. The structures of unbound Fab fragments or Fab-peptide complexes were solved by molecular replacement using PHASER⁴⁷. Iterative cycles of the manual model building were performed using COOT⁴⁸ and TLS as well as restrained refinement with Phenix or REFMAC5⁴⁹ until R-factors converged. Refinement statistics are given in table S3. About 5% of the reflections were randomly selected and set aside for unbiased cross-validation (calculation of R_{free}). The “Protein Interfaces, Surfaces and Assemblies” service PISA at the European Bioinformatics Institute (www.ebi.ac.uk/pdbe/prot_int/pistart.html)⁵⁰ was used to analyze molecular surfaces. Structure comparisons and RMSD calculations were performed with SSM⁵¹ as implemented in PyMOL or COOT. Figures were prepared with PyMOL. The crystallographic coordinates and structure factors have been deposited in the PDB with the accession codes 6YXK, 6YXM, 6YXN and 6ZJG.

Molecular-dynamics (MD) simulations - The crystal structures of $7E4_{Fab}$, $3F3_{Fab}$ and $1F2_{Fab}$ were used as initial structures for the MD simulation. Quick MD Simulator integrated with a module of Glycan Reader at the CHARMM-GUI website (www.charmm-gui.org) was used for preparing the input files for simulation⁵². The N-glycans were predicted by NetNGlyc1.0 Server (www.cbs.dtu.dk/services/NetNGlyc/)⁵³. For simulation, we adopted the default setting from CHARMM-GUI for preparing the input files. Briefly, the TIP3P model was used for explicit water molecules. A distance of 15 Å between the protein atoms and the cubic system boundary was introduced and 150 mM NaCl was added to the system. The CHARMM36 force field was used for proteins and carbohydrates. All calculations were performed at 300 K. The particle mesh Ewald algorithm

was applied to calculate electrostatic forces. Each system was equilibrated in constant particle number, volume, and temperature condition with restraints using CHARMM36. An additional short period of constant particle number, pressure, and temperature equilibration was also applied without restraints for each system. The simulation was performed in Amber 18⁵⁴. All analyses were performed in Visual Molecular Dynamics⁵⁵.

Protein citrullination and citrullinated peptide synthesis - Vinculin, fibrinogen, myelin basic protein (MBP) and OVA (Sigma Aldrich) protein modification (citrullination) was performed as previously described⁵⁶. Four linear N-terminal biotinylated peptides fibrinogen α 27-42, fibrinogen β 36-52, vimentin 59-74 and enolase 5-20 and two cyclic N-terminal biotinylated peptides CCP1 and CCP2 (patent EP2071335) were synthesized including the native arginine and the altered citrullinated residue(s) at the same positions within the peptide sequence²³. The integrity of the synthesized peptides after purification was examined by ultra-performance liquid chromatography (UPLC) on an Acquity instrument (Waters), and the exact mass was measured via MS on a Microflex instrument (Bruker) and crosschecked with the calculated masses.

Antigen-binding assays - To identify the impact of VDGs on antigen binding, ELISAs were performed as described earlier²³. Briefly, 1 to 10 $\mu\text{g/ml}$ of biotinylated citrulline or arginine containing peptides were coupled to pre-coated streptavidin plates (Microcoat, #65001) for 1 hour at RT. mAbs were added in PBS/1% bovine serum albumin (BSA)/0.05% Tween (PBT) (Sigma Aldrich) and incubated for 1 hour at 37 °C. For protein ELISAs citrullinated or native proteins (10 $\mu\text{g/ml}$) were directly coupled to Nunc Maxisorp plates (Thermo Fisher Scientific) and incubated overnight on ice at 4 °C. Following blocking with PBS/2% BSA for 6 hours, mAbs were added in PBT and incubated overnight on ice at 4 °C. Antibody interactions were detected using a horseradish peroxidase (HRP) conjugated monoclonal mouse anti-human IgG (Fc) C_H2 antibody (Bio Rad, MK1A6) to prevent VDG influences on secondary antibody binding. ELISA readout was performed using ABTS and H₂O₂. For SPR measurements, biotinylated citrullinated-peptides were mounted on a streptavidin iSPR chip (Ssenc BV), and mAb analyte binding was assessed. An SPR imaging system for multiplexing 96 biomolecular interactions (IBISMX96, IBIS Technologies, Enschede, The Netherlands) was used.

Human Ramos B-cell transfectants - Human Ramos B-cell transfectants carrying 7E4 and 3F3 mIgG BCRs were generated as described earlier²³. In brief, HC and LC containing single vector constructs were created with the In-Fusion HD Cloning Kit (Clontech) using the pMIG-IRES-GFP-2AP vector backbone including the IGHG1 transmembrane domain. Variable gene sequences were cloned with and without N-linked glycan sites to generate WT and NG constructs. Inserts were verified by Sanger sequencing performed on Applied Biosystems 96-capillary (ABI3730) systems (LGTC facility, Macrogen). Retroviral transductions were performed as previously described⁵⁷. Briefly, Phoenix-ECO (ATCC CRL-3212TM) cells were transfected with PolyJet DNA

transfection reagent (SignaGen Laboratories). Retrovirus containing supernatants were collected 72 hours after transfection and used for the transduction of MDL-AID (IGHM, IGHD, IGLC and AID KO lymphoma Ramos B cells carrying *slc7a1*. Ramos cell lines were cultured in RPMI1640/GlutaMAX™/10% fetal calf serum (FCS)/10 mM Hepes medium (Thermo Fisher Scientific) with penicillin/streptomycin (100 U/ml; P/S) (Lonza).

Ramos BCR glycan analysis - For BCR glycan analysis, 20 million human Ramos B cells were lysed in PBS+1% Triton- X100 for 60 min at 37 °C, followed by total IgG BCR capturing using CaptureSelect™ FcXL Affinity Matrix (Thermo Fisher Scientific) and an overnight incubation at 4 °C. Laemmli buffer (4×) was added to the IgG BCR/FcXL bead slurry, boiled for 5 min at 95 °C, and loaded on a 4 to 15% SDS gel (Bio Rad). Proteins were detected with Coomassie Brilliant Blue G-250 Dye (Thermo Fisher Scientific). The visualized IgG BCR bands were extracted from the gel, to exclude glycosylated contaminants, and transferred to Eppendorf tubes. The gel pieces were washed first with 25 mM ammonium bicarbonate (ABC), followed by ACN and, for protein reduction, incubated for 30 min at 56 °C in 10 mM dithiothreitol (DTT)/25 mM ABC. After the reduction step, the gel pieces were washed with ACN and, for alkylation, incubated for 30 min at RT in the dark in 55 mM iodoacetamide/25 mM ABC to block reactive cysteine groups. After washing steps with 25 mM ABC and ACN, the gel bands were dried in a centrifugal vacuum concentrator for 5 min. N-linked glycans were released with 30 U of PNGase F (Roche Diagnostics, Germany) in 2%- NP-40/2.5× PBS by an overnight incubation at 37 °C. Released glycans were subsequently labeled with 2-aminobenzoic acid (Sigma Aldrich) and 2-picoline borane (Sigma Aldrich) and purified with 15 µl cotton HILIC tips as described above. Glycans were separated on an Ultimate 3000 UHPLC system (Dionex/ Thermo Fisher Scientific, Breda, The Netherlands) coupled to a MaXis Impact HD quadrupole-TOF mass spectrometer (MaXis HD, Bruker Daltonics, Bremen, Germany) equipped with a CaptiveSpray NanoBooster source (Bruker Daltonics, Bremen, Germany) as previously described⁵⁸. In short, 20% of the released, purified, and labeled glycans were loaded onto a C18 trap column (Acclaim PepMap 100; 100 µm by 2 cm, particle size of 5 µm, pore size 100 Å; Dionex/Thermo Fisher Scientific) and washed for 2 min with 15 µl/min of 0.1% formic acid (FA)/ 1% ACN. Glycans were subsequently separated on a C18 analytical column (Acclaim PepMap 100; 75 µm by 15 cm, particle size of 3 µm, pore size of 100 Å; Dionex/Thermo Fisher Scientific), and elution was performed at a flow rate of 700 nl/min with buffer A [0.1% FA (v/v)] and buffer B [95% ACN/ 0.1% FA (v/v)]. A gradient of 1% to 70% buffer B in 70 min was applied (t = 0 min, B = 1%; t = 5 min, B = 1%; t = 30 min, B = 50%; t = 31 min, B = 70%; t = 35 min, B = 70%; t = 36 min, B = 1%; t = 70 min, B = 1%). The CaptiveSpray NanoBooster was operated with ACN-enriched gas (0.2 bar) and dry gas (3 liters/min) at 180 °C and a capillary voltage of 1150 V. Mass spectra were acquired within a mass range of m/z 550 to 1800. LC-MS data were first examined manually using DataAnalysis (Bruker Daltonics). Data processing, including peak integration, was performed using LaCyTools v1.1.0. Glycans with a S/N above nine, a mass accuracy of +/-20, and an isotopic peak quality of 0.2 were included into the analysis⁵⁹.

Cell surface biotinylating and surface IgG Ramos BCR glycan analysis - Ramos cell surface biotinylating was performed according to the manufacturer's instructions of the Pierce Cell Surface Protein Biotinylating and Isolation Kit (#A44390). In brief, 24 million cells were harvested and biotinylated using Sulfo-NHS-SS-Biotin for 10 min at RT. The label was removed by washing with tris-buffered saline following cell lysis for 30 min on ice. Biotinylated surface proteins were captured using NeutrAvidin™ Agarose and eluted in elution buffer containing 10 mM DTT. Subsequently, 2% SDS was added, and the samples were incubated for 30 min at 60 °C. The denatured, reduced and biotinylated surface proteins were treated with 2 U of Endo H (Roche Diagnostics, Germany) in 50 mM sodium acetate buffer (pH 5.5) or 2 U of PNGase F (Roche Diagnostics, Germany) in 1:1 5XPBS/4% NP-40 overnight at 37 °C. The presence of high-mannose (Endo H treatment) or complex-type (PNGase F treatment) N-glycans on the surface IgG BCRs was identified via western blot analysis as described below.

Assembly of ribonucleoprotein complexes - Assembly of ribonucleoproteins (RNPs) was performed in a similar way as described in the CRISPR genome editing user guide from integrated DNA technologies (IDT). Briefly, pre-annealed CD22 exon 1 specific complexes of CRISPR-targeting RNA (crRNA) and transactivating crRNA (tracrRNA) were designed via IDT. The single guide RNA (sgRNA) Hs.Cas9.CD22.1.AB (sequence: 5'-TGTCATTGAGGTGCACCGGG-3'; position: 35332832; on-target score: 52; off-target score: 76) was diluted to 44 µM in IDTE buffer (IDT). Alt-R S.p. Cas9 Nuclease V3 (IDT) was diluted to 36 µM in resuspension buffer R (IDT). 90 pmol sgRNA was combined with 30 pmol of Cas9 to form the RNP complex.

Ramos cell electroporation with RNP complexes - Two million 3F3 WT and NG mIgG-expressing Ramos B cells were used per transfection reaction and washed with PBS to remove culture medium FCS. Ramos cell pellet was homogenously resuspended with 100 µl of 11 µM RNP and 11 µM Cas9 Electroporation Enhancer (IDT) diluted in resuspension buffer R (Invitrogen). Electrolyte buffer (3 ml; Invitrogen) was added to the transfection tube of the Neon transfection machine (Invitrogen). Cell/RNP mixture was pipetted into the Neon tip and transferred to the transfection tube. Electroporation was performed using the following settings: V = 1350, W = 30 ms and P = 1. Electroporated cells were transferred into a 24-well plate and supplemented with 1 ml of prewarmed medium. Fluorescence activated cell sorting (FACS) or flow cytometry validation experiments were performed after 1 week of culturing using an anti-CD22 allophycocyanin (APC) labeled antibody (BD, #562850) on a BD 4 laser Aria1 FACS or a BD LSRII-flow cytometry instrument, respectively.

Genomic DNA isolation, bulk sequencing and TIDE analysis - Genomic DNA was isolated from 5 million 3F3 WT/NG Ramos B cells with and without CD22 CRISPR Cas9 KO using the Isolate II Genomic DNA Kit (Bioline, BIO-52066) according to the manufacturer's instructions. Isolated genomic DNA (50 ng) was PCR amplified 500 to 1500 base pairs enclosing the designed editing

site using the pre-designed forward and reverse primers (10 μ M) and myTaq mix (Bioline, BIO-25041). PCR gel bands were purified using the PCR Clean-up Gel Extraction Kit (Takara), and 25 to 50 ng/ μ l were prepared for Sanger sequencing performed on an Applied Biosystems 96-capillary (ABI3730) system (LGTC facility, Macrogen). Sequences were analyzed using SnapGene software V5.0.4. The efficiency of the CD22 KO was quantified using TIDE analysis version 3.3.0 (alignment window: 100 to 217, decomposition window: 242 to 481, indel size: 10, and p threshold: 0.001)⁶⁰.

Flow cytometer experiments - Binding of the generated 7E4/ 3F3 WT and NG mIgG and GFP-expressing B-cell lines to citrullinated antigens was analyzed by flow cytometry. Ramos B cells were stained with APC-labeled cit-peptide SA-tetramers (0 to 5 μ g/ml) (CCP2, CCP1, cit-fibrinogen α 27-43, cit-fibrinogen β 38-52 and cit-vimentin 59-74) and 0.5 μ g/ml goat anti-human IgG-Fc phycoerythrin (PE) (#12-4998-82) in staining solution (PBS/0.5%BSA/ 0.02% NaN₃) via incubation for 30 min on ice. Tetramer formation was performed as previously described²⁷. Unmodified peptides including arginine residues were measured as negative controls in the same concentration range (0 to 5 μ g/ml) to analyze antigen-specificity.

B-cell activation was measured via calcium release of the generated B-cell lines after stimulation. Therefore, 1 million mIgG and GFP-expressing B cells were collected and stained with 200 μ l of calcium-indicator loading dye medium, 2 μ M Indo-1 AM (#ab142778) and 0.05% pluronic acid (#P6866) in 1 ml of stimulation medium (RPMI1640/100 U/ml P/S/GlutaMAX™/10 mM Hepes/2%FCS), for 35 min at 37 °C in the dark. After washing with stimulation medium only, B cells were incubated with 500 μ l stimulation medium plus 2 mM calcium and incubated on ice, in the dark until usage. Fifteen min before the analysis, B cells were prewarmed in a water bath at 37 °C to decrease baseline activation upon measurement. The analysis was performed on a BD LSRII-flow cytometry or a Cytex Aurora 5L instrument including a UV laser and acquiring 500 cells/s at a high speed. After 2 min of baseline measurement, 100 μ l of stimulus [CCP2/CArgP2 (5 μ g/ml) or anti-human IgG F(ab)'₂ (80 μ g/ml)] was added to the samples and mixed adequately, and the measurement continued for another 5 min until the signal reached almost baseline again. The calcium flux was measured as the ratio of calcium-bound Indo-1 to unbound Indo-1. MDL-AID KO B cells, without an endogenous BCR, were used as negative controls in all experiments. The maximal calcium flux (peak-baseline signal) and its speed (slope of the curve) were analyzed.

BCR signaling was analyzed via the intracellular expression of pSyk after activation. Therefore, 1 million mIgG and GFP-expressing B cells were collected and stimulated with CCP2-strep. tetramer (5 μ g/ml) or 15 μ g of anti-human IgG F(ab)'₂ for 0, 2, 5, 10, 15, or 20 min at 37 °C in stimulation medium (RPMI/100 U/ml P/S/GlutaMAX™/10 mM Hepes/1% FCS). Afterward, cells were fixed (BioLegend Fixation Buffer, #420801) and permeabilized (True-Phos™ Perm Buffer, #425401). After washing, the intracellular expression of phosphorylated Syk was analyzed with a mouse anti-human pSyk(Y348)-PE mAb (#moch1ct, eBioscience™) diluted 1:20 in staining

solution. The rate of pSyk expression in Ramos cells was calculated as the percentage of pSyk(Y348)⁺ cells or the pSyk median fluorescence intensity (MFI) ratio between stimulated and unstimulated cells. Gating was based on the MDL-AID KO control cell line stimulated with CCP2 or anti-IgG F(ab)² respectively.

To assess BCR modulation, 0.2 million mIgG and GFP-expressing Ramos B cells were first incubated for 30 min on ice followed by a 15 min stimulation at 4 °C with either control PBS or CCP2-/CAArgP2-strep. tetramers (5 µg/ml) in PBS/2% FCS. The stimulated B cells were then incubated for 0, 5, 15 or 30 min at 37 °C to allow BCR downmodulation. The remaining surface BCRs were stained with a AF647 NHS (*N*-hydroxysuccinimide) ester (Thermo Fisher Scientific, #A20006) labeled Fab goat anti-human IgG (Jackson ImmunoResearch, #109007003) diluted 1:2000 in staining solution. Stained cells were analyzed on a BD LSR-II flow cytometry instrument. Data were analyzed with FlowJo_V10.

Western blot analysis - CD22, Syk, pCD22, pSyk and glyceraldehyde-3-phosphate dehydrogenase (GAPDH)-expression of Ramos cells before and after stimulation were analyzed via western blot analyses. Therefore, 4 million Ramos cells were lysed in 20 µl NP40 cell lysis buffer (Thermo Fisher Scientific) including 1× Protease/ Phosphatase Inhibitor Cocktail (100×; Cell Signaling Technology) via incubation for 30 min on ice. Before cell lysis, cells were either stimulated with 20 µg/ml CCP2 or anti-human IgG F(ab)² or incubated with stimulation medium (RPMI1640/100 U/ml P/S/GlutaMAX™/10 mM Hepes/2% FCS) only for 5 min at 37 °C. The supernatant of the lysed cells was stored at 20 °C for further usage. Lysates (10 µl; 1 million cells) were subjected to 4 to 15% SDS-polyacrylamide gels (Bio Rad) together with 4× Laemmli buffer (Bio Rad) after incubation for 5 min at 95 °C. Subsequently, immunoblotting was performed on a nitrocellulose membrane (Bio Rad). Blots were incubated in PTE (3% skim milk powder/PBS/0.05% Tween) for 2 hours at RT. Following washing with PBS/0.05% Tween (PT), the blots were incubated at 4 °C overnight with 1:20,000 mouse anti-human GAPDH (#MAD374, Bio Rad) or 1:3000 rabbit anti-human β-actin (D6A8, #8457S), 1:15,000 rabbit anti-human CD22 (#ab207727, BioLegend), and 1:300 rabbit anti-human Syk (#2712S, Cell Signaling Technology) or 1:200 rabbit anti-human pCD22 (Y822, #ab32123, BioLegend) and 1:1000 rabbit anti-human pSyk (p-Zap-70, Y319, #2717S, Cell Signaling Technology), respectively diluted in 5 ml of PTE. After washing with PT, blots were incubated for 1 hour at RT with 5 ml of PTE containing 1:1000 goat anti-rabbit- Ig HRP (#P0448, DAKO) and 1:5000 goat anti-mouse-Ig HRP (#P0447, DAKO) secondary antibodies. Blots were washed, and bound antibodies were visualized using enhanced chemiluminescence (GE Healthcare, RPN2109). The readout was performed on a Bio Rad Chemidoc Touch Imaging system. For biotinylated surface IgG BCR detection after Endo H or PNGase F treatment, samples were mixed with 4× Laemmli buffer, incubated for 5 min at 95 °C and loaded on 4 to 15% gels (Bio Rad). Western blot analysis was performed as described above using a goat anti-human IgG (#31410, Invitrogen) HRP labeled antibody diluted 1:1000 in PTE.

Spinning disk confocal microscopy - BCR modulation and antigen internalization were identified using spinning disk confocal microscopy. One million Ramos B cells were incubated for 30 min on ice followed by a 10 min stimulation at 4 °C with 5 ug/ml CCP2-strep. AF568 tetramers in PBS/2% FCS. The stimulated B cells were then incubated for 0, 5, or 15 min at 37 °C to allow BCR downmodulation and antigen internalization. After fixation with 2% paraformaldehyde (PFA), the cells were stained for 15 min with an AF647 NHS ester (Thermo Fisher Scientific, #A20006) labeled Fab goat anti-human IgG (Jackson ImmunoResearch, #109007003) antibody diluted 1:2000 in staining solution to detect the remaining BCRs on the fixed cell surface. After washing, the cells were settled to poly D-lysine precoated coverslips (Ibidi) for at least 40 min. Imaging was performed on an Andor Dragonfly 500 spinning disk confocal microscope at the Light and Electron Microscopy Facility of the LUMC, The Netherlands. Z-stacks of 20 slices per cell were acquired for three laser lines (488, 561, and 637), and the mean signal intensity on the B-cell membrane or inside the cell was assessed using Fiji/Image J.

Statistical analysis - Antigen-binding data of mAbs were analyzed using two-tailed unpaired t-tests assuming that all samples show the same scatter (SD). LC-MS mIgG BCR glycan data were analyzed using multiple t-tests assuming that all samples show the same SD and corrected for multiple comparisons using the Bonferroni-Dunn method. Paired two-tailed t-tests were performed for B-cell activation and BCR downmodulation assays with a number of 3 to 5 pairs. Ordinary one-way analysis of variance (ANOVA) tests were performed for parametric non-matched confocal microscopy data. Significant differences are denoted as follows: not significant (ns; $p > 0.05$), * ($p < 0.05$), ** ($p < 0.01$), *** ($p < 0.001$) or **** ($p < 0.0001$).

Acknowledgments

We thank J.-W. Drijfhout (LUMC, Leiden, The Netherlands) for providing the citrullinated peptides, J. Eken (LUMC, Leiden, The Netherlands) for expert assistance with the CRISPR-Cas9 KOs, the Protein Science Facility at Karolinska Institute for providing crystallization infrastructure, and the whole group of Affinity Proteomics at SciLifeLab Stockholm for efforts, and we thankfully acknowledge access to beamlines at the Diamond Light Source and MAX IV Laboratory as well as the staff for assistance with crystal testing and data collection. Furthermore, we thank the LUMC Flow cytometry Core Facility (FCF) and the Light and Electron Microscopy Facility for help with cell sorting and imaging.

Funding

This work was supported by the ReumaNederland 17-1-402 (to R.E.M.T.), the IMI-funded project RTCure 777357 (to T.W.J.H.), ZonMw TOP 91214031 (to R.E.M.T.), Target-to-B LSHM18055-SGF (to R.E.M.T.), NWO-ZonMW clinical fellowship 90714509 (to H.U.S.), NWO-ZonMW VENI grant 91617107 (to H.U.S.), ZonMW Enabling Technology Hotels grant 435002030 (to H.U.S.), Dutch Arthritis Foundation 15-2-402 and 18-1-205 (to H.U.S.), Excellence Initiative of the German Federal and State Governments EXC 294 (to M.R.), DFG through TRR130-P02 (to M.R.), RO1 grant A031503 (to M.R.), Knut and Alice Wallenberg Foundation 2019.0059 (to R.H.), The Swedish Research Council 2017-06014 (to R.H.), National Science Foundation of China, 1R15AI154248-01A1 (KR-K210) (to R.H.), and European Community's Seventh Framework Programme (FP7/2007-2013) under BioStruct-X grant agreement no. 283570 (to R.H.).

Author contributions

All authors were involved in drafting the article or revising it critically for important intellectual content, and all authors approved the final version to be published. Conceptualization: T.K., C.G., L.H., T.W.J.H., H.U.S., M.R., R.H., and R.E.M.T. Methodology: T.K., C.G., L.M.V., L.H., L.M.S., M.C., G.J.M.P., and M.W. Software: C.G., L.M.V., and L.H. Investigation: T.K., C.G., L.H., J.C.K., L.M.S., Y.H., K.A.J.v.S., R.D.V., A.S.B.K., S.R., G.S.-R., and B.X. Visualization: T.K., C.G., and L.H. Supervision: M.C., R.H., T.W.J.H., H.U.S., and R.E.M.T. Writing—original draft: T.K. and R.E.M.T. Writing—review and editing: C.G., L.D., J.C.K., L.M.S., M.C., Y.H., K.A.J.v.S., R.D.V., A.S.B.K., S.R., G.S.-R., L.M.V., L.H., B.X., G.J.M.P., M.W., T.R., T.W.J.H., H.U.S., M.R., and R.H.

Conflict of interest

C.G., B.X., T.R., and R.H. are named as coinventors of a patent application (PCT/EP2018/082236) regarding the arthritis-protective effects of ACPA. H.U.S., T.W.J.H., and R.E.M.T. are mentioned as inventors on a patent on ACPA IgG V-domain glycosylation. G.J.M.P. is mentioned as inventor on the CCP2-related patent EP2071335. The other authors declare that they have no competing interests.

Data and materials availability

We confirm that the data supporting the findings of this study are available within the article and/or the Supplementary Materials. The CCP2 peptide can be provided by G.J.M.P. (Radboud University, The Netherlands) pending scientific review and a completed material transfer agreement. Requests for the CCP2 peptide should be submitted to G.Pruijn@ncmls.ru.nl. The 7E4 sequence and antibodies can be provided by R.H. (Karolinska Institutet, Sweden) or T.R. (Sanquin Research, The Netherlands) under the protection of a completed material transfer agreement. Requests for the 7E4 sequence should be submitted to Rikard.Holmdahl@ki.se.

References

- 1 Barnas, J. L., Looney, R. J. and Anolik, J. H., B cell targeted therapies in autoimmune disease. *Curr Opin Immunol* 2019. 61: 92-99.
- 2 Hampe, C. S., B Cell in Autoimmune Diseases. *Scientifica (Cairo)* 2012. 2012.
- 3 Erikson, J., Radic, M. Z., Camper, S. A., Hardy, R. R., Carmack, C. and Weigert, M., Expression of anti-DNA immunoglobulin transgenes in non-autoimmune mice. *Nature* 1991. 349: 331-334.
- 4 Goodnow, C. C., Crosbie, J., Adelstein, S., Lavoie, T. B., Smith-Gill, S. J., Brink, R. A., et al., Altered immunoglobulin expression and functional silencing of self-reactive B lymphocytes in transgenic mice. *Nature* 1988. 334: 676-682.
- 5 Hartley, S. B., Crosbie, J., Brink, R., Kantor, A. B., Basten, A. and Goodnow, C. C., Elimination from peripheral lymphoid tissues of self-reactive B lymphocytes recognizing membrane-bound antigens. *Nature* 1991. 353: 765-769.
- 6 Pelanda, R., Schwers, S., Sonoda, E., Torres, R. M., Nemazee, D. and Rajewsky, K., Receptor editing in a transgenic mouse model: site, efficiency, and role in B cell tolerance and antibody diversification. *Immunity* 1997. 7: 765-775.
- 7 Tiegs, S. L., Russell, D. M. and Nemazee, D., Receptor editing in self-reactive bone marrow B cells. *J Exp Med* 1993. 177: 1009-1020.
- 8 Wardemann, H., Yurasov, S., Schaefer, A., Young, J. W., Meffre, E. and Nussenzweig, M. C., Predominant autoantibody production by early human B cell precursors. *Science* 2003. 301: 1374-1377.
- 9 Diaz, M. and Klinman, N. R., Relative roles of somatic and Darwinian evolution in shaping the antibody response. *Immunol Res* 2000. 21: 89-102.
- 10 Burnett, D. L., Langley, D. B., Schofield, P., Hermes, J. R., Chan, T. D., Jackson, J., et al., Germinal center antibody mutation trajectories are determined by rapid self/foreign discrimination. *Science* 2018. 360: 223-226.
- 11 Sabouri, Z., Schofield, P., Horikawa, K., Spierings, E., Kipling, D., Randall, K. L., et al., Redemption of autoantibodies on anergic B cells by variable-region glycosylation and mutation away from self-reactivity. *Proc Natl Acad Sci U S A* 2014. 111: E2567-2575.
- 12 Bretscher, P. and Cohn, M., A theory of self-nonself discrimination. *Science* 1970. 169: 1042-1049.
- 13 Reijm, S., Kissel, T. and Toes, R. E. M., Checkpoints controlling the induction of B cell mediated autoimmunity in human autoimmune diseases. *Eur J Immunol* 2020. 50: 1885-1894.
- 14 Schellekens, G. A., de Jong, B. A., van den Hoogen, F. H., van de Putte, L. B. and van Venrooij, W. J., Citrulline is an essential constituent of antigenic determinants recognized by rheumatoid arthritis-specific autoantibodies. *J Clin Invest* 1998. 101: 273-281.
- 15 Ge, C., Xu, B., Liang, B., Lonnblom, E., Lundstrom, S. L., Zubarev, R. A., et al., Structural Basis of Cross-Reactivity of Anti-Citrullinated Protein Antibodies. *Arthritis Rheumatol* 2019. 71: 210-221.
- 16 Hafkenscheid, L., Bondt, A., Scherer, H. U., Huizinga, T. W., Wuhler, M., Toes, R. E., et al., Structural Analysis of Variable Domain Glycosylation of Anti-Citrullinated Protein Antibodies in Rheumatoid Arthritis Reveals the Presence of Highly Sialylated Glycans. *Mol Cell Proteomics* 2017. 16: 278-287.
- 17 Rombouts, Y., Willemze, A., van Beers, J. J., Shi, J., Kerkman, P. F., van Toorn, L., et al., Extensive glycosylation of ACPA-IgG variable domains modulates binding to citrullinated antigens in rheumatoid arthritis. *Ann Rheum Dis* 2016. 75: 578-585.
- 18 Vergroesen, R. D., Slot, L. M., Hafkenscheid, L., Koning, M. T., van der Voort, E. I. H., Grooff, C. A., et al., B-cell receptor sequencing of anti-citrullinated protein antibody (ACPA) IgG-expressing B cells indicates a selective advantage for the introduction of N-glycosylation sites during somatic hypermutation. *Ann Rheum Dis* 2018. 77: 956-958.

- 19 Hafkenschied, L., de Moel, E., Smolik, I., Tanner, S., Meng, X., Jansen, B. C., et al., N-Linked Glycans in the Variable Domain of IgG Anti-Citrullinated Protein Antibodies Predict the Development of Rheumatoid Arthritis. *Arthritis Rheumatol* 2019. 71: 1626-1633.
- 20 Vletter, E. M., Koning, M. T., Scherer, H. U., Veelken, H. and Toes, R. E. M., A Comparison of Immunoglobulin Variable Region N-Linked Glycosylation in Healthy Donors, Autoimmune Disease and Lymphoma. *Front Immunol* 2020. 11: 241.
- 21 Biermann, M. H., Griffante, G., Podolska, M. J., Boeltz, S., Sturmer, J., Munoz, L. E., et al., Sweet but dangerous - the role of immunoglobulin G glycosylation in autoimmunity and inflammation. *Lupus* 2016. 25: 934-942.
- 22 van de Bovenkamp, F. S., Derksen, N. I. L., Ooijevaar-de Heer, P., van Schie, K. A., Kruithof, S., Berkowska, M. A., et al., Adaptive antibody diversification through N-linked glycosylation of the immunoglobulin variable region. *Proc Natl Acad Sci U S A* 2018. 115: 1901-1906.
- 23 Kissel, T., Reijm, S., Slot, L. M., Cavallari, M., Wortel, C. M., Vergroesen, R. D., et al., Antibodies and B cells recognising citrullinated proteins display a broad cross-reactivity towards other post-translational modifications. *Ann Rheum Dis* 2020. 79: 472-480.
- 24 van de Stadt, L. A., van Schouwenburg, P. A., Bryde, S., Kruithof, S., van Schaardenburg, D., Hamann, D., et al., Monoclonal anti-citrullinated protein antibodies selected on citrullinated fibrinogen have distinct targets with different cross-reactivity patterns. *Rheumatology (Oxford)* 2013. 52: 631-635.
- 25 Dekkers, G., Plomp, R., Koeleman, C. A., Visser, R., von Horsten, H. H., Sandig, V., et al., Multi-level glyco-engineering techniques to generate IgG with defined Fc-glycans. *Sci Rep* 2016. 6: 36964.
- 26 Chiodin, G., Allen, J. D., Bryant, D., Rock, P., Martino, E. A., Valle-Argos, B., et al., Insertion of atypical glycans into the tumor antigen-binding site identifies DLBCLs with distinct origin and behavior. *Blood* 2021.
- 27 Kerkman, P. F., Fabre, E., van der Voort, E. I., Zaldumbide, A., Rombouts, Y., Rispens, T., et al., Identification and characterisation of citrullinated antigen-specific B cells in peripheral blood of patients with rheumatoid arthritis. *Ann Rheum Dis* 2016. 75: 1170-1176.
- 28 Klasener, K., Maity, P. C., Hobeika, E., Yang, J. and Reth, M., B cell activation involves nanoscale receptor reorganizations and inside-out signaling by Syk. *Elife* 2014. 3: e02069.
- 29 Suwannalai, P., van de Stadt, L. A., Radner, H., Steiner, G., El-Gabalawy, H. S., Zijde, C. M., et al., Avidity maturation of anti-citrullinated protein antibodies in rheumatoid arthritis. *Arthritis Rheum* 2012. 64: 1323-1328.
- 30 Volkov, M., van Schie, K. A. and van der Woude, D., Autoantibodies and B Cells: The ABC of rheumatoid arthritis pathophysiology. *Immunol Rev* 2020. 294: 148-163.
- 31 Kissel, T., van Schie, K. A., Hafkenschied, L., Lundquist, A., Kokkonen, H., Wuhler, M., et al., On the presence of HLA-SE alleles and ACPA-IgG variable domain glycosylation in the phase preceding the development of rheumatoid arthritis. *Ann Rheum Dis* 2019. 78: 1616-1620.
- 32 Kissel, T., van Wesemael, T. J., Lundquist, A., Kokkonen, H., Kawakami, A., Tamai, M., et al., Genetic predisposition (HLA-SE) is associated with ACPA-IgG variable domain glycosylation in the predisease phase of RA. *Ann Rheum Dis* 2021.
- 33 Chan, T. D., Wood, K., Hermes, J. R., Butt, D., Jolly, C. J., Basten, A., et al., Elimination of germinal-center-derived self-reactive B cells is governed by the location and concentration of self-antigen. *Immunity* 2012. 37: 893-904.
- 34 Schneider, D., Duhren-von Minden, M., Alkhatib, A., Setz, C., van Bergen, C. A., Benkisser-Petersen, M., et al., Lectins from opportunistic bacteria interact with acquired variable-region glycans of surface immunoglobulin in follicular lymphoma. *Blood* 2015. 125: 3287-3296.
- 35 Zhu, D., McCarthy, H., Ottensmeier, C. H., Johnson, P., Hamblin, T. J. and Stevenson, F. K., Acquisition of potential N-glycosylation sites in the immunoglobulin variable region by somatic mutation is a distinctive feature of follicular lymphoma. *Blood* 2002. 99: 2562-2568.

- 36 Radcliffe, C. M., Arnold, J. N., Suter, D. M., Wormald, M. R., Harvey, D. J., Royle, L., et al., Human follicular lymphoma cells contain oligomannose glycans in the antigen-binding site of the B-cell receptor. *J Biol Chem* 2007. 282: 7405-7415.
- 37 Peaker, C. J. and Neuberger, M. S., Association of CD22 with the B cell antigen receptor. *Eur J Immunol* 1993. 23: 1358-1363.
- 38 Cao, A., Alluqmani, N., Buhari, F. H. M., Wasim, L., Smith, L. K., Quaile, A. T., et al., Galectin-9 binds IgM-BCR to regulate B cell signaling. *Nat Commun* 2018. 9: 3288.
- 39 Hou, P., Araujo, E., Zhao, T., Zhang, M., Massenburg, D., Veselits, M., et al., B cell antigen receptor signaling and internalization are mutually exclusive events. *PLoS Biol* 2006. 4: e200.
- 40 Stoddart, A., Jackson, A. P. and Brodsky, F. M., Plasticity of B cell receptor internalization upon conditional depletion of clathrin. *Mol Biol Cell* 2005. 16: 2339-2348.
- 41 Aletaha, D., Neogi, T., Silman, A. J., Funovits, J., Felson, D. T., Bingham, C. O., 3rd, et al., 2010 rheumatoid arthritis classification criteria: an American College of Rheumatology/European League Against Rheumatism collaborative initiative. *Ann Rheum Dis* 2010. 69: 1580-1588.
- 42 Koning, M. T., Kielbasa, S. M., Boersma, V., Buermans, H. P. J., van der Zeeuw, S. A. J., van Bergen, C. A. M., et al., ARTISAN PCR: rapid identification of full-length immunoglobulin rearrangements without primer binding bias. *Br J Haematol* 2017. 178: 983-986.
- 43 Reiding, K. R., Lonardi, E., Hipgrave Ederveen, A. L. and Wührer, M., Ethyl Esterification for MALDI-MS Analysis of Protein Glycosylation. *Methods Mol Biol* 2016. 1394: 151-162.
- 44 Sauter, N. K., Grosse-Kunstleve, R. W. and Adams, P. D., Robust indexing for automatic data collection. *J Appl Crystallogr* 2004. 37: 399-409.
- 45 Evans, P. R. and Murshudov, G. N., How good are my data and what is the resolution? *Acta Crystallogr D Biol Crystallogr* 2013. 69: 1204-1214.
- 46 Collaborative Computational Project, N., The CCP4 suite: programs for protein crystallography. *Acta Crystallogr D Biol Crystallogr* 1994. 50: 760-763.
- 47 McCoy, A. J., Grosse-Kunstleve, R. W., Adams, P. D., Winn, M. D., Storoni, L. C. and Read, R. J., Phaser crystallographic software. *J Appl Crystallogr* 2007. 40: 658-674.
- 48 Emsley, P., Lohkamp, B., Scott, W. G. and Cowtan, K., Features and development of Coot. *Acta Crystallogr D Biol Crystallogr* 2010. 66: 486-501.
- 49 Murshudov, G. N., Vagin, A. A. and Dodson, E. J., Refinement of macromolecular structures by the maximum-likelihood method. *Acta Crystallogr D Biol Crystallogr* 1997. 53: 240-255.
- 50 Krissinel, E. and Henrick, K., Inference of macromolecular assemblies from crystalline state. *J Mol Biol* 2007. 372: 774-797.
- 51 Krissinel, E. and Henrick, K., Secondary-structure matching (SSM), a new tool for fast protein structure alignment in three dimensions. *Acta Crystallogr D Biol Crystallogr* 2004. 60: 2256-2268.
- 52 Jo, S., Kim, T., Iyer, V. G. and Im, W., CHARMM-GUI: a web-based graphical user interface for CHARMM. *J Comput Chem* 2008. 29: 1859-1865.
- 53 Steentoft, C., Vakhrushev, S. Y., Joshi, H. J., Kong, Y., Vester-Christensen, M. B., Schjoldager, K. T., et al., Precision mapping of the human O-GalNAc glycoproteome through SimpleCell technology. *EMBO J* 2013. 32: 1478-1488.
- 54 Case, D. A., Cheatham, T. E., 3rd, Darden, T., Gohlke, H., Luo, R., Merz, K. M., Jr., et al., The Amber biomolecular simulation programs. *J Comput Chem* 2005. 26: 1668-1688.
- 55 Humphrey, W., Dalke, A. and Schulten, K., VMD: visual molecular dynamics. *J Mol Graph* 1996. 14: 33-38, 27-38.
- 56 Kampstra, A. S. B., Dekkers, J. S., Volkov, M., Dorjee, A. L., Hafkenscheid, L., Kempers, A. C., et al., Different classes of anti-modified protein antibodies are induced on exposure to antigens expressing only one type of modification. *Ann Rheum Dis* 2019. 78: 908-916.

- 57 He, X., Klasener, K., Iype, J. M., Becker, M., Maity, P. C., Cavallari, M., et al., Continuous signaling of CD79b and CD19 is required for the fitness of Burkitt lymphoma B cells. *EMBO J* 2018. 37.
- 58 Plomp, R., de Haan, N., Bondt, A., Murli, J., Dotz, V. and Wuhrer, M., Comparative Glycomics of Immunoglobulin A and G From Saliva and Plasma Reveals Biomarker Potential. *Front Immunol* 2018. 9: 2436.
- 59 Jansen, B. C., Falck, D., de Haan, N., Hipgrave Ederveen, A. L., Razdorov, G., Lauc, G., et al., LaCyTools: A Targeted Liquid Chromatography-Mass Spectrometry Data Processing Package for Relative Quantitation of Glycopeptides. *J Proteome Res* 2016. 15: 2198-2210.
- 60 Brinkman, E. K., Kousholt, A. N., Harmsen, T., Leemans, C., Chen, T., Jonkers, J., et al., Easy quantification of template-directed CRISPR/Cas9 editing. *Nucleic Acids Res* 2018. 46: e58.

Supplemental Tables

Table S1. SPR Kd1 and Kd2 values of monoclonal ACPA IgG with VDGs (WT) and w/o VDGs (NG) calculated based on biphasic curve fits.

Kd1	CCP2	cit-fibrinogen α 27-43	cit-fibrinogen β 36-52
7E4 WT	8.80E-05	nd*	7.14E-05
7E4 WT+neu	2.89E-04	6.10E-04	1.19E-04
7E4 NG	9.36E-05	7.33E-05	nd*
7E4 NG+neu	nd*	7.93E-04	nd*
Kd2	CCP2	cit-fibrinogen α 27-43	cit-fibrinogen β 36-52
7E4 WT	3.74E-05	2.22E-04	nd*
7E4 WT+neu	nd*	1.39E-04	nd*
7E4 NG	1.94E-04	4.36E-05	nd*
7E4 NG+neu	5.39E-05	6.06E-05	nd*

*nd = not-determined, negative Kon values.

Table S2. Equilibrium K_D values of monoclonal ACPA IgG with VDGs (WT) and without VDGs (NG).
Equilibrium K_D and B_{max} values were calculated based on ELISA curves and shown including their standard errors.

peptide	7E4 WT		7E4 WT + neu	
	K _D [M]	B _{max}	K _D [M]	B _{max}
CCP2	1.04E-08 ± 6.56E-10	2.54 ± 0.048	6.78E-09 ± 5.02E-10	2.81 ± 0.051
Cit-fibrinogen α 27-43	6.64E-09 ± 5.67E-10	3.20 ± 0.066	5.26E-09 ± 6.84E-10	3.48 ± 0.097
CCP1	NM*	NM*	NM*	NM*
Cit-vimentin 59-74	NM*	NM*	NM*	NM*
Cit-enolase 5-20	NM*	NM*	NM*	NM*
Cit-fibrinogen β 36-52	1.30E-08 ± 3.67E-10	2.11 ± 0.022	9.24E-09 ± 3.54E-10	2.31 ± 0.029

*NM = not-measurable, ELISA curves not at saturation.

cit-vimentin 59-74	cit-enolase 5-20	Kd1	CCP2
1.78E-05	3.72E-05	2D11 WT	1.21E-04
2.90E-05	5.18E-05	2D11 WT+neu	7.82E-05
4.83E-04	3.99E-03	2D11 NG	5.94E-05
3.96E-05	nd*	2D11 NG+neu	7.53E-05
cit-vimentin 59-74	cit-enolase 5-20	Kd2	CCP2
1.41E-04	3.20E-04	2D11 WT	nd*
nd*	4.60E-03	2D11 WT+neu	5.75E-05
nd*	nd*	2D11 NG	7.96E-05
nd*	nd*	2D11 NG+neu	nd*

7E4 NG		7E4 NG + neu	
K _D [M]	B _{max}	K _D [M]	B _{max}
2.66E-09 ± 4.77E-10	3.25 ± 0.082	2.88E-09 ± 2.29E-10	3.16 ± 0.037
2.83E-09 ± 3.47E-10	3.43 ± 0.062	2.32E-09 ± 3.47E-10	3.29 ± 0.063
7.16E-08 ± 6.38E-09	4.83 ± 0.280	5.82E-08 ± 6.91E-09	4.11 ± 0.298
4.91E-08 ± 9.56E-09	4.44 ± 0.497	4.76E-08 ± 1.03E-08	4.51 ± 0.553
1.73E-07 ± 2.10E-08	5.39 ± 0.453	1.81E-07 ± 1.92E-08	5.54 ± 0.413
5.53E-09 ± 6.03E-11	2.70 ± 0.009	5.12E-09 ± 1.81E-10	2.61 ± 0.028

Table S3. Data collection and refinement statistics. Statistics for the highest-resolution shell are shown in parentheses.

3F3:cit-vimentin 59-74	
Wavelength [Å]	0.91840
Resolution range [Å]	52.28 - 2.0 (2.071 - 2.0)
Space group	P 21 21 21
Unit cell a, b, c [Å]	53.379, 82.094, 135.613
Unit cell a, b, c [Å]	90, 90, 90
Total reflections	325932 (33061)
Unique reflections	40868 (4035)
Multiplicity	8.0 (8.2)
Completeness [%]	99.37 (99.51)
Mean I/sigma [I]	9.93 (2.16)
Wilson B-factor	32.61
R-merge	0.1256 (0.886)
R-meas	0.1344 (0.9457)
R-pim	0.04728 (0.3275)
CC1/2	0.996 (0.682)
CC*	0.999 (0.901)
Reflections used in refinement	40845 (4025)
Reflections used for R-free	2023 (193)
R-work	0.2011
R-free	0.2414
Number of non-hydrogen atoms	3762
macromolecules	3395
ligands	64
solvent	303
Protein residues	447
RMS [bonds]	0.019
RMS [angles]	2.39
Ramachandran favored [%]	97.00
Ramachandran allowed [%]	3.00
Ramachandran outliers [%]	0.00
Number of TLS groups	3

1F2:cit-CII-C-39	1F2	7E4:cit-CII-C-48
0.97622	0.97622	0.91840
36.19 - 2.85 (2.952 - 2.85)	35.01 - 3.05 (3.159 - 3.05)	59.78 - 2.45 (2.538 - 2.45)
P 21 21 21	C 1 2 1	C 2 2 21
53.01, 89.65, 118.68	152.43, 88.8, 88.02	77.183, 151.774, 97.066
90, 90, 90	90, 113.26, 90	90, 90, 90
121917 (11635)	95969 (9446)	195694 (19513)
13784 (1351)	20678 (2032)	21351 (2104)
8.8 (8.5)	4.6 (4.6)	9.2 (9.3)
98.10 (98.69)	99.63 (99.61)	99.96 (99.86)
9.97 (3.66)	9.92 (3.31)	22.47 (4.80)
44.66	77.47	57.62
0.1524 (0.5557)	0.09467 (0.3793)	0.05246 (0.4131)
0.1623 (0.5933)	0.1073 (0.4305)	0.05567 (0.438)
0.05479 (0.2044)	0.04964 (0.2002)	0.01827 (0.1431)
0.992 (0.901)	0.993 (0.938)	0.999 (0.951)
0.998 (0.974)	0.998 (0.984)	1 (0.987)
13532 (1351)	20638 (2032)	21348 (2104)
638 (74)	1054 (102)	1129 (106)
0.2117	0.2349	0.2384
0.2610	0.2663	0.2746
3372	6444	3363
3275	6392	3276
64	52	39
33		48
434	848	440
0.013	0.012	0.013
1.77	1.84	1.89
95.01	96.12	96.69
4.75	3.03	3.31
0.24	0.85	0.00
3	4	3

Table S4. H-bond interaction details between the ACPA 7E4 HC and LC Fab fragments and the respective N-linked glycan. Shown are the H-bond donor and acceptor pairs (three letter code of the respective amino acids and monosaccharides) and the occupancy of the interaction in percentage. GlcNAc: *N*-acetyl glucosamine, Neu5Ac: *N*-acetylneuraminic acid, Fuc: fucose, Gal: galactose, Man: mannose.

7E4 HC			7E4 LC		
donor	acceptor	oc. [%]	donor	acceptor	oc. [%]
Asn 29	GlcNAc 221	5.85	Asn 16	GlcNAc 214	10.76
GlcNAc 221	Pro 73	1.15	Fuc 226	Gly 14	8.84
Ser 74	GlcNAc 222	0.94	Fuc 226	Asn 16	2.44
GlcNAc 222	Ser 74	0.84	Fuc 226	Gln 15	1.56
Ser 74	GlcNAc 222	0.49	Gln 15	Fuc 226	1.36
Fuc 233	Asn 29	0.49	Arg 52	Neu5Ac 220	1.04
His 53	Fuc 233	0.36	Man 217	Ala 60	0.9
Fuc 233	His 53	0.35	Arg 52	Neu5Ac 220	0.88
Lys 75	GlcNAc 225	0.35	Neu5Ac 220	Asn 66	0.73
GlcNAc 222	Ser 74	0.35	Neu5Ac 220	Ser 65	0.55
Lys 75	GlcNAc 232	0.32	GlcNAc 214	Asp 74	0.42
Met 28	GlcNAc 221	0.29	Arg 52	GlcNAc 218	0.37
Lys 75	GlcNAc 229	0.22	Arg 54	Man 217	0.35
Asn 76	GlcNAc 221	0.22	Gly 77	Fuc 226	0.31
Asn 76	GlcNAc 222	0.19	Man 217	Ser 63	0.28
GlcNAc 222	Asn 76	0.14	Ser 63	Man 217	0.28
Gal 226	Thr 22	0.14	Arg 54	Neu5Ac 220	0.26
Gln 77	Gal 226	0.11	Neu5Ac 220	Ser 63	0.25
Thr 22	Gal 226	0.1	Neu5Ac 220	Ser 63	0.21
Ser 20	Gal 226	0.04	Neu5Ac 220	Ile 58	0.21
GlcNAc 232	Lys 75	0.04	Neu5Ac 220	Gly 57	0.17
GlcNAc 232	Ser 74	0.04	Arg 54	Gal 219	0.16
Gal 226	Ser 74	0.02	Ala 60	GlcNAc 218	0.11
Gal 226	Lys 75	0.02	Ser 56	Neu5Ac 220	0.08
Ser 74	GlcNAc 221	0.01	GlcNAc 215	Ala 60	0.08
Fuc 233	His 53	0.01	Ile 58	Neu5Ac 220	0.06
Lys 75	Neu5Ac 231	0.01	Neu5Ac 220	Ser 56	0.05
His 53	GlcNAc 221	0.01	Ala 60	Man 217	0.05
GlcNAc 221	Ser 74	0.01	Neu5Ac 220	Ser 56	0.05
Neu5Ac 231	Thr 56	0.01	Arg 61	Man 217	0.04
Gal 230	Thr 54	0.01	Gal 223	Gln 79	0.04
Glu 30	GlcNAc 221	0.01	Arg 54	GlcNAc 218	0.04
His 53	Gal 230	0.01	GlcNAc 215	Ala 76	0.03
			Neu5Ac 224	Gly 14	0.03
			Neu5Ac 224	Gln 15	0.03

Table S4. Continued

7E4 HC			7E4 LC		
donor	acceptor	oc. [%]	donor	acceptor	oc. [%]
			Ser 56	Gal 219	0.02
			Gal 219	Ser 56	0.01
			Gln 79	Neu5Ac 224	0.01
			Neu5Ac 224	Gln 79	0.01
			Neu5Ac 224	Pro 13	0.01
			Arg 61	Man 217	0.01
			Arg 80	Neu5Ac 224	0.01
			Neu5Ac 224	Pro 13	0.01
			Gln 15	Neu5Ac 224	0.01
			Neu5Ac 220	Gly 57	0.01
			Gly 57	Neu5Ac 220	0.01
			GlcNAc 214	Ala 76	0.01
			Gal 223	Pro 13	0.01

Table S5. H-bond interaction details between the ACPA 3F3 HC and LC Fab fragments and the respective N-linked glycan. Shown are the H-bond donor and acceptor pairs (three letter code of the respective amino acids and monosaccharides) and the occupancy of the interaction in percentage. GlcNAc: N-acetylglucosamine, Neu5Ac: N-acetylneuraminic acid, Fuc: fucose, Gal: galactose, Man: mannose.

3F3 HC #1 N-glycan			3F3 HC #2 N-glycan			3F3 LC		
donor	acceptor	oc. [%]	donor	acceptor	oc. [%]	donor	acceptor	oc. [%]
Fuc 236	Glu 81	13.02	Fuc 249	Glu 22	10.53	Ser 71	GlcNAc 219	15.43
Lys 18	Fuc 236	1.68	Fuc 249	Ser 74	4.57	Asn 78	GlcNAc 219	8.69
Fuc 236	Thr 70	1.21	Gal 246	Gly 25	2.00	GlcNAc 220	Asp 76	5.96
Fuc 236	Gln 64	0.68	Phe 28	GlcNAc 237	0.47	GlcNAc 219	Asp 76	4.23
GlcNAc 224	Glu 81	0.65	GlcNAc 237	Ser 24	0.41	Lys 24	GlcNAc 227	1.18
Thr 70	Fuc 236	0.26	Gal 246	Ser 24	0.21	Gal 228	Ser 26	0.96
Neu5Ac 230	Gly 65	0.24	Neu5Ac 243	Tyr 100	0.08	Lys 24	GlcNAc 220	0.54
Asn 68	GlcNAc 224	0.21	Lys 53	Man 240	0.03	Lys 24	Man 226	0.50
Fuc 236	Asn 68	0.14	Asn 29	GlcNAc 237	0.03	Thr 20	Fuc 231	0.34
Neu5Ac 230	Gln 64	0.12	Lys 53	GlcNAc 238	0.03	GlcNAc 227	Thr 75	0.31
Gln 64	Fuc 236	0.06	Neu5Ac 247	Gly 25	0.03	Neu5Ac 229	Asp 9	0.28
Met 69	GlcNAc 224	0.04	Tyr 100	Neu5Ac 243	0.03	Fuc 231	Thr 20	0.26
Lys 53	Neu5Ac 234	0.03	Lys 53	Neu5Ac 243	0.02	Neu5Ac 229	Asp 9	0.21
Lys 53	Gal 229	0.02	Ile 27	Gal 246	0.01	GlcNAc 219	Asp 76	0.19
Neu5Ac 230	Gly 14	0.02	Tyr 100	Neu5Ac 243	0.01	Ser 28	Gal 228	0.17
Fuc 236	Gly 65	0.02				Fuc 231	Thr 20	0.14

Table S5. Continued

3F3 HC #1 N-glycan			3F3 HC #2 N-glycan			3F3 LC		
donor	acceptor	oc. [%]	donor	acceptor	oc. [%]	donor	acceptor	oc. [%]
Lys 53	Neu5Ac 230	0.01				Neu5Ac 225	Ser 26	0.14
Thr 83	Neu5Ac 230	0.01				GlcNAc 227	Ser 25	0.14
GlcNAc 224	Thr 83	0.01				Thr 75	GlcNAc 227	0.13
Thr 70	Neu5Ac 234	0.01				GlcNAc 227	Asp 76	0.08
						Neu5Ac 225	Ser 73	0.06
						Arg 18	Fuc 231	0.05
						Gal 228	Tyr 7	0.05
						Gal 228	Gln 27	0.05
						Asp 9	Gal 228	0.04
						Neu5Ac 229	Tyr 7	0.03
						Ser 73	Neu5Ac 225	0.03
						Tyr 7	Neu5Ac 229	0.02
						Neu5Ac 225	Gln 27	0.02
						Tyr 7	Gal 228	0.02
						Fuc 231	Asn 22	0.02
						Tyr 7	GlcNAc 227	0.02
						Gal 228	Thr 75	0.02
						Thr 5	Neu5Ac 229	0.01
						Neu5Ac 225	Thr 75	0.01
						Ser 28	Neu5Ac 225	0.01
						Ser 73	Neu5Ac 225	0.01
						Gal 228	Asp 9	0.01
						Gln 27	Gal 228	0.01
						Thr 75	Gal 228	0.01
						Neu5Ac 225	Ser 71	0.01

Table S6. H-bond interaction details between the ACPA 1F2 HC and LC Fab fragments and the respective N-linked glycan. Shown are the H-bond donor and acceptor pairs (three letter code of the respective amino acids and monosaccharides) and the occupancy of the interaction in percentage. GlcNAc: *N*-acetylglucosamine, Neu5Ac: *N*-acetylneuraminic acid, Fuc: fucose, Gal: galactose, Man: mannose.

1F2 HC #1 N-glycan			1F2 HC #2 N-glycan			1F2 LC		
donor	acceptor	oc. [%]	donor	acceptor	oc. [%]	donor	acceptor	oc. [%]
Ser 30	GlcNAc 223	11.08	GlcNAc 236	Thr 55	4.27	Gal 222	Asp 151	21.55
His 31	Fuc 235	9.5	Lys 54	Neu5Ac 246	2.7	Neu5Ac 223	Gly 156	10.44
Fuc 235	His 31	2.4	Fuc 248	Ala 56	1.65	GlcNAc 224	Thr 160	10.39

Table S6. Continued

1F2 HC #1 N-glycan			1F2 HC #2 N-glycan			1F2 LC		
donor	acceptor	oc. [%]	donor	acceptor	oc. [%]	donor	acceptor	oc. [%]
Lys 54	Fuc 235	1.98	Thr 55	GlcNAc 236	0.93	Neu5Ac 219	Gln 161	9.88
Fuc 235	Ser 30	1.32	Fuc 248	Thr 55	0.86	Lys 153	Gal 222	7.29
Neu5Ac 233	Leu 102	1.14	Neu5Ac 246	Lys 54	0.74	Gal 218	Thr 157	5.81
Ser 30	GlcNAc 223	1.13	Asn 57	GlcNAc 236	0.22	Gln 161	GlcNAc 224	4.83
Phe 29	GlcNAc 223	0.89	Gal 245	Asn 57	0.2	Neu5Ac 219	Thr 183	3.81
Thr 74	GlcNAc 224	0.25	GlcNAc 236	Ala 56	0.15	GlcNAc 213	Thr 3	2.83
Ile 104	Fuc 235	0.13	Fuc 248	Asn 57	0.12	Thr 157	Neu5Ac 223	2.75
Fuc 235	Asn 28	0.09	Lys 54	Neu5Ac 246	0.1	Gal 218	Gln 161	2.48
Asn 28	GlcNAc 223	0.05	Thr 55	Fuc 248	0.1	Fuc 225	Asn 25	2.15
GlcNAc 231	Lys 54	0.04	Thr 55	Gal 245	0.07	Neu5Ac 223	Gly 156	1.85
GlcNAc 224	Thr 74	0.03	Neu5Ac 246	Thr 55	0.03	Neu5Ac 223	Thr 157	1.74
Fuc 235	Leu 102	0.02	Gal 245	Lys 54	0.02	Asn 1	GlcNAc 213	1.59
Lys 54	Gal 232	0.02	Leu 58	Fuc 248	0.01	Gln 161	Neu5Ac 219	1.42
His 31	GlcNAc 223	0.01	Thr 55	GlcNAc 236	0.01	Gal 218	Gln 161	1.34
GlcNAc 224	Ser 75	0.01				Gln 161	GlcNAc 217	1.16
Neu5Ac 233	Gly 103	0.01				GlcNAc 224	Gln 161	1.04
						Thr 160	GlcNAc 224	1.02
						GlcNAc 217	Gln 161	0.85
						Gal 222	Gly 156	0.84
						Fuc 225	Asn 25	0.81
						Gln 161	GlcNAc 224	0.62
						Lys 153	Neu5Ac 223	0.55
						Lys 133	Neu5Ac 219	0.53
						Neu5Ac 223	Asp 155	0.49
						Neu5Ac 219	Gln 161	0.46
						Fuc 225	Asn 1	0.42
						Neu5Ac 219	Thr 183	0.39
						Thr 205	Neu5Ac 223	0.39
						GlcNAc 217	Gln 161	0.34
						Fuc 225	Thr 3	0.27
						Thr 160	GlcNAc 224	0.27
						Thr 157	Gal 218	0.26
						Gal 218	Thr 160	0.23
						Gln 161	Gal 218	0.22
						GlcNAc 217	Thr 160	0.22
						Thr 160	Gal 218	0.2

Table S6. Continued

1F2 HC #1 N-glycan			1F2 HC #2 N-glycan			1F2 LC		
donor	acceptor	oc. [%]	donor	acceptor	oc. [%]	donor	acceptor	oc. [%]
						Thr 3	Fuc 225	0.18
						GlcNAc 213	Leu 2	0.17
						Fuc 225	Asn 1	0.16
						Gly 162	Neu5Ac 219	0.15
						GlcNAc 224	Pro 158	0.15
						Neu5Ac 223	Gly 203	0.15
						Neu5Ac 223	Asp 155	0.14
						Gal 222	Thr 157	0.13
						GlcNAc 221	Asp 151	0.13
						Thr 185	Neu5Ac 219	0.13
						Asn 25	Fuc 225	0.1
						Gal 222	Thr 205	0.08
						Gln 198	Gal 222	0.07
						Neu5Ac 223	Thr 157	0.05
						Arg 191	Neu5Ac 219	0.05
						GlcNAc 221	Thr 160	0.05
						Thr 160	GlcNAc 217	0.04
						Thr 183	Neu5Ac 219	0.03
						GlcNAc 217	Thr 160	0.03
						Neu5Ac 223	Glu 207	0.03
						Gln 161	Man 216	0.02
						Gln 161	GlcNAc 217	0.02
						Thr 205	Neu5Ac 223	0.02
						Thr 185	Neu5Ac 219	0.02
						Gal 222	Glu 207	0.02
						Thr 183	Neu5Ac 219	0.01
						Thr 160	GlcNAc 221	0.01
						Gal 218	Pro 158	0.01
						Gal 218	His 192	0.01
						Neu5Ac 219	Thr 185	0.01
						Gal 218	Val 154	0.01
						Thr 157	GlcNAc 224	0.01
						Fuc 225	Gly 26	0.01
						Thr 157	Neu5Ac 223	0.01

Supplemental Figures

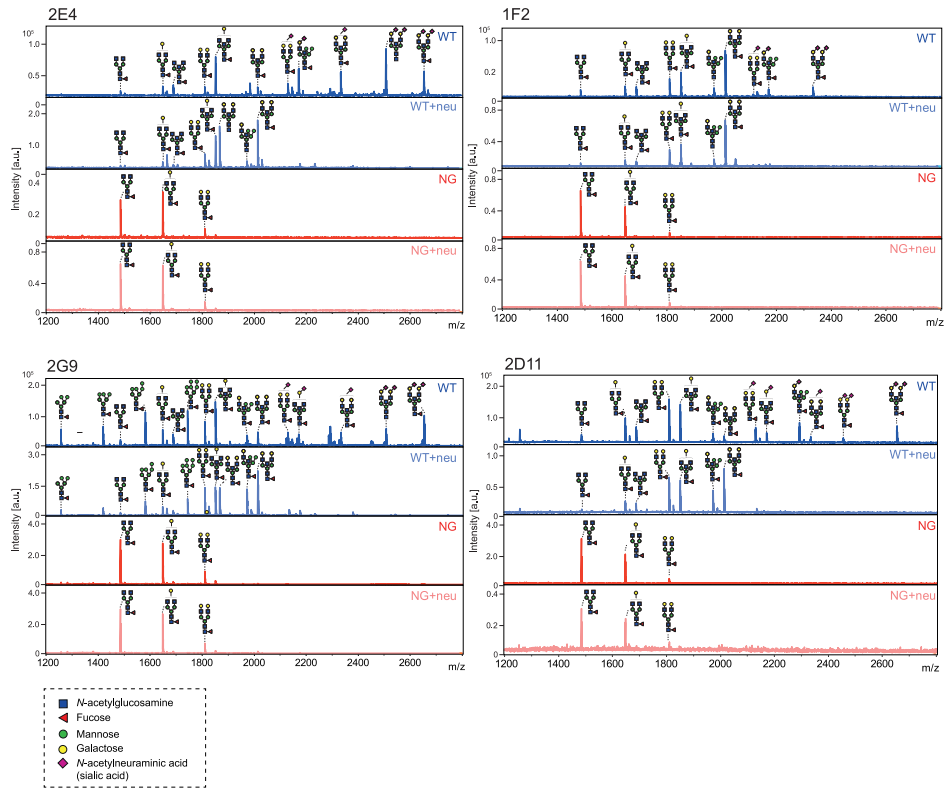
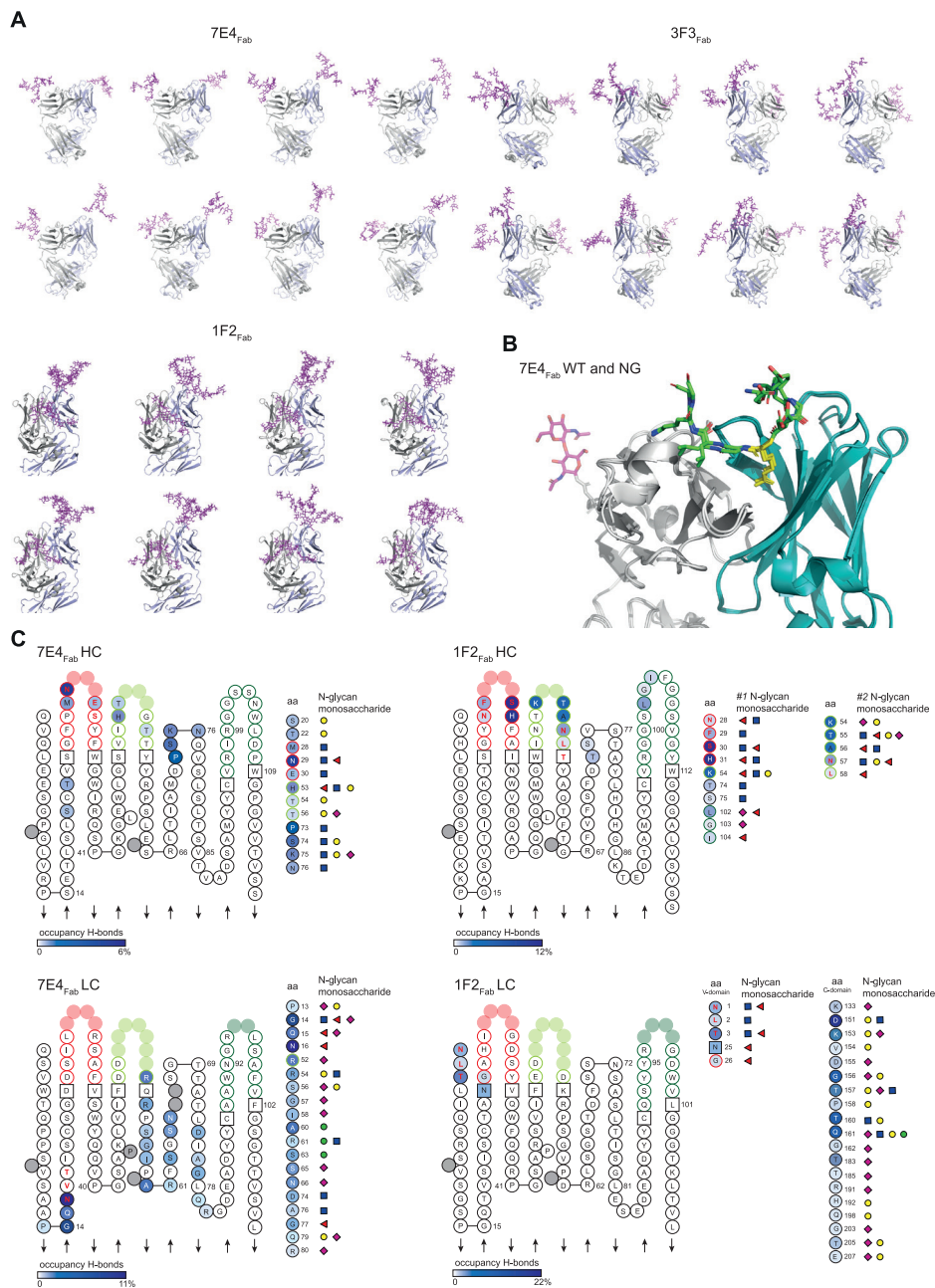


Figure S1. MALDI-TOF analysis of released and stabilized N-linked variable domain and Fc glycans from WT (blue), WT+neu (light blue), NG (red) and NG+neu (light red) ACPA IgG 2E4, 1F2, 2G9 and 2D11. Glycan structures of the most abundant N-linked glycan peaks are depicted. Blue square: N-acetylglucosamine (GlcNAc), green circle: mannose, yellow circle: galactose, red triangle: fucose, purple diamond: α 2,6-linked N-acetylneuraminic acid.



◀ **Figure S2. Molecular dynamics (MD)-simulations to predict VDG-antibody interactions and 7E4_{Fab} crystal structure comparison with and without N-linked glycan sites.** (A) MD-simulations, 8 time-points, of 7E4_{Fab}, 3F3_{Fab} and 1F2_{Fab} crystal structures modelled with full length disialylated VDG (sticks in magenta). (B) Superposition of 7E4_{Fab} crystal structures expressed with and without N-linked glycan sites. 7E4_{Fab} WT including N-linked glycan sites was crystallized together with the first two GlcNAcs (sticks in magenta) of the LC VDG. LC is depicted in light gray, HC in steel blue, the peptides bound to the respective Fab as sticks with carbon (green), oxygen (red) and nitrogen (blue) atoms. (C) ACPA 7E4_{Fab} and 1F2_{Fab} HC and LC variable gene aa-sequences, based on IMGT (2D), are depicted. Acceptor/ donor pairs of H-bond interactions between the antibody and HC (#1 and #2)/LC N-glycans are visualized. A high occupancy is depicted in dark blue (HC: 6%; 12%, LC: 11%; 22%) and a low occupancy is depicted in light blue (0.01 to 0.2%). Amino acids and their respective interaction partners (N-glycan monosaccharides) are shown. Blue square: *N*-acetylglucosamine, green circle: mannose, yellow circle: galactose, red triangle: fucose, purple diamond: α 2,6-linked *N*-acetylneuraminic acid (sialic acid).

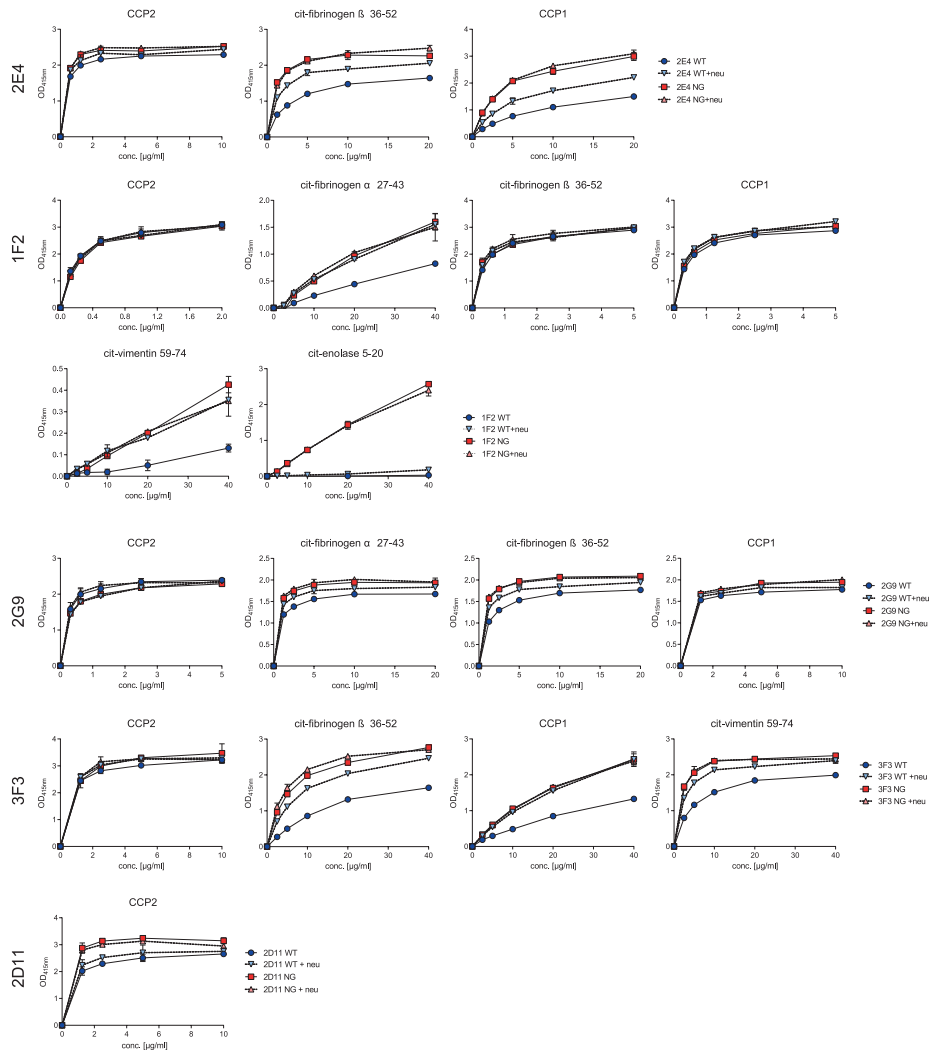


Figure S3. Impact of disialylated ACPA VDG on citrullinated peptide binding. ELISA titration binding curves of the ACPA 2E4, 1F2, 2D11, 2G9 and 3F3 (0 to 40 $\mu\text{g/ml}$) variants (WT, WT+neu, NG and NG+neu) towards citrullinated peptides (CCP2, CCP1, cit-fibrinogen α 27-43, cit-fibrinogen β 36-52, cit-vimentin 59-74, cit-enolase 5-20). Binding to the arginine control peptide was subtracted. Reactivity was determined via the OD at 415 nm. Each data point represents the mean of two technical replicates. N = 2 to 3.

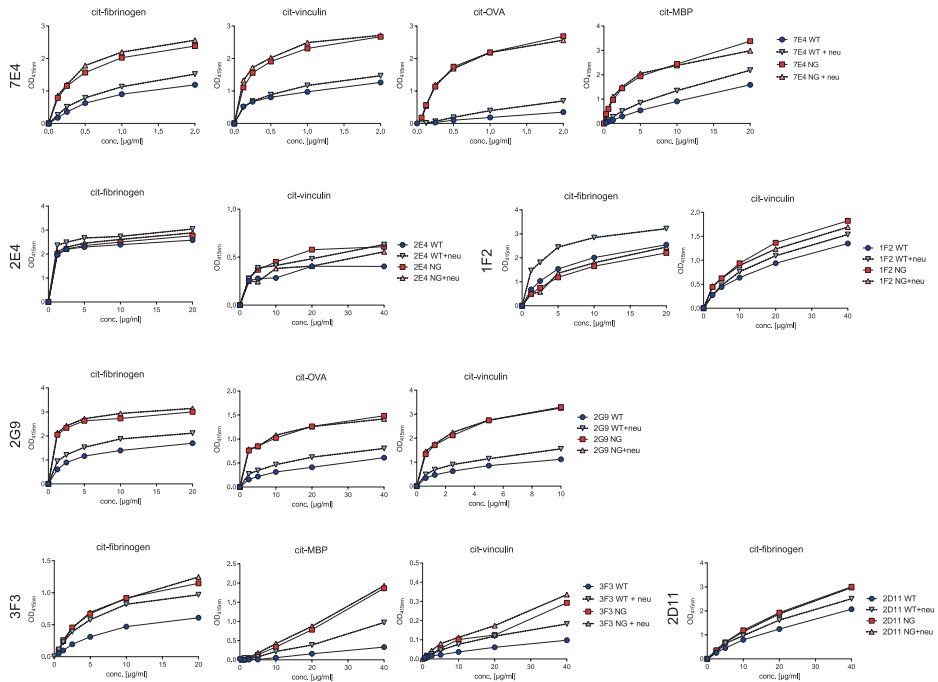
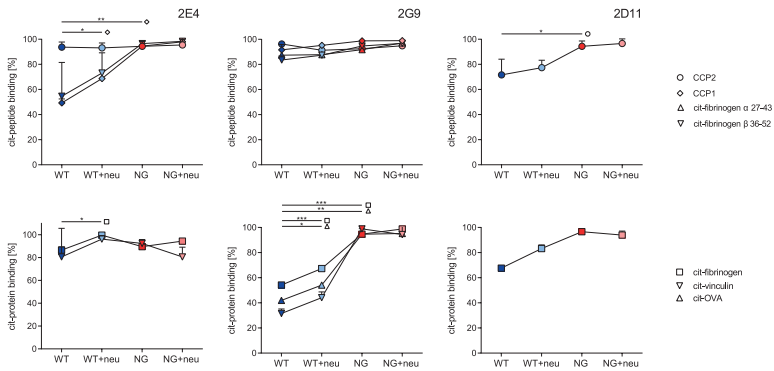
A**B**

Figure S4. Impact of disialylated ACPA VDG on citrullinated protein binding. (A) ELISA titration binding curves of the ACPA 2E4, 1F2, 2D11, 2G9 and 3F3 (0 to 40 μg/ml) variants (WT, WT+neu, NG and NG+neu) towards citrullinated proteins (cit-fibrinogen, cit-vinculin, cit-MBP and cit-OVA). Binding to the arginine control protein was subtracted. Reactivity was determined via the OD at 415 nm. N = 2 to 3. **(B)** Relative binding of the ACPA mAb 2E4, 2G9 and 2D11 (10 to 40 μg/ml) variants (WT, WT+neu, NG, NG+neu) towards citrullinated peptides and proteins. N = 2 to 3. Unpaired two-tailed t-tests assuming the same SD. 2E4WT-NG: **p (CCP1) = 0.0028; 2E4WT-WT+neu: *p (CCP1) = 0.0143, *p (cit-fibrinogen) = 0.0226; 2G9WT-NG: ***p (cit-fibrinogen) = 0.0009, **p (cit-OVA) = 0.0047; 2G9WT-WT+neu: ***p (cit-fibrinogen) = 0.0004, *p (cit-OVA) = 0.0297; 2D11WT-NG: *p (CCP2) = 0.0406.

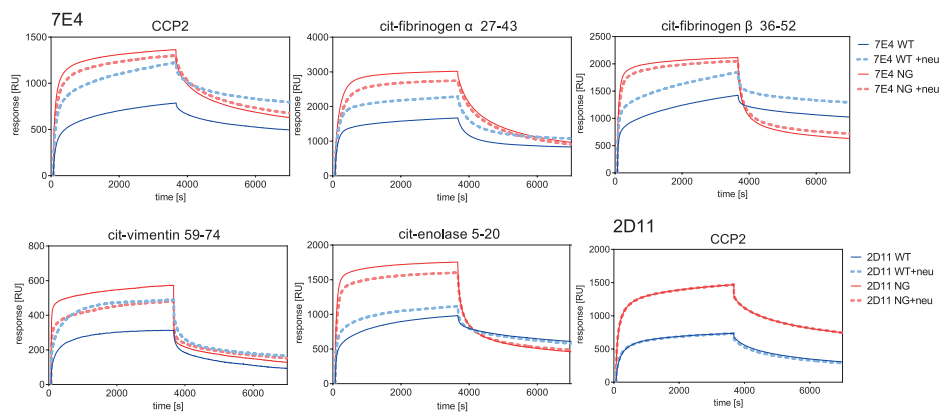


Figure S5. SPR sensorgrams of ACPA IgG 7E4 and 2D11 binding to citrullinated peptides. Antigen association and dissociation are represented as response units (RU) over time (s). The experiment represents 2 technical replicates. Four different monoclonal antibody variants were assessed: WT, WT+neu, NG and NG+neu.

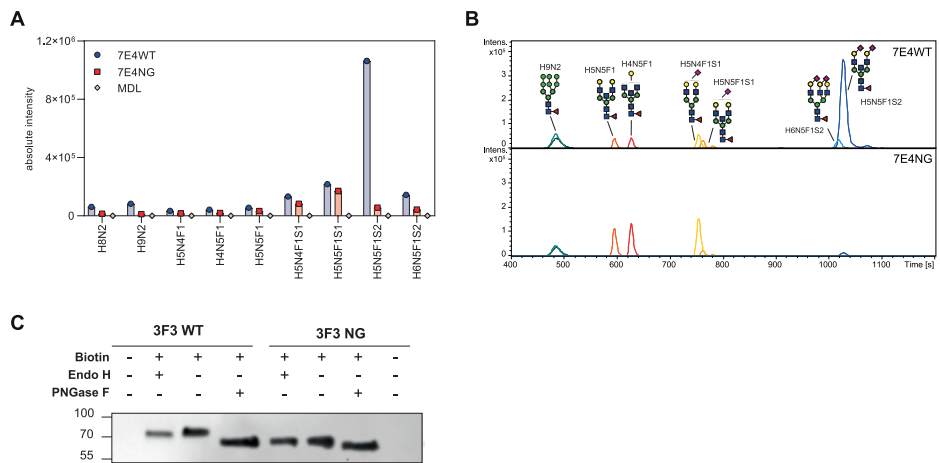


Figure S6. Human Ramos IgG B-cell receptor glycan analysis. (A) Absolute intensity of glycan traits expressed on the 7E4 WT, NG and MDL IgG BCR after passing QC settings. (B) LC-chromatogram of glycan traits expressed on the 7E4 WT and NG (IgG BCR after passing QC settings). The respective glycan traits are schematically illustrated. (C) Western blot analyses of PBS-treated (- Biotin) or biotinylated (+ Biotin) surface IgG 3F3 WT and NG BCRs after NeutrAvidin capturing. Biotinylated mIgG with and without VDG were treated with 2 U Endo H (cleavage of high-mannose structures) or 2 U PNGase F (cleavage of all N-glycans).

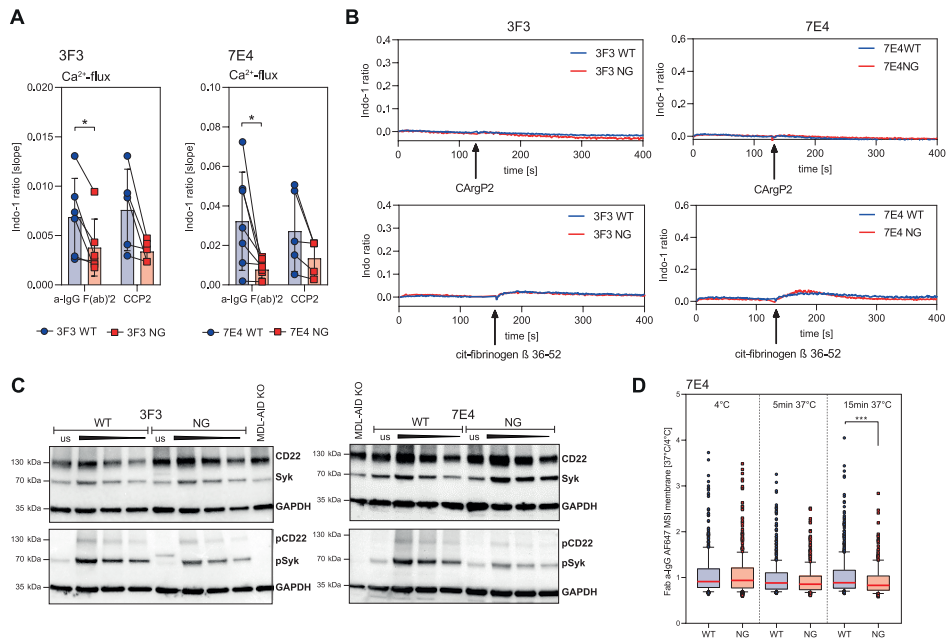


Figure S7. Impact of mIgG VDGs on human Ramos B-cell activation and BCR downmodulation. (A) Paired analysis of Ca^{2+} -flux speed (slope) for mIgG 3F3/ 7E4 WT and NG Ramos B cells after a-IgG F(ab)₂ and antigen (CCP2-strep.) stimulation. Paired two-tailed t-test. N = 5 to 7. 3F3: *p = 0.0377; 7E4: *p = 0.0206. (B) Overlays of WT and NG Ca^{2+} -flux (Ca^{2+} bound Indo-1/ unbound Indo-1) of mIgG 3F3/ 7E4 WT and NG Ramos B cells after stimulation with CArgP2-SA or cit-fibrinogen β 36-52. (C) Western blot analyses of mIgG 3F3/ 7E4 WT and NG Ramos B cells after 5 min of CCP2 stimulation or unstimulated (us). CD22, Syk, pCD22 (Y822) and pSyk(Y352) expression are shown. Cell lysis of 1 million (unstimulated and stimulated 1st slot), 0.5 million (stimulated 2nd slot) and 0.25 million (stimulated 3rd slot) were blotted. GAPDH was used as loading control. Cell lysates of 1 million MDL-AID KO cells were added as additional control. (D) Remaining mIgG 7E4 WT and NG expression after CCP2-strep. stimulation and incubation at 4°C or 5, 15 min at 37 °C. N = 619, 459, 645, 433, 738 and 302 cell slices respectively. Ordinary one-way ANOVA, ***p = 0.0002.

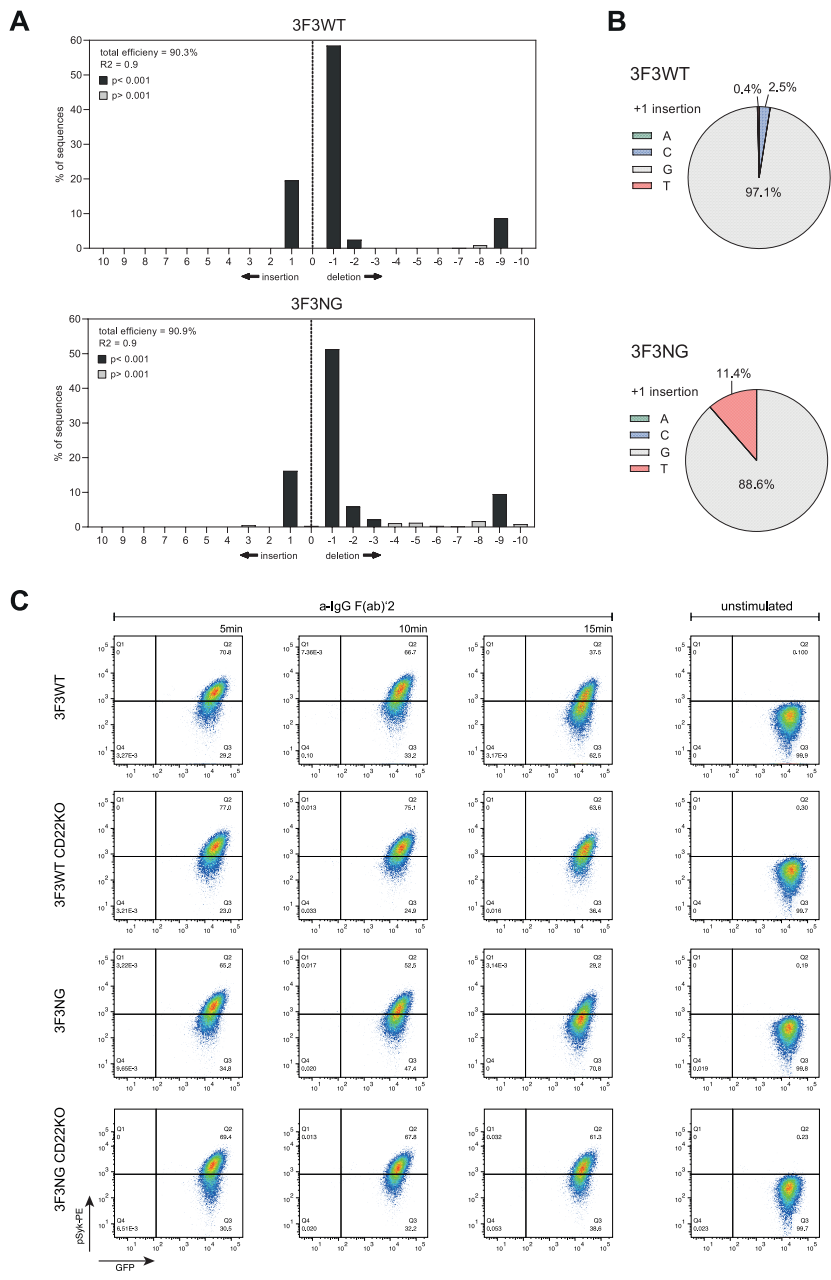


Figure S8. TIDE analysis 3F3 CD22KO Ramos B cells. (A) Comprehensive profile of all insertions and deletions (indels) in the CD22 KO edited sample according to the TIDE analysis. The total KO efficiency is depicted. (B) An estimate of the +1 insertion base composition according to the TIDE analysis. (C) pSyk(Y348) expression of mlgG 3F3 WT, WT CD22KO, NG and NG CD22KO BCRs after 5, 10 and 15 min of α-IgG F(ab)'2 stimulation. Gating is based on the unstimulated cells. The pSyk expression is depicted on the y-axis and the GFP expression on the x-axis. One experiment is exemplarily shown.



N-linked glycans attached to the immunoglobulin variable domain affect the recruitment of complement

Theresa Kissel, Sanne van de Bovenkamp, Hugo J. van Dooren, Astrid S. Brehler, Joanneke C. Kwekkeboom, Eva M. Stork, Carolien Koeleman, Manfred Wuhrer, Tom W.J. Huizinga, Hans U. Scherer, Leendert A. Trouw, René E.M. Toes

Abstract

Recruitment and activation of the complement system represents an important effector mechanism of (auto)antibodies. Previous studies have shown that the autoantibodies characteristic of Rheumatoid Arthritis (RA), anti-citrullinated protein antibodies (ACPAs), are capable of activating the classical and alternative complement cascade. ACPA immunoglobulin gamma (IgG) are extensively N-linked glycosylated in their variable domains. In contrast to the role of the evolutionary conserved Fc glycan at position 297, the influence of variable domain glycans (VDGs) on the biological function of antibodies remains to be elucidated.

In this study, we investigated the effects of VDGs on complement activation using patient-derived monoclonal ACPA IgG with and without naturally occurring N-linked glycans in the variable domain. We show that monoclonal ACPA IgG activated the classical and alternative complement cascade in a dose-dependent manner consistent with the results observed for polyclonal ACPA. Interestingly, the presence of VDGs resulted in impaired initiation of the classical but not the alternative complement pathway. This was explained by reduced C1q binding and decreased subsequent C4 and C3c deposition, especially for ACPA IgG carrying a high amount of VDGs. The decreased binding of C1q was explained by the reduced ability of VDG-bearing IgG to hexamerize, which is crucial for IgG to interact efficiently with C1q, rather than by differences in antigen binding.

Collectively, these results show that glycans attached to the variable domain of autoantibodies inhibit initiation of the classical complement pathway and reveal a novel mechanism that affects the ability of antibodies to recruit a key immune effector mechanism. These data suggest that glycan modifications in the variable domain could potentially be employed to influence the complement-activating potential of IgG (auto)antibodies.

Introduction

The complement system is an important innate defense cascade that can mediate a plethora of functions in the host defense against invading pathogens and protection against autoimmunity¹⁻³. Complement can be activated via the classical, the alternative and the lectin pathway⁴. The classical pathway is initiated by binding of C1q to antibody-antigen immune complexes, preferentially hexamers, and often assessed by circulating levels of activated C4. The lectin pathway is triggered by mannose-binding lectin (MBL) or ficolins whereas the alternative pathway is initiated by an “autoactivation” of the complement factor C3. Central to complement activation is the formation of C3 convertases (C3c) that cleave C3 to biologically active complement fragments resulting in the recruitment and activation of immune cells as well as cell lysis after formation of the membrane attack complex. Importantly, the induction of complement is tightly regulated and aberrant activation can lead to severe tissue damage. Complement is likely also playing a role in human autoimmune diseases as complement inhibition has been proven effective^{5,6} and complement activation products are often found at sites of inflammation. For example, in the synovial fluid of RA patients elevated levels of complement activation products such as SC5b-9, Bb or C1q-C4 complexes are readily detected⁷⁻⁹. Similarly, complement deposits can be visualized in the synovial membrane¹⁰, indicating local complement activation in the synovium of RA patients.

The prominent autoimmune disease RA is characterized by autoantibodies directed against citrullinated residues expressed by proteins, termed anti-citrullinated protein antibodies (ACPAs). ACPAs have a remarkably specificity for RA, can be present several years before the actual onset of RA and their presence is associated with a worsened disease course¹¹⁻¹⁴. Recent studies have shown that ACPA are capable of activating both the classical and alternative complement cascade in an antigen-dependent in vitro assay¹⁵ suggesting a potential contribution to disease pathogenesis via the complement system. As an integral feature, ACPA IgG harbor glycans not only at the evolutionary conserved N-linked glycosylation site at position 297 in the Fc domain, but also in the variable domains of the heavy and light chains (V_H and V_L , respectively). Structural analysis revealed that ACPA IgG VDGs are predominantly fully processed diantennary complex type glycans presenting a bisecting *N*-acetylglucosamine and two terminal sialic acids¹⁶. Intriguingly, VDGs are present on more than 90% of the RA-specific autoantibodies¹⁶ and their introduction has been reported to be predictive for disease development with increasing levels towards RA-onset¹⁷⁻¹⁹. Recently, it has been suggested that the abundant introduction of N-glycosylation sites in the hypervariable regions of ACPA IgG molecules^{20,21} likely provides a selective advantage to citrullinated protein-reactive B cells²².

Nevertheless, VDGs are not unique to ACPA, but also present on conventional IgG molecules albeit at a lower level of approximately 15%²³. Interestingly elevated levels of VDGs were also found on (auto)antibodies from ANCA-associated vasculitis (AAV)-patients (anti-MPO, anti-

PR3, anti-GBM)²⁴, primary Sjorgen's syndrome (pSS), multiple sclerosis (MS) or systemic lupus erythematosus (SLE) patients^{25,26}. VDGs were also found to be present in monoclonal muscle-specific kinase (MuSK) autoantibodies, suggesting a potential role for myasthenia gravis^{27,28}. In addition, glycans are frequently presented in the variable domains of anti-drug antibodies that emerge in patients treated with adalimumab or infliximab²⁹. Thus, increased variable domain glycosylation appears to be a common feature of several (autoreactive) B-cell responses potentially triggered by chronic, systemic antigen exposure and may pursue important immunomodulatory functions.

It is well established that the conserved N-linked glycans in the IgG Fc domain can modulate immune effector functions by interacting with the complement system³⁰⁻³². The composition of the Fc glycans is variable and it has been reported that Fc galactosylation and sialylation affect binding to C1q and, thereby, complement-dependent cytotoxicity (CDC). For Fc galactosylation enhanced binding to C1q has been reported^{30,33}, whereas conflicting data have been observed for IgG sialylation^{30,34,35}. Recently, the mechanism by which Fc galactosylation affects complement activation has been elucidated, as it has been shown that hypergalactosylation enhances the potential of IgG to form hexameric structures, which is a pre-requisite for efficient C1q binding and subsequent CDC, rather than directly impacting on the affinity/avidity of individual Fc tails to C1q³⁵.

Given the importance of IgG-Fc N-linked glycans on immune effector functions and the abundant occurrence of glycans in the variable domains on ACPAs, we now wished to determine the potential impact of VDGs on complement activation. To study this, we created a set of glycoengineered monoclonal antibodies (mAbs) expressing N-linked glycans in the variable domain and analyzed their ability to facilitate complement binding and activation. Furthermore, we assessed the impact of VDGs on the propensity of IgG molecules to form hexamer structures, accompanied by efficient C1q binding, by generating RGY triple mutants (E345R, E430G and S440Y).

Results

Glycoengineered human monoclonal antibodies with and without N-linked variable domain glycans

To investigate the effect of antibody VDGs on complement activation, we generated monoclonal ACPA IgG, derived from B-cell receptor sequences obtained from RA patients. These mAbs harbor 2 to 4 naturally occurring N-linked glycan sites in the heavy chain (HC) and light chain (LC) variable regions (Figure 1A). To produce non-variable domain glycosylated monoclonal antibody (mAb) counterparts, the N-linked glycan motifs were mutated back to the respective

germline sequences (Table S1). The integrity of the wild-type (WT, i.e. the sequence with N-glycosylation sites), and non-glycosylated (NG) mAbs (lacking the VDGs) was verified by gel electrophoresis (Figure 1B). The shift in the apparent molecular weight between both variants indicates the presence of glycans and was in line with an increasing number of glycan-sites ($7E4 < 3F3 < 2G9$). As indicated by the gel bands depicted in figure 1B, all glycosylation sites in the mAb HC and LC were occupied by a glycan, except for a fraction of the ACPA 2G9 HC and LC glycan sites which were only partially used. Next to the ACPA IgG, we further cloned and expressed an anti-tetanus toxoid (anti-TT) IgG mAb (D2) with and without its natural LC N-glycan site to determine whether the findings generated were specific for ACPAs or likely reflect a general effect of VDGs (Figure S1A). As for monoclonal ACPA IgG, also the sequence of the anti-TT mAb was derived from sorted antigen-specific B cells obtained from RA patients.

Since ACPA VDGs mainly consist of diantennary glycans harboring terminal sialic acids, we produced glycoengineered (+ge) variants of the mAbs (see Materials and Methods)¹⁶. To investigate the effect of different glycan compositions, the mAb 7E4 was generated in the presence and absence of glycoengineering. Different Fc-glycan profiles for the mAb variants were observed as determined by liquid chromatography coupled to mass spectrometry (LC-MS) with an increased percentage of galactosylation, sialylation and bisection for the glycoengineered molecules (Figure 1, C and E). Importantly, the Fc-glycan profiles between the WT and NG variant of each set of mAbs were similar when generated under the same conditions (Figure 1 and S1). Glycan analysis after total glycan release revealed a dominating complex-type, bisected and disialylated VDG profile ($m/z = 2651$) after glycoengineering (Figure 1F and S2). Consequently specific glycoengineering of Freestyle™ 293-F cells enables the generation of mAbs with complex-type disialylated VDG-glycan profiles similar to those obtained on secreted autoantibodies from RA patients. Together, we generated and characterized four different mAbs with VDGs and their non-VDG containing counterparts to address the functional relevance of antibody VDGs on complement activation.

IgG variable domain glycosylation hampers the activation of the classical complement pathway

To assess whether the presence of VDGs affects the complement cascade, we determined the ability of the different mAb IgG variants to activate the classical or alternative complement pathway. Because antigen binding is a pre-requisite for complement activation, ACPA IgG were first incubated on a plate coated with the antigen cyclic citrullinated peptide 2 (CCP2) (Figure 2A). To obtain similar binding for the WT and NG antibody variants (Figure 2B) we adjusted antigen-coating for the 7E4 mAbs (see Materials and Methods). No effect of the VDGs on CCP2 binding was observed for the 3F3 and 2G9 mAbs (Figure 2B).

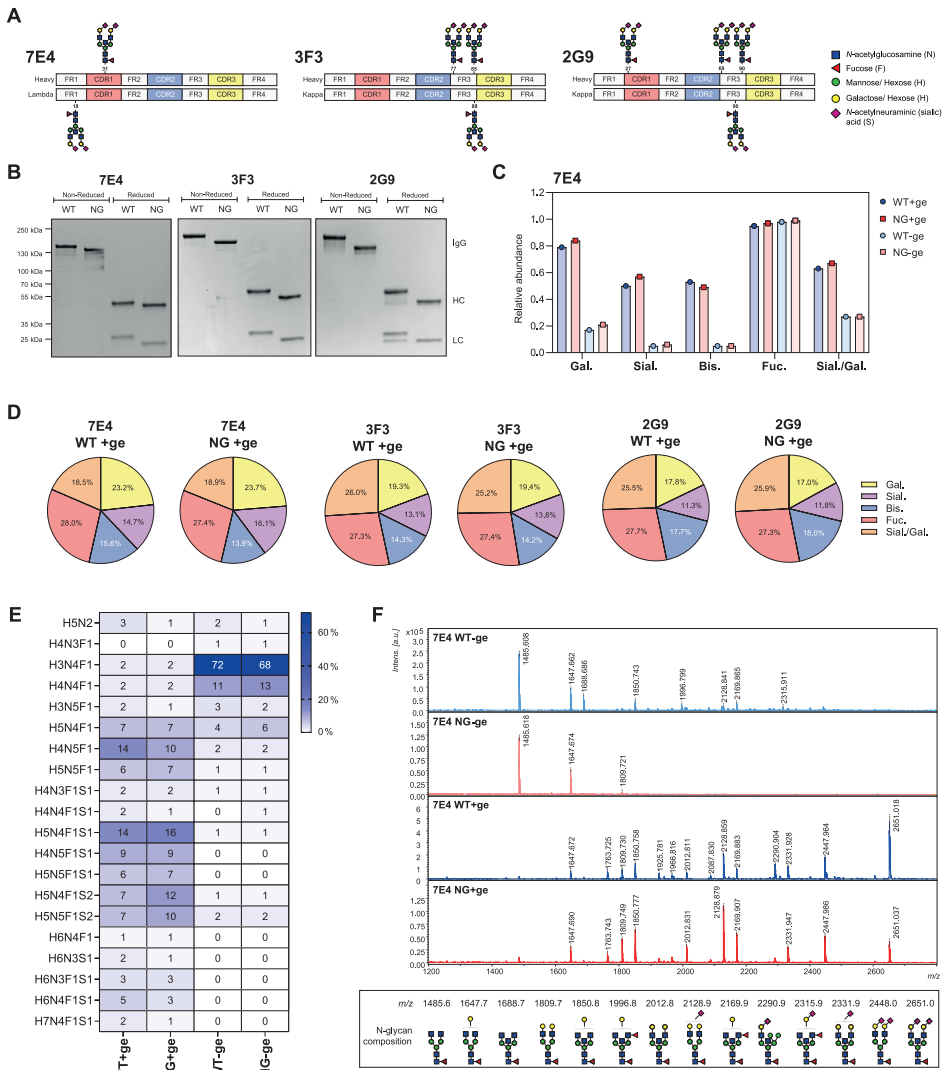
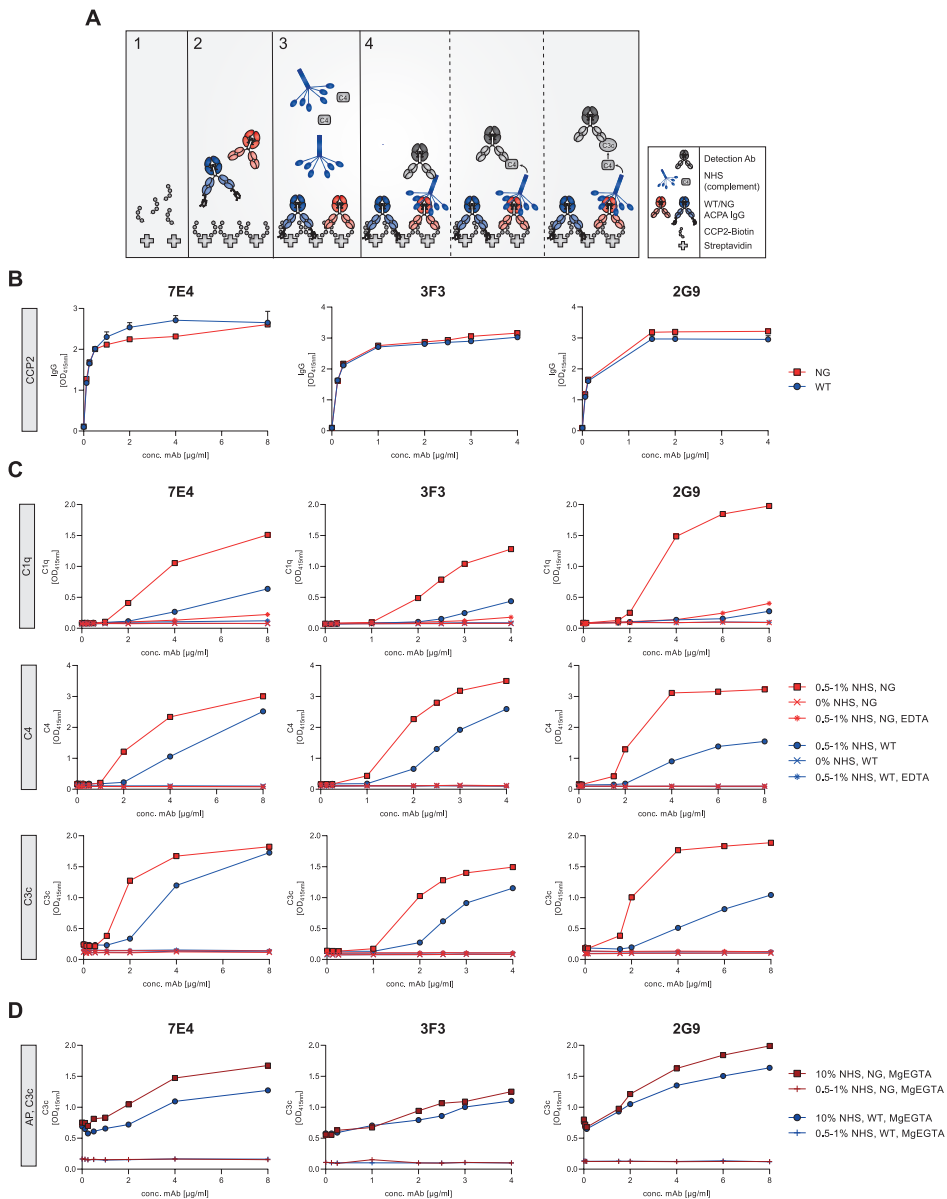


Figure 1. Production of RA patient derived monoclonal ACPA IgG with (wild-type, WT) and without (non-glycosylated, NG) naturally occurring variable domain glycan sites. (A) Schematic representation of the 7E4, 3F3 and 2G9 heavy and lambda or kappa light chain variable regions including the respective positions of the naturally occurring N-linked glycan sites. **(B)** 4 to 15% gradient SDS protein gel (BioRad) of purified WT and NG monoclonal ACPA IgG 7E4, 3F3 and 2G9 under non-reduced (IgG) and reduced (HC and LC) conditions. The size-shift caused by the presence of VDGs is visible per mAb-family. The size was determined using the PageRuler™ Plus Prestained Protein Ladder (Thermo Fisher Scientific). **(C)** Relative abundance of Fc galactosylation (Gal.), sialylation (Sial.), bisection (Bis.) and fucosylation (Fuc.) on 7E4 WT and NG +/-ge mAb variants determined by LC-MS Fc-glycopeptide analysis. **(D)** Pie chart graphs of WT+ge and NG+ge mAbs 7E4, 3F3 and 2G9. The percentage of galactosylation, sialylation, bisection and fucosylation are shown. **(E)** Fc-peptide glycan compositions of 7E4 WT and NG +/-ge mAb variants. The percentages of the respective glycan traits are shown. **(F)** MALDI-TOF MS analysis of released and stabilized VD and Fc glycans from 7E4 WT and NG +/-ge mAbs. The respective m/z and schematic N-glycan compositions are depicted. Blue square: N-acetylglucosamine (GlcNAc), green circle: mannose, red triangle: fucose, purple diamond: α 2,6-linked N-acetylneuraminic acid (sialic acid).

Next, we assessed classical complement pathway activation by addition of exogenous complement (normal human serum, NHS) and subsequent detection of C1q, C4 and C3c deposition on the mAbs bound to the antigen-coated plates (Figure 2A). The findings confirmed the results of previous studies investigating the influence of Fc-glycan compositions on complement activation^{30,33}, and showed that elevated levels of galactosylation and sialylation, as seen for our glycoengineered (+ge) versus non-glycoengineered (-ge) mAb variants, increased the classical pathway initiation and thus downstream C3c deposition (Figure S3A). Intriguingly, our data showed a substantial reduction in classical pathway activation in the presence of additional glycans attached to the mAb variable domains (WT) (Figure 2C and Figure S3A). We observed a consistently lower degree of C1q, C4 and C3c deposition for all WT mAbs compared to their NG counterparts. No complement activation was detected in the absence of NHS or in the presence of EDTA (Figure 2C). For efficient alternative pathway (AP) activation we used a buffer containing Mg-EGTA, that blocks both the classical and lectin pathway, in the presence of 10% NHS¹⁵. Under the AP conditions C3c deposition was only marginally reduced when WT antibodies were compared to their NG counterparts, indicating that alternative complement pathway activation is hardly influenced by the presence of VDGs (Figure 2D). No C4 deposition (classical complement pathway component) was observed using the AP-specific buffer (Figure S3D). The effect of VDGs on the classical pathway activation (C1q, C4 and C3c deposition) was observed for all WT compared to their NG mAb variants assessed (Figure 3). The largest difference, particularly for C3c deposition, was noted for the mAb 2G9 (Figure 2C and Figure 3) that expresses in total eight N-linked glycans in the variable domain.

To identify, if VDGs only impact complement activation in the context of ACPA IgG molecules or if this post-translational glycan modification also changes the antibody effector functions for IgG with other specificities, we assessed an anti-TT mAb (D2), which contains one natural LC VDG. Also in this case, we observed a reduced C1q and C3c deposition of the WT mAb compared to its NG counterpart, despite an identical binding to the ELISA plate (Figure S3, B and C).

Next, we investigated whether also polyclonal ACPA IgG with an increased amount of VDGs hinder classical complement activation. To this end, we captured ACPA IgG from two RA patients that showed different VDG quantities. The isolated polyclonal ACPA IgG from patient 2 exhibited, on average, a higher molecular weight likely reflecting a higher degree of VDGs (Figure S4A). This notion was confirmed by LC-MS (Figure S4B) as the obtained glycan profiles revealed a higher degree of the bisected and disialylated glycan traits among the VDGs of ACPA IgG from patient 2 (Figure S4, B and C). In line with our previous observations on the monoclonal level, the polyclonal ACPA IgG with a higher degree of VDGs showed, despite a similar antigen-binding behavior (Figure S4D), a reduced C1q and C3c deposition in the complement activation assay (Figure S4E). We were not able to analyze polyclonal ACPA IgG without VDGs as an increased level of variable domain glycosylation is present in all RA patients. Thus, these results indicate that glycan modifications on the variable domain of both monoclonal and polyclonal antibodies impair C1q binding and the initiation of the classical complement pathway.



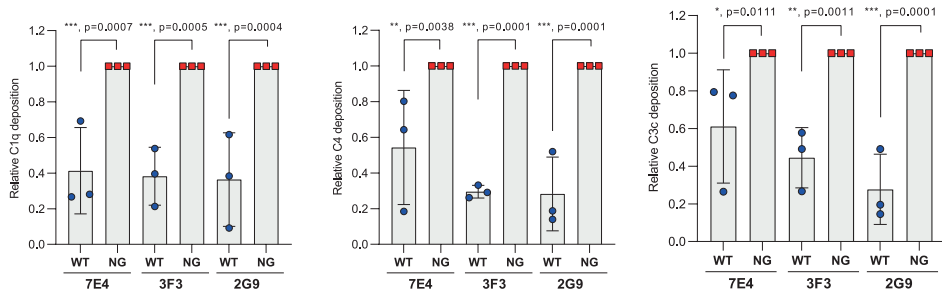


Figure 3. Classical complement pathway activation of WT and NG monoclonal ACPA IgG. Relative C1q, C4 and C3c deposition on CCP2 bound WT mAb compared to its NG counterpart (2 μ g/ml). Each experiment was repeated 3 times and each dot represents one independent experiment. Ordinary one-way ANOVA was performed and the respective p-values are depicted: ns $p > 0.05$, * $p \leq 0.05$, ** $p \leq 0.01$, *** $p \leq 0.001$ or **** $p \leq 0.0001$.

Impaired C1q binding correlates with the amount of N-linked glycans on the variable domain

We next wished to analyze whether the effect on the initiation of complement activation was dependent on the abundance or location of the N-linked glycans. Therefore, we generated mAb variants of 7E4 and 3F3 with VDGs presented only in the HC (HCWT) or the LC (LCWT), respectively (Figure 4A). As depicted in figure 4B, the apparent molecular weight of the antibodies produced was in line with the number and location of the N-linked glycosylation sites expressed by the respective Ab chains. When assessing these variants in complement activation assays, we observed a clear and significant stepwise decrease in C1q and C3c deposition with an increasing number of VDGs (Figure 4) despite an identical antigen (CCP2)-binding (Figure S5A). The same effect was observed for C4 deposition as assessed using 7E4 (Figure S5, B and C).

In case of 7E4, the glycan expressed by the LC (LCWT) associated with a more potent inhibitory effect compared to the VDG expressed by the HC (HCWT) (Figure 4 and Figure S5). The mAb 3F3 expressing two VDGs in the antibody HC and one in the LC, showed accordingly less complement component deposition when expressed as HCWT variant (Figure 4, C and E). Thus, the data described above indicate that the degree of variable domain glycosylation correlates with its ability to diminish classical complement activation.

To address whether the localization of VDGs in relation to the Fab-arm interacting with its antigen influences the ability of VDGs to hinder classical complement activation, we next generated bispecific antibodies (bsAbs) of the 3F3 clone that is only able to bind with one Fab-arm to its antigenic target. The other arm of the antibody molecule is not “fixed” to the antigen and conceivably flexible and potentially able to interact with the C1q-binding site (Figure 5A). We made use of the structure of the mAb 3F3 co-crystallized with the citrullinated vimentin 59-74 antigen (PDB: 6YXK) and identified T100 located in the HC as the main amino acid involved in citrulline binding. The production of T100V mutants allowed us to generate 3F3 WT and NG

parental mAbs (Figure 5B) unable to bind antigen and, as a consequence, complement (Figure 5C). To generate bsAb molecules with only one citrulline binding arm, we introduced additional mutations in the Fc region allowing a controlled Fab-arm exchange³⁶. More specifically, we expressed the 3F3 WT/NG and WT(T100V)/NG(T100V) mutants as parental IgG molecules including two matching point mutations, K409R and F405L respectively, at the C_H3:C_H3 interface. Controlled reduction and reoxidation of the interchain disulfide bonds allowed the mutation-based recombination of H-L pairs resulting in four different 3F3 bsAb (WT+WT(T100V), NG+WT(T100V), WT+NG(T100V) and NG+NG(T100V)) (Figure 5A). The bsAb carrying only one glycosylated Fab-arm (NG+WT(T100V) and WT+NG(T100V)) showed a molecular weight between the fully glycosylated and non-glycosylated variants implying a successful Fab-arm exchange of the parental molecules (Figure 5D). Using these antibody variants, we addressed the question whether C1q binding is more restricted when VDGs are located on the Fab-arm directed towards the C1q-docking interface.

Despite similar antigen-binding strengths (Figure 5E), we observed a decreased C1q deposition to the 3F3WT+WT(T100V) bsAb carrying VDGs on either Fab-arm (Figure 5F). The highest C1q binding was observed for the bsAb depicting no VDGs and an intermediate C1q binding for the bsAb molecules with only one variable region glycosylated Fab-arm. No additional inhibitory effect was detected when the glycans were presented on the Fab-arm pointing towards the C1q binding interface or vice versa [(3F3NG+WT(T100V) or 3F3WT+NG(T100V)] (Figure 5F). Consequently, these results indicate that the impairment of complement activation by VDGs is independent of the glycan location in relation to the C1q-binding interface.

Variable domain glycosylation affects the hexamerization potential of IgG

We reasoned that the inhibitory effect of VDGs on complement activation might be caused by a potentially lower ability of Fab-glycosylated IgG to form hexamers (immune complex formation). The latter has been shown essential for the ability of IgG to activate the classical complement pathway^{37,38}. Therefore, we next wished to determine the extent to which IgG variable domain glycosylation affects the propensity to form hexamers. For this reason, we generated RGY triple mutants (E345R, E430G and S440Y) of the 3F3 WT and NG mAbs. The combination of these three mutations induces effective IgG hexamerization in solution³⁸. We identified the formation of monomeric or oligomeric IgG via size-exclusion chromatography. The data presented in figure 6A reveal predominantly hexameric (IgG)₆ species for both the WT and NG RGY mutants at a concentration of 0.5 mg/ml. As expected, the self-assembling RGY mutants showed a reduced hexamer formation at lower concentrations (Figure 6A).

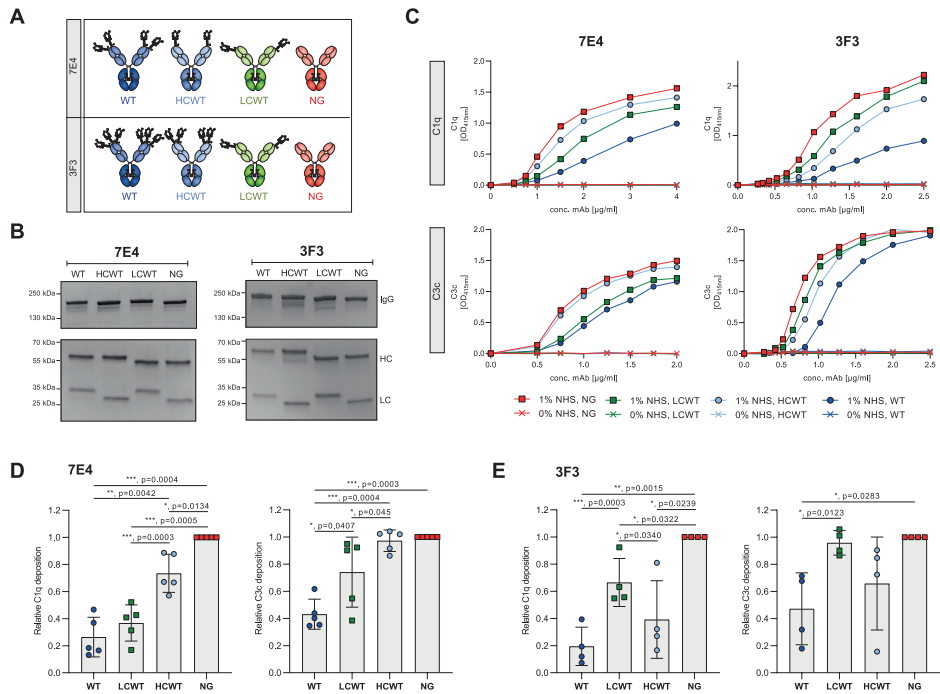


Figure 4. Classical complement pathway activation of monoclonal ACPA IgG 7E4 and 3F3 with a different number of N-linked glycosylation sites in the variable domain of the heavy and light chain. (A) Schematic illustration of the generated 7E4 and 3F3 mAbs. **(B)** 4 to 15% gradient SDS protein gel (BioRad) of purified WT, HCWT, LCWT and NG monoclonal ACPA IgG 7E4 and 3F3. The size-shift caused by the presence of VDGs is visible per mAb-family. The size was determined using the PageRuler™ Plus Prestained Protein Ladder (Thermo Fisher Scientific). **(C)** Classical complement activation. Detection of C1q and C3c deposition on CCP2 bound WT, HCWT, LCWT and NG 7E4 and 3F3 mAbs in the presence of 0% or 1% NHS in GVB++. **(D)** Relative C1q and C3c deposition on CCP2 bound WT, HCWT, LCWT mAb 7E4 compared to its NG counterpart. Each experiment was repeated 5 times and each dot represents one independent experiment. **(E)** Relative C1q and C3c deposition on CCP2 bound WT, HCWT, LCWT mAb 3F3 compared to its NG counterpart. Each experiment was repeated 4 times and each dot represents one independent experiment. Repeated measure one-way ANOVA was performed including the Geissner-Greenhouse correction. The respective p-values are depicted: ns $p > 0.05$, * $p \leq 0.05$, ** $p \leq 0.01$, *** $p \leq 0.001$ or **** $p \leq 0.0001$.

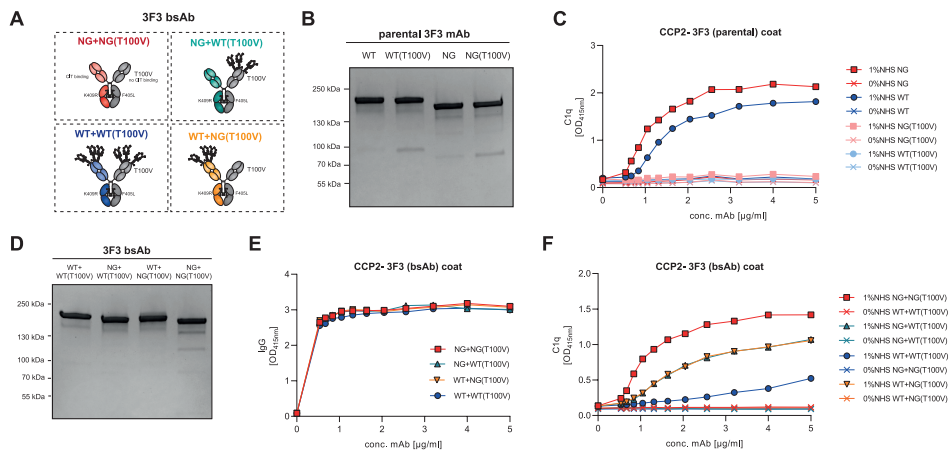


Figure 5. 3F3 bispecific antibodies (bsAb) with only one citrullinated antigen-binding arm (T100V) and varying amounts of VDGs generated via controlled Fab-arm exchange. **(A)** Schematic illustration of the four 3F3 bsAb variants generated including a T100V mutation in one of the Fab-arms to abrogate antigen-specific C1q deposition [NG+NG(T100V), NG+WT(T100V), WT+NG(T100V) and WT+WT(T100V)]. The 3F3 bsAbs harbor a K409R and F405L point-mutation in the $C_H3:C_H3$ interface to allow controlled Fab-arm exchange³⁶. **(B)** 4 to 15% gradient SDS protein gel (BioRad) of the parental 3F3 mAbs under non-reducing (IgG) conditions. The size-shift between the different variants depicts the amount of VDGs present: NG and NG(T100V) < WT and WT(T100V). **(C)** C1q deposition on CCP2 bound parental 3F3 mAbs after adding 0% or 1% NHS in GVB++. **(D)** 4 to 15% gradient SDS protein gel (BioRad) of 3F3 bsAb under non-reducing (IgG) conditions. The size-shift between the different variants depicts the amount of VDGs present: NG+NG(T100V) < NG+WT(T100V) = WT+NG(T100V) < WT+WT(T100V). **(E)** Detection of 3F3 IgG bsAb [WT+WT(T100V), WT+NG(T100V), NG+WT(T100V), NG+NG(T100V)] binding to CCP2-coated ELISA plate. **(F)** C1q deposition on CCP2 bound 3F3 bsAbs after adding 0% or 1% NHS in GVB++.

Interestingly, a reduction in hexamer formation was most prominently observed for the WT RGY mutant indicating that under these conditions, the presence of VDGs lowers hexamerization (Figure 6A). Thus, the WT and NG RGY mutants showed different oligomerization efficiencies at the concentrations tested (Figure 6, B and C). The decreased ability of WT RGY mutants to form hexamers was further confirmed by native gel-electrophoresis, showing less prominent intensities at a high molecular weight expected for (IgG)₆ molecules as compared to the NG RGY (Figure 6D). The clear size difference between the WT and NG RGY reflects the presence or absence of VDGs (Figure 6, C and D). Despite a similar IgG deposition to the ELISA plate (Figure 6F), we observed, as anticipated, a considerably higher C1q and C3c deposition for the NG RGY mutant compared to the non-mutated monomeric NG variant (Figure 6, E and F). This reflects the increased ability of IgG hexamers to bind C1q as compared to the monomeric molecules when coated to the ELISA plate. When comparing the WT RGY to the NG RGY variant, we detected a significantly decreased C1q and C3c deposition to the variable domain glycosylated variant (Figure 6, E and F). The observed difference in the classical pathway activation is in line with the inhibitory effect of VDGs on the propensity of IgG to form hexamers. An effect of Fc glycans can be excluded as both RGY variants showed a similar Fc glycan composition (Figure S1D).

To further validate the observations described above, we coated the ELISA plate with recombinant C1q and assessed binding of the RGY mutants and the monomeric 3F3 IgG respectively. No binding of the monomeric IgG to C1q was observed (Figure 6G) as IgG is only capable of interacting with C1q in an oligomeric form or when complexed on the ELISA plate. In contrast, the RGY (IgG)₆ antibodies showed binding to the recombinant C1q in a dose-dependent manner. Importantly, also in this assay increased interaction with C1q was noted for the NG RGY mutant as compared to the WT RGY mutant (Figure 6G). The presence of NaCl abrogated the binding of both WT and NG RGY mutants to C1q to the same extent, indicating similar affinities of both variants to the C1q globular head domains when oligomerized (Figure S6A). We further confirmed the increased binding of human C1q to the NG RGY mutants compared to their VDG counterparts with western blot analysis (Figure S6D). The data thus show that VDGs decrease the potential of Fc:Fc interactions and thereby affect C1q interactions and complement activity.

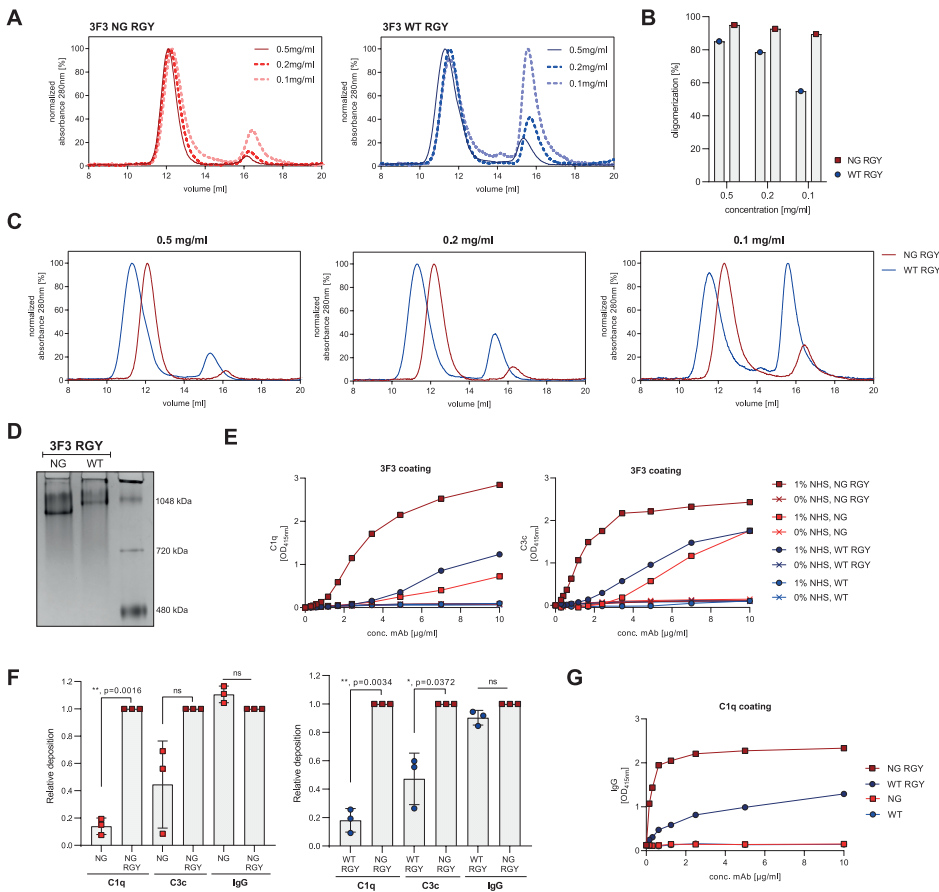


Figure 6. Propensity of 3F3 WT and NG 3F3 mAb IgG RGY mutants to form hexamers and their ability to activate the classical complement pathway. (A) Size exclusion chromatograms (SEC) of WT and NG RGY mutants in a concentration dependent manner (0.5 mg/ml, 0.2 mg/ml and 0.1 mg/ml), which elute at a size of oligomeric or monomeric structures. (B) Oligomerization efficiency of WT and NG RGY mutants at a concentration of 0.1 mg/ml, 0.2 mg/ml and 0.5 mg/ml. (C) Representative SEC chromatogram overlays of WT and NG RGY mutants at the different concentrations analyzed. (D) Native 7% TRIS-acetate gel (Novex NuPAGE) of WT and NG RGY mutants depicting a high apparent molecular weight. The size was determined using the NativeMark unstained protein standard (Invitrogen). (E) C1q and C3c deposition after mAb WT, NG, WT RGY and NG RGY (0 to 10 µg/ml) coating and in the presence of 0% or 1% NHS in GVB++. (F) Relative C1q, C3c and IgG deposition of NG vs. NG RGY and of WT RGY vs. NG RGY. Each experiment was repeated 3 times and each dot represents one independent experiment. Repeated measure one-way ANOVA was performed including the Geissner-Greenhouse correction. The respective p-values are depicted: ns $p > 0.05$, * $p \leq 0.05$, ** $p \leq 0.01$, *** $p \leq 0.001$ or **** $p \leq 0.0001$. (G) Detection of WT, NG, WT RGY and NG RGY (0 to 10 µg/ml) binding to C1q-coated ELISA plate.

Discussion

The disease-specific autoantibodies from RA patients, ACPA IgG, are hyperglycosylated in the variable domains. Recent studies have shown that the degree of ACPA IgG variable domain glycosylation rises towards RA-onset^{17,19} and is predictive for disease development¹⁸, suggesting a functional relevance of this post-translational glycan modification. Intriguingly, VDGs are also profoundly expressed on (auto)antibodies from individuals with AAV, MS, SLE and pSS as well as on inflammation-associated anti-hinge antibodies^{26,39-41}. However, in contrast to IgG Fc glycans, the functional significance of IgG VDGs and their contribution to immune effector mechanisms of antibodies are thus far unknown.

In this study, we characterized the impact of hyperglycosylated variable domains on complement initiation and activation. We generated three ACPA IgG and one anti-TT IgG mAb with a different number of naturally occurring VDGs as well as variants with germline-encoded amino acids lacking the N-linked glycan sites. Our results show a notably decreased C1q-binding ability and deposition of classical complement components in the presence of VDGs. We noted greater complement inhibition in the presence of increasing numbers of VDGs, which correlated with a gradual reduction in C1q binding and subsequent C4 and C3c deposition. As no or only a marginal impact of VDGs on the alternative pathway activation was observed, in contrast to a prominent effect on C1q binding, the influence of VDGs to modulate complement activation is likely restricted to the initiation of the classical pathway. Because evolutionary conserved IgG Fc glycans are known to modulate the complement-activating abilities of IgG, we ruled out the possibility that the observed differences were due to variations in Fc glycan compositions. We therefore confirmed that all mAb-pairs (WT and NG) were generated with a similar Fc glycan profile. In line with previous studies, different Fc glycan profiles, as observed for the glycoengineered versus non-glycoengineered mAb variants, showed somewhat elevated complement deposition with increasing levels of Fc galactosylation^{30,33}.

To provide mechanistic insight into how VDGs regulate the ability of IgG to activate complement, we hypothesized different scenarios. As VDGs affect the (thermo)stability⁴² and thus potentially the structure of IgG molecules, we assumed that they may affect the flexibility of the C_H2 domains, the known binding interfaces for C1q. Thereby VDGs may directly alter C1q-binding affinity. However, our data showing a similar abrogated binding of antibodies with or without VDGs in the presence of NaCl, indicate similar avidities of both variants to the C1q globular heads. Another possibility could be that the bulky glycans attached to the variable domain directly interact with C1q. Our results based on bispecific antibody molecules presenting VDGs either in the Fab-arm pointing towards the C1q-binding interface or the Fab-arm interacting with the antigen, argue however against this hypothesis. The position of the VDGs in relation to the C1q-docking site was not relevant

for the dampening effect on C1q binding. A third possibility could be that VDGs alter the spatial orientation of IgG molecules resulting in diminished Fc:Fc interactions and thus hexamerization. This would be in line with previous findings showing that antibody Fab-arms can contribute to immune complex formation and thereby influence C1 activation³⁸. Our results also support this scenario, as VDGs decreased the potential of IgG molecules to form hexamers in solution. We observed a decreased tendency of WT RGY variants to form spontaneous hexamers in the absence of their cognate antigen. Accordingly, it can be assumed that glycans attached to variable domain impact on IgG oligomerization, potentially by steric repulsion, which provides a mechanistic explanation for the decreased C1q-binding ability and diminished classical complement activation.

Further studies need to investigate how glycans impact on the oligomerization efficiency of IgG molecules. For example, it still needs to be elucidated, if distinct VDG compositions (differences in sialylation, galactosylation or bisection) impact differently on the oligomerization propensity of IgG. However, this analysis is likely challenging because changes in Fab glycan compositions, due to treatment with specific glycosidases, are always accompanied by changes in the Fc-glycan profile. In addition, it remains to be investigated, whether the location of the N-linked glycan site is important for the observed effects. Based on our results, it is tempting to speculate that glycans attached to the V_L have a more pronounced effect because they may be more flexible and thus sterically more demanding compared to V_H N-linked glycans. However, further studies need to be performed analyzing multiple clones that express V_H or V_L restricted VDGs. Exploring which VDGs have the most pronounced effect on hexamerization and subsequent complement activation, would allow us to specifically design monoclonal antibodies with boosted therapeutic potencies by taming down their Fc domain-mediated effector functions, such as complement-dependent cytotoxicity (CDC).

In conclusion, although it is not possible to conclude from our data, if and how hyperglycosylated autoantibodies from RA patients contribute to disease pathogenesis or if they might have a protective effect, our results clearly show that a post-translational glycan modification on top of the IgG variable domain can be exploited to “switch off” the antibody-dependent classical complement pathway.

Materials and Methods

Blood samples from patients diagnosed with RA - Peripheral blood samples from ACPA-positive (ACPA⁺, > 340 U/ml) patients with RA visiting the outpatient clinic of the Rheumatology Department at the Leiden University Medical Center (LUMC) were included in this study. All patients fulfilled the EULAR/ACR 2010-criteria for classification of RA⁴³. None of the patients

were previously treated with B-cell depletion therapies. Blood samples were obtained on written informed consent prior to inclusion and with approval from the local ethics committee of the LUMC, The Netherlands. Patient characteristics were previously described⁴⁴.

Recombinant mAb production, generation of RGY mutants and bsAb molecules - Monoclonal antibodies (mAbs) were generated based on full-length BCR sequences from ACPA-positive patients with RA or healthy donors. Labelled CCP2- and CArgP2-streptavidin tetramers or tetanus toxoid (TT) (Statens Serum Institute) were used to single cell isolate ACPA or anti-TT-expressing B cells as previously described⁴⁵. RNA isolation, cDNA synthesis, ARTISAN PCR and BCR sequencing were performed as described earlier^{27,46}. The 7E4 sequence was provided by Dr. Rispens, Sanquin, The Netherlands⁴⁷. To generate mAbs without the naturally occurring variable domain glycans, N-linked glycan motifs (N-X-S/T, X ≠ P) in the Fab-domains were specifically mutated back to the germline amino acid sequence (based on IMGT) at the respective position (Table S1). Wild-type (WT), including N-linked glycan sites, and non-glycosylated (NG), including only the conserved Fc N-linked glycan sites, BCR sequences were codon-optimized and the HC/LC variable genes together with 5'-BamHI and 3'-XhoI restriction sites, the Kozak sequence, and the IGHV1-18*01 leader sequence ordered from GeneArt (Life Technologies). The constructs were ligated into the pcDNA3.1 (+) expression vector (Invitrogen) carrying the IGHG1 or the IGLC3/IGKC constant regions (UniProt) respectively flanking 3'-XhoI site. The recombinant monoclonal antibodies were produced in Freestyle™ 293-F cells (Gibco) as previously stated⁴⁴. Glycoengineering (ge) was performed by adding D-galactose substrate (Sigma, G0750-5G) and by a co-transfection with 1% β-1,4-N-acetylglucosaminyltransferase III (GnTIII), 2.5% α2,6-sialyltransferase 1 (ST6galT) and 1% β-1,4-galactosyltransferase 1 (B4GalT1). The supernatants were harvested 5 to 6 days post-transfection. IgG1 antibodies were purified using a 1 ml HiTrap® Protein G HP affinity column (GE Healthcare) followed by a direct buffer exchange (53 ml HiPrep™ 26/10 Desalting column, GE Healthcare). In total three ACPA (7E4, 3F3 and 2G9) and one anti-TT (D2) monoclonal were generated as IgG1. Additionally, we produced the 7E4 and 3F3 mAbs with only the HC (HCWT) or the LC (LCWT) N-linked glycans, respectively. For RGY mutants, the 3F3 WT and NG HC were generated including three point-mutations (E345R, E430G and S440Y) in the IGHG1*01 constant domain³⁷. The mutated HC sequences were ordered from GeneArt (Life Technologies) and cloned as described above. 3F3 RGY mutants were produced in Freestyle™ 293-F cells (Gibco) with glycoengineering as mentioned above.

To produce 3F3 bispecific antibodies (bsAbs) that bind only with one Fab-arm to citrullinated antigens, we made use of the 3F3 crystal structure (PDB: 6YXK) and introduced the T100V point-mutation into the HC CDR3. Next, two matching point-mutations, K409R and F405L, were introduced into the C_H3 interface of 3F3WT/NG or 3F3WT(T100V)/NG(T100V), respectively. All point-mutations were introduced using the Q5 Site-Directed Mutagenesis Kit (NEB, E0554S). After the production of the parental 3F3 WT(K409R), NG(K409R), WT(T100V, F405L) and NG(T100V,

F405L) mAbs in Freestyle™ 293-F cells (Gibco) as described above, the bsAb molecules were generated with the controlled Fab-arm exchange method as previously described³⁶. In brief, 50 µg of the parental 3F3 mAb pairs were mixed in equimolar amounts and incubated with 750 mM cysteamide hydrochloride (Sigma Aldrich) for 5 hours at 31 °C for reduction. Reoxidation and buffer exchange was performed using ultra centrifugal filters (50,000 MWCO, Merck Millipore) and PBS. This method allows a mutation-based recombination of HC-LC pairs resulting in four 3F3 bsAb molecules [WT+WT(T100V), NG+WT(T100V), WT+NG(T100V) and NG+NG(T100V)].

Integrity and size characterization of mAbs - The human mAb integrity and the expression of the VDGs was analyzed via size-exclusion chromatography (SEC), SDS gel electrophoresis and native gel electrophoresis. SEC was performed using a Superose6Increase, 10/300 GL column (GE Healthcare). The recombinant proteins were monitored by UV absorption at 280 nm. For sodium dodecyl sulfate (SDS) polyacrylamide gel electrophoresis (PAGE), 1.5 µg of the mAbs were diluted in 4× Laemmli buffer (Bio Rad) with (reduced) or without (non-reduced) 2% β-mercaptoethanol (Sigma Aldrich) and incubated for 5 min at 95 °C. Samples and PageRuler™ Plus Prestained Protein Ladder (Thermo Fisher Scientific) were loaded on 4 to 15% SDS-polyacrylamide gels (Bio Rad). For native gel electrophoresis, 1 to 4 µg of the RGY mutants were diluted in 2× TRIS-glycine native sample buffer (Novex) and applied to a 7% TRIS-acetate gel (Novex NuPAGE) together with the NativeMark Unstained Protein Standard (Invitrogen). For protein detection gels were stained with Coomassie Brilliant Blue G-250 Dye (Thermo Fisher Scientific).

Fc-glycopeptide and variable domain glycosylation mass spectrometry (MS) analysis -

Matrix Assisted Laser Desorption Ionization Time of Flight (MALDI-TOF) MS analysis of released N-glycans was performed as previously described⁴⁸. In brief, the IgG samples (10 µg) were reduced in 2% SDS and incubated with 0.5 U N-glycosidase F, PNGase F, (Roche Diagnostics, Germany), in 1:1 5xPBS/ 4% NP-40, overnight at 37 °C. The total released glycans were stabilized with ethylation reagent (0.5 M EDC hydrochloride and 0.5 M 1-hydroxybenzotriazole hydrate) for 1 hour at 37 °C. Glycans were purified in 85% acetonitrile (ACN) (Biosolve, Valkenswaard, The Netherlands) with 15 µl cotton hydrophilic interaction liquid chromatography (HILIC) tips using 85% ACN and 85% ACN+1% TFA for washing. Released and purified N-glycans were eluted from the HILIC tips using MQ and 1 µl spotted on a MALDI target (MTP AnchorChip 800/384 TF; Bruker Daltonics) together with 1 µl 5 mg/ml super-DHB in 50% ACN and 1 mM NaOH. Spots were dried on room temperature (RT) and analyzed on an UltrafleXtreme (Bruker Daltonics) operated under flexControl 3.3 (Build 108; Bruker Daltonics). A mass spectrum from m/z 1000 to 3000 was recorded, combining 10000 shots in a random walk pattern at 1000 Hz. The instrument was calibrated with a peptide calibration standard (Bruker Daltonics). MS data were analyzed using flexControl 3.3 and glycan peaks above S/N of nine were included into the analysis.

Liquid chromatography-mass spectrometry (LC-MS) Fc-glycopeptide analysis was performed as previously described⁴⁹. Briefly, denatured mAbs were trypsinized using 200 ng sequencing grade modified trypsin (Promega) in 50 mM ammonium bicarbonate overnight at 37 °C. For total N-glycan LC-MS analysis, glycans were released using 2 U PNGase F as described above, labeled with 2-aminobenzoic acid (2-AA, Sigma Aldrich) and 2-picoline borane (2-PB, Sigma Aldrich) and purified using 15 µl cotton HILIC tips as described earlier. Trypsinized samples or released and purified glycans were separated and analyzed on an Ultimate 3000 UHPLC system (Dionex/ Thermo Fisher Scientific, Breda, The Netherlands) coupled to a MaXis Impact HD quadrupole-TOF mass spectrometer (MaXis HD, Bruker Daltonics, Bremen, Germany) equipped with a CaptiveSpray NanoBooster source (Bruker Daltonics, Bremen, Germany) as previously described⁴⁹⁻⁵¹. Mass spectra were acquired within a mass range of m/z 550 to 1800. LC-MS data were first examined manually using DataAnalysis (Bruker Daltonics). Data processing, including peak integration, was performed using LaCyTools v1.1.0. Glycans with a S/N above nine, a mass accuracy of ± 20 and an isotopic peak quality (IPQ) of 0.2 were included into the analysis⁵².

Complement activation assays - To analyze the complement activating potential of mAbs with different quantities of VDGs, enzyme-linked immunosorbent assays (ELISA) were performed in a similar way than previously described¹⁵. In short, mAbs were coated directly to Nunc Maxisorp plates (Thermo Fisher Scientific) in coating buffer [100 mM Na₂CO₃/NaHCO₃ (pH 9.6)] overnight at 4 °C. Or mAbs were diluted in PBS/ 0.05% Tween/ 1% BSA (PBT) and added to streptavidin plates (Microcoat, #65001) pre-coated with biotinylated CCP2 (1 µg/ml) overnight at 4 °C⁴⁴. The mAb concentrations used are mentioned in the respective figure legends. To obtain a similar coating, the CCP2 concentrations were adjusted for the 7E4 WT (1.9 µg/ml) and NG (0.95 µg/ml) mAb variants. Comparable deposition of WT and NG mAbs to the ELISA plate was verified using a HRP-conjugated rabbit-anti-human IgG secondary detection antibody (DAKO, P0214, 1:5000).

For complement activation, 0%, 0.5%, 1% or 10% complement-active normal human serum (NHS) diluted either in GVB++ (veronal buffered saline [VBS] containing 0.5 mM MgCl₂, 2 mM CaCl₂, 0.05% Tween 20, and 0.1% gelatin [pH 7.5]) or Mg-EGTA (VBS containing 10 mM EGTA, 5 mM MgCl₂, 0.05% Tween 20, and 0.1% gelatin [pH 7.5]) buffer was added for 1 hour at 37 °C. Complement deposition on the mAbs was determined by adding rabbit anti-C1q (DAKO, A0136, 1:1000), goat anti-C4 (QUIDEL, A305, 1:1000) or rabbit anti-C3c (DAKO, A0062, 1:1000) secondary antibodies in PBT for 1 hour at 37 °C. Binding was detected using matched and HRP-labelled goat anti-rabbit (DAKO, P0448, 1:3000) or rabbit anti-goat (DAKO, P0449, 1:3000) detection antibodies diluted in PBT for 1 hour at 37 °C. The plates were developed using the substrate ABTS, and absorbance was read at 415 nm. A schematic overview of this assay is shown in figure 2A. To identify direct interactions with C1q, 10 µg/ml of the recombinant C1q protein was directly coated to Nunc Maxisorp plates (Thermo Fisher Scientific) in coating buffer

for 1 hour at 37 °C. After blocking with PBS/ 1% BSA for 1 hour at 37 °C, mAbs were added in PBT and incubated for 1 hour at 37 °C. Binding of the IgG mAbs to C1q was detected using HRP-labelled F(ab')₂ Fragment rabbit anti-human IgG (Jackson ImmunoResearch, #309-036-003) diluted 1:5000 in PBT and incubated for 1 hour at 37 °C. The plates were developed using the substrate ABTS, and absorbance was read at 415 nm.

Western blot analysis - C1q binding to the 3F3 WT and NG RGY mutants was analyzed via western blot analyses. Therefore, 1 to 4 µg of the respective RGY mutants was diluted in 2× TRIS-glycine native sample buffer (Novex) and applied to a 7% TRIS-acetate gel (Novex NuPAGE). The native gel was incubated for 1 hour in a buffer containing 0.05% SDS, 0.0125M Tris and 0.1 M glycine to achieve a negative protein charge and subsequently immunoblotted on a Nitrocellulose membrane (Bio Rad). The blot was incubated in PTE (3% skim milk powder/ PBS/0.05% tween) for 1 hour at RT. Following washing with PBS/0.05% tween (PT), the blot was incubated at 4 °C overnight with 8 µg human native C1q (CompTech) diluted in 5 ml PTE. After washing with PT, the blot was incubated for 1 hour at RT with 5 ml PTE containing 1:1000 rabbit anti-human C1q (#A0136, DAKO). Binding was detected using an HRP-labelled goat anti-rabbit (DAKO, P0448, 1:1000) detection antibody diluted in PT for 2 hours at 37 °C. The blot was washed and bound antibodies visualized using enhanced chemiluminescence (GE Healthcare, RPN2109). The readout was performed on a Bio Rad Chemidoc Touch Imaging system.

Statistical analysis - Repeated measure (RM) one-way ANOVA including the Geissner-Greenhouse correction, ordinary (no pairing) one-way ANOVA or paired t-tests were performed using the GraphPad Prism software (GraphPad Prism 8.0.1 software). P values less than 0.05 were considered significant: ns $p > 0.05$, * $p \leq 0.05$, ** $p \leq 0.01$, *** $p \leq 0.001$ or **** $p \leq 0.0001$.

Acknowledgments

We thank J.-W. Drijfhout (LUMC, Leiden, The Netherlands) for providing the citrullinated peptides.

Funding

This work was supported by ReumaNederland 17-1-402 (to R.E.M.T.), the IMI-funded project RTCure 777357 (to T.W.J.H.), ZonMw TOP 91214031 (to R.E.M.T.), Target-to-B LSHM18055-SGF (to R.E.M.T.), NWO-ZonMW clinical fellowship 90714509 (to H.U.S.), NWO-ZonMW VENI grant 91617107 (to H.U.S.), ZonMW Enabling Technology Hotels grant 435002030 (to H.U.S.) and the Dutch Arthritis Foundation 15-2-402 and 18-1-205 (to H.U.S.).

Author contributions

All authors were involved in drafting the article or revising it critically for important intellectual content, and all authors approved the final version to be published. Conceptualization: T.K. and R.E.M.T. Methodology: T.K., S.v.d.B., H.J.v.D., A.S.B., J.C.K., E.M.S., C.K. Investigation: T.K., S.v.d.B., H.J.v.D., A.S.B., E.M.S. Visualization: T.K. Supervision: L.A.T. and R.E.M.T. Writing—original draft: T.K. and R.E.M.T. Writing—review and editing: T.K., S.v.d.B., H.J.v.D., A.S.B., J.C.K., E.M.S., C.K., M.W., T.W.J.H., H.U.S., L.A.T. and R.E.M.T.

Conflict of interest

H.U.S., T.W.J.H., and R.E.M.T. are mentioned as inventors on a patent on ACPA IgG V-domain glycosylation. The other authors declare that they have no competing interests.

Data and materials availability

We confirm that the data supporting the findings of this study are available within the article and/or the Supplementary Materials. The 7E4 sequence and antibodies can be provided by T.R. (Sanquin Research, The Netherlands) under the protection of a completed material transfer agreement.

References

- 1 Walport, M. J., Complement. Second of two parts. *N Engl J Med* 2001. 344: 1140-1144.
- 2 Walport, M. J., Complement. First of two parts. *N Engl J Med* 2001. 344: 1058-1066.
- 3 Trouw, L. A., Blom, A. M. and Gasque, P., Role of complement and complement regulators in the removal of apoptotic cells. *Mol Immunol* 2008. 45: 1199-1207.
- 4 Sjoberg, A. P., Trouw, L. A. and Blom, A. M., Complement activation and inhibition: a delicate balance. *Trends Immunol* 2009. 30: 83-90.
- 5 Dhillon, S., Eculizumab: A Review in Generalized Myasthenia Gravis. *Drugs* 2018. 78: 367-376.
- 6 Jayne, D. R. W., Bruchfeld, A. N., Harper, L., Schaier, M., Venning, M. C., Hamilton, P., et al., Randomized Trial of C5a Receptor Inhibitor Avacopan in ANCA-Associated Vasculitis. *J Am Soc Nephrol* 2017. 28: 2756-2767.
- 7 Wouters, D., Voskuyl, A. E., Molenaar, E. T., Dijkmans, B. A. and Hack, C. E., Evaluation of classical complement pathway activation in rheumatoid arthritis: measurement of C1q-C4 complexes as novel activation products. *Arthritis Rheum* 2006. 54: 1143-1150.
- 8 Brodeur, J. P., Ruddy, S., Schwartz, L. B. and Moxley, G., Synovial fluid levels of complement SC5b-9 and fragment Bb are elevated in patients with rheumatoid arthritis. *Arthritis Rheum* 1991. 34: 1531-1537.
- 9 Swaak, A. J., Van Rooyen, A., Planten, O., Han, H., Hattink, O. and Hack, E., An analysis of the levels of complement components in the synovial fluid in rheumatic diseases. *Clin Rheumatol* 1987. 6: 350-357.
- 10 Konttinen, Y. T., Ceponis, A., Meri, S., Vuorikoski, A., Kortekangas, P., Sorsa, T., et al., Complement in acute and chronic arthritides: assessment of C3c, C9, and protectin (CD59) in synovial membrane. *Ann Rheum Dis* 1996. 55: 888-894.
- 11 Nielen, M. M., van Schaardenburg, D., Reesink, H. W., van de Stadt, R. J., van der Horst-Bruinsma, I. E., de Koning, M. H., et al., Specific autoantibodies precede the symptoms of rheumatoid arthritis: a study of serial measurements in blood donors. *Arthritis Rheum* 2004. 50: 380-386.
- 12 van Boekel, M. A., Vossenaar, E. R., van den Hoogen, F. H. and van Venrooij, W. J., Autoantibody systems in rheumatoid arthritis: specificity, sensitivity and diagnostic value. *Arthritis Res* 2002. 4: 87-93.
- 13 van Gaalen, F. A., Linn-Rasker, S. P., van Venrooij, W. J., de Jong, B. A., Breedveld, F. C., Verweij, C. L., et al., Autoantibodies to cyclic citrullinated peptides predict progression to rheumatoid arthritis in patients with undifferentiated arthritis: a prospective cohort study. *Arthritis Rheum* 2004. 50: 709-715.
- 14 Kuhn, K. A., Kulik, L., Tomooka, B., Braschler, K. J., Arend, W. P., Robinson, W. H., et al., Antibodies against citrullinated proteins enhance tissue injury in experimental autoimmune arthritis. *J Clin Invest* 2006. 116: 961-973.
- 15 Trouw, L. A., Haisma, E. M., Levarht, E. W., van der Woude, D., Ioan-Facsinay, A., Daha, M. R., et al., Anti-cyclic citrullinated peptide antibodies from rheumatoid arthritis patients activate complement via both the classical and alternative pathways. *Arthritis Rheum* 2009. 60: 1923-1931.
- 16 Hafkenscheid, L., Bondt, A., Scherer, H. U., Huizinga, T. W., Wuhler, M., Toes, R. E., et al., Structural Analysis of Variable Domain Glycosylation of Anti-Citrullinated Protein Antibodies in Rheumatoid Arthritis Reveals the Presence of Highly Sialylated Glycans. *Mol Cell Proteomics* 2017. 16: 278-287.
- 17 Kissel, T., van Schie, K. A., Hafkenscheid, L., Lundquist, A., Kokkonen, H., Wuhler, M., et al., On the presence of HLA-SE alleles and ACPA-IgG variable domain glycosylation in the phase preceding the development of rheumatoid arthritis. *Ann Rheum Dis* 2019. 78: 1616-1620.
- 18 Hafkenscheid, L., de Moel, E., Smolik, I., Tanner, S., Meng, X., Jansen, B. C., et al., N-Linked Glycans in the Variable Domain of IgG Anti-Citrullinated Protein Antibodies Predict the Development of Rheumatoid Arthritis. *Arthritis Rheumatol* 2019. 71: 1626-1633.

- 19 Kissel, T., Hafkenscheid, L., Wesemael, T. J., Tamai, M., Kawashiri, S. Y., Kawakami, A., et al., ACPA-IgG variable domain glycosylation increases before the onset of rheumatoid arthritis and stabilizes thereafter; a cross-sectional study encompassing 1500 samples. *Arthritis Rheumatol* 2022.
- 20 Vergoesen, R. D., Slot, L. M., Hafkenscheid, L., Koning, M. T., van der Voort, E. I. H., Grooff, C. A., et al., B-cell receptor sequencing of anti-citrullinated protein antibody (ACPA) IgG-expressing B cells indicates a selective advantage for the introduction of N-glycosylation sites during somatic hypermutation. *Ann Rheum Dis* 2018. 77: 956-958.
- 21 Vergoesen, R. D., Slot, L. M., van Schaik, B. D. C., Koning, M. T., Rispens, T., van Kampen, A. H. C., et al., N-Glycosylation Site Analysis of Citrullinated Antigen-Specific B-Cell Receptors Indicates Alternative Selection Pathways During Autoreactive B-Cell Development. *Front Immunol* 2019. 10: 2092.
- 22 Kissel, T., Ge, C., Hafkenscheid, L., Kwekkeboom, J. C., Slot, L. M., Cavallari, M., et al., Surface Ig variable domain glycosylation affects autoantigen binding and acts as threshold for human autoreactive B cell activation. *Sci Adv* 2022. 8: eabm1759.
- 23 Kasermann, F., Boerema, D. J., Rueggsegger, M., Hofmann, A., Wymann, S., Zuercher, A. W., et al., Analysis and functional consequences of increased Fab-sialylation of intravenous immunoglobulin (IVIg) after lectin fractionation. *PLoS One* 2012. 7: e37243.
- 24 Xu, P. C., Gou, S. J., Yang, X. W., Cui, Z., Jia, X. Y., Chen, M., et al., Influence of variable domain glycosylation on anti-neutrophil cytoplasmic autoantibodies and anti-glomerular basement membrane autoantibodies. *BMC Immunol* 2012. 13: 10.
- 25 Hamza, N., Hersherberg, U., Kallenberg, C. G., Vissink, A., Spijkervet, F. K., Bootsma, H., et al., Ig gene analysis reveals altered selective pressures on Ig-producing cells in parotid glands of primary Sjogren's syndrome patients. *J Immunol* 2015. 194: 514-521.
- 26 Visser, A., Hamza, N., Kroese, F. G. M. and Bos, N. A., Acquiring new N-glycosylation sites in variable regions of immunoglobulin genes by somatic hypermutation is a common feature of autoimmune diseases. *Ann Rheum Dis* 2018. 77: e69.
- 27 Huijbers, M. G., Vergoossen, D. L., Fillie-Grijpma, Y. E., van Es, I. E., Koning, M. T., Slot, L. M., et al., MuSK myasthenia gravis monoclonal antibodies: Valency dictates pathogenicity. *Neurol Neuroimmunol Neuroinflamm* 2019. 6: e547.
- 28 Mandel-Brehm, C., Fichtner, M. L., Jiang, R., Winton, V. J., Vazquez, S. E., Pham, M. C., et al., Elevated N-Linked Glycosylation of IgG V Regions in Myasthenia Gravis Disease Subtypes. *J Immunol* 2021. 207: 2005-2014.
- 29 van de Bovenkamp, F. S., Derksen, N. I. L., Ooijevaar-de Heer, P., van Schie, K. A., Kruithof, S., Berkowska, M. A., et al., Adaptive antibody diversification through N-linked glycosylation of the immunoglobulin variable region. *Proc Natl Acad Sci U S A* 2018. 115: 1901-1906.
- 30 Dekkers, G., Treffers, L., Plomp, R., Bentlage, A. E. H., de Boer, M., Koeleman, C. A. M., et al., Decoding the Human Immunoglobulin G-Glycan Repertoire Reveals a Spectrum of Fc-Receptor- and Complement-Mediated-Effector Activities. *Front Immunol* 2017. 8: 877.
- 31 Lund, J., Takahashi, N., Pound, J. D., Goodall, M. and Jefferis, R., Multiple interactions of IgG with its core oligosaccharide can modulate recognition by complement and human Fc gamma receptor I and influence the synthesis of its oligosaccharide chains. *J Immunol* 1996. 157: 4963-4969.
- 32 Tao, M. H. and Morrison, S. L., Studies of aglycosylated chimeric mouse-human IgG. Role of carbohydrate in the structure and effector functions mediated by the human IgG constant region. *J Immunol* 1989. 143: 2595-2601.
- 33 Peschke, B., Keller, C. W., Weber, P., Quast, I. and Lunemann, J. D., Fc-Galactosylation of Human Immunoglobulin Gamma Isotypes Improves C1q Binding and Enhances Complement-Dependent Cytotoxicity. *Front Immunol* 2017. 8: 646.

- 34 Quast, I., Keller, C. W., Maurer, M. A., Giddens, J. P., Tackenberg, B., Wang, L. X., et al., Sialylation of IgG Fc domain impairs complement-dependent cytotoxicity. *J Clin Invest* 2015. 125: 4160-4170.
- 35 van Osch, T. L. J., Nouta, J., Derksen, N. I. L., van Mierlo, G., van der Schoot, C. E., Wuhrer, M., et al., Fc Galactosylation Promotes Hexamerization of Human IgG1, Leading to Enhanced Classical Complement Activation. *J Immunol* 2021. 207: 1545-1554.
- 36 Labrijn, A. F., Meesters, J. I., Priem, P., de Jong, R. N., van den Bremer, E. T., van Kampen, M. D., et al., Controlled Fab-arm exchange for the generation of stable bispecific IgG1. *Nat Protoc* 2014. 9: 2450-2463.
- 37 Diebold, C. A., Beurskens, F. J., de Jong, R. N., Koning, R. I., Strumane, K., Lindorfer, M. A., et al., Complement is activated by IgG hexamers assembled at the cell surface. *Science* 2014. 343: 1260-1263.
- 38 Wang, G., de Jong, R. N., van den Bremer, E. T., Beurskens, F. J., Labrijn, A. F., Ugurlar, D., et al., Molecular Basis of Assembly and Activation of Complement Component C1 in Complex with Immunoglobulin G1 and Antigen. *Mol Cell* 2016. 63: 135-145.
- 39 Vletter, E. M., Koning, M. T., Scherer, H. U., Veelken, H. and Toes, R. E. M., A Comparison of Immunoglobulin Variable Region N-Linked Glycosylation in Healthy Donors, Autoimmune Disease and Lymphoma. *Front Immunol* 2020. 11: 241.
- 40 Biermann, M. H., Griffante, G., Podolska, M. J., Boeltz, S., Sturmer, J., Munoz, L. E., et al., Sweet but dangerous - the role of immunoglobulin G glycosylation in autoimmunity and inflammation. *Lupus* 2016. 25: 934-942.
- 41 Kempers, A. C., Hafkenscheid, L., Dorjee, A. L., Moutousidou, E., van de Bovenkamp, F. S., Rispens, T., et al., The extensive glycosylation of the ACPA variable domain observed for ACPA-IgG is absent from ACPA-IgM. *Ann Rheum Dis* 2018. 77: 1087-1088.
- 42 van de Bovenkamp, F. S., Derksen, N. I. L., van Breemen, M. J., de Taeye, S. W., Ooijevaar-de Heer, P., Sanders, R. W., et al., Variable Domain N-Linked Glycans Acquired During Antigen-Specific Immune Responses Can Contribute to Immunoglobulin G Antibody Stability. *Front Immunol* 2018. 9: 740.
- 43 Aletaha, D., Neogi, T., Silman, A. J., Funovits, J., Felson, D. T., Bingham, C. O., 3rd, et al., 2010 rheumatoid arthritis classification criteria: an American College of Rheumatology/European League Against Rheumatism collaborative initiative. *Ann Rheum Dis* 2010. 69: 1580-1588.
- 44 Kissel, T., Reijm, S., Slot, L. M., Cavallari, M., Wortel, C. M., Vergroesen, R. D., et al., Antibodies and B cells recognising citrullinated proteins display a broad cross-reactivity towards other post-translational modifications. *Ann Rheum Dis* 2020. 79: 472-480.
- 45 Kerkman, P. F., Fabre, E., van der Voort, E. I., Zaldumbide, A., Rombouts, Y., Rispens, T., et al., Identification and characterisation of citrullinated antigen-specific B cells in peripheral blood of patients with rheumatoid arthritis. *Ann Rheum Dis* 2016. 75: 1170-1176.
- 46 Koning, M. T., Kielbasa, S. M., Boersma, V., Buermans, H. P. J., van der Zeeuw, S. A. J., van Bergen, C. A. M., et al., ARTISAN PCR: rapid identification of full-length immunoglobulin rearrangements without primer binding bias. *Br J Haematol* 2017. 178: 983-986.
- 47 van de Stadt, L. A., van Schouwenburg, P. A., Bryde, S., Kruithof, S., van Schaardenburg, D., Hamann, D., et al., Monoclonal anti-citrullinated protein antibodies selected on citrullinated fibrinogen have distinct targets with different cross-reactivity patterns. *Rheumatology (Oxford)* 2013. 52: 631-635.
- 48 Reiding, K. R., Lonardi, E., Hipgrave Ederveen, A. L. and Wuhrer, M., Ethyl Esterification for MALDI-MS Analysis of Protein Glycosylation. *Methods Mol Biol* 2016. 1394: 151-162.
- 49 Rombouts, Y., Ewing, E., van de Stadt, L. A., Selman, M. H., Trouw, L. A., Deelder, A. M., et al., Anti-citrullinated protein antibodies acquire a pro-inflammatory Fc glycosylation phenotype prior to the onset of rheumatoid arthritis. *Ann Rheum Dis* 2015. 74: 234-241.
- 50 Plomp, R., de Haan, N., Bondt, A., Murli, J., Dotz, V. and Wuhrer, M., Comparative Glycomics of Immunoglobulin A and G From Saliva and Plasma Reveals Biomarker Potential. *Front Immunol* 2018. 9: 2436.

- 51 Selman, M. H., Derks, R. J., Bondt, A., Palmblad, M., Schoenmaker, B., Koeleman, C. A., et al., Fc specific IgG glycosylation profiling by robust nano-reverse phase HPLC-MS using a sheath-flow ESI sprayer interface. *J Proteomics* 2012. 75: 1318-1329.
- 52 Jansen, B. C., Falck, D., de Haan, N., Hipgrave Ederveen, A. L., Razdorov, G., Lauc, G., et al., LaCyTools: A Targeted Liquid Chromatography-Mass Spectrometry Data Processing Package for Relative Quantitation of Glycopeptides. *J Proteome Res* 2016. 15: 2198-2210.

Supplemental Tables

Table S1. ACPA IgG BCR variable region sequence details. ACPA IgG BCR sequences isolated from single B cells of 3 RA patients and anti-TT IgG BCR sequence isolated from a healthy donor. Immunoglobulin (IG) heavy and kappa (K) or lambda (L) light chain CDR3 amino-acid sequences are depicted. The N-linked glycan motifs presented in the variable heavy (V_H) or light (V_L) chain are visualized together with their respective location. The germline motifs are depicted based on the IMGT database.

IgG	Patient	IGH-CDR3	IGK/L-CDR3
7E4 (ACPA)	4	CVRIIRGGSSNW	CAAWNGRLSAFVF
2G9 (ACPA)	2	CVRWGEDRTEGLW	CMQRLRFPLTF
3F3 (ACPA)	1	CARGTYLPVDESAAFDVW	CQQYYEAPYTF
D2 (anti-TT)	7	CARRGGKDNVWGDW	CQQYNDWPVTF

* Amino-acid sequence and location.

† Determined by IMGT/ V-QUEST.

N-linked glycan motifs V _H ⁺	N-linked glycan motifs V _L ⁺	Germline motifs V _H ⁺	Germline motifs V _L ⁺
NES (CDR1)	NVT (FR1)	SES (CDR1)	KVT (FR1)
NGS (CDR1), NTS (FR3) and NMT (FR3)	NIS (FR3)	GGG (CDR1), NPS (FR3) and KLS (FR3)	KIS (FR3)
NMT (FR3) and NTS (FR3)	NLT (FR3)	TMT (FR3) and STA (FR3)	TLT (FR3)
NFT (CDR1)	x	SFT (CDR1)	x

Supplemental Figures

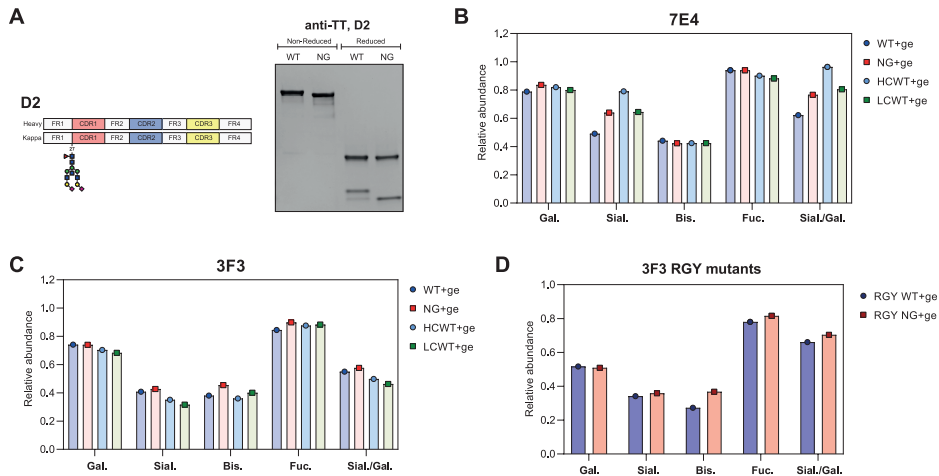


Figure S1. Production data of monoclonal ACPA and anti-TT IgG with (wild-type, WT) and without (non-glycosylated, NG) naturally occurring VDGs. (A) Schematic depiction of the D2 (anti-TT) heavy and kappa light chain variable regions including the position of the naturally occurring N-linked glycan site. 4-15% gradient SDS protein gel (BioRad) of purified WT and NG monoclonal anti-TT IgG D2 under non-reduced (IgG) and reduced (HC and LC) conditions. The size-shift caused by the presence of VDGs is visible. The size was determined using the PageRuler™ Plus Prestained Protein Ladder (Thermo Fisher Scientific). (B) LC-MS Fc-peptide glycan analysis of WT, HCWT, LCWT and NG 7E4 and (C) 3F3 mAb variants. The amount of galactosylation (Gal), sialylation (Sial), bisection (Bis) and fucosylation (Fuc) per N-glycan is shown. (D) LC-MS Fc-peptide glycan analysis of WT and NG RGY mutants. The amount of galactosylation (Gal), sialylation (Sial), bisection (Bis) and fucosylation (Fuc) per N-glycan is shown.

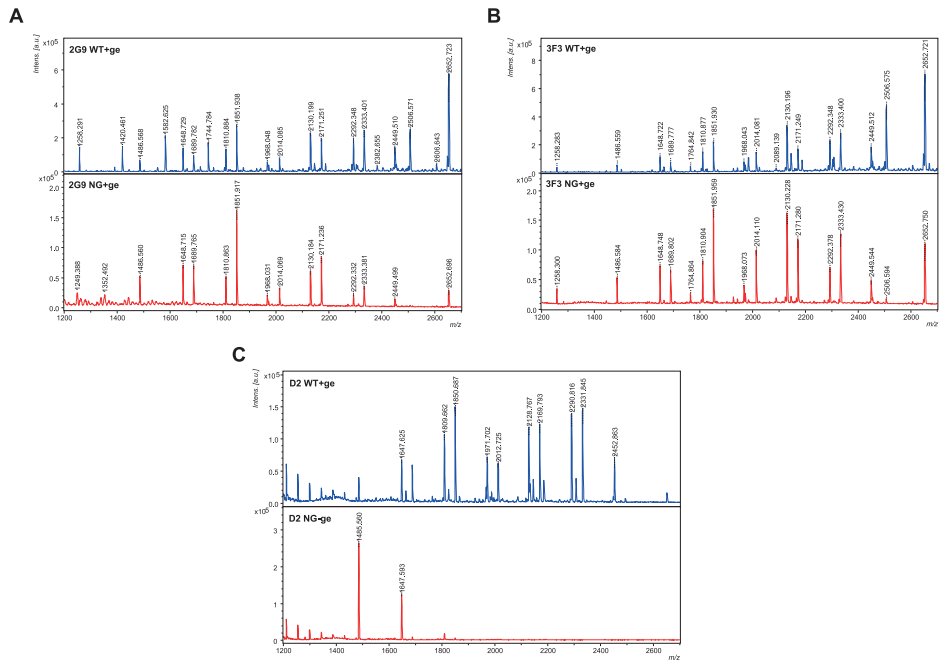


Figure S2. MALDI-TOF MS analysis of released and stabilized VD and Fc glycans from WT and NG 2G9, 3F3 and D2 mAbs. The m/z of the glycan peaks are depicted. Blue square: *N*-acetylglucosamine (GlcNAc), green circle: mannose, yellow circle: galactose, red triangle: fucose, purple diamond: α 2,6-linked *N*-acetylneuraminic acid (sialic acid).

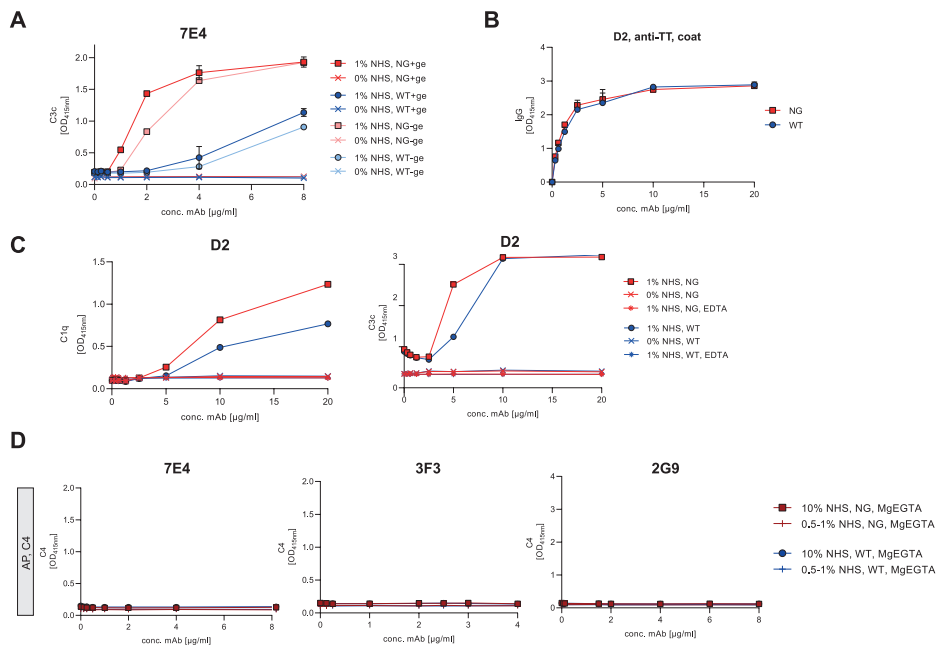


Figure S3. Complement pathway activation of mAbs. (A) Classical pathway activation. C3c deposition on WT and NG +/-ge 7E4 mAbs (0 to 8 µg/ml) after adding 0% or 1% NHS in gelatin veronal buffer containing Ca²⁺ and Mg²⁺ (GVB++). Each data point represents the mean of two technical replicates. (B) Detection of WT and NG mAb D2 (a-TT) binding to ELISA plates. Each data point represents the mean of two technical replicates. (C) Classical pathway activation. C1q and C3c deposition on WT and NG mAb D2 after adding 0% or 1% NHS in GVB++. (D) C4 deposition on WT and NG mAb (7E4, 3F3 and 2G9) after adding alternative pathway buffer (1% or 10% NHS in Mg-EGTA).

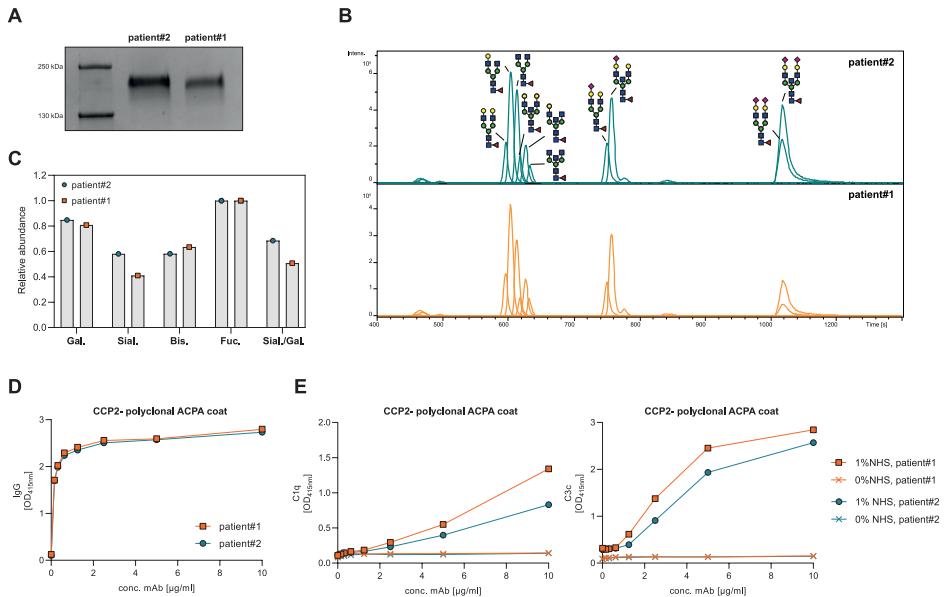


Figure S4. Classical complement pathway activation of polyclonal ACPA IgG with different quantities of VDGs isolated from RA patient serum samples. (A) 4 to 15% gradient SDS protein gel (BioRad) of patient isolated polyclonal ACPA IgG. The size-shift between the polyclonal ACPA IgG from patient #1 vs. patient #2 caused by the presence of different quantities of VDGs is visible. The size was determined using the PageRuler™ Plus Prestained Protein Ladder (Thermo Fisher Scientific). (B) LC-chromatogram of released and stabilized VD and Fc glycans from patient#1 and #2. The schematic N-glycan composition per elution peak is depicted. Blue square: *N*-acetylglucosamine (GlcNAc), green circle: mannose, yellow circle: galactose, red triangle: fucose, purple diamond: α 2,6-linked *N*-acetylneuraminic acid (sialic acid). (C) Amount of galactosylation (Gal), sialylation (Sial), bisection (Bis) and fucosylation (Fuc) per N-glycan (VD and Fc glycans) based on the quantified LC-MS results. (D) Detection of polyclonal ACPA IgG (0 to 10 µg/ml) binding to CCP2-coated ELISA plate. (E) Classical pathway activation. C1q and C3c deposition on polyclonal ACPA IgG (0 to 10 µg/ml) from patient #1 and #2 with different VDG quantities after adding 0% or 0.5% NHS in GVB++.

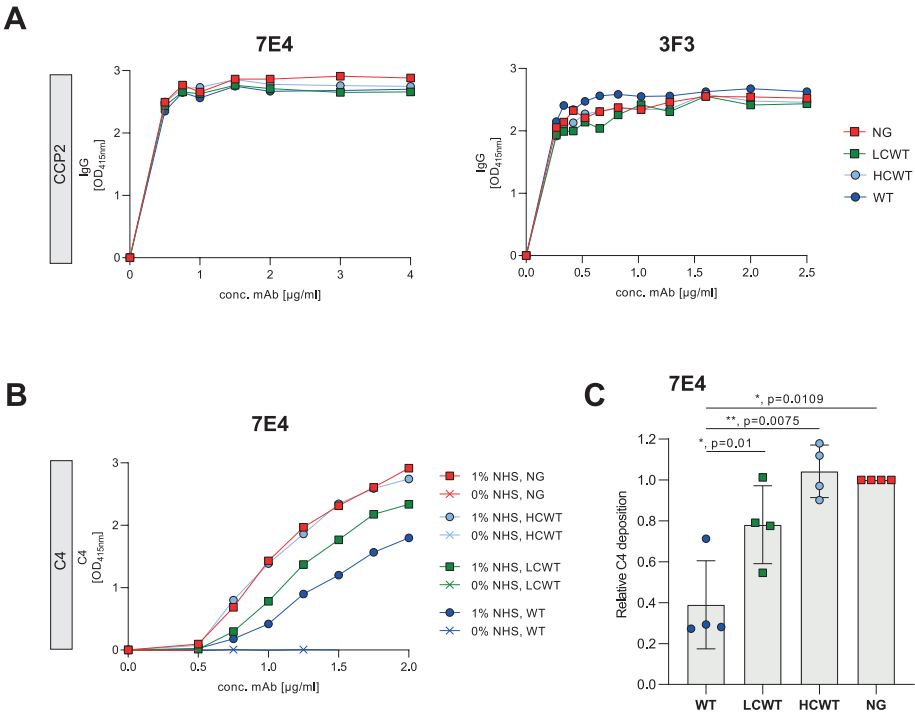


Figure S5. CCP2-binding (3F3 and 7E4) and C4 deposition (7E4) of monoclonal ACPA IgG with different quantities of VDGS in heavy and light chain. (A) Detection of WT, HCWT, LCWT and NG binding to CCP2-coated ELISA plate for mAb 7E4 and mAb 3F3. **(B)** Classical pathway activation. C4 deposition on WT, HCWT, LCWT and NG 7E4 after adding 0% or 1% NHS in GVB++. **(C)** Relative C4 deposition of WT, HCWT, LCWT mAb 7E4 (2 μg/ml) compared to its NG counterpart. Each binding experiment was repeated 4 times and each dot represents one independent experiment. The respective p-values are depicted: ns $p > 0.05$, * $p \leq 0.05$, ** $p \leq 0.01$, *** $p \leq 0.001$ or **** $p \leq 0.0001$.

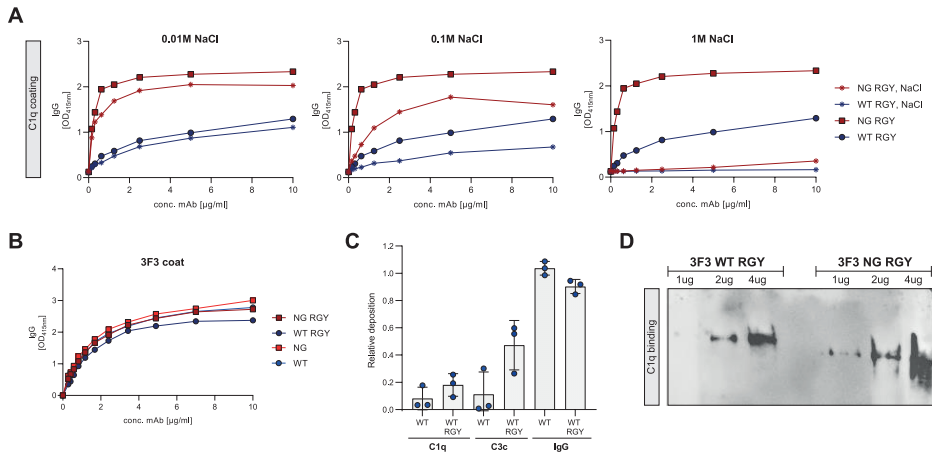


Figure S6. C1q binding of 3F3 RGY mutants. (A) Detection of WT, NG, WT RGY and NG RGY 3F3 mAb binding to C1q-coated ELISA plate after incubation with 0.01 M, 0.1 M or 1 M NaCl to specifically disrupt the C1q head domain interactions. (B) Detection of monomeric WT and NG and WT RGY and NG RGY 3F3 mAb (0 to 10 μg/ml) binding to CCP2-coated ELISA plate. (C) Relative C1q, C3c and IgG deposition of WT vs. WT RGY. Each experiment was repeated 3 times and each dot represents one independent experiment. (D) Western blot of native 7% TRIS-acetate gel after incubation in 0.05% SDS. Binding to recombinantly added human native C1q (CompTech) was detected using rabbit anti-C1q (DAKO) and HRP-labelled goat anti-rabbit (DAKO) detection antibodies.



General discussion and perspectives

General discussion and perspectives

Loss of humoral tolerance is a hallmark of many autoimmune diseases and leads to the appearance of self-reactive B cells and the autoantibodies they secrete. This also applies to the prototypical human autoimmune disease Rheumatoid Arthritis (RA), which is characterized by inflammation of the synovial tissue of the joints. The pathways of autoreactive B cells to overrun tolerance checkpoints and thereby drive the development of RA are largely unknown. Nevertheless detailed analyses of the RA-specific autoantibody responses in the past decades, have provided important insights into how autoreactive responses could arise in RA and how checkpoints could be violated. RA is a heterogeneous autoimmune disease that emerges most likely through the accumulation of genetic, epigenetic and environmental factors, such as the microbiome. Immunologically, the autoimmune disease can be divided into at least two different subgroups, characterized by the presence or the absence of the disease-specific autoantibodies, anti-citrullinated protein antibodies (ACPAs). The fact that ACPA-positivity associates with more severe clinical outcomes¹ and that these autoantibodies appear already many years before the onset of the disease², suggests an early break in B-cell tolerance and highlights the importance of autoantibodies and the underlying B-cell response for the development and maintenance of RA. Additionally, the most important genetic risk factor for RA, the HLA-shared epitope (SE) alleles predispose only to the development of ACPA-positive RA³. Thus, it is likely that autoreactive citrullinated protein (CP)-directed B cells in RA can recruit HLA-SE restricted T-cell help necessary for the induction and the maturation of the ACPA-specific B-cell response. Several studies indicate that ACPA responses differ from conventional antibody responses as they are characterized, despite an extensive amount of somatic mutations, by a relatively low avidity for antigen⁴ combined with a high promiscuity, a reactivity to several antigenic-backbones and post-translational modifications (PTMs)⁵⁻¹⁴. Moreover, unlike most antigen-specific antibody responses, most ACPA in RA harbor N-linked glycans in their hypervariable regions¹⁵.

The presented work in this thesis deals with these specific features of autoreactive B cells and their secreted autoantibodies in RA. The aspect of cross-reactivity is described on the monoclonal antibody level and on the level of autoreactive B-cell responses (**Chapter 3**). Furthermore, the emergence of variable domain glycans (VDGs) (**Chapter 4, Chapter 5** and **Chapter 6**) and their functional consequences for CP-directed B cells and their secreted autoantibodies (**Chapter 7** and **Chapter 8**) are evaluated. These aspects will be discussed in the following sections along with the latest findings and a focus on how these characteristics might help ACPA-expressing B cells to overrun peripheral B-cell checkpoints, which are highlighted in **Chapter 2**.

The promiscuity of anti-modified protein antibodies in RA

The molecular nature of the antigens recognized by most of the disease-specific antibodies, anti-citrullinated protein antibodies (ACPAs), in RA, was identified in 1998 and has since been used as a biomarker to aid in RA diagnosis. ACPAs are already detectable years before the onset of inflammation and persist in patients with established RA and in individuals with drug-free sustained remission. Hence it has been hypothesized that the “quality” of the ACPA response rather than their first emergence determines its involvement in the inflammatory responses observed in RA. This includes their fine-specificity (epitope recognition)¹⁶, the degree and type of glycosylation in the Fc and the variable domain^{15,17}, their isotype usage¹⁸⁻²⁰, their avidity⁴ and the potential of ACPA to activate the complement cascade²¹. An important characteristic of ACPAs in “full-blown” RA is for example their extensive poly-reactivity to several citrullinated epitopes. Next to that, ACPAs can cross-react to multiple post-translationally modified epitopes, including carbamylated-lysine and acetylated-lysine residues. Initial studies suggested that ACPAs, anti-carbamylated protein antibodies (ACarPAs) and anti-acetylated protein antibodies (AAPAs) represent three independent autoantibody systems²², due to the positional and structural differences of the targeted modified epitopes. However, there is more and more evidence indicating that a large proportion of these antibodies are cross-reactive and relate to a single antibody family, defined in **Chapter 3** as anti-modified protein antibodies (AMPAs)¹³. Particularly, characterizations of fourteen RA-derived monoclonal ACPAs confirmed their cross-reactivity and highlighted their promiscuity to modified amino acid residues that share similar physicochemical and structural properties with citrulline (**Chapter 3**). However, it should also be noted that not all ACPAs exhibit the same degree of cross-reactivity towards all modifications (**Chapter 3**). This has not only been observed at the monoclonal antibody level, but autoantibody-positive patients have also been described to exhibit reactivity to either one, two or all three modifications^{23,24}.

The first crystal structures of monoclonal ACPA Fab domains provided structural background that could explain the extensive cross-reactivity of ACPAs²⁵. The superposition of crystal structures from three ACPA Fabs co-crystallized with diverse citrullinated antigens, revealed that next to their individual structural features and differential electrostatic potentials, all Fab domains share two deep polar and hydrophobic binding pockets able to accommodate a citrullinated residue (**Chapter 7**). Importantly, the primary interactions were observed between the terminal nitrogen and oxygen atoms of the citrulline side chain, and secondary interactions only with the peptide backbone of the flanking amino acids. Hence, except for the citrulline modification, no “specific” interactions to determined flanking amino acids are needed for ACPAs to interact with their cognate antigens. The antibodies can promiscuously accommodate different citrullinated peptide variants as long as the modified residue is in a favorable and accessible position (Figure 1A). The accessibility of the modification also depends on the nature

of the secondary contacts formed with the surrounding peptide scaffold. Thus, antigens could be excluded from the binding repertoire due to steric repulsion with certain spatially demanding amino acids proximal to the citrulline (Figure 1A). This might explain why glycine residues, with only minor spatial requirements are potentially preferred amino acids in the surrounding of the modification^{11,25,26}. The importance of secondary contacts is likely to be different for different ACPAs accommodating different antigens. It has been postulated that certain ACPAs that require only interactions with the modification are more “promiscuous”, whereas others that bind depending on the specific flanking regions are more “private specific”²⁷. The rather “shallow” binding mode of RA-specific autoantibodies might also explain the low avidity/affinity of ACPAs towards many of their antigens, despite the fact that ACPA-expressing B cells undergo extensive somatic hypermutation (SHM), a process that is usually accompanied by affinity maturation^{11,28,29}. It further explains the broad cross-reactivity of ACPAs to other post-translational modifications (PTMs) harboring terminal nitrogen and oxygen atoms and comparable structural requirements to citrulline, such as acetylated- and carbamylated-lysine residues (Figure 1, A and B). All three modified residues exhibit similar physicochemical properties, such as size, shape, charge and hydrophobicity.

Thus, existing theories regarding the main role of citrullination as the driver of the autoimmune response connected to RA might be incorrect as possibly other post-translational modifications (PTMs), such as carbamylation or acetylation, presented by for example microbe derived antigens, might be involved in the initial breach of tolerance. This hypothesis is reinforced by our findings showing that autoreactive B cells expressing B-cell receptors (BCRs) directed against one particular PTM can also be activated by antigens expressing different modifications (**Chapter 3**). Additionally, recent studies revealed already a high cross-reactive nature and thus promiscuity of ACPA IgM, despite limited mutational load. Intriguingly, cross-reactivity even remained in two antibody variants which were mutated back to germline further emphasizing that multiple antigens could be involved in the initial B-cell activation and that the breach of tolerance towards several PTMs occurs already before extensive SHM and class switching³⁰. It is tempting to speculate that a particular PTM initiates the AMPA response and that further exposure to other PTMs determines its direction towards a more ACPA-, ACPA- or AAPA-like response. Furthermore, it can be hypothesized that this response is highly dynamic and can be “re-routed” up upon a new encounter with a different modification (Figure 1C). This dynamic behavior of the AMPA response associated with the plasticity of the paratope-epitope interactions is highlighted in a recent study showing that the AMPA recognition profile is skewed towards the most recently encountered PTM, suggesting that the PTM responsible for the initial induction of the response and the PTM predominant in established RA are not necessarily identical³¹. Indeed, an ongoing antigen triggering, with potentially different modifications, is also in line with the activated proliferative phenotype of ACPA-expressing B cells in RA³².

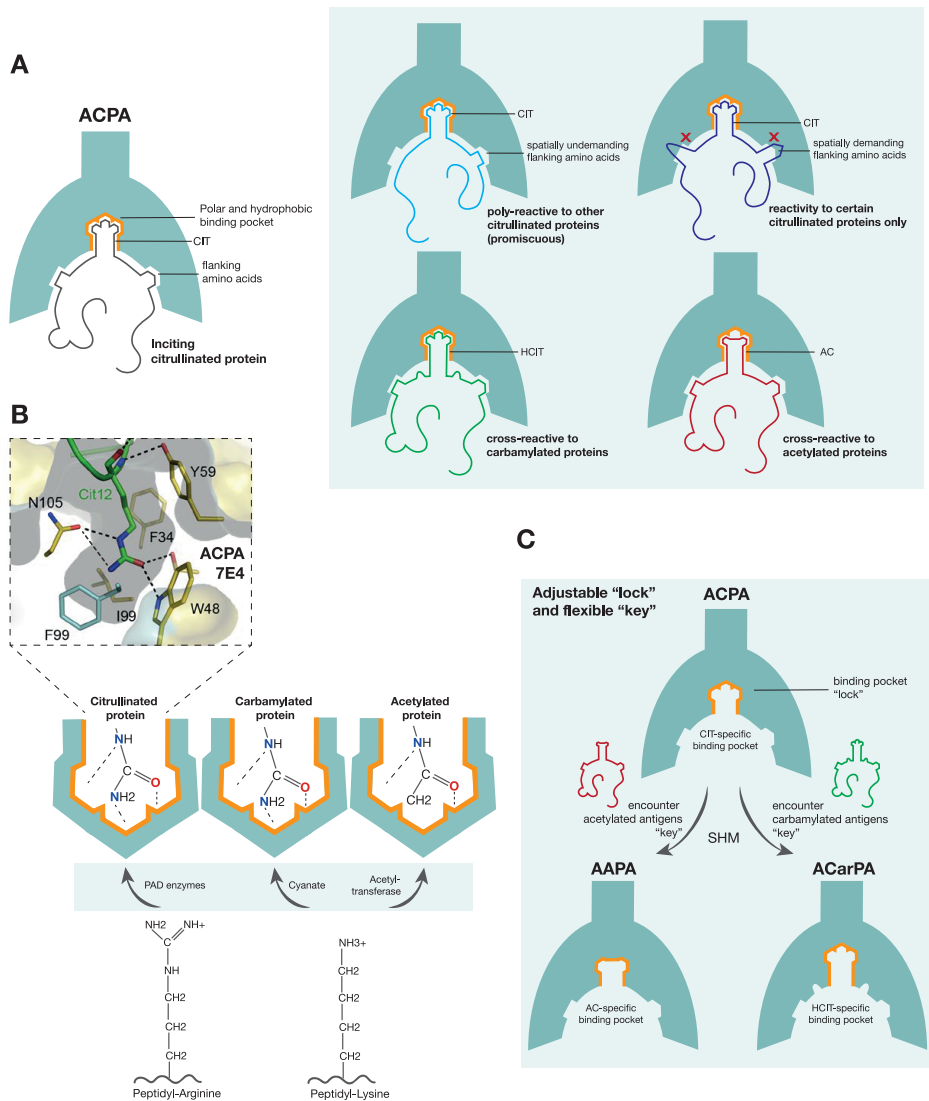


Figure 1. The binding mode of anti-citrullinated protein antibodies (ACPAs). (A) Schematic representation of the polar and hydrophobic ACPA binding pocket accommodating a citrulline (CIT) side chain. Illustration of the promiscuous binding mode to CIT proteins with flanking amino acids of minor spatial requirements and specificity for only certain CIT proteins due to steric repulsion with demanding flanking amino acids. Cross-reactivity to carbamylated (homocitrullinated, HCIT) and acetylated (AC) proteins with similar structural requirements. (B) Depiction of the formation of citrullination, carbamylation and acetylation. Illustration of the main hydrogen-bond interactions formed between the antibody binding pocket and the terminal nitrogen and oxygen atoms of the respective modification. Crystal structure of the CIT binding pocket of the monoclonal ACPA 7E4 is depicted. (C) Plasticity of the ACPA binding pocket (adjustable "lock") upon encounter of a differently modified antigen (flexible "key") and somatic hypermutation (SHM).

Nevertheless, it remains unknown which modification, or which modified antigen incites the autoantibody specific B-cell response in RA. Although previous studies have identified ACPAs as the dominant autoantibody response in patients with established RA, it still needs to be further investigated whether ACPAs are already prevalent years before the onset of clinical symptoms or if the pre-RA response is characterized by the presence of AAPAs and/or ACarPAs. It can also be speculated that the AMPA response is initiated by acetylated or carbamylated foreign-antigens presented at mucosal surfaces³³ or by acetylated antigens generated upon cell death and NETosis¹². That carbamylation might play an important role for the initiation of the AMPA response, is also in line with the findings that the extracellular matrix protein collagen, which has a long half-life and represents one of the potential autoantigens in RA, can be easily carbamylated³⁴. This response may then be the bridge to the production of ACPAs in RA by a skewing of the immune response to citrullinated proteins presented at the side of inflammation^{35,36}. However it is also conceivable that carbamylation and acetylation represent epitopes that have no relevance for disease pathogenesis.

Overall, it can be concluded that the generation of cross-reactive antibodies directed against a broad range of potentially unrelated self or non-self-proteins carrying structural epitopes that mimic the primary immunogen, is adding another layer of complexity to the already heterogeneous autoimmune disease³⁷. Further studies, focusing on the cross-reactive nature of AMPAs in the phase prior to the onset of arthritis combined with more comprehensive analyses of AMPA epitope structures, are evidently important to understand the initiation, the evolution and variety of the autoreactive responses observed in RA. Furthermore, more structural insights will allow us to improve the diagnostic assays used in the clinic to detect autoantibodies and therefore to improve disease diagnosis.

The emergence of variable domain glycans during the ACPA B-cell development

N-linked glycosylation sites, a pre-requisite for the introduction of N-glycans, were found to be present in almost 90% of ACPA IgG variable regions, which by far exceeds the frequency of such sites in the healthy repertoire²⁹. However, it has been hardly described when, during the autoreactive B-cell development, N-glycans are introduced into the ACPA IgG variable domains. Based on previous studies it can be assumed that N-linked glycan sites are introduced into the ACPA variable domains following class-switch recombination (CSR) and SHM, as no sites were found to be preset on ACPA IgM³⁸ or in the germline-encoded ACPA IgG V-gene repertoire^{29,39}. SHM occurs in germinal centers (GC) following T-cell help provided to B cells. It can therefore be assumed that N-glycans are accumulated in the ACPA IgG variable domains during the repeated passage of ACPA-expressing B cells through GCs and are thus part of the maturation process of

the ACPA B-cell response. However, GC responses, CSR and SHM are common processes that occur in all humoral immune responses and do not normally lead to a frequent accumulation of N-glycans in the variable domain of the BCR. It can therefore be assumed that “specific” T cell contacts are required and that the introduction of glycans in the variable domain is not just the result of the accumulation of multiple somatic mutations. Indeed, the frequency of N-glycosylation sites does not correlate with the mutational load of ACPA IgG BCRs, suggesting that the sequons are introduced during a selective process²⁹.

Furthermore this hypothesis was confirmed by our findings, presented in **Chapter 4** and **Chapter 5**, showing that the most prominent genetic risk factor predisposing to ACPA-positive RA, the HLA-SE alleles, associates with ACPA IgG presenting N-glycans in their variable domains. More specifically, the data depict an association between ACPA IgG carrying VDGs and the HLA-SE alleles in the pre-disease phase as shown for healthy individuals from Japan, pre-symptomatic individuals from Sweden and individuals with arthralgia from the Amsterdam area of The Netherlands. This finding is intriguing and indicates that SE-restricted T-cell help might drive the introduction of N-linked VDGs. The fact that two different T helper cell responses are at play during the ACPA B-cell development is also in line with the finding that no association between ACPA and HLA-SE was observed in healthy individuals, despite class switching to IgG, but in individuals with ACPA-positive disease that also abundantly incorporated VDGs into their ACPA IgG. Thus, N-glycosylation sites are potentially accumulated during SHM following help of T cells restricted to the predisposing HLA molecules. In line with this assumption we observed an increased association between the presence of VDGs and the HLA-SE alleles after correcting for ACPA-positivity. Thus, HLA-SE alleles predominantly associate with variable domain glycosylated ACPA IgG and not with ACPA IgG as such.

We observed not only an association between the HLA-SE alleles and the presence of VDGs, but also identified increased VDG levels in HLA-SE-positive individuals, highlighted in **Chapter 5**, and no association between HLA-SE and ACPA levels after correcting for the presence of VDGs. Additionally, our data depicted primarily an association between HLA-SE and the most prominent bisected and disialylated glycan trait (G2FBS2) found on the ACPA IgG variable domains and again this association remained after correcting for ACPA levels. Thus, these data have solved another piece of the jig-saw puzzle unraveling the development of RA as it can now be hypothesized that, in the phase preceding the onset of RA, T cells restricted to the HLA molecules predisposing to RA development provide help to ACPA-expressing B cells, which results in extensive SHM leading to the introduction of N-linked glycosylation sites and hence the abundant expression of VDGs. The HLA-SE risk effect together with the subsequent expression of VDGs on ACPA IgG can thus be seen as an accelerating factor and important “hit” for the development of the autoimmune disease RA.

This notion is in line with the findings presented in **Chapter 5** showing that individuals with an “incomplete” VDG profile (< 75%) were more prone to develop RA, if they were HLA-SE-positive. The presence of HLA-SE alleles will likely lead to an accelerated introduction of VDGs which will conceivably promote the transition to RA. That increased VDG levels in the asymptomatic phase are a strong predictor for the development of inflammatory arthritis has also been shown in a previous study within a healthy Canadian population⁴⁰. Together with the observation that N-glycans are selectively introduced into the variable regions of ACPA BCRs and are not the results of a random accumulation of somatic mutations²⁹, and the finding that ACPA B cells do not undergo avidity maturation⁴, these observations point towards a different selection mechanism of ACPA-expressing B cells, in which post-translational glycan modifications most likely play a crucial role.

However, our results also indicate that, in certain individuals, VDGs can already be abundantly present several years before the actual onset of RA (**Chapter 4** and **Chapter 5**) indicating that several “hits”, over a period of multiple years, are likely involved in the transition to RA. To investigate the emergence and the momentum of VDGs on ACPA IgG in greater detail and to understand their contribution to the autoreactive B-cell response in RA, we cross-sectionally investigated their presence and abundance in 1498 samples from individuals in various disease stages (**Chapter 6**). The percentages of ACPA IgG VDGs were analyzed in the “pre”-RA phase in samples of healthy individuals from Japan and Canada, of pre-symptomatic individuals from Sweden and of individuals with arthralgia from the Amsterdam and the Leiden area of The Netherlands. Additionally, the abundance of ACPA IgG VDGs in the “post”-RA phase was determined including the influence of treatment and changes upon drug-free remission (DFR) or late disease flares. We therefore made use of a well-controlled treatment strategy trial and furthermore analyzed individuals whose RA achieved long-term drug free remission (DFR) or late flares and had been followed up to 16 years. The data show that VDGs were already abundantly (58%) expressed on ACPA IgG isolated from healthy individuals. Levels increased further towards the arthralgia phase (75%) and towards RA-onset (93%). Thus, in agreement with the results presented above, VDGs are already present on ACPA IgG of asymptomatic healthy individuals and their abundance rises further during the progression to arthralgia and ultimately clinically detectable arthritis/ early RA. In established RA, we observed a stable expression of the glycan modification with a slight decrease upon start of immunosuppressive therapy. Furthermore, especially in the “pre”-RA phase, we identified a correlation between the abundance of VDGs and the evolution of the ACPA immune response, as expressed by an increase in ACPA levels and epitope spreading, implying again the involvement of VDGs in the progression of disease. Notably, our data illustrated that patients whose RA achieved long-term DFR later in time had introduced significantly less glycans into their variable domains compared to patients with persistent or relapsing disease.

Thus the data, presented in **Chapter 4**, **Chapter 5** and **Chapter 6** highlight the association of VDGs with the transition from autoimmunity to autoimmune disease as well as with the persistence of the disease. Therefore, it is relevant to uncover and understand the biological impact of VDGs on autoreactive B cells and their secreted autoantibodies in general and on the RA-specific ACPA response in particular. Further it remains to be elucidated, whether VDGs are presented by all AMPA classes and to what extent the selective introduction of VDGs is influenced by the nature of the antigen.

Functional impact of VDGs on secreted autoantibodies

Current findings showing that ACPAs do not undergo strong avidity maturation, but selectively and abundantly introduce N-glycans into their variable domains, strongly indicate that VDGs are involved in the selection and regulation mechanisms involved in the expansion of ACPA-expressing B cells. This assumption is further reinforced by the predictive value of VDGs for disease development and their association with the most prominent genetic risk factor, the HLA-SE alleles. Intriguingly, not only ACPAs, but also other human (auto)antibody responses, including anti-MPO or anti-PR antibodies from ANCA-associated vasculitis patients⁴¹, are characterized by a hyperglycosylation of the variable domain.

Despite the probably important involvement of VDGs in the mechanisms leading to the maturation of the autoimmune responses underlying human autoimmune diseases, we currently only have a glimpse on the functional role of these glycan modifications for autoreactive B cells and the antibodies they secrete. In the studies described in **Chapter 7**, we identified the impact of complex-type, bisected and disialylated ACPA IgG VDGs on (auto)antigen binding by analyzing the binding mode of six monoclonal antibodies with and without their naturally occurring VDGs. N-linked glycosylation sites presented in the variable domains are, contrarily to Fc N-glycans, not necessarily occupied with a glycan and constrained by the accessibility of the N-glycosylation sites⁴². Thus, it might be exceptional that almost all glycan sites expressed in the variable domain of the ACPA IgG mAbs were found to be completely occupied by a complex-type N-glycan. With an exception of the N-linked glycosylation site in the LC of two mAbs, which appeared to be only partially occupied. It is also exceptional that some monoclonal ACPA IgG presented up to a total of eight glycans in their variable domains.

Based on the crystallographic data of three ACPA Fab domains and dynamic modeling, we were able to show that VDGs attached to the FR3 or the CDR1 regions can interact with amino acids in or in close proximity to the antigen-binding pocket and thus potentially compete with the antigens for binding. The suspected negative impact on binding was confirmed for all six mAbs by ELISA-based antigen-binding studies. Particularly low-affine antigens were outcompeted by

the (potentially higher affine) VDGs, while the binding towards high-affine antigens was less affected. The impact of VDGs on antigen binding depends on the specific glycan structure and the location of the N-glycan in the variable domain. In this respect it is noteworthy that a differential impact of VDGs on antigen binding has been reported in literature^{43,44}. Further site-specific analyses are necessary to draw more comprehensive conclusions on the impact of VDGs on antigen binding. Indeed, it is also conceivable that N-glycans interact with the antigens upon binding, holding them in the binding-pocket and thereby enhancing binding. This would be in line with the decreased apparent dissociation rates observed in our SPR experiments presented in **Chapter 7**. Next to the effect on antigen binding, VDGs can increase the thermostability of antibodies, possibly by shielding hydrophobic residues (Figure 2D). This positive impact on antibody stability is not mediated by the terminal sialic acids⁴⁵.

Next to the impact on stability, VDGs may affect the propensity of immunoglobulins to form immune complexes/ aggregates⁴⁶ and thus potentially impact on IgG effector functions. In the studies described in **Chapter 8** we investigated the influence of VDGs on hexamer formation of IgG molecules and the subsequent effect on complement activation. Monoclonal antibodies with identical Fc glycan patterns, but different amounts of VDGs depicted a clearly reduced classical complement pathway activation in the presence of N-linked VDGs. This difference is likely caused by a decreased ability of variable domain glycosylated IgG to form hexamers, due to steric repulsion, leading to a lowered binding to the classical pathway initiator C1q (Figure 2E). These results indicate that not only Fc glycans, but also glycans presented on the IgG variable domain can have immunomodulatory effects and impact on the effector functions of antibodies. Therefore, VDGs might be thought to affect not only complement but also binding to Fc gamma receptors (FcγR), including the neonatal FcR (FcRn), which is critical for the half-life of serum IgG.

Functional impact of VDGs on autoreactive B cells

In addition to the functional impact of VDGs on secreted antibodies, it is of importance to investigate the effects of VDGs for surface-bound immunoglobulins, BCRs. In this way, we can determine whether glycans can interfere with B-cell functions and thus could be a potential trigger for B-cell selection and disease development. Interestingly, an inhibitory effect on binding to low-affine antigens was also observed for the CP-directed BCRs harboring N-glycan modifications in their variable regions. Thus, it can be hypothesized that VDGs reduce the self-antigen recognition profile in the GC preventing negative selection and promoting B-cell survival only through a retained cross-reactivity to potentially higher affine foreign-epitopes (Figure 2A). This “redemption” hypothesis is in line with a study in mouse models showing that self-reactive antibodies mutate away from autoreactivity through the introduction of N-linked

variable domain glycans and thereby prevent elimination through clonal deletion or receptor editing⁴⁷. Another important functionality reported for glycans on BCRs is the interaction with glycan-binding proteins, lectins. For follicular lymphoma B cells it has been proposed that high mannosylated VDGs presented on the BCR variable domain interact with mannose-binding lectins causing B-cell activation without the need for antigen⁴⁸⁻⁵⁰. These B cells are thus selected for the presence of VDGs, which is in line with the abundant expression of N-linked glycosylation sites in the variable regions of follicular lymphoma BCRs⁵¹. Concordantly, it has been suggested that the abundant expression of glycans in the hypervariable domains of CP-directed BCRs provide a selection/ survival advantage to ACPA-expressing B cells through the interaction with lectins in vicinity to the BCR (in *cis*) or on neighboring cells (in *trans*). In line with this hypothesis, we identified an increased activation potential of B cells carrying variable domain glycosylated BCRs (**Chapter 7**, Figure 2B). This observation was made by transducing human Ramos B cells with two CP-directed BCRs from RA patients. We consistently observed an increased and prolonged BCR signaling after antigenic-stimulation or BCR cross-linking. Consequently, VDGs seem to change the activation threshold of RA-specific B cells which could lead to the loss of control of the self-reactive response and thus may play an important role for the pathogenesis of the disease. This activation/ survival advantage will in turn lead to the selection of these B cells in the germinal center reaction and thereby the secretion of abundantly variable domain glycosylated autoantibodies.

However, against the hypothesis that lectins provide this survival signal⁵², we could not identify an impact of the negative regulator, the sialic acid-binding immunoglobulin-type lectin (Siglec) CD22, on the VDG-mediated effects on B-cell signaling. CD22 knock-outs showed no impact on the increased activation status of N-glycosylated BCRs, despite the fact that we mainly identified complex-type disialylated glycans expressed by the BCR variable regions. Nevertheless, VDGs might interact with other (soluble) lectins leading to an increase in activation. It has for example been suggested that galectin-9 facilitates interactions between N-glycosylated IgM BCRs and either of the inhibitory proteins CD45 or CD22 and thus attenuating B-cell signaling upon antigen-stimulation^{53,54}. Therefore galectin-9 interactions could also play a role for signaling of CP-directed B cells carrying a large amount of N-glycans in the variable regions of their BCRs although binding has been reported primarily for *N*-acetylglucosamine (LacNAc) containing multi-antennary N-glycans⁵⁵. Additionally, we observed decreased antigen uptake and BCR downmodulation rates in the presence of VDGs (**Chapter 7**, Figure 2C). The prolonged surface expression of antigen-bound BCRs might be an explanation for the observed differences in signaling strength and duration. This would be in line with previous studies showing an increased BCR signaling after inhibition of BCR uptake⁵⁶. The impact of VDGs on BCR downmodulation may also affect the turnover rate of the surface immunoglobulins. It is conceivable that non variable domain glycosylated BCRs are less stably expressed on the B-cell surface and have thus a lower turnover rate. This may cause BCR surface expression to decrease over time,

which in turn may affect the overall signaling strength of the B cell and its activation. The stable and abundant expression of N-glycosylated CP-directed B-cell receptors on the surface of autoreactive B cells in RA might explain why a large population of actively proliferating autoreactive B cells are found that do not “die out” by negative selection or “exhaustion” even after more than 30 years of disease. Nevertheless further studies, using for example endocytosis inhibitors, are needed to delineate whether the observed effects of VDGs on BCR signaling and downmodulation are directly linked to these cellular phenotypes.

In addition, the altered B-cell activation installed by VDGs might also be explained by altered nanoscale organization of the BCR structures. It could be envisioned that the incorporation of VDGs by a BCR will lead to the formation of distinct clusters in a resting or an activated state which could in turn influence signaling. The negatively charged sialic acids terminating the N-linked glycan structures on the variable domain of the BCR could repel similarly sialylated glycoproteins in close proximity as e.g. neighboring BCRs. This could lead to an “open” BCR conformation, which according to the “dissociation activation model” could determine the activated state of variable domain glycosylated B cells, particularly after monovalent antigen exposure⁵⁷. According to this model, BCRs form a closed autoinhibited oligomeric structure on the surface of resting B cells. Antigen binding disturbs this structure leading to an opening and thus activation of the BCRs as evidenced by proximity ligation assays⁵⁷. Further insights could be obtained by tracking the BCRs with and without VDGs after antigenic-stimulation using live cell imaging. This would enable us to detect potential spatial differences of BCRs due to the presence of VDGs. A differential formation of BCR signaling-active caps in the presence of spatially demanding N-glycans could lead to an altered organization of the molecular adaptor Cbl with the tyrosine kinase Syk, causing altered ubiquitination of phosphorylated Syk and thus differences in BCR signaling⁵⁸. In addition, it is conceivable that VDGs impact on the metabolic fitness of B cells. The two major pathways that provide energy for cells are glycolysis and oxidative phosphorylation or in short OXPHOS. Glycolysis is a relatively inefficient, but rapid way of generating energy for cells as compared to OXPHOS. Recently it has been shown that germinal center B cells acquiring higher-affinity mutations and thereby undergoing clonal expansion and positive selection, showed elevated levels of OXPHOS genes⁵⁹. Therefore, it is also conceivable that ACPA-expressing B cells, that potentially have a selective advantage through the introduction of VDGs, show an increased oxidative phosphorylation. BCRs have been shown to affect the metabolic fitness of B cells⁶⁰, and it can be hypothesized that N-glycans bound to these receptors and affecting B-cell activation may thus also be able to control the metabolic state of the cells.

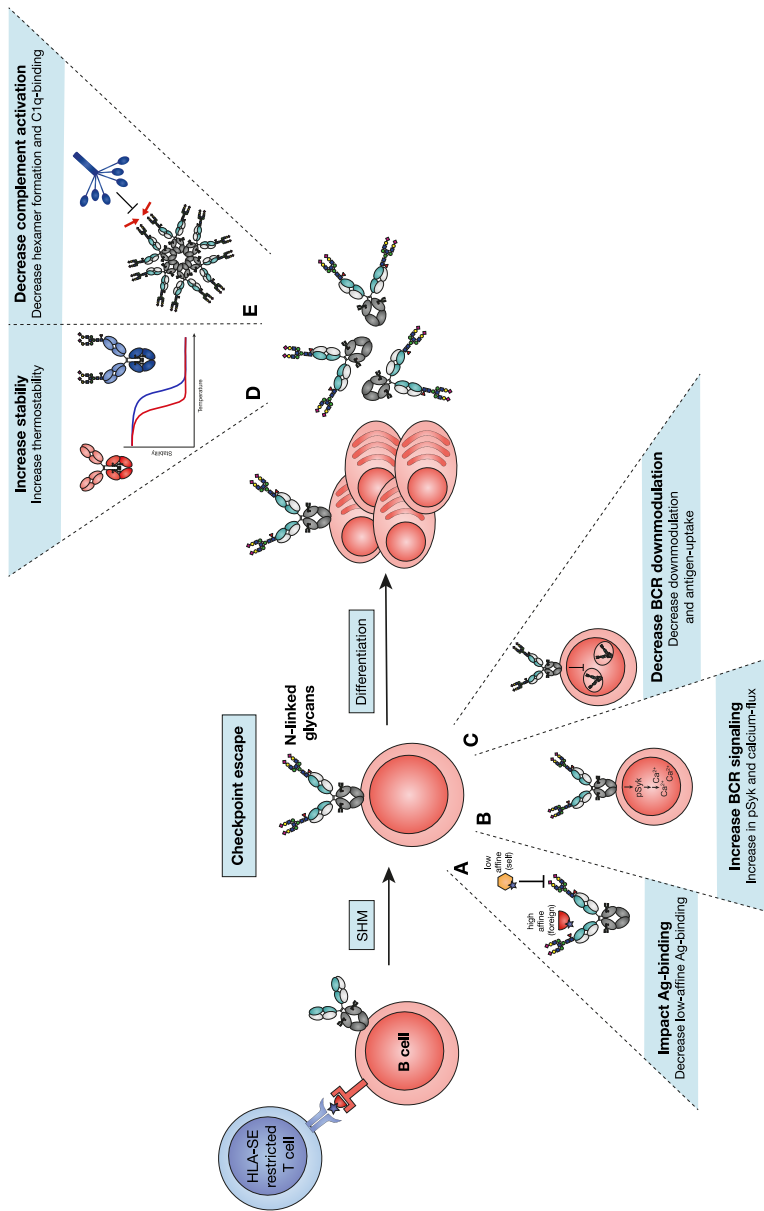


Figure 2. The functional impact of variable domain glycans (VDGs) for autoreactive citrullinated-protein (CP) directed B cells and their secreted ACPAs. N-linked glycans are introduced into the variable domains following HLA-SE restricted T-cell help and somatic hypermutation (SHM). VDGs might allow the B cells to overcome checkpoint control mechanisms by (A) lowering binding to low-affine (self)-antigens, while retaining binding to high-affine (potentially foreign)-antigens. (B) Increasing B-cell receptor (BCR) signaling and thus decreasing the activation threshold. (C) Decreasing BCR downmodulation and antigen-uptake. VDGs potentially also impact on (D) the thermostability of secreted ACPAs, (E) the propensity of ACPA IgG to form hexamers and thus on C1q-binding and complement activation.

Thus, our data, together with the current literature presented above, indicate that VDGs seem to have important immunomodulatory effects on autoreactive B cells and their secreted autoantibodies. Variable domain glycans can affect antigen recognition, positively influence the stability of immunoglobulins, impact on the effector functions of immunoglobulins (complement activation) and importantly influence antigen uptake, BCR downmodulation and signaling. Further explorations of the functional consequences of VDGs could therefore provide more insights into the regulation of humoral immune responses and possibly the pathogenesis of B cell-mediated autoimmune diseases.

The evolution from autoimmunity to autoimmune disease - “multiple hit” model

The development of ACPA-positive RA is thought to be a multistep process which is here described as a “multiple-hit” model (Figure 3). The initial immunological trigger for the induction of an ACPA immune response might be a combination of environmental risk factors, such as smoking, and/or post-translationally modified microbe derived antigens. Recently, we showed that the first responding naïve IgM B cells can already express cross-reactive BCRs³⁰ that promiscuously accommodate citrullinated/ carbamylated and/or acetylated foreign- and/or self-proteins in their binding pockets. The high cross-reactive nature complicates the identification of the “inciting” antigen underlying the first activation of the ACPA immune response that is responsible for the recruitment of T-cell help. A “wealth” of antigens could activate the CP-directed B cells, and different antigens may play a role in different patients and at different stages of disease. However, it is conceivable that the inciting B cells are activated by a normal response against (opsonized) microbes presenting foreign-epitopes that mimic self-epitopes as presented in the “mucosal origin hypothesis”⁶¹. Such antigens are then recognized by citrullinated protein specific T cells, conceivably non-self-directed, that provide help to the B cells, followed by SHM and class switch recombination. This can be defined as a “1st hit” responsible for B cell-mediated immunity to PTM proteins, including self-proteins through cross-reactivity. Although autoantibodies occur, individuals are still healthy, and the induction of the “PTM protein-directed immunity” will only lead to the transition to an autoimmune disease in conjunction with other factors (hits), possibly including certain genetic risk factors. This probably also explains why some individuals are more prone to transition to disease than others.

The most prominent genetic risk factor for ACPA-positive RA are the HLA-DRB1 shared epitope (SE) alleles. That HLA-SE alleles are not involved in the initial breach of tolerance, but rather facilitate a further maturation of the ACPA response occurring before RA-onset, is supported by the findings showings that HLA-SE alleles only associate with ACPA-positive disease and not with ACPA-positivity in healthy individuals^{62,63}. Thus, it is likely that in a 2nd immunological

hit, modified (citrullinated) antigens facilitate the help of additional T cells directed against citrullinated antigens presented by HLA-SE molecules. The findings described in this thesis, now indicate that this “2nd” HLE-SE restricted T-cell response expedites the introduction of N-linked glycosylation sites into the variable regions of the CP-directed BCRs through SHM (**Chapter 4** and **Chapter 5**). Thus, upon repetitive passages of CP-directed B cells through germinal centers and the accompanied T-cell help, N-linked glycans will be presented in the variable domains of the autoreactive BCRs and their secreted autoantibodies. The introduced VDGs alter antigen binding and the activation threshold of the CP-directed B cells (**Chapter 7**) and may thus be considered as “the spark that lights the fire”. VDGs potentially help the B cells to proliferate and to overcome important B-cell checkpoints ultimately leading to the induction of the autoimmune disease RA. This concept of VDGs as a “master switch” for the expansion of the ACPA immune response, is reinforced by the fact that ACPAs display a relatively low avidity to their antigens, even after extensive SHM^{4,64}. Apparently, CP-directed B cells are not following “conventional” affinity maturation concepts that underly the outgrowth of the “fittest” B cells in germinal centers, but rather acquire crucial survival and proliferation signals through their ability to incorporate N-glycans into their variable regions. Thus, the second expansion of ACPA B cells is most likely regulated through the selective introduction of N-glycans into the variable regions rather than by avidity maturation. This is also in line with previous studies showing that the introduction of VDGs is associated with the transition towards disease⁴⁰ and with the findings presented in **Chapter 6** indicating that their abundance rises significantly towards disease progression. In addition, the high abundance of VDGs on ACPA IgG in all patients indicates that they are likely an important pre-requisite for disease development. As evidenced by the results presented in **Chapter 7**, the introduction of VDGs potentially explains the activated phenotype of the CP-directed B cells. The abundant expression of VDGs might hinder the autoreactive B cells to reach a state of quiescence through a continuous activation, potentially even in the absence of antigens, via e.g. the interaction with other glycan-binding molecules. However, further studies are needed to bring these two findings into context. It is also conceivable that the hyperresponsiveness of CP-directed B cells can be explained by the fact that these B cells almost exclusively interact with post-translational modifications that are repeatedly present on the respective antigens. Thus, BCRs are efficiently cross-linked through multiple interactions with the repeated epitopes, resulting in extensive and rapid B-cell activation. In comparison, tetanus toxoid directed B cells, which can only interact with one specific epitope, receive only monovalent antigenic stimulation and therefore show a reduced activation status.

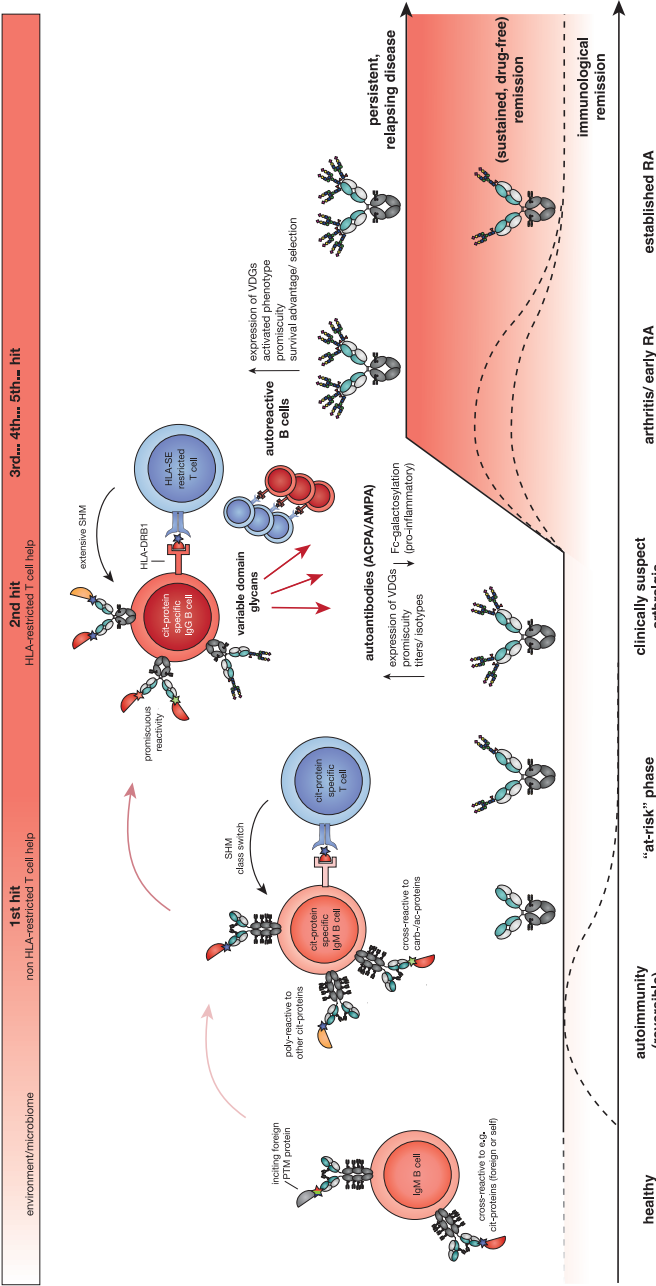


Figure 3. "Multiple hit" model potentially explaining the development of ACPA-positive RA inspired by⁴⁵. Environmental factors or the microbiome generate post-translational modified proteins likely involved in the earliest breach of self-tolerance. Naïve IgM B cells able to accommodate these modified-proteins [citrullinated (blue), carbamylated (green), acetylated (red)] via their cross-reactive (promiscuous) BCRs, receive help from PTM protein specific T cells followed by somatic hypermutation (SHM) and class switching (1st hit). These early events lead to autoimmunity as evidenced by the presence of ACPAs and already occurs several years before the onset of arthritis. Further hits are likely at play involving the ongoing help of HLA-SE restricted T cells (2nd hit) followed by the ongoing and ultimately abundant introduction of N-linked variable domain glycans (VDGs) via SHM (3rd, 4th, 5th hit). VDGs likely give a selective advantage to ACPA-expressing B cells which is eventually instrumental in the transition to an autoimmune disease. The "quality" of the ACPA response, characterized by its cross-reactivity, antibody titres, isotype-usage, Fc glycosylation and expression of VDGs, potentially predetermines the transition to a persistent, relapsing disease or the chance that the RA of patients achieves remission at a later stage.

The “multiple hit” model also explains why ACPAs can already be present several years before the onset of clinical symptoms. The “constitution” of the ACPA response changes however during disease development, as evidenced by an increase in ACPA titres, isotype-usage, an expansion of the recognition profile (increased cross-reactivity), an increase in the introduction of VDGs as well as a change in the Fc-glycan profile (reduced Fc-galactosylation). These changes are likely obtained via “multiple hits” requiring multiple rounds of repetitive HLA-SE restricted T-cell help over a period of several years and are thus responsible for the transition from a (potentially reversible) autoimmunity to autoimmune disease. The “type” of the ACPA response also correlates with outcomes, more specifically, if individuals will develop an irreversible (chronic), relapsing disease or if their disease achieves remission at a later time point. This was also demonstrated in **Chapter 6**, where individuals who had introduced a lower amount of VDGs into the ACPA variable domains had a higher chance of achieving drug-free remission at a later stage. The results presented in this chapter indicate that once a specific ACPA response is present in disease, it seems to be relatively stable over time. The ACPA response in individuals with persistent disease is characterized by low avidity, but this is balanced by a high cross-reactive nature and an abundant expression of N-linked glycans in the variable domains. The high expression of VDGs can possibly shift the B cells into a more active phenotype by e.g. affecting the metabolic state. This might explain why these B cells can persist for several years and eventually cause the onset of RA.

Concluding remarks

The last few years, we have made great progress in our understanding of the immunological processes underlying the human autoimmune disease Rheumatoid Arthritis (RA) and identified mechanisms potentially involved in the breach of tolerance. The data described in this thesis reinforce the hypothesis that the disease-specific autoantibodies (ACPAs, ACarPAs and AAPAs) are highly cross-reactive to several post-translational modifications (PTMs) and thus potentially belong to one family of anti-modified protein antibodies (AMPAs). The studies show that ACPA-expressing B cells can be activated by multiple PTM antigens indicating that various modifications can be involved in the initial breach of tolerance. In addition, the studies unravel the important role of variable domain glycans (VDGs) for the disease progression to RA. Our data show that VDGs associate with the most prominent genetic risk factor for ACPA-positive RA, the HLA-SE alleles, and that the abundance of VDGs can be predictive for the development of a chronic, persistent disease or the chance that RA patients achieve remission at a later time. Functionally, we identified that VDGs can impact complement activation and reduce binding to low-affine (potential self) antigens, while binding to high-affine (potential foreign) antigens is retained. Importantly, VDGs were able to decrease the activation threshold of CP-directed B cells and thus display important immunomodulatory functions. The results presented in this

thesis show that autoreactive B-cell responses in RA most likely evolve via “multiple hits”, and that both, the highly cross-reactive nature of the response and the abundant expression of VDGs might help the B cells to overcome important immune checkpoints and to breach tolerance. Stratifying patients with RA on the basis of their cross-reactivity and the abundance of VDGs together with the specific Fc glycosylation profile might therefore allow us to identify more homogeneous patient groups, with respect to both disease course and the response to treatment. We are looking forward to the coming years and the many more important discoveries that are waiting to be made to unravel the role of variable domain N-glycans (sweet) on autoreactive B cells and their secreted autoantibodies (bitter) and thus to understand this Bitter Sweet Symphony.

References

- 1 van der Kooij, S. M., Goekoop-Ruiterman, Y. P., de Vries-Bouwstra, J. K., Guler-Yuksel, M., Zwinderman, A. H., Kerstens, P. J., et al., Drug-free remission, functioning and radiographic damage after 4 years of response-driven treatment in patients with recent-onset rheumatoid arthritis. *Ann Rheum Dis* 2009. 68: 914-921.
- 2 Nielen, M. M., van Schaardenburg, D., Reesink, H. W., van de Stadt, R. J., van der Horst-Bruinsma, I. E., de Koning, M. H., et al., Specific autoantibodies precede the symptoms of rheumatoid arthritis: a study of serial measurements in blood donors. *Arthritis Rheum* 2004. 50: 380-386.
- 3 Huizinga, T. W., Amos, C. I., van der Helm-van Mil, A. H., Chen, W., van Gaalen, F. A., Jawaheer, D., et al., Refining the complex rheumatoid arthritis phenotype based on specificity of the HLA-DRB1 shared epitope for antibodies to citrullinated proteins. *Arthritis Rheum* 2005. 52: 3433-3438.
- 4 Suwannalai, P., Scherer, H. U., van der Woude, D., Ioan-Facsinay, A., Jol-van der Zijde, C. M., van Tol, M. J., et al., Anti-citrullinated protein antibodies have a low avidity compared with antibodies against recall antigens. *Ann Rheum Dis* 2011. 70: 373-379.
- 5 Schellekens, G. A., de Jong, B. A., van den Hoogen, F. H., van de Putte, L. B. and van Venrooij, W. J., Citrulline is an essential constituent of antigenic determinants recognized by rheumatoid arthritis-specific autoantibodies. *J Clin Invest* 1998. 101: 273-281.
- 6 Takizawa, Y., Suzuki, A., Sawada, T., Ohsaka, M., Inoue, T., Yamada, R., et al., Citrullinated fibrinogen detected as a soluble citrullinated autoantigen in rheumatoid arthritis synovial fluids. *Ann Rheum Dis* 2006. 65: 1013-1020.
- 7 Burkhardt, H., Koller, T., Engstrom, A., Nandakumar, K. S., Turnay, J., Kraetsch, H. G., et al., Epitope-specific recognition of type II collagen by rheumatoid arthritis antibodies is shared with recognition by antibodies that are arthritogenic in collagen-induced arthritis in the mouse. *Arthritis Rheum* 2002. 46: 2339-2348.
- 8 Vossenaar, E. R., Despres, N., Lapointe, E., van der Heijden, A., Lora, M., Senshu, T., et al., Rheumatoid arthritis specific anti-Sa antibodies target citrullinated vimentin. *Arthritis Res Ther* 2004. 6: R142-150.
- 9 Lundberg, K., Kinloch, A., Fisher, B. A., Wegner, N., Wait, R., Charles, P., et al., Antibodies to citrullinated alpha-enolase peptide 1 are specific for rheumatoid arthritis and cross-react with bacterial enolase. *Arthritis Rheum* 2008. 58: 3009-3019.
- 10 Ioan-Facsinay, A., el-Bannoudi, H., Scherer, H. U., van der Woude, D., Menard, H. A., Lora, M., et al., Anti-cyclic citrullinated peptide antibodies are a collection of anti-citrullinated protein antibodies and contain overlapping and non-overlapping reactivities. *Ann Rheum Dis* 2011. 70: 188-193.
- 11 Steen, J., Forsstrom, B., Sahlstrom, P., Odowd, V., Israelsson, L., Krishnamurthy, A., et al., Recognition of Amino Acid Motifs, Rather Than Specific Proteins, by Human Plasma Cell-Derived Monoclonal Antibodies to Posttranslationally Modified Proteins in Rheumatoid Arthritis. *Arthritis Rheumatol* 2019. 71: 196-209.
- 12 Lloyd, K. A., Wigerblad, G., Sahlstrom, P., Garimella, M. G., Chemin, K., Steen, J., et al., Differential ACPA Binding to Nuclear Antigens Reveals a PAD-Independent Pathway and a Distinct Subset of Acetylation Cross-Reactive Autoantibodies in Rheumatoid Arthritis. *Front Immunol* 2018. 9: 3033.
- 13 Reed, E., Jiang, X., Kharlamova, N., Ytterberg, A. J., Catrina, A. I., Israelsson, L., et al., Antibodies to carbamylated alpha-enolase epitopes in rheumatoid arthritis also bind citrullinated epitopes and are largely indistinct from anti-citrullinated protein antibodies. *Arthritis Res Ther* 2016. 18: 96.
- 14 Kampstra, A. S. B., Dekkers, J. S., Volkov, M., Dorjee, A. L., Hafkenscheid, L., Kempers, A. C., et al., Different classes of anti-modified protein antibodies are induced on exposure to antigens expressing only one type of modification. *Ann Rheum Dis* 2019. 78: 908-916.
- 15 Rombouts, Y., Willemze, A., van Beers, J. J., Shi, J., Kerkman, P. F., van Toorn, L., et al., Extensive glycosylation of ACPA-IgG variable domains modulates binding to citrullinated antigens in rheumatoid arthritis. *Ann Rheum Dis* 2016. 75: 578-585.

- 16 Verpoort, K. N., Cheung, K., Ioan-Facsinay, A., van der Helm-van Mil, A. H., de Vries-Bouwstra, J. K., Allaart, C. F., et al., Fine specificity of the anti-citrullinated protein antibody response is influenced by the shared epitope alleles. *Arthritis Rheum* 2007. 56: 3949-3952.
- 17 Scherer, H. U., van der Woude, D., Ioan-Facsinay, A., el Bannoudi, H., Trouw, L. A., Wang, J., et al., Glycan profiling of anti-citrullinated protein antibodies isolated from human serum and synovial fluid. *Arthritis Rheum* 2010. 62: 1620-1629.
- 18 Ioan-Facsinay, A., Willemze, A., Robinson, D. B., Peschken, C. A., Markland, J., van der Woude, D., et al., Marked differences in fine specificity and isotype usage of the anti-citrullinated protein antibody in health and disease. *Arthritis Rheum* 2008. 58: 3000-3008.
- 19 Verpoort, K. N., Jol-van der Zijde, C. M., Papendrecht-van der Voort, E. A., Ioan-Facsinay, A., Drijfhout, J. W., van Tol, M. J., et al., Isotype distribution of anti-cyclic citrullinated peptide antibodies in undifferentiated arthritis and rheumatoid arthritis reflects an ongoing immune response. *Arthritis Rheum* 2006. 54: 3799-3808.
- 20 van der Woude, D., Syversen, S. W., van der Voort, E. I., Verpoort, K. N., Goll, G. L., van der Linden, M. P., et al., The ACPA isotype profile reflects long-term radiographic progression in rheumatoid arthritis. *Ann Rheum Dis* 2010. 69: 1110-1116.
- 21 Trouw, L. A., Haisma, E. M., Levarht, E. W., van der Woude, D., Ioan-Facsinay, A., Daha, M. R., et al., Anti-cyclic citrullinated peptide antibodies from rheumatoid arthritis patients activate complement via both the classical and alternative pathways. *Arthritis Rheum* 2009. 60: 1923-1931.
- 22 Trouw, L. A., Rispens, T. and Toes, R. E. M., Beyond citrullination: other post-translational protein modifications in rheumatoid arthritis. *Nat Rev Rheumatol* 2017. 13: 331-339.
- 23 Nijjar, J. S., Morton, F. R., Bang, H., Buckley, C. D., van der Heijde, D., Gilmour, A., et al., The impact of autoantibodies against citrullinated, carbamylated, and acetylated peptides on radiographic progression in patients with new-onset rheumatoid arthritis: an observational cohort study. *Lancet Rheumatol* 2021. 3: e284-e293.
- 24 Juarez, M., Bang, H., Hammar, F., Reimer, U., Dyke, B., Sahbudin, I., et al., Identification of novel antiacetylated vimentin antibodies in patients with early inflammatory arthritis. *Ann Rheum Dis* 2016. 75: 1099-1107.
- 25 Ge, C., Xu, B., Liang, B., Lonnblom, E., Lundstrom, S. L., Zubarev, R. A., et al., Structural Basis of Cross-Reactivity of Anti-Citrullinated Protein Antibodies. *Arthritis Rheumatol* 2019. 71: 210-221.
- 26 Fanelli, I., Rovero, P., Hansen, P. R., Frederiksen, J., Houen, G. and Trier, N. H., Specificity of Anti-Citrullinated Protein Antibodies to Citrullinated alpha-Enolase Peptides as a Function of Epitope Structure and Composition. *Antibodies (Basel)* 2021. 10.
- 27 Ge, C. and Holmdahl, R., The structure, specificity and function of anti-citrullinated protein antibodies. *Nat Rev Rheumatol* 2019. 15: 503-508.
- 28 Elliott, S. E., Kongpachith, S., Lingampalli, N., Adamska, J. Z., Cannon, B. J., Mao, R., et al., Affinity Maturation Drives Epitope Spreading and Generation of Proinflammatory Anti-Citrullinated Protein Antibodies in Rheumatoid Arthritis. *Arthritis Rheumatol* 2018. 70: 1946-1958.
- 29 Vergroesen, R. D., Slot, L. M., Hafkenscheid, L., Koning, M. T., van der Voort, E. I. H., Grooff, C. A., et al., B-cell receptor sequencing of anti-citrullinated protein antibody (ACPA) IgG-expressing B cells indicates a selective advantage for the introduction of N-glycosylation sites during somatic hypermutation. *Ann Rheum Dis* 2018. 77: 956-958.
- 30 Reijm, S., Kissel, T., Stoeken-Rijsbergen, G., Slot, L. M., Wortel, C. M., van Dooren, H. J., et al., Cross-reactivity of IgM anti-modified protein antibodies in rheumatoid arthritis despite limited mutational load. *Arthritis Res Ther* 2021. 23: 230.
- 31 Volkov, M., Kampstra, A. S. B., van Schie, K. A., Kawakami, A., Tamai, M., Kawashiri, S., et al., Evolution of anti-modified protein antibody responses can be driven by consecutive exposure to different post-translational modifications. *Arthritis Res Ther* 2021. 23: 298.

- 32 Kristyanto, H., Blomberg, N. J., Slot, L. M., van der Voort, E. I. H., Kerkman, P. F., Bakker, A., et al., Persistently activated, proliferative memory autoreactive B cells promote inflammation in rheumatoid arthritis. *Sci Transl Med* 2020. 12.
- 33 Zhang, X., Ning, Z., Mayne, J., Yang, Y., Deeke, S. A., Walker, K., et al., Widespread protein lysine acetylation in gut microbiome and its alterations in patients with Crohn's disease. *Nat Commun* 2020. 11: 4120.
- 34 Mydel, P., Wang, Z., Brisslert, M., Hellvard, A., Dahlberg, L. E., Hazen, S. L., et al., Carbamylation-dependent activation of T cells: a novel mechanism in the pathogenesis of autoimmune arthritis. *J Immunol* 2010. 184: 6882-6890.
- 35 Wang, F., Chen, F. F., Gao, W. B., Wang, H. Y., Zhao, N. W., Xu, M., et al., Identification of citrullinated peptides in the synovial fluid of patients with rheumatoid arthritis using LC-MALDI-TOF/TOF. *Clin Rheumatol* 2016. 35: 2185-2194.
- 36 Kinloch, A., Lundberg, K., Wait, R., Wegner, N., Lim, N. H., Zendman, A. J., et al., Synovial fluid is a site of citrullination of autoantigens in inflammatory arthritis. *Arthritis Rheum* 2008. 58: 2287-2295.
- 37 Sahlstrom, P., Hansson, M., Steen, J., Amara, K., Titcombe, P. J., Forsstrom, B., et al., Different Hierarchies of Anti-Modified Protein Autoantibody Reactivities in Rheumatoid Arthritis. *Arthritis Rheumatol* 2020. 72: 1643-1657.
- 38 Kempers, A. C., Hafkenscheid, L., Dorjee, A. L., Moutousidou, E., van de Bovenkamp, F. S., Rispens, T., et al., The extensive glycosylation of the ACPA variable domain observed for ACPA-IgG is absent from ACPA-IgM. *Ann Rheum Dis* 2018. 77: 1087-1088.
- 39 Vergroesen, R. D., Slot, L. M., van Schaik, B. D. C., Koning, M. T., Rispens, T., van Kampen, A. H. C., et al., N-Glycosylation Site Analysis of Citrullinated Antigen-Specific B-Cell Receptors Indicates Alternative Selection Pathways During Autoreactive B-Cell Development. *Front Immunol* 2019. 10: 2092.
- 40 Hafkenscheid, L., de Moel, E., Smolik, I., Tanner, S., Meng, X., Jansen, B. C., et al., N-Linked Glycans in the Variable Domain of IgG Anti-Citrullinated Protein Antibodies Predict the Development of Rheumatoid Arthritis. *Arthritis Rheumatol* 2019. 71: 1626-1633.
- 41 Xu, P. C., Gou, S. J., Yang, X. W., Cui, Z., Jia, X. Y., Chen, M., et al., Influence of variable domain glycosylation on anti-neutrophil cytoplasmic autoantibodies and anti-glomerular basement membrane autoantibodies. *BMC Immunol* 2012. 13: 10.
- 42 Petrescu, A. J., Milac, A. L., Petrescu, S. M., Dwek, R. A. and Wormald, M. R., Statistical analysis of the protein environment of N-glycosylation sites: implications for occupancy, structure, and folding. *Glycobiology* 2004. 14: 103-114.
- 43 Koelsch, K. A., Cavett, J., Smith, K., Moore, J. S., Lehoux, S. D., Jia, N., et al., Evidence of Alternative Modes of B Cell Activation Involving Acquired Fab Regions of N-Glycosylation in Antibody-Secreting Cells Infiltrating the Labial Salivary Glands of Patients With Sjogren's Syndrome. *Arthritis Rheumatol* 2018. 70: 1102-1113.
- 44 van de Bovenkamp, F. S., Derksen, N. I. L., Ooijevaar-de Heer, P., van Schie, K. A., Kruithof, S., Berkowska, M. A., et al., Adaptive antibody diversification through N-linked glycosylation of the immunoglobulin variable region. *Proc Natl Acad Sci U S A* 2018. 115: 1901-1906.
- 45 van de Bovenkamp, F. S., Derksen, N. I. L., van Breemen, M. J., de Taeye, S. W., Ooijevaar-de Heer, P., Sanders, R. W., et al., Variable Domain N-Linked Glycans Acquired During Antigen-Specific Immune Responses Can Contribute to Immunoglobulin G Antibody Stability. *Front Immunol* 2018. 9: 740.
- 46 Courtois, F., Agrawal, N. J., Lauer, T. M. and Trout, B. L., Rational design of therapeutic mAbs against aggregation through protein engineering and incorporation of glycosylation motifs applied to bevacizumab. *MAbs* 2016. 8: 99-112.
- 47 Sabouri, Z., Schofield, P., Horikawa, K., Spierings, E., Kipling, D., Randall, K. L., et al., Redemption of autoantibodies on anergic B cells by variable-region glycosylation and mutation away from self-reactivity. *Proc Natl Acad Sci U S A* 2014. 111: E2567-2575.

- 48 Linley, A., Krysov, S., Ponzoni, M., Johnson, P. W., Packham, G. and Stevenson, F. K., Lectin binding to surface Ig variable regions provides a universal persistent activating signal for follicular lymphoma cells. *Blood* 2015. 126: 1902-1910.
- 49 Radcliffe, C. M., Arnold, J. N., Suter, D. M., Wormald, M. R., Harvey, D. J., Royle, L., et al., Human Follicular Lymphoma Cells Contain Oligomannose Glycans in the Antigen-binding Site of the B-cell Receptor. *Journal of Biological Chemistry* 2007. 282: 7405-7415.
- 50 Coelho, V., Krysov, S., Ghaemmaghami, A. M., Emara, M., Potter, K. N., Johnson, P., et al., Glycosylation of surface Ig creates a functional bridge between human follicular lymphoma and microenvironmental lectins. *Proc Natl Acad Sci U S A* 2010. 107: 18587-18592.
- 51 Zhu, D., McCarthy, H., Ottensmeier, C. H., Johnson, P., Hamblin, T. J. and Stevenson, F. K., Acquisition of potential N-glycosylation sites in the immunoglobulin variable region by somatic mutation is a distinctive feature of follicular lymphoma. *Blood* 2002. 99: 2562-2568.
- 52 Peaker, C. J. and Neuberger, M. S., Association of CD22 with the B cell antigen receptor. *Eur J Immunol* 1993. 23: 1358-1363.
- 53 Cao, A., Alluqmani, N., Buhari, F. H. M., Wasim, L., Smith, L. K., Quaile, A. T., et al., Galectin-9 binds IgM-BCR to regulate B cell signaling. *Nat Commun* 2018. 9: 3288.
- 54 Smith, L. K., Fawaz, K. and Treanor, B., Galectin-9 regulates the threshold of B cell activation and autoimmunity. *Elife* 2021. 10.
- 55 Giovannone, N., Liang, J., Antonopoulos, A., Geddes Sweeney, J., King, S. L., Pochebit, S. M., et al., Galectin-9 suppresses B cell receptor signaling and is regulated by I-branching of N-glycans. *Nat Commun* 2018. 9: 3287.
- 56 Stoddart, A., Jackson, A. P. and Brodsky, F. M., Plasticity of B cell receptor internalization upon conditional depletion of clathrin. *Mol Biol Cell* 2005. 16: 2339-2348.
- 57 Volkmann, C., Brings, N., Becker, M., Hobeika, E., Yang, J. and Reth, M., Molecular requirements of the B-cell antigen receptor for sensing monovalent antigens. *EMBO J* 2016. 35: 2371-2381.
- 58 Sohn, H. W., Gu, H. and Pierce, S. K., Cbl-b negatively regulates B cell antigen receptor signaling in mature B cells through ubiquitination of the tyrosine kinase Syk. *J Exp Med* 2003. 197: 1511-1524.
- 59 Chen, D., Wang, Y., Manakkat Vijay, G. K., Fu, S., Nash, C. W., Xu, D., et al., Coupled analysis of transcriptome and BCR mutations reveals role of OXPHOS in affinity maturation. *Nat Immunol* 2021. 22: 904-913.
- 60 Juma, H., Caganova, M., McAllister, E. J., Hoenig, L., He, X., Saltukoglu, D., et al., Immunoglobulin expression in the endoplasmic reticulum shapes the metabolic fitness of B lymphocytes. *Life Sci Alliance* 2020. 3.
- 61 Holers, V. M., Demoruelle, M. K., Kuhn, K. A., Buckner, J. H., Robinson, W. H., Okamoto, Y., et al., Rheumatoid arthritis and the mucosal origins hypothesis: protection turns to destruction. *Nat Rev Rheumatol* 2018. 14: 542-557.
- 62 Hensvold, A. H., Magnusson, P. K., Joshua, V., Hansson, M., Israelsson, L., Ferreira, R., et al., Environmental and genetic factors in the development of anticitrullinated protein antibodies (ACPAs) and ACPA-positive rheumatoid arthritis: an epidemiological investigation in twins. *Ann Rheum Dis* 2015. 74: 375-380.
- 63 Terao, C., Ohmura, K., Ikari, K., Kawaguchi, T., Takahashi, M., Setoh, K., et al., Effects of smoking and shared epitope on the production of anti-citrullinated peptide antibody in a Japanese adult population. *Arthritis Care Res (Hoboken)* 2014. 66: 1818-1827.
- 64 Suwannalai, P., van de Stadt, L. A., Radner, H., Steiner, G., El-Gabalawy, H. S., Zijde, C. M., et al., Avidity maturation of anti-citrullinated protein antibodies in rheumatoid arthritis. *Arthritis Rheum* 2012. 64: 1323-1328.
- 65 Scherer, H. U., Haupl, T. and Burmester, G. R., The etiology of rheumatoid arthritis. *J Autoimmun* 2020. 110: 102400.



Addendum

Summary

Nederlandse samenvatting

Deutsche Zusammenfassung

Curriculum Vitae

List of publications

Acknowledgments

Summary

The studies described in this thesis focus on the chronic, lifelong inflammatory joint disease Rheumatoid Arthritis (RA), which is widespread in our society. RA is an autoimmune disease that occurs when our immune system, which is supposed to protect us from bacterial, viral, and parasitic infections, gets out of control and mistakenly begins to “attack” our own body’s tissue. In RA, this causes immune cells such as T cells, B cells, and macrophages to infiltrate joint tissue, which can lead to inflammation and eventually cartilage and bone damage. Despite recent advances in therapy and the identification of the involvement of both, genetic and environmental factors contributing to the disease, the underlying cause of the autoimmune response in RA remains unknown. Up to 80% of RA patients display disease-specific antibodies (soluble B-cell receptors) directed against the body’s own proteins (self-antigens). These autoantibodies arise as a result of the loss of the immune system’s ability to distinguish between self and non-self (foreign) antigens. Their abundant presence in patients with RA and the effectiveness of targeted B-cell therapies suggest that the underlying autoreactive B-cell response plays an important role in disease development.

The different classes of autoantibodies characteristic of the disease are described in the general introduction (**Chapter 1**). RA is characterized by autoantibodies directed against post-translational modifications (PTMs), i.e. biochemical modifications on individual amino acids of a protein that occur after translation of mRNA into proteins. The most disease-specific autoantibodies are directed against citrulline [anti-citrullinated protein antibodies (ACPAs)], an enzymatic conversion of the amino acid arginine. In addition to ACPAs, autoantibodies against carbamylated [anti-carbamylated protein antibodies (ACarPAs)] or acetylated proteins [anti-acetylated protein antibodies (AAPAs)] have also been observed in patients with RA. Both modifications result from a post-translational modification of the amino acid lysine. In previous studies, the different autoantibody systems were found to occur simultaneously in RA patients, suggesting cross-reactivity of one autoantibody class against several PTMs. In addition to their reactivity against PTMs, ACPA molecules have another important feature: they carry additional sugar structures (glycans) in the region of the antibody molecule responsible for binding to the modified proteins. Glycans consist of individual sugar residues (monosaccharides) that together form sugar chains. The antibodies (immunoglobulins) of class G (IgG) normally carry glycans in the constant domain (Fc) of the antibody molecule. However, ACPA IgG molecules are also abundantly glycosylated in the antigen-binding region (variable domain). With the studies described in this work, we aim to understand how the characteristics of RA-specific autoreactive B cells - their cross-reactivity and the glycosylation of the variable domain - help these cells to survive and escape the strict control mechanisms our body has in place that normally prevent the development of autoimmunity.

To this end, **Chapter 2** reviews the current literature on the checkpoints controlling the induction of autoreactive B cells. In order to be able to ward off pathogens, they are recognized as foreign by our immune system. In contrast, the body's own proteins are tolerated by the immune system (self-tolerance). This self-tolerance develops in the thymus and bone marrow (central tolerance). There are also various control mechanisms in other parts of the body, such as the lymph nodes (peripheral tolerance), which prevent the immune system from getting out of control. In this chapter, we focus specifically on these peripheral control mechanisms which ensure that potentially autoreactive B cells do not cause autoimmunity. We highlighted antigen presentation by follicular dendritic cells (FDCs), somatic hypermutation (SHM) - a mechanism by which the immune system adapts to new antigens through mutations in the variable domains of the B-cell receptor - and cross-reactivity of T-/ B-cell receptors to self- and foreign (microbial/ environmental)-proteins. Furthermore, it is highlighted that autoreactive B cells in RA potentially escape this self-tolerance through their cross-reactivity and variable domain glycans (VDGs).

The data described in **Chapter 3** reinforce the hypothesis that the three autoantibody classes characteristic of RA (ACPA, ACPA and AAPA) cross-react and thus may belong to one family of antibodies. We therefore introduced the term anti-modified protein antibodies (AMPAs). The finding that AMPAs are cross-reactive was obtained by generating monoclonal antibodies. The B-cell receptor sequences that form the basis for these monoclonal antibodies were isolated from single B cells of RA patients. The binding potential of these antibodies to different antigen candidates (proteins and peptides) carrying citrullinated, carbamylated or acetylated amino acids was analyzed, which revealed high cross-reactivity against at least two different modifications. In this chapter, we also show that B cells originally directed against citrullinated proteins can also be stimulated by acetylated or carbamylated antigens. Taken together, these data suggest that autoreactive B cells in RA can be activated by multiple proteins carrying different modifications. Accordingly, different PTMs may be involved in the initial breach of self-tolerance, such as endogenous acetylated proteins that may have been acetylated during bacterial infection.

In addition to their cross-reactivity to various PTMs, ACPA IgGs themselves carry post-translational modifications, as they are abundantly glycosylated in their variable domains. In the studies described in **Chapter 4** and **Chapter 5**, we were able to elucidate an important function of these glycans in the development of RA. Previous findings already indicated that VDGs confer an advantage to autoreactive B cells producing ACPAs. These results showed that VDGs are selectively introduced into ACPA antigen-binding domains after T-cell help and SHM. It was also already known that the presence of VDGs in ACPAs increases the likelihood that a person who is still symptom-free will later develop RA. The results described in these chapters now show that the presence of VDGs is associated with the most prominent genetic risk factor

for ACPA-positive RA. These are the human leukocyte antigen (HLA) alleles, which encode so-called “shared epitopes” (SE). HLA-SE are involved in the recruitment of T-cell help, which is necessary for the development of a “full-fledged” B-cell response. Accordingly, it is likely that VDGs are introduced into the autoreactive B-cell receptors during SHM after receiving help signals from T cells restricted to the HLA-molecules predisposing to the disease.

This unfavorable “hit” may occur multiple times, which is shown by the increasing frequency of VDGs on autoreactive B cells during the course of disease development as demonstrated by the studies presented in **Chapter 6**. The percentage of variable domain glycosylation was analyzed in 1498 samples from individuals at various clinical stages of disease. The glycosylation of the variable domain of ACPA IgGs increased steadily starting with 56% in healthy individuals, already showing autoantibodies, to 75% in patients with joint pain (arthralgia) and 93% in patients with incipient RA. Once the disease is established, ACPA molecules from RA patients consistently show high expression of VDGs, although there is a slight decrease upon immunosuppression. The data described in this chapter further show that the “quality” of the ACPA immune response, i.e. the frequency of VDGs on ACPA IgGs at disease-onset, may be predictive of the development of chronic persistent disease or the chance of RA patients achieving drug-free remission at a later stage.

The study described in **Chapter 7** focuses on the functional importance of VDGs for autoreactive B cells and their secreted autoantibodies. The data show that the presence of VDGs can reduce the binding of autoreactive B-cell receptors and autoantibodies to citrullinated proteins. The presence of VDGs had no effect on the binding of citrullinated proteins that are recognized with high-affinity. However, it reduced binding to citrullinated proteins that are less well recognized and consequently have low affinity. Structural analyses and modelling of the interactions between autoantibody and antigen confirmed that VDGs interact with the part of the antibody involved in citrulline recognition. In addition, the data showed that VDGs increase the activation status of autoreactive B cells. This may be a consequence of the reduced internalization of glycosylated B-cell receptors after binding to citrullinated proteins. These important functional consequences of VDGs – both the decreased binding to low-affine (potentially self) antigens while retaining binding to high-affine (potentially foreign)-antigens, and a lower activation threshold – may allow autoreactive B cells to overcome important immune checkpoints and thus to breach self-tolerance.

Chapter 8 describes that VDGs, in addition to their functional importance for B-cell receptors, can also influence the effector functions of secreted antibodies. In this study, we observed a lower formation of hexamers of variable domain glycosylated ACPA IgGs. This leads to a reduced binding to the effector molecule C1q and thus a lower activation of the complement cascade, an important pathway within the immune system for the activation and recruitment

of immune cells. Whether this reduced complement activation of glycosylated ACPA IgGs has an impact on the pathogenesis of the disease and possibly makes ACPA less immunogenic, or whether it is just a bystander effect, can only be speculated and requires further investigation. Nevertheless, it can be concluded that IgG VDGs can be exploited to downregulate the antibody-dependent classical complement pathway.

All data are jointly discussed in **Chapter 9** in the context of the current literature. The ability of RA-specific autoantibodies to bind to various modified proteins is demonstrated and explained by the structural analyses of ACPA molecules. ACPA interact specifically with the citrulline modification and not, or only to a minor extent, with the flanking amino acids surrounding this modification. Since the modifications that arise after carbamylation and acetylation (homocitrulline and acetyl-lysine) of proteins are structurally very similar to citrulline, ACPA can also recognize these post-translational modifications “promiscuously”. In addition, the selective introduction of glycans into the variable domains of ACPA IgGs and its functional consequences are discussed. The data described in this thesis have led to the hypothesis that VDGs help autoreactive B cells to bypass tolerance checkpoints by influencing binding to modified proteins and B-cell activation. In conclusion, it is discussed that autoreactive B-cell responses in RA most likely result from sequential events (“multiple hits”) in which the cross-reactive nature of the response and abundant expression of VDGs play an important role. This new “glycan mechanism” may be useful to improve the diagnosis of RA even before the disease develops. This knowledge is also valuable in understanding how the immune system gets out of control and how autoimmunity develops. However, much more research is needed to understand how and why autoimmune diseases like RA develop (*bitter*) and to unravel the important role of glycan modifications (*sweet*) during disease development.

Nederlandse samenvatting

Dit proefschrift richt zich op de chronische, vaak levenslange en veelvoorkomende auto-immuunziekte Reumatoïde Artritis (RA). Ons immuunsysteem beschermt tegen bacteriële, virale en parasitaire infecties, maar kan soms ontsporen en zich richten tegen het eigen lichaam. Bij RA zorgt dit ervoor dat immuuncellen zoals T-cellen, B-cellen en macrofagen het gewrichtsweefsel infiltreren. Dit kan leiden tot gewrichtsontsteking en uiteindelijk schade aan kraakbeen en bot. Ondanks de recente vooruitgang in de identificatie van betrokken genetische en omgevingsfactoren, is de onderliggende oorzaak van de auto-immunreactie bij RA onbekend. Tot 80% van de mensen met RA hebben specifieke antilichamen (oplosbare B-cel-receptoren) die zijn gericht tegen lichaamseigen eiwitten. Deze auto-antilichamen ontstaan doordat het immuunsysteem onvoldoende onderscheid maakt tussen lichaamseigen en lichaamsvreemde moleculen. De frequente aanwezigheid van auto-antilichamen bij mensen met RA en de effectiviteit van B-celgerichte behandelingen suggereren dat de onderliggende autoreactieve B-cel activiteit een belangrijke rol speelt in de ontwikkeling van de ziekte.

De verschillende klassen van auto-antilichamen die kenmerkend zijn voor de ziekte worden beschreven in de algemene inleiding (**Hoofdstuk 1**). RA wordt gekenmerkt door autoantilichamen die gericht zijn tegen post-translationele modificaties (PTM's). Dit zijn biochemische veranderingen van aminozuren die optreden na de vertaling van RNA naar eiwitten. Het grootste deel van de ziektespecifieke autoantilichamen bij mensen met RA zijn gericht tegen citrulline [anti-citrullinated protein antilichamen (ACPA)]. Citrulline ontstaat na een enzymatische omzetting van het aminozuur arginine. Naast ACPA worden ook auto-antilichamen tegen "gecarbamylerde" of "geacetylerde" eiwitten gevonden bij mensen met RA [anti-gecarbamylerd protein antilichamen (ACarPA), respectievelijk anti-geacetylerd protein antilichamen (AAPA)]. Beide modificaties ontstaan na verandering van het aminozuur lysine. In eerdere studies is vastgesteld dat de verschillende autoantilichamen gelijktijdig voorkomen bij RA-patiënten. Dit wijst op kruisreactiviteit van één auto-antilichaamklasse tegen verschillende PTM's. Naast de reactiviteit van ACPA tegen verschillende PTM's hebben deze auto-antilichamen nog een ander belangrijk kenmerk. Zij dragen suikerstructuren (glycanen) in het gedeelte van het antilichaammolecuul dat verantwoordelijk is voor binding aan de gemodificeerde eiwitten. Glycanen bestaan uit afzonderlijke suikers (monosachariden). Deze zijn aan elkaar gebonden en vormen samen ketens. Antilichamen van klasse G, ook wel immunoglobulinen G (IgG) genoemd, dragen normaliter alleen glycanen in het constante domein (Fc) van de antilichaammolecuul. ACPA IgG-moleculen dragen echter ook glycanen in de antigeenbindende regio's (variabele domeinen). De studies die staan beschreven in dit proefschrift zijn gericht op een beter begrip van de kenmerken van de RA-specifieke autoreactieve B-celreactie, hoe deze kenmerken bijdragen aan de ontsporing van het immuunsysteem en hoe de autoreactieve B-cellen kunnen ontsnappen aan de strikte controlemechanismen in ons lichaam die normaliter de ontwikkeling van auto-immuniteit voorkomen.

In **Hoofdstuk 2** is de stand van de huidige literatuur beschreven over de controlemechanismen die de ontsporing van autoreactieve B-cellen voorkomen. Om ziekteverwekkers op te ruimen, worden deze door ons immuunsysteem als lichaamsvreemd herkend. Lichaamseigen eiwitten worden daarentegen door het immuunsysteem geaccepteerd (zelftolerantie). De ontwikkeling van zelftolerantie gebeurt in de thymus en het beenmerg. Ook op andere plaatsen in het lichaam, zoals in lymfeklieren, bevinden zich verschillende controlemechanismen die ontsporing van het immuunsysteem voorkomen. In dit hoofdstuk richten we ons specifiek op deze “perifere” controlemechanismen die ervoor zorgen dat potentieel autoreactieve B-cellen geen auto-immuniteit veroorzaken. Hier belichten wij de antigeenpresentatie door folliculaire dendritische cellen (FDC’s), somatische hypermutatie (SHM), een mechanisme waarbij het immuunsysteem zich verbetert door mutaties aan te brengen in de variabele domeinen van de B-celreceptor (BCR), en kruisreactiviteit van T-/B-cel-receptoren op zelf- en lichaamsvreemde eiwitten. Er wordt benadrukt dat autoreactieve B-cellen die voorkomen bij mensen met RA potentieel zijn ontsnapt aan deze zelftolerantie door kruisreactiviteit met lichaamsvreemde moleculen en de aanwezigheid van variabele domein glycanen (VDG).

De studies beschreven in **Hoofdstuk 3** ondersteunen de hypothese dat de drie auto-antilichamen die kenmerkend zijn voor RA (ACPA, ACarPA en AAPA) kruisreageren en dus mogelijk tot één familie van antilichamen behoren. Daarom hebben wij de term anti-gemodificeerde proteïne antilichamen (AMPA) geïntroduceerd. Deze bevinding werd verkregen door het genereren van monoklonale antilichamen. De BCR sequenties die de basis vormen voor deze monoklonale antilichamen werden geïsoleerd uit B-cellen van RA-patiënten. De binding van deze antilichamen aan verschillende moleculen (eiwitten en peptiden) met gecitrullineerde, gecarbamylerde of geacetylerde aminozuren werd geanalyseerd. Alle monoklonale antilichamen vertonen een hoge kruisreactiviteit tegen ten minste twee verschillende modificaties. De studies beschreven in dit hoofdstuk laten ook zien dat B-cellen die oorspronkelijk gericht zijn tegen gecitrullineerde eiwitten ook gestimuleerd kunnen worden door geacetylerde of gecarbamylerde eiwitten. Deze bevindingen suggereren dat autoreactieve B-cellen afkomstig van mensen met RA geactiveerd kunnen worden door meerdere eiwitten die verschillende modificaties kunnen dragen. Dit wil zeggen dat verschillende PTM’s betrokken kunnen zijn bij de initiële inbreuk op de zelftolerantie, zoals bijvoorbeeld geacetylerde eiwitten die tijdens een infectie door bacteriën geacetyleerd zijn geraakt.

Naast de kruisreactiviteit op diverse PTM’s, dragen ACPA IgG’s zelf ook post-translationele modificaties in de vorm van glycanen die zijn geplaatst in de variabele domeinen. In het werk dat staat beschreven in **Hoofdstuk 4** en **Hoofdstuk 5**, waren we in staat om een belangrijke functie van deze glycanen in de ontwikkeling van de RA op te helderen. Eerdere bevindingen wezen er al op dat VDG een voordeel bieden aan autoreactieve B-cellen die ACPA aanmaken. Deze bevindingen hadden al aangetoond dat VDG selectief zijn ingebouwd na T-cel hulp en SHM.

Ook wisten we al dat de aanwezigheid van VDG in ACPA de kans verhogen dat een persoon, indien nog klachtenvrij, later RA ontwikkelt. De resultaten beschreven in deze hoofdstukken tonen aan dat de aanwezigheid van VDG geassocieerd is met de belangrijkste genetische risicofactor voor ACPA-positieve RA. Dit zijn de HLA (humaan leukocytenantigenen) allelen die betrokken zijn bij de rekrutering van de T-celhelp die nodig is voor de ontwikkeling van een “volwaardige” B-celreactie. Het is daarom waarschijnlijk dat deze glycanen tijdens SHM in de variabele domeinen van de autoreactieve B-cel-receptoren worden ingebracht na signalen te hebben ontvangen van T-cellen die nodig zijn om de B-celreactie te laten ontspreiden.

Deze nadelige “T-cel hit” kan meerdere malen voorkomen, zoals blijkt uit de toenemende frequentie van VDG op autoreactieve B-cellen in de tijd die voorafgaat aan ontwikkeling van ziekte. Dit staat beschreven in **Hoofdstuk 6**. De aanwezigheid van VDG op ACPA werd geanalyseerd in 1498 monsters van personen in verschillende klinische ziektestadia. De aanwezigheid van VDG op ACPA IgG nam toe van 56% bij gezonde personen tot 75% bij patiënten met gewrichtspijn tot 93% bij patiënten met beginnende RA. Als ziekte eenmaal aanwezig is, hebben de ACPA moleculen van RA patiënten een constant hoge aanwezigheid van VDG, hoewel er een lichte daling optreedt na behandeling. De bevindingen beschreven in dit hoofdstuk tonen ook aan dat de “kwaliteit” van de ACPA immuunrespons, d.w.z. de frequentie van VDG op ACPA IgG bij het begin van de ziekte, voorspellend kan zijn voor de ontwikkeling van chronische persisterende ziekte of de kans dat RA patiënten medicijnvrije remissie bereiken op een later tijdstip.

De studies beschreven in **Hoofdstuk 7**, richtten zich op de functionele betekenis van VDG op autoreactieve B-cellen en de afgescheiden auto-antilichamen. De bevindingen tonen aan dat de aanwezigheid van VDG de binding van autoreactieve B-cel-receptoren en ACPA aan gecitrullineerde eiwitten kunnen verminderen. De aanwezigheid van VDG had geen invloed op herkenning van gecitrullineerde eiwitten die goed werden herkend, maar verminderde de binding aan gecitrullineerde eiwitten die minder goed werden herkend. Structuuranalyse en modellering van interacties tussen auto-antilichaam en gecitrullineerd eiwit bevestigden dat VDG een interactie aangaan met het gedeelte van het antilichaam dat betrokken is bij de herkenning van citrulline. Daarnaast hebben onze bevindingen laten zien dat VDG de activeringsstatus van autoreactieve B-cellen verhogen. Dit is mogelijk een gevolg van een verminderde opname van de BCR door de B-cel na binding van gecitrullineerde eiwitten. Deze belangrijke functionele gevolgen van VDG, zowel de verminderde binding aan (potentieel lichaamseigen) gecitrullineerde eiwitten die al minder goed werden herkend, terwijl binding aan (potentieel vreemde) gecitrullineerde eiwitten die goed worden herkend behouden blijft, als de lagere activeringsdrempel, kunnen autoreactieve B-cellen in staat stellen belangrijke controlemechanismen te omzeilen. Op deze wijze zouden ze kunnen ontsnappen aan zelftolerantie.

In **Hoofdstuk 8** wordt beschreven dat VDG ook de effectormechanismen van uitgescheiden antilichamen kunnen beïnvloeden. Wij constateren in deze studie een geringere vorming van hexameren van geglycosyleerd ACPA IgG. Dit leidt tot een geringere binding aan het effectormolecuul C1q. Hierdoor vindt een verminderde activering plaats van het complementcascade, een belangrijk route binnen het immuunsysteem voor de activatie en rekrutering van immuuncellen. Of deze verminderde complementactivatie van geglycosyleerd ACPA IgG invloed heeft op de pathogenese van de ziekte en ACPA mogelijk minder “actief” maken, of dat het slechts een bijeffect is, is niet duidelijk. Dit moet verder worden onderzocht. Niettemin kan worden geconcludeerd dat IgG VDG gebruikt kunnen worden om de antilichaamafhankelijke complementactivatie te doen verminderen.

De resultaten beschreven in dit proefschrift worden in **Hoofdstuk 9** besproken en geplaatst in de context van de huidige literatuur. Het vermogen van RA-specifieke auto-antilichamen om aan verschillende gemodificeerde eiwitten te binden wordt belicht en verklaard aan de hand van de structuuranalyse van ACPA-moleculen. ACPA gaan een specifieke interactie aan met de citrulline modificatie en niet, of slechts in geringe mate, met de flankerende aminozuren rond deze modificatie. Aangezien de modificaties die ontstaan na carbamylering en acetylering (homocitrulline en acetyl-lysine) van eiwitten structureel zeer vergelijkbaar zijn met citrulline, kunnen ACPA deze modificaties ook herkennen. Daarnaast worden de selectieve introductie van glycanen in het variabele domein van ACPA IgG en de functionele gevolgen daarvan in dit hoofdstuk besproken. Het werk beschreven in dit proefschrift heeft geleid tot de hypothese dat VDG autoreactieve B-cellen helpen om de “tolerantiecontrolepunten” te omzeilen doordat ze de binding aan gemodificeerde eiwitten en de activatie van B-cellen beïnvloeden. Tot slot wordt besproken dat autoreactieve B-celresponsen bij RA hoogstwaarschijnlijk het gevolg zijn van opeenvolgende gebeurtenissen (“multiple hits”) waarbij het kruisreactieve karakter van de BCR en AMPA en de overvloedige introductie van VDG een belangrijke rol spelen. Dit nieuwe “glycaanmechanisme” zou nuttig kunnen zijn om de diagnose van RA al voor de ziekte is ontstaan te verbeteren. Ook is deze kennis belangrijk om te kunnen begrijpen hoe het immuunsysteem ontspoord en hoe auto-immuniteit zich ontwikkelt. Er is echter veel meer onderzoek nodig om te begrijpen hoe en waarom auto-immuunziekten zoals RA zich ontwikkelen (*bitter*) en om de belangrijke rol van glycaanmodificaties (*sweet*) in ziekte-ontwikkeling te ontrafelen.

Deutsche Zusammenfassung

Diese Arbeit befasst sich mit der chronischen und entzündlichen Gelenkerkrankung Rheumatoide Arthritis (RA), die in unserer Gesellschaft weit verbreitet ist. Rheumatoide Arthritis ist eine Autoimmunerkrankung, die entsteht, wenn unser Immunsystem, das uns eigentlich vor bakteriellen, viralen und parasitären Infektionen schützen soll, aus dem Ruder läuft und fälschlicherweise beginnt unser eigenes Körpergewebe anzugreifen. Bei RA wird dabei das Gelenkgewebe von Immunzellen wie T-Zellen, B-Zellen und Makrophagen infiltriert, was zu Entzündungen und schließlich zu Knorpel- und Knochenschäden führen kann. Trotz jüngster Fortschritte in der Therapie und der Erkenntnis, dass sowohl genetische als auch umweltbedingte Faktoren eine Rolle bei der Krankheitsentstehung spielen, ist die Ursache der Autoimmunreaktion bei RA nach wie vor unbekannt. Bis zu 80% der RA-Patienten weisen spezifische Antikörper (lösliche B-Zell-Rezeptoren) auf, die sich gegen körpereigene Proteine (Antigene) richten. Diese Autoantikörper entstehen, weil das Immunsystem nicht hinreichend zwischen körpereigenen und -fremden Antigenen unterscheiden kann. Das häufige Auftreten von Autoantikörpern bei Patienten mit RA und die Wirksamkeit gezielter B-Zell-Therapien deuten darauf hin, dass die zugrundeliegende autoreaktive B-Zell-Reaktion eine wichtige Rolle bei der Krankheitsentstehung spielt.

Die verschiedenen Klassen von Autoantikörpern, die für die Krankheit charakteristisch sind, werden in der allgemeinen Einleitung (**Kapitel 1**) beschrieben. RA ist durch Autoantikörper gekennzeichnet, die sich gegen posttranslationale Modifikationen (PTM) richten, d.h. gegen biochemische Veränderungen einzelner Aminosäuren eines Proteins, die nach der Übersetzung (Translation) von mRNA in Proteine auftreten. Die Autoantikörper mit der größten Spezifität für RA richten sich gegen die Citrullinierung [anti-citrullinierte Protein-Antikörper (ACPA)], eine enzymatische Umwandlung der Aminosäure Arginin. Neben ACPA werden bei Patienten mit RA auch Autoantikörper gegen carbamylierte [anti-carbamylierte Protein-Antikörper (ACarPA)] und acetylierte [anti-acetylierte Protein-Antikörper (AAPA)] Proteine beobachtet. Beide Modifikationen entstehen durch eine posttranslationale Veränderung der Aminosäure Lysin. In vorherigen Studien wurde festgestellt, dass die verschiedenen Autoantikörpersysteme gleichzeitig bei RA-Patienten auftreten, was auf eine Kreuzreaktivität einer Autoantikörperklasse gegenüber mehreren PTM schließen lässt. Neben ihrer Reaktivität gegen PTM weisen ACPA-Moleküle ein weiteres wichtiges Merkmal auf: sie tragen Zuckerstrukturen (Glykane) in der Region des Antikörpermoleküls, die für die Bindung an die modifizierten Proteine zuständig ist. Glykane bestehen aus einzelnen aneinander gebundenen Zuckerbausteinen (Monosacchariden), die sich zu Ketten verbinden. Die Antikörper (Immunglobuline) der Klasse G (IgG) tragen normalerweise Glykane in der konstanten Domäne (Fc) des Antikörpermoleküls. ACPA-IgG-Moleküle sind jedoch auch in der Antigen-bindenden Region (variablen Domäne) reichlich glykosyliert. Mit den in dieser Arbeit beschriebenen Studien wollen wir verstehen wie die Merkmale von RA-

spezifischen autoreaktiven B-Zellen – ihre Kreuzreaktivität und die Glykosylierung der variablen Domäne – diesen Zellen dazu verhilft zu überleben und den strengen Kontrollmechanismen in unserem Körper zu entkommen, die normalerweise die Entwicklung von Autoimmunität verhindern.

Daher wird in **Kapitel 2** die aktuelle Literatur zu den Kontrollmechanismen erläutert, die die Entstehung autoreaktiver B-Zellen verhindern. Um Krankheitserreger abwehren zu können, werden sie von unserem Immunsystem als fremd erkannt. Korpereigene Proteine werden hingegen vom Immunsystem toleriert (Selbsttoleranz). Diese Selbsttoleranz entwickelt sich im Thymus und im Knochenmark (zentrale Selbsttoleranz). Auch an anderen Stellen im menschlichen Körper, etwa in den Lymphknoten, gibt es verschiedene Kontrollmechanismen (periphere Selbsttoleranz), die verhindern, dass das Immunsystem „entgleist“. In diesem Kapitel konzentrieren wir uns speziell auf diese „peripheren“ Kontrollmechanismen, die sicherstellen, dass potenziell autoreaktive B-Zellen keine Autoimmunität verursachen. Dabei beleuchten wir die Antigenpräsentation durch folliculäre dendritische Zellen (FDCs), die somatische Hypermutation (SHM) – ein Mechanismus, bei dem sich das Immunsystem durch Mutationen in den variablen Domänen des B-Zell-Rezeptors an neue Antigene anpasst – sowie die Kreuzreaktivität von T-/B-Zell-Rezeptoren gegenüber körpereigenen und fremden (mikrobiellen/umweltbedingten) Proteinen. Es wird hervorgehoben, dass autoreaktive B-Zellen in RA potentiell durch ihre Kreuzreaktivität und die Glykosylierung der variablen Domäne dieser Selbsttoleranz entkommen.

Die in **Kapitel 3** beschriebenen Daten bekräftigen die Hypothese, dass die drei für RA charakteristischen Autoantikörperklassen (ACPA, ACPA und AAPA) kreuzreagieren und somit möglicherweise zu einer Familie von Antikörpern gehören. Wir haben daher den Term anti-modifizierte Protein-Antikörper (AMPA) eingeführt. Diese Erkenntnis wurde durch die Generierung von monoklonalen Antikörpern erlangt. Die B-Zell-Rezeptor-Sequenzen, die die Grundlage für diese monoklonalen Antikörper bilden, wurden aus B-Zellen von RA-Patienten isoliert. Die Bindung dieser Antikörper an verschiedene Antigenkandidaten (Proteine und Peptide), die citrullinierte, carbamylerte oder acetylierte Aminosäuren tragen, wurde analysiert. Alle monoklonalen Antikörper zeigten eine hohe Kreuzreaktivität gegen mindestens zwei verschiedene Modifikationen. In diesem Kapitel zeigen wir zudem, dass B-Zellen, die sich ursprünglich gegen citrullinierte Proteine richten, auch durch acetylierte oder carbamylerte Antigene stimuliert werden können. Diese Daten deuten darauf hin, dass autoreaktive B-Zellen in RA durch mehrere Proteine aktiviert werden können, die unterschiedliche Modifikationen tragen. Demnach können verschiedene PTM an der anfänglichen Verletzung der Selbsttoleranz beteiligt sein, wie zum Beispiel körpereigene acetylierte Proteine, die möglicherweise während einer bakteriellen Infektion acetyliert wurden.

Neben ihrer Kreuzreaktivität gegenüber verschiedenen PTM tragen ACPA-IgG selbst posttranslationale Modifikationen, da sie Glykane in ihren variablen Domänen aufweisen. In den in **Kapitel 4** und **Kapitel 5** beschriebenen Studien konnten wir eine wichtige Funktion dieser variablen Domänenglykane (VDG) bei der Entstehung von RA aufklären. Frühere Erkenntnisse deuteten bereits darauf hin, dass VDG autoreaktiven B-Zellen, die ACPA produzieren, einen Vorteil verschaffen. Diese Ergebnisse zeigten, dass VDG selektiv nach T-Zell-Hilfe und SHM in die ACPA-Antigenbindungsdomänen eingefügt werden. Auch war bereits bekannt, dass das Vorhandensein von VDG in ACPA die Wahrscheinlichkeit erhöht, dass eine Person, die noch symptomfrei ist, später RA entwickelt. Die in diesen Kapiteln beschriebenen Ergebnisse zeigen, dass das Vorhandensein von VDG mit dem wichtigsten genetischen Risikofaktor für ACPA-positive RA assoziiert ist. Dabei handelt es sich um die Humanen Leukozytenantigen (HLA)-Allele, die für sogenannte „shared epitopes“ (SE) kodieren. Sie sind an der Rekrutierung der T-Zell-Unterstützung beteiligt, die für die Entwicklung einer 'vollwertigen' B-Zell-Reaktion erforderlich ist. Es ist demnach wahrscheinlich, dass diese Glykane während der SHM in die variablen Domänen der autoreaktiven B-Zell-Rezeptoren eingefügt werden, nachdem sie Signale von T-Zellen erhalten haben, die auf die für die Krankheit prädisponierenden HLA-Moleküle beschränkt sind.

Dieser ungünstige „T-Zell Hit“ erfolgt möglicherweise mehrfach, wie die in **Kapitel 6** aufgezeigte zunehmende Häufigkeit von VDG auf autoreaktiven B-Zellen im Verlauf der Krankheitsentwicklung zeigt. Die prozentuale Glykosylierung der variablen Domäne wurde in 1498 Proben von Personen in verschiedenen klinischen Krankheitsstadien analysiert. Die Glykosylierung der variablen Domäne von ACPA-IgG stieg stetig an, angefangen mit 56% bei gesunden Personen, die bereits Autoantikörper aufweisen, bis zu 75% bei Patienten mit Gelenkschmerzen (Arthralgie) und 93% bei Patienten mit beginnender RA. Ist die Krankheit erst einmal ausgebrochen (etablierte RA), weisen ACPA-IgG-Moleküle von RA-Patienten eine durchgängig hohe Expression von VDG auf, wobei jedoch ein leichter Rückgang bei Immunsuppression zu verzeichnen ist. Die in diesem Kapitel beschriebenen Daten zeigen außerdem, dass die „Qualität“ der ACPA-Immunantwort, d.h. die Häufigkeit von VDG auf ACPA-IgG bei Krankheitsbeginn, prädiktiv sein kann für die Entwicklung einer chronischen, persistierenden Krankheit oder der Chance von RA-Patienten, zu einem späteren Zeitpunkt eine medikamentenfreie Remission zu erreichen.

Die in **Kapitel 7** beschriebene Studie konzentriert sich auf die funktionelle Bedeutung von VDG für autoreaktive B-Zellen und ihre sezernierten Autoantikörper. Die Daten zeigen, dass die Anwesenheit von VDG die Bindung von autoreaktiven B-Zell-Rezeptoren und Autoantikörpern an citrullinierte Proteine verringern kann. Das Vorhandensein von VDG hatte keinen Einfluss auf die Bindung von citrullinierten Proteinen die mit hoher Affinität erkannt werden, verringerte jedoch die Bindung an citrullinierte Proteine, die weniger gut erkannt werden und demnach eine geringe Affinität aufweisen. Strukturanalysen und die Modellierung der

Wechselwirkungen zwischen Autoantikörper und Antigen bestätigten, dass VDG mit dem Teil des Antikörpers interagieren, der an der Erkennung von Citrullin beteiligt ist. Darüber hinaus zeigten die Daten, dass VDG den Aktivierungsstatus autoreaktiver B-Zellen erhöhen. Dies ist möglicherweise eine Folge der verringerten Internalisierung von glykosylierten B-Zell-Rezeptoren nach der Bindung an citrullinierte Proteine. Diese wichtigen funktionellen Folgen von VDG – sowohl die verringerte Bindung an niedrig-affine (potenziell körpereigene) Antigene, während die Bindung an hoch-affine (potenziell fremde) Antigene beibehalten wird, als auch die geringere Aktivierungsschwelle – könnten es den autoreaktiven B-Zellen ermöglichen, wichtige Kontrollmechanismen zu überwinden und damit die Selbsttoleranz zu durchbrechen.

In **Kapitel 8** wird beschrieben, dass VDG, neben ihrer funktionellen Bedeutung für B-Zell-Rezeptoren, auch die Effektorfunktionen sekretierter Antikörper beeinflussen können. In dieser Studie beobachteten wir eine geringere Bildung von Hexameren bei glykosylierten ACPA-IgG, was folglich zu einer geringeren Bindung an das Effektormolekül C1q und somit zu einer geringeren Aktivierung des klassischen Komplementsystems führt. Das Komplementsystem ist eines der wichtigsten Netzwerke innerhalb des Immunsystems, das für die Aktivierung und Rekrutierung von Immunzellen verantwortlich ist. Ob diese verringerte Komplementaktivierung von glykosylierten ACPA-IgG Auswirkungen auf die Pathogenese der Krankheit hat und ACPA möglicherweise weniger „aktiv“ (immunogen) macht, oder ob es sich nur um einen Nebeneffekt handelt, kann nur spekuliert werden und bedarf weiterer Untersuchungen. Dennoch kann geschlussfolgert werden, dass VDG auf IgG-Antikörpern genutzt werden können, um die Antikörper-abhängigen klassische Komplementaktivierung herunterzuregulieren.

Die in dieser Arbeit beschriebenen Ergebnisse werden in **Kapitel 9** diskutiert und in den Kontext der aktuellen Literatur gestellt. Die Fähigkeit von RA-spezifischen Autoantikörpern an verschiedene modifizierte Proteine zu binden wird anhand der Strukturanalysen von ACPA-Molekülen aufgezeigt und erklärt. ACPA interagieren spezifisch mit der Citrullin-Modifikation und nicht oder nur in geringem Ausmaß mit den flankierenden Aminosäuren, die diese Modifikation umgeben. Da die Modifikationen, die nach der Carbamylierung und Acetylierung von Proteinen entstehen (Homocitrullin und Acetyllysine), strukturell sehr ähnlich zu Citrullin sind, kann ACPA auch diese posttranslationalen Modifikationen „promiskuitiv“ erkennen. Darüber hinaus werden die selektive Einführung von Glykanen in die variable Domäne von ACPA-IgG und ihre funktionellen Konsequenzen diskutiert. Die in dieser Thesis beschriebenen Daten haben zu der Hypothese geführt, dass VDG autoreaktiven B-Zellen dazu verhelfen können Toleranzkontrollpunkte zu umgehen, indem sie die Bindung an modifizierte Proteine und die Aktivierung von B-Zellen beeinflussen. Abschließend wird erörtert, dass autoreaktive B-Zell-Reaktionen bei RA höchstwahrscheinlich aus sequenziellen Ereignissen („multiplen Hits“) resultieren, bei denen die Kreuzreaktivität von B-Zell-Rezeptoren und AMPA und die reichliche Expression von VDG eine wichtige Rolle spielen. Dieser neue „Glykan-Mechanismus“

könnte nützlich sein, um die frühzeitige Diagnose von RA - vor Entstehen der Erkrankung - zu verbessern. Dieses Wissen ist zudem wertvoll, um zu verstehen, wie das Immunsystem "entgleist" und wie Autoimmunität entsteht. Es ist jedoch noch viel mehr Forschung erforderlich, um zu verstehen wie und warum sich Autoimmunerkrankungen wie RA entwickeln (*bitter*) und um die wichtige Rolle von Glykanmodifikationen (*sweet*) bei dieser Krankheitsentwicklung zu entschlüsseln.

Curriculum Vitae

Theresa Kissel was born in Bensheim, Germany, on December 14, 1992, and grew up in Zwingenberg. She graduated from “Altes Kurfürstliches Gymnasium” in Bensheim, Germany, in 2012, majoring in biology and mathematics. In 2015, she graduated with a bachelor’s degree in Biomolecular Engineering from the Technical University (TU) Darmstadt, Germany, where she worked on pH-sensitive, shark-derived variable domains of IgNARs for therapeutic applications under the supervision of Prof. dr. Harald Kolmar. She continued with the master’s program Biomolecular Engineering at the TU Darmstadt. During her study, she completed a semester abroad at the University of Massachusetts in Boston, USA, focusing on immunology and medical biochemistry. She completed her master’s thesis at Sanofi in Frankfurt, Germany, in the Biologics Research department to investigate trispecific T-cell engaging antibodies. In 2017, she obtained her Master of Science (cum laude) and started as a PhD student under the supervision of Prof. dr. René Toes and Dr. Hans Ulrich Scherer in the department of Rheumatology at Leiden University Medical Center in The Netherlands. During her PhD training, she studied the cause and consequence of the hyperglycosylation of the variable domain of (auto)antibodies and B cells characteristic for patients with Rheumatoid Arthritis. The results of the research at the interface of immunology and glycobiology are described in this thesis.

List of publications

Kampstra, A. S. B., Dekkers, J. S., Volkov, M., Dorjee, A. L., Hafkenscheid, L., Kempers, A. C., van Delft, M., Kissel, T., Reijm, S., Janssen, G. M. C., van Veelen, P. A., Bang, H., Huizinga, T. W. J., Trouw, L. A., van der Woude, D. and Toes, R. E. M., Different classes of anti-modified protein antibodies are induced on exposure to antigens expressing only one type of modification. *Ann Rheum Dis* 2019. 78: 908-916.

Kissel, T., van Schie, K. A., Hafkenscheid, L., Lundquist, A., Kokkonen, H., Wuhler, M., Huizinga, T. W., Scherer, H. U., Toes, R. and Rantapaa-Dahlqvist, S., On the presence of HLA-SE alleles and ACPA-IgG variable domain glycosylation in the phase preceding the development of rheumatoid arthritis. *Ann Rheum Dis* 2019. 78: 1616-1620.

Kissel, T.[†], Reijm, S.[†], Slot, L. M., Cavallari, M., Wortel, C. M., Vergroesen, R. D., Stoeken-Rijsbergen, G., Kwekkeboom, J. C., Kampstra, A., Levarht, E., Drijfhout, J. W., Bang, H., Bongers, K. M., Janssen, G., van Veelen, P. A., Huizinga, T., Scherer, H. U., Reth, M. and Toes, R., Antibodies and B cells recognising citrullinated proteins display a broad cross-reactivity towards other post-translational modifications. *Ann Rheum Dis* 2020. 79: 472-480.

Reijm, S.[†], Kissel, T.[†] and Toes, R. E. M.[†], Checkpoints controlling the induction of B cell mediated autoimmunity in human autoimmune diseases. *Eur J Immunol* 2020. 50: 1885-1894.

Kissel, T.[†], van Wesemael, T. J.[†], Lundquist, A., Kokkonen, H., Kawakami, A., Tamai, M., van Schaardenburg, D., Wuhler, M., Huizinga, T. W., Scherer, H. U., van der Woude, D., Rantapaa-Dahlqvist, S. and Toes, R. E. M., Genetic predisposition (HLA-SE) is associated with ACPA-IgG variable domain glycosylation in the predisease phase of RA. *Ann Rheum Dis* 2021.

Reijm, S.[†], Kissel, T.[†], Stoeken-Rijsbergen, G., Slot, L. M., Wortel, C. M., van Dooren, H. J., Levarht, N. E. W., Kampstra, A. S. B., Derksen, V., Heer, P. O., Bang, H., Drijfhout, J. W., Trouw, L. A., Huizinga, T. W. J., Rispen, T., Scherer, H. U. and Toes, R. E. M., Cross-reactivity of IgM anti-modified protein antibodies in rheumatoid arthritis despite limited mutational load. *Arthritis Res Ther* 2021. 23: 230.

Derksen, V., Kissel, T., Lamers-Karnebeek, F. B. G., van der Bijl, A. E., Venhuizen, A. C., Huizinga, T. W. J., Toes, R. E. M., Roukens, A. H. E. and van der Woude, D., Onset of rheumatoid arthritis after COVID-19: coincidence or connected? *Ann Rheum Dis* 2021.

Kissel, T.[†], Ge, C.[†], Hafkenscheid, L., Kwekkeboom, J. C., Slot, L. M., Cavallari, M., He, Y., van Schie, K. A., Vergroesen, R. D., Kampstra, A. S. B., Reijm, S., Stoeken-Rijsbergen, G., Koeleman, C., Voortman, L. M., Heitman, L. H., Xu, B., Pruijn, G. J. M., Wuhler, M., Rispens, T., Huizinga, T. W. J., Scherer, H. U., Reth, M., Holmdahl, R. and Toes, R. E. M., Surface Ig variable domain glycosylation affects autoantigen binding and acts as threshold for human autoreactive B cell activation. *Sci Adv* 2022. 8: eabm1759.

Kissel, T., Hafkenscheid, L., Wesemael, T. J., Tamai, M., Kawashiri, S. Y., Kawakami, A., El-Gabalawy, H. S., van Schaardenburg, D., Rantapaa-Dahlqvist, S., Wuhler, M., van der Helm-van Mil, A. H. M., Allaart, C. F., van der Woude, D., Scherer, H. U., Toes, R. E. M. and Huizinga, T. W. J., ACPA-IgG variable domain glycosylation increases before the onset of rheumatoid arthritis and stabilizes thereafter; a cross-sectional study encompassing 1500 samples. *Arthritis Rheumatol* 2022.

Oskam, N., Ooijevaar-de Heer, P., Derksen, N. I. L., Kruithof, S., de Taeye, S. W., Vidarsson, G., Reijm, S., Kissel, T., Toes, R. E. M. and Rispens, T., At Critically Low Antigen Densities, IgM Hexamers Outcompete Both IgM Pentamers and IgG1 for Human Complement Deposition and Complement-Dependent Cytotoxicity. *J Immunol* 2022. 209: 16-25.

[†] These authors contributed equally to this work as co-first authors.

Acknowledgments

Even if you jumped straight to the acknowledgments, thank you reading my thesis and making the last few years of my (PhD) life an incredible experience!

I could not have undertaken this journey without René. Thank you for your guidance, support and for giving me the freedom that I needed to grow into a scientist. I will always remember your saying “you never prove something in science” and I will never start an experiment without having a positive and negative control. Uli, together with René you gave me the opportunity to start as a PhD student in the lab. I would like to thank you for this opportunity which was the start into a new chapter of my life.

Tom, your enthusiasm for science is infectious. Thank you for your support, your input and advice.

Ellen, we all know that the lab would not exist without you! Thank you for all the hard work you are doing every day for all of us. Also special thanks to Joanneke and Gerrie you contributed enormously to this PhD work. Extra thanks to Manfred and the entire CPM department. I have always felt a bit at home in the German environment of the CPM labs.

Next, I would like to thank my paranymphs Mikhail and Sanne. Mikhail, “Mitschkov”, thank you for being there for me right at the beginning of my PhD. Being pushed out of my German “comfort” zone, this was the most difficult time for me and I am more than happy that you started your PhD at the same time. You always had my back and I am happy about this wonderful friendship. Sanne, I think we are truly “cross-reactive”, reflected not only by our first thesis chapters, but also because we are both enjoying the same sports and holidays. Thank you for pushing me through the difficult long distance runs, for being my PhD, climbing, surfing and running buddy. To many more great waves in life together!

Extra special thanks to Nienke. I am grateful for all the happy moments we spent together, inside and outside of the lab, the great conversations, your sarcasm and honesty. To all the amazing people working in the lab (Veerle, Tineke, Esther, Alice, Miles, Eva Maria, Hugo, Wieke, Renee, Sam, Sanne, Sophie-Anne, Anouk, Roxane, Lars, Abdulallah, Jolien and Cynthia) and all other C5 citizens (Marc and Tjardo): a PhD is so much more than just pipetting. Thank you all for drinking liters of coffee and eating bags of cookies with me, for new friendships, fun borrel nights and congresses. Rochelle, Corrie, Linda and Sanne (the 1st), thank you for getting me started in the lab. Also special thanks to Karin and Lise for guiding me with my first steps in the glyco-world!

To my friends outside of the department, you are the best and I am very lucky to have friends like you. Dani and Alena, you two will always be my gymnastic buddies, and I can't thank you enough for your thoughtful conversations, the laughter and the memories we made together. Patrick, Lena, Doro, Anja and Chris, you saved me during the pandemic with our weekly Jizzi-gymnastic work outs. Michi and Maike (M&M), thank you for your enthusiastic encouragement. For making me take breaks on the beaches of Spain, France and Portugal and for "living in harmony, harmony (always)". Jana, thank you for being a supportive, always kind and lifelong friend. Giggling during our skype dates made me feel better every single time. Nadja, Philip, Jana, Julia, Paul, Alica, and everyone else from "la familia", thank you all for the great memories throughout the years, our holidays together, the fun songs and games. Ale and Louise, thank you for the best dinner evenings in Leiden. Looking forward to eat more home-made marmalade with the two of you. Jeremy and Anna, thank you for the great climbing sessions together! Julia, thank you for your support as a neighbor and friend!

Finally, and most importantly, I am fortunate to have incredible support from my family. Mama und Papa, danke, dass ihr wirklich immer für mich da seid, für eure Unterstützung in jeglicher Hinsicht, dafür dass ihr mich daran erinnert mir eine Auszeit zu nehmen wenn ich es brauche und für eure Liebe - ihr seid einfach wunderbar! Kai, Anna, Nicky, René, Frieda, Greta, Lucia, Oma Inge, Oma Irene, und alle anderen - danke für die beste Unterstützung und Liebe, die man sich wünschen kann! Ich weiß, dass ich immer auf euch zählen kann!

And Simon(tje), thank you for starting this adventure with me. You are truly my resting place! Thank you for always being there for me, for supporting me mentally and culinarily, helping me with technical problems during virtual times, and of course for being my confidante and for your love.

